Studies of the Active Site of the HIV-1 Fusion Cofactor CCR5

by

Shawn E. Kuhmann

A DISSERTATION

Presented to the Department of Biochemistry and Molecular Biology

and the Oregon Health Sciences University

School of Medicine

in partial fulfillment of the requirements for the degree of

Doctor of Philosophy

November 1999

School of Medicine

Oregon Health Sciences University

CERTIFICATE OF APPROVAL

This is to certify that the Ph.D. thesis of

Shawn E. Kuhmann

has been approved.

[redacted]

[redacted]

Member

[redacted]

[redacted]

Member

[redacted]

Member

Table of Contents

List of Tables and Figures

Acknowledgements

I would like to express my deepest thanks to my mentor Dr. David Kabat for his support and wisdom. I would like to thank those people with whom I have had the pleasure of working closely: Sue Kozak, Navid Madani, Mariana Marin, Ali Nouri, Emily Platt, Ethel Polonoff, and Chet Tailor. My grad school experience has been more enjoyable because of their advice, discussion, and support.

I would like to acknowledge my labmates who have contributed to the manuscripts contained in this work. Emily Platt performed the infectivity assays with SIV_{mac251} for Chapter 2, and contributed the JRCSF and Y14N adapted virus stocks used in the studies in Chapters 3 and 4. Sue Kozak assisted in data collection for Chapter 2 and did the analysis of CCR5 glycosylation and sulfation shown in Chapter 4. Navid Madani performed the electrophysiology for Chapter 3. David Kabat purified the BaL gp120 used for binding studies in Chapters 3 and 4.

I gratefully acknowledge the contributions of our collaborators at Merck Research Laboratories, especially Salvatore Siciliano and Julie DeMartino, for their contributions to the work in Chapter 3, specifically the binding studies performed with the YU2 and SF162 gp120s.

This work is dedicated to the memory of Frank R. Smith.

Abstract

The retrovirus human immunodeficiency virus type-1 (HIV-1) is the causative agent of acquired immune deficiency syndrome. Infection of a target cell by HIV-1 requires the sequential interaction with two cell surface proteins, CD4 and a coreceptor. The most biologically relevant coreceptor in HIV-1 infection is CCR5. We have undertaken preliminary studies of the active site within CCR5 for coreceptor function. We find that CCR5 coreceptor activity depends on multiple extracellular regions of CCR5. We have identified an amino acid critical to coreceptor activity and HIV-1 binding within the extracellular amino-terminal domain of CCR5. In addition, we identified an amino acid substitution in the second extracellular loop near the transmembrane domain which inhibits HIV-1 binding and coreceptor activity. We also initiated studies of clonal cell lines expressing varying amounts of CCR5s containing the amino-terminal or second extracellular loop substitutions. These studies indicate that the amino-terminal substitution requires higher expression for maximum infectivity than wild-type CCR5, and also exhibits reduced infectivity when the mutant is present at saturating concentrations. In contrast, the mutation in the second extracellular loop requires higher expression levels for maximum infectivity, but infectivity plateaus at approximately the same level as wild-type. The CCR5 concentration *versus* infectivity curves appear to have sigmoid shapes. We interpret the sigmoid shapes as an indication that multiple CCR5 molecules reversibly associate with an HIV-1 virion to form a complex that is required to promote fusion of the viral and cellular membranes. We believe that the amino-terminal substitution inhibits both the assembly and activity of this complex, whereas the substitution in the second extracellular loop inhibits only the assembly of this complex.

Chapter 1. Introduction

Pathogenesis of HIV-1

Acquired immune deficiency syndrome (AIDS) was first identified as a disease in 1981 (64). HIV-1 was recognized as a unique human retrovirus in 1983 and shown to occur in AIDS patients and in those at high risk for AIDS (64). Soon thereafter HIV-1 was generally accepted as the causative agent of AIDS (186). According to the World Health Organization, AIDS was the fourth leading cause of death in the world during 1998 (10). As of December 1998, an estimated 33 million people were infected with HIV-1 world-wide, and the number of infections is estimated to be increasing at a rate of approximately 6 million infections per year (10, 11). During 1998 an estimated 2.5 million people died from AIDS (11). In Africa, AIDS was the single leading cause of death during 1998, killing 1.8 million people (10). Intense research has led to an increased understanding of the mechanisms by which HIV-1 causes AIDS, which are only briefly reviewed here.

HIV-1 infects cells of the monocyte/macrophage lineage, including terminally differentiated macrophages, as well as CD4+ T-lymphocytes (T-cells) (64). Primary infection with HIV-1 often leads to a mononucleosis-like illness within three to six weeks of infection that coincides with a burst of viral replication and a sharp decline in blood CD4+ T-cells (64). This primary infection is followed by a decrease in viremia and a partial recovery in CD4+ T-cell numbers (64). The recovery of CD4+ T-cells is thought to be due to immune responses against the virus and sequestration of HIV-1 replication to the lymphoid organs (64). There is a long period of clinical latency before the onset of AIDS, which occurs an average of 8 to 10 years after infection (64). During clinical latency, there is continuous viral replication, killing of CD4+ T-cells, and a gradual decline in the number of CD4+ T-cells in the blood (64). Amino acid substitutions in the Env glycoproteins of HIV-1 accumulate at a rate of approximately 2.5% per year and occur mainly within the hypervariable regions (see below) (64). This implies the

selection of advantageous mutations within these regions, most likely as a means of escaping the immune system (64). Indeed, most HIV-1+ individuals continuously have antibody and T-cell responses against viral proteins throughout the course of infection (64). When CD4+ T-cell counts drop below approximately 200 cells/μl infected individuals become susceptible to the opportunistic infections which define AIDS (64).

Progressive HIV-1 infection results in extensive killing of CD4+ T-cells (64). In addition, uninfected CD4+ T-cells and other immune cells (such as CD8+ T-cells, B-cells, monocytes, and macrophages) exhibit decreased function (64). The exact mechanisms of immune dysfunction in the absence of cell killing are not entirely understood (64). The dysfunction may result from interactions of susceptible cells with circulating viral gene products or from impaired interactions of other cell types with CD4+ T-cells and the lymphoid organs, which are being destroyed (64). The mechanism of CD4+ T-cell killing is also poorly understood (64). HIV-1 is extremely cytopathic for CD4+ T-cells *in vitro*, but less so for macrophages (64). Killing may be a result of direct toxicity to infected cells by sequestration of the cellular machinery during viral replication (64). Formation of multinucleated cells (syncytia) by fusion of infected cells with uninfected CD4+ cells may lead to killing of both infected and uninfected cells (64). Other mechanisms which have been suggested to contribute to pathogenicity include immune attack of infected cells, defects in T-cell regeneration due to infection of thymic precursors, and apoptosis induced by circulating viral gene products (64). Interestingly, expression of the *nef* gene product in T-cells, monocytes, and macrophages of transgenic mice is sufficient to induce an AIDS-like illness in the absence of other viral gene products, suggesting that *nef* may be a major determinant of viral pathogenicity (76). HIV-1 pathogenicity also includes destruction of the lymphoid organs (64). The mechanisms of this destruction are not clear, but the lymph nodes are major centers of HIV-1 replication, especially during the clinical latency stage of disease (64).

Although a vaccine is the ideal solution to the AIDS epidemic, little success has been made in the search for an effective candidate (58). Recently, pharmacological control of HIV-1 infection has been more promising (58). Several inhibitors of the viral protease and reverse-transcriptase proteins, when used in combination, have proven effective in decreasing circulating virus to undetectable levels (58). In the absence of active viral replication, CD4+ T-cell counts and immune function partially recover and disease progression is delayed (58). However, viral resistance to these drugs, as well as the persistence of integrated HIV-1 proviruses in resting T-cells which are not actively producing virus, are problems limiting the utility of these drugs (58, 66). HIV-1 entry is an attractive target for new drugs to control viral replication (58). Therefore, an increased understanding of the entry process may lead to improved treatments for HIV-1 infection.

Molecular virology of HIV-1

Taxonomy of HIV-1. HIV-1 is a member of the virus family retroviridae and subfamily lentivirinae (41). In addition to HIV-1, this subfamily consists of the simian immunodeficiency viruses (SIVs), feline immunodeficiency virus, and several other pathogenic animal viruses (41). HIV-1 is thought to have arisen in human populations by several zoonotic transmissions of SIV_{cpz} from chimpanzees (*Pan troglodytes*), in particular a subspecies (*P. t. troglodytes*) found primarily in Gabon (70, 187). Distinct transmission events are believed to have resulted in three groups of HIV-1 subspecies (M, N, and O) and occurred at least as early as 1959 (70, 169, 187, 203). The M group is responsible for the global AIDS pandemic and can be further divided into eight subgroups or clades (termed A-H) (64) which likely arose after the virus entered the human population (187). SIV_{cpz} and HIV-1 are related to other primate lentiviruses which can be grouped into five distinct evolutionary lineages: HIV-1/SIV_{cpz}, HIV-2/SIV_{smm} (from sooty mangabey monkeys), SIV_{agm} (from African green monkeys), SIV_{mnd} (from mandrills), and SIV_{syk} (from sykes monkeys) (64). SIV_{agm} is of particular interest because African green monkeys (AGMs) (*Chlorocebus* sp.) are divided into four distinct but closely related subspecies all of which are infected to high prevalence with viruses from distinct subspecies-specific SIV_{agm} groups, none of which cause disease in their natural hosts (4, 20, 128, 132). This suggests that SIV_{agm} has coevolved with its hosts since before the subspeciation of AGMs and that both virus and host may have evolved such that the virus is nonpathogenic.

Virion structure. Retroviruses have a genome consisting of two identical RNA strands (41). These strands are identical to the full length transcription product from the viral long terminal repeat (LTR) promoter, but do not direct protein synthesis when the virus enters a cell (41). Rather, the RNA is reverse transcribed into a double stranded DNA (dsDNA) provirus which is inserted into the nuclear DNA of the cell (41). The organization of the HIV-1 genome, like the genomes of all lentiviruses, is more complex

than that of other retrovirus subfamilies (41). Whereas other retroviruses contain as few as three and as many as six genes, lentiviruses have at least nine genes (41). HIV-1 has three genes which code for the proteins common to all retroviruses: *gag*, *pro-pol*, and *env* (41). The function of the products of these genes is discussed below. In addition, HIV-1 codes for six other genes known to produce protein products: *vif*, *vpr*, *tat*, *rev*, *vpu*, and *nef* (41). In the inserted proviral DNA, the coding region is flanked by LTR sequences (41). There are several important RNA elements in the HIV-1 genome: the packaging sequence (Ψ), the primer binding site (PBS), the Tat-responsive region (TAR), and the Rev-response element (RRE) (147).

HIV-1 particles consist of cores composed mainly of the viral *gag* and *pro-pol* gene products and the viral RNAs, surrounded by a lipid bilayer acquired from the host cell plasma membrane during budding (180). Inserted in the lipid bilayer are "knobs" consisting of the glycoprotein products of the *env* gene (180). Electron microscopy of HIV-1 virions reveals that the core of immature virions consists of an electron dense shell just inside the membrane, whereas the core of mature virions has collapsed into a dense cone or tube shaped structure (174). Virion maturation is a result of cleavage of the Gag and Gag-Pro-Pol precursor proteins by the viral protease (PR) (180). The mature core consists mainly of the *gag* gene products MA, CA, and NC (for matrix, capsid, and nucleocapsid, respectively) (180). Associated with the core are the genomic RNAs, and the enzymatic proteins RT and IN (for reverse-transcriptase and integrase, respectively) (180).

Early events in the HIV-1 life-cycle. Retroviruses are surrounded by a lipid bilayer acquired from the host cell as the virion buds through the plasma membrane (41). The initial steps of infection for any retrovirus are the attachment to the target cell and fusion of the virus membrane with a membrane of the cell (41). The membrane fusion of HIV-1 is thought to occur at the plasma membrane (41). This step is dependent on the protein products of the viral *env* gene termed the surface (SU) and transmembrane (TM)

subunits, which mediate receptor binding and fusion, respectively (85). This process releases the viral core into the cytoplasm, where reverse transcription takes place (41). At this stage there is a poorly defined step at which the structure necessary for reverse transcription is formed (41). RT, IN, and NC are thought to form this structure, although other *gag* protein products may also be involved (41).

Reverse transcription is a process in which the RNA genome is copied into a dsDNA provirus (41). During this process the flanking LTRs are formed from sequences at the 5' and 3' ends of the RNA genome (41). The RT protein is an RNA and DNA directed DNA polymerase and is responsible for all of the DNA synthesis required for formation of the provirus (41). The PBS is complimentary to the 3' end of a lysine(3) tRNA which is packaged with the viral genome (175). This tRNA serves as a primer for initiating DNA synthesis (175).

The next stage of the viral life cycle requires the integration of the viral DNA into the genome of the host cell where the host transcription machinery can synthesize viral mRNAs and genomic RNA (41). Integration is required for replication and the newly synthesized DNA must move to the nucleus for this process to occur (29). Unlike many other retroviruses, lentiviruses have the capacity to replicate in non-dividing cells, such as terminally differentiated macrophages (29). Therefore, HIV-1 need not always rely on the breakdown of the nuclear membrane during cell division to gain access to the host chromosomes (29). In non-dividing cells, HIV-1 requires the translocation of a preintegration complex (PIC) from the cytoplasm to the nucleus via nuclear pores (29). The PIC contains viral proteins, the proviral dsDNA, and possibly some cellular proteins (29). Functional nuclear localization signals can be found in some HIV-1 proteins thought to be part of the PIC, including MA and Vpr (29), and seem to be sufficient for nuclear translocation in non-dividing cells (29). There is no known sequence specificity in the host DNA for HIV-1 integration, although nucleosomal DNA is preferred and studies suggest that mechanisms exist to direct integration to sites favorable for

transcription (29). The integration reaction is catalyzed by IN and requires the interaction of IN with specific features at the ends of the viral DNA (29).

HIV-1 gene expression. The newly integrated HIV-1 provirus must be transcribed by the host machinery to produce mRNAs for protein synthesis and genomic RNAs for packaging (41). Transcription is mediated by RNA polymerase II, and induction relies on *cis* acting sequences in the 5' LTR (147). HIV-1 transcription is induced by members of the NF-κB/Rel family of transcription activators upon activation of T-cells and monocytes by cytokines and TCR signaling (147). Other transcription factors such as Sp1 can act with NF-κB family members to enhance transcription (147). Lentiviruses encode a *trans*-activator protein known as Tat (147). Tat is required for high level expression of viral gene products (147). Tat binds to an RNA structure in the nascent RNA called the TAR and recruits a cyclin-T1/CDK9 elongation complex (185). This complex is thought to hyperphosphorylate the RNA polymerase II carboxyl-terminal domain leading to increased processivity (185).

RNA transcripts are processed by the cellular mRNA processing machinery (147). They are cleaved at the 3' end and are polyadenylated (147). The transcripts are also capped at the 5' end (147). The resulting RNA serves as the genomic RNA and the mRNA for Gag and Gag-Pro-Pol synthesis (147). RNA splicing also occurs through the cellular machinery, and multiply spliced RNAs for Tat, Rev, and Nef expression are found in the cytoplasm at early times after infection (147). The singly spliced RNAs for Env and Vpu, Vif, and Vpr expression, as well as the unspliced RNA accumulate in the cytoplasm after sufficient accumulation of Rev (147). These RNAs contain a *cis*-acting element (the RRE) in the *env* gene that interacts with Rev, and the resulting complex recruits components of the nuclear export machinery and promotes the export of the late RNAs (147).

Late events in the HIV-1 life-cycle. Translation also takes advantage of the host cell machinery (174). Of the major structural proteins, Gag and Gag-Pro-Pol are

synthesized by free ribosomes in the cytoplasm (174). The synthesis of the Gag-Pro-Pol fusion protein occurs by an inefficient frameshift and readthrough event near the end of the *gag* gene (174). The inefficiency of this event allows for the production of Gag and Gag-Pro-Pol in the correct proportions (174). The Gag and Gag-Pro-Pol proteins are directed to the inner leaflet of the plasma membrane by an amino-terminal membrane association domain that includes a myristate post-translational modification (174). The protein product of the singly spliced *env* mRNA is cotranslationally secreted from membrane bound ribosomes into the rough endoplasmic reticulum (RER) (174). Env remains embedded in the ER membrane through its single transmembrane domain and proceeds to the plasma membrane through the secretory pathway (174).

Assembly of infectious virions occurs at the plasma membrane, and the Gag polyprotein is sufficient to mediate assembly of virus particles (174). Gag interactions are responsible for incorporation of the *pro-pol* gene products by way of interactions between Gag and Gag-Pro-Pol (174). The amino-terminus of the MA domain of the Gag precursor is responsible for membrane binding, and the NC domain insures specific incorporation of viral RNAs (174). Specific incorporation of HIV-1 Env into virions may occur through the interaction of the cytoplasmic tail of gp41 with the MA region of Gag (174). The incorporation of Vpr into virions is also mediated by interactions with Gag (174). After budding of virions through the plasma membrane, immature virions are formed in which the Gag proteins form a shell close to the viral membrane (174). The viral PR is active in the context of the Gag-Pro-Pol precursor, and after budding it cleaves the Gag and Gag-Pro-Pol precursors into the mature proteins products (174). Subsequent rearrangement of the core proteins results in maturation of the virion and collapse of the core into a condensed cone or rod shaped structure (174). These mature particles represent the infectious HIV-1 virions (174).

Many of the viral accessory genes play specific parts in the production of mature virions (174). The Vif protein acts at the level of the producer cell to counteract an

unidentified factor found in T-cells and monocytes that reduces the infectivity of produced virions (111, 170). In addition to its role in translocating the PIC (see above), Vpr also plays a poorly understood role in producer cells by modulating the cell-cycle (174). Vpu and Nef play crucial roles in producing infectious virions by downmodulating CD4 in infected cells (174). Because Env proteins are capable of receptor binding before budding occurs, downmodulation of CD4 probably allows for increased Env incorporation (174). In addition, the downmodulation of cell surface MHC class I molecules by Nef may reduce immune recognition of infected cells (140).

HIV-1 membrane fusion

Viral and cellular proteins. As mentioned above, receptor binding and entry of retroviruses into host cells is strictly dependent on the glycoprotein products of the *env* gene. These products are synthesized as a precursor protein with an apparent M_r of ~160,000 referred to as gp160. The HIV-1 gp160 amino acid sequence is preceded by a signal sequence (c.a., 30 amino acids), which is cleaved by the signal peptidase in the RER (85). The precursor remains anchored in the membrane by the transmembrane domain (85). Carbohydrates are added in the ER and gp160 is cleaved by a cellular protease in the Golgi apparatus into SU and TM subunits, which remain noncovalently associated (85). The SU protein is responsible for receptor binding, and the TM protein is required for membrane fusion (180). The HIV-1 SU and TM products are referred to as gp120 and gp41 respectively, the numbers reflecting the apparent M_r in thousands from SDS-PAGE analysis (85). gp120 and gp41 remain noncovalently associated on the virion after cleavage and form higher order multimers, most likely a trimer of gp120-gp41 heterodimers (referred to below as the Env trimer) (85). Fusion is also dependent on two cellular proteins. The first of these cellular proteins is CD4, which is a cell-surface marker found primarily on T-cells and cells of the monocyte/macrophage lineage (85). The other cellular protein thus far identified as being required for fusion is termed the coreceptor. Coreceptors are members of the family of chemokine receptors and other closely related members of the seven-transmembrane spanning G protein-coupled (7TM) receptor superfamily (107). While a number of different 7TM receptors exhibit coreceptor activity under certain conditions, CCR5 and CXCR4 are the most important of these for HIV-1 entry *in vivo* (3, 38, 50, 53, 54, 65, 107, 202). An overview of the proposed mechanism of HIV-1 mediated fusion, as well as the structures and functions of each of these four proteins (gp120, gp41, CD4, and coreceptor) are discussed in more detail below.

Proposed mechanism. The initial step in HIV-1 infection is attachment to the surface of the target cell and binding to CD4. Attachment of retroviruses to cells has been shown to be dependent on the SU protein (gp120 of HIV-1) and in most cases on the presence of the viral receptor (85). For HIV-1, attachment to most cell types is dependent on the presence of CD4 in the membrane (85). After attachment to the surface of the target cell, virion associated gp120 must interact with both CD4 and the coreceptor for fusion to occur (85). It has been shown that the interaction with coreceptor takes place after binding of gp120 to CD4 (154). Thus, it has been proposed that the interaction of gp120 with CD4 induces a conformational change in gp120 that forms a site on gp120 for the interaction with the coreceptor (34).

Because HIV-1 is thought to fuse at the plasma membrane in a pH independent manner, it has been suggested that an interaction of gp120 with a receptor induces conformational changes in the Env trimer leading to initiation of the fusion process by gp41 (34). Prior to the identification of the coreceptors, this role was suggested to belong to CD4 (85). However, some observations are inconsistent with this view and suggest the presence of a fusion cofactor. Foremost, CD4 expression in most non-human and some human cultured cells is insufficient for viral entry, although CD4 dependent virus attachment still occurs in these cells (85). Second, HIV-1 strains are known to exhibit distinct tropisms for different cultured human cells which can not be accounted for by CD4 expression, and the determinants of tropism map to the viral *env* gene (85). As discussed below, coreceptors account for most of these observations and are thus assumed to be the viral receptors responsible for triggering fusion. Binding of the coreceptor to gp120 is thought to alter the conformation of the Env trimers in such a way as to allow gp41 to initiate fusion of the two membranes (34).

Fusion is thought to be triggered by extension of the amino terminal hydrophobic region (fusion peptide) of the gp41 trimers into the plasma membrane of the target cell (34). Subsequent conformational changes in trimeric gp41 lead to rearrangement of its

coiled-coil conformation to a six-stranded helical bundle and to apposition of the viral and cellular membranes (34). It is unclear how this leads to fusion. One proposal is that clustering of multiple gp41 trimers could form a "fusion pore" which, once opened would widen to allow entry of the viral core (34).

gp41 mediated fusion. gp41 is an approximately 350 amino acid protein modified by asparagine-linked (N-linked) oligosaccharides (34). The extracellular domain of gp41 consists of an amino terminal hydrophobic sequence (c.a., 30 amino acids) known as the fusion peptide which, by analogy to influenza A virus, is thought to insert into the target membrane (34). The fusion peptide is followed by a region characterized by a heptad repeat motif common to coiled-coil proteins (c.a., 50 amino acids) (33, 190). A short linker connects this region to an additional heptad repeat region (c.a., 40 amino acids) (33, 190). Oligomerization of the gp120-gp41 complex is mediated by gp41 through the heptad repeat regions (34). An additional spacer region connects this domain to the transmembrane domain, which spans the viral membrane (34). The carboxyl terminal domain of HIV-1 gp41 is relatively large for a retrovirus (c.a., 160 amino acids), is intracellular in virus producing cells, and lies inside the viral membrane after budding (34). This domain has been proposed to interact with the viral *gag* gene products, perhaps as a means of insuring incorporation of Env proteins into budding virions (174).

Two high resolution crystallographic structures of portions of HIV-1 gp41 have been recently reported (33, 190). The findings of both groups are in concordance and similar to those for related proteins from simian immunodeficiency virus (30, 114, 200), murine leukemia virus (63), influenza A virus (85), and Ebola virus (115, 188, 189), all of which are believed to have similar fusion mechanisms (171). Essentially, both groups determined the structure of a protease resistant fragment consisting of two peptides that correspond to the two heptad repeat regions (33, 190). A trimer of the amino terminal heptad repeat forms a core coiled-coil, and the three carboxyl terminal repeats form α-helices packed anti-parallel into grooves on the surface of the coiled-coil, such that the

fusion peptide and transmembrane domain would lie at the same ends of a six-stranded helical bundle (33, 190). This conformation is thought to represent the post-fusion state, after insertion into the target bilayer and subsequent rearrangement (33, 190). This conclusion is in part by analogy with structures of the influenza A virus HA protein (see below) (34). Additionally, this conclusion is supported by the fact that the structure forms in the absence of gp120, and loss of contacts with gp120 is thought to lead to the structural rearrangements in gp41 that occur during fusion (34). Finally, fusion can be inhibited by peptides corresponding to the carboxyl terminal heptad repeat, suggesting that the grooves on the amino-terminal coiled-coil are unoccupied prior to fusion, and that the rearrangement of the carboxyl-terminal heptad repeats to fit into these grooves is required for fusion (34).

The proposed mechanism of membrane fusion mediated by the gp41 protein of HIV-1 closely resembles that of other enveloped viruses, the most extensively studied of which is the influenza A virus (171). Therefore, it is useful to examine the similarities and differences between the fusion mechanisms of influenza A virus and HIV-1. Like HIV-1 Env, influenza hemagglutinin (HA) is synthesized as a single precursor, which is proteolytically processed into HA1 and HA2 subunits (85). HA2 is the fusion subunit, and has structural features in common with gp41 (85). HA1 is the receptor binding subunit and shares no structural homology with gp120 (100). HA1 binds to sialic acid on the surface of target cells, however fusion is not induced by receptor binding, but rather by a change in the pH of vesicles after endocytosis of the virus (85). HA forms trimers on the cell surface, with the oligomerization being mediated by the coiled-coil interactions of the HA2 subunits (85). Crystal structures of HA at neutral pH and of an HA2 fragment at low pH have been solved (85). In the neutral pH structure, the carboxyl-terminus of HA2 forms a coiled-coil and the amino terminus containing the fusion peptide is bent back against the carboxyl terminus (85). The HA1 subunit makes contacts with the intervening loop (85). In the low pH structure, the loop and the amino-

terminus form an extension of the coiled-coil, such that the fusion peptides would be at the end of the coil (171). In addition, the carboxyl-terminus is now bent back around the outside of the amino-terminal coiled-coil (171). This structure is similar to the structures of gp41 described above, with the carboxyl-terminus and the amino-terminus pointed toward to same end of a rod-like structure and an amino-terminal coiled-coil at its core (171). This has led to the proposal that the low pH structure is the post-fusion conformation and to the following hypothetical mechanism for influenza A virus membrane fusion (171). First, the HA1 subunit binds to sialic acid and the virus is endocytosed (171). The low pH triggers HA2 to form of an extended coiled-coil with the amino terminal fusion peptide inserted into the target membrane (171). The extended coiled-coil rearranges so that the carboxyl-terminus packs tightly against the amino-terminus and the fusion peptide and transmembrane domain are drawn together pulling the two membranes close together (171). The clustering of several HA2 subunits is thought to form a pore which expands to allow complete fusion (122). The structural similarities suggest that the mechanism for gp41 mediated fusion is similar to that of HA2 (34). However, HIV-1 fusion is expected to be initiated by the interaction of the gp120 subunit with a coreceptor rather than by a change in pH (34). The elucidation of the interaction of gp120 with the coreceptor is therefore of great importance for understanding the process of HIV-1 entry.

Receptor binding by gp120. The mature gp120 protein is approximately 480 amino acids in length, and contains 18 cysteine residues (see Fig 1-1) (105). These cysteine residues are involved in nine disulfide linkages which form five loops (105). Two of these loops contain a single disulfide bond and three contain two or more disulfide bonds (105). Approximately 50% of the apparent M_r of gp120 is oligosaccharides (105). Analysis has shown that all 24 potential sites for asparagine-linked (N-linked) glycosylation are utilized in the gp120 protein of the prototype IIIB strain of HIV-1 (105). gp120 sequences from different HIV-1 isolates are highly

variable, with most of the variable sequences falling into five hypervariable regions termed V1 through V5, which vary both in sequence and length (85). V1 and V2 form a large disulfide bonded loop (referred to as V1/2) containing three disulfide bonds, V3 and V4 each comprise a disulfide bonded loop, and V5 is not delimited by disulfide bonds (85). The variable regions are flanked by five conserved regions (the short semi-conserved sequence between V1 and V2 is not counted) termed C1 through C5 (85). The C1 and C5 regions at the amino-and carboxyl-termini, respectively, have been shown to be important for association with the gp41 trimer (79, 196). The variable regions have been shown to be surface exposed by their antigenicity and extensive glycosylation (197). The role of these variable loops and of the carbohydrates has been suggested to be to shield the receptor binding domains from immune surveillance by presenting a surface covered with "self" oligosaccharides and protein sequences which can be altered without a loss of replicative capacity (100, 126, 197) .

The CD4 binding site on gp120 has been extensively analyzed (85). Neutralizing antibodies against gp120 which compete with CD4 for binding to gp120 (termed CD4BS antibodies) map to discontinuous sequences within conserved regions of CD4 (85). Site-directed mutagenesis of gp120 has also shown that amino acid substitutions that disrupt CD4 binding are found in constant regions of CD4 (85). Taken together the results suggest that portions of the C2, C3, and C4 regions fold to form a tertiary structure critical for CD4 binding (85). The importance of these regions was confirmed in the atomic structure of the core of gp120 bound to a fragment CD4 (100), and the nature of the tertiary structure involved is described below.

Determination of the coreceptor binding site has begun more recently and is less definitive. Most work to date has focused on regions of gp120 that determine which coreceptor is used by a given virus strain. The V3 loop has been identified as the major determinant of discrimination between CCR5 and CXCR4 coreceptor usage (21, 38, 91, 160, 172). Increased basic character of V3 has been implicated in CXCR4 usage (87,

91). Specific sequence alterations in gp120s from CXCR4 dependent strains can promote the use of CCR5 instead (84, 183, 199). However, the sequence alterations required depend on the HIV-1 isolate, and there is not yet a specific consensus sequence that can predict coreceptor use (84, 91, 172, 183, 199). Sequences that allow use of both coreceptors are often produced in gp120 chimeras or mutants (91, 172) and also arise *in vivo* (17). These results suggest that coreceptor choice, while clearly controlled by the V3 region, may be dependent on structural features rather than an absolute sequence requirement, or that other unidentified regions interact with V3 in determining coreceptor choice. In addition, the determinants of CXCR4 and CCR5 use must be at least partially overlapping.

Further studies have attempted to address coreceptor binding as opposed to coreceptor choice. Studies have demonstrated that purified monomeric gp120 competes for chemokine binding to CCR5 when CD4 or a soluble fragment of CD4 is present (177, 193). This competition has been interpreted as a direct CD4 dependent interaction of gp120 with the chemokine receptor (177, 193). The integrity of the V3 region is necessary for this competition to be observed (177, 193). Additionally, the interaction is blocked by monoclonal antibodies that bind to gp120 epitopes induced by CD4 binding (CD4i epitopes). CD4i epitopes are formed from the constant regions near the base of the V1/2 and in C4 (177, 193). Studies of gp120 binding to CXCR4 also implicate the V3 and CD4i regions of gp120 in coreceptor binding (123). The importance of CD4i regions in coreceptor binding is underscored by the mutation of gp120 residues shown to directly contact a CD4i epitope recognizing monoclonal antibody (mAb) (151). Mutation of these amino acids disrupts CCR5 binding by gp120 (151). Other studies have examined the binding of virion associated gp120 to coreceptors by less direct methods. A recent study indicates that a single amino acid change in the V1 loop of gp120 from one virus isolate can enable it to exploit extremely low concentrations of CCR5, most likely by increasing the affinity of gp120 for CCR5 (49). In addition, we have recently found that

a point mutation in the V3 region of a cloned HIV-1 isolate enhances its affinity for mutant CCR5s which bind the wild-type gp120 poorly (142). Taken together, the above results suggest that the coreceptor binding site is likely to involve a tertiary structure comprised of both conserved and variable regions.

A high resolution crystal structure has been solved of the core of gp120 from the HXB2 isolate complexed to the D1D2 fragment of CD4 (see below) and an Fab fragment of the CD4i human anti-gp120 mAb 17b (100). This structure lacks the variable regions V1/2 and V3, is truncated at the amino and carboxyl termini, and all carbohydrates have been enzymatically removed (100). In addition, the V4 region is disordered in the structure (100). However, this gp120 core fragment binds CD4 and retains much of the antigenic character of native gp120 (22, 100), suggesting that the structure of the gp120 core is relevant to the native structure. The structure is significant because it demonstrates the nature of the CD4 binding site, and because it suggests a mechanism for coreceptor binding. The gp120 core consists of two domains, termed the inner and outer domains based on their presumed positions in the gp41 associated trimer (100, 197). Although gp120 is monomeric in the absence of association with gp41, the assignment of the inner and outer domains was made based on the fact that the gp41 binding regions, although not present in the crystal structure, would be located on the face of the inner domain opposite the CD4 binding site (100). Non-neutralizing antibodies, which are elicited to epitopes on monomeric gp120 that are occluded in the trimeric structure, map to the same face of the inner domain as the gp41 binding site (100, 197). The inner and outer domains are bridged by a four stranded β-sheet (termed the bridging sheet) formed by the stem of the V1/2 loop (the C1 and C2 residues immediately flanking the V1/2 loop) and part of the C4 region (100). The presumed locations of the V1/2, V3, V4, and V5 regions are exposed on the surface of the predicted trimeric structure (100).

The CD4 binding site on gp120 is formed from a depression at the interface of the inner and outer domains and part of the bridging sheet which includes the V1/2 stem

(100). The gp120 residues that make direct contacts with CD4 are short stretches of conserved amino acids contributed by the C2, C3, C4, and C5 regions (100). The binding interface is unusual because about half of the contacts with CD4 are not from side-chain atoms, but from the main-chain (100). The interface is not a continuous protein-protein surface, but is interrupted by a water-filled cavity on the gp120 surface, which is lined with variable residues, but maintains an electrostatic complementarity to CD4 (100). A critical gp120 binding residue of CD4, phenylalanine 43, is inserted into the opening of a large cavity in the interior of the gp120 structure (100). When the four domain structure of the extracellular fragment of CD4 (soluble CD4, sCD4) is modeled in place of the two domain fragment found in the crystals, the gp120 molecule is oriented such that, viewing the structure from the plane of the target membrane, CD4 contacts the molecule from the side (100). This orientation results in the base of the bridging sheet and V3 loop facing the target cell membrane (100). Several features of the CD4 binding site are suggested to contribute to immune evasion (100). First, the residues which contact CD4 are dispersed throughout the linear sequence of gp120 (100). Second, main-chain atoms make a major contribution to the CD4 binding site (100). Third, the conserved portions of the binding site are interrupted by a large cavity lined with more variable side-chains (100). Finally, the critical contacts with CD4 are recessed in a narrow cavity (100).

CD4i epitopes are more exposed after CD4 binding (197) and in unusual viruses isolated *in vitro* which infect cells independent of CD4 (82). CD4i mAbs also compete with coreceptor for binding to gp120 (197). The similarities betwen CD4i antibody binding to gp120 and coreceptor binding to gp120 suggest that CD4i epitopes overlap the coreceptor binding site. Indeed, mutation of conserved residues in gp120 involved in the binding of mAb 17b also disrupt gp120 binding to coreceptor (151). The core gp120 structure solved by Kwong and coworkers was solved as a complex with an Fab fragment of 17b (100), allowing a clear delineation of the conserved structures proposed to be involved in coreceptor binding. The 17b Fab makes contact with the base of the bridging

sheet on the side of gp120 facing the target cell membrane (100). The 17b contact surface is basic and hydrophobic in character (100). If present in the structure, the V3 loop would also be oriented toward the target cell membrane adjacent to the 17b binding site (100). Based on these considerations, it is attractive to speculate that the structure solved by Kwong and coworkers represents a gp120 intermediate primed for coreceptor binding, and that the highly acidic amino-termini of the coreceptors interact with the basic surface of the bridging sheet (100). In this model, the V3 loop region would be likely to interact with other coreceptor regions and the coreceptor binding site would be formed from both conserved and variable regions of gp120 (100).

Although the structure solved by Kwong and coworkers represents only one conformation of the extremely flexible gp120 protein, and is missing key regions needed for a full understanding, the structure and other work in the field allow the authors to form a speculative model of the sequential mechanism of receptor binding (100). This model is detailed in references (100, 126), and only briefly summarized here. Initially, binding of the Env trimers to the D1 domain of CD4 positions the gp120 proteins with the chemokine receptor binding regions oriented towards the target cell membrane (100). Although the pre-CD4 binding conformation is unknown, the authors suggest that CD4 binding forms or stabilizes the bridging sheet by its interaction with residues from three of the four strands in the sheet and by a reorientation of the inner and outer domains with respect to one another, thereby forming the large internal cavity which is stabilized by phenylalanine 43 of CD4 (100). The V1/2 loop is probably masking the V3 and bridging sheet regions before CD4 binding and is shifted by the subsequent conformational changes (100, 198). The structure of V3 may also be altered by CD4 binding (100). Thus, the coreceptor binding site of gp120 is revealed and correctly oriented by CD4 binding (100). The next step is the interaction of gp120 with the coreceptor which is probably facilitated by the flexibility of CD4 at the D1D2 to D3D4 junction (see below) (100). This flexibility allows the virus bound above the glycocalyx to make close contact

with the extracellular domains of the coreceptors which lie close to the membrane (100). The coreceptor then binds to the base of the bridging sheet and the V3 loop (100). It seems that selectivity is conferred on a conserved coreceptor binding site by the variable regions because the binding site consists of both variable regions of gp120 and regions conserved between virus isolates that utilize different coreceptors (100). Because the V3 region is variable even among viruses using the same coreceptor, the tertiary structure of V3 and main-chain contributions from this region may be key to coreceptor recognition, similar to the CD4 binding site (100). After the coreceptor interaction, gp120 must undergo further structural changes to allow exposure of the fusion peptide of gp41 and initiation of the membrane fusion mechanism described in the previous section. The structure of gp120 does not reveal how this rearrangement may occur, but it is proposed that a rearrangement between the gp120 subunits of the Env trimer may loosen the interaction of gp120 with gp41 (100).

Structure and function of CD4. CD4 was identified as a receptor for HIV-1 soon after the virus was identified (44, 94). The initial identification was based on several observations: i) CD4+ T-cells are depleted in AIDS patients (85); ii) HIV-1 replication is restricted to CD4+ cells *in vitro* (85); iii) CD4 levels on the surface of T-cells are decreased after HIV-1 infection (85); and iv) Monoclonal antibodies against CD4 block HIV-1 infection (85). When the cDNA encoding CD4 is transfected into some otherwise resistant cultured human cells, it renders them susceptible to HIV-1 infection (113). In addition, it has been shown that CD4 mediates attachment of HIV-1 virions to the surfaces of CD4+ T-cells by binding to gp120 (118, 119). Although endocytosis was initially implicated in entry, later studies showed that entry is independent of pH and it is now generally accepted that fusion occurs at the plasma membrane through a receptor rather than pH initiated process (85).

CD4 is a glycoprotein with an apparent M_r of approximately 60,000 which is expressed mainly on major histocompatibility complex class II (MHC class II)

recognizing T-cells, which are primarily T-helper cells (12). CD4 can also be found on cells of other lineages including monocytes and macrophages (85). In T-cells, CD4 functions in immune responses as an accessory factor to T-cell receptor (TCR) activation by MHC class II complexes on antigen presenting cells (12). CD4 binds to non-polymorphic sequences on MHC class II molecules and strengthens the interaction between MHC class II and the TCR (12). In addition to strengthening this interaction, CD4 may also transmit a costimulatory signal through the associated tyrosine kinase $p56^{lck}$ (12).

CD4 is an integral membrane protein and contains a large extracellular segment (c.a., 370 amino acids) consisting of four immunoglobulin-like domains, D1 to D4, numbered from the amino terminus (156, 182). The immunoglobulin-like domains are attached to a transmembrane anchor, and a short cytoplasmic tail (c.a., 38 amino acids) which contains the carboxyl terminus and is involved in signaling through $p56^{lck}$ (156, 182). Like the reciprocal site on gp120, the CD4 structures involved in gp120 binding have been thoroughly investigated and are reviewed in reference (85). The D1 domain has been implicated in this process through mapping of anti-CD4 mAbs able inhibit attachment and infection (85). These results are supported by chimeric and mutational analyses of the human CD4 gene expressed in cells which are rendered susceptible to HIV-1 by CD4 expression (85). Specifically, residues 30 to 60 of human CD4 have been implicated HIV-1 infection and phenylalanine 43 is a critical amino acid determinant from this region (85). Notably, the transmembrane domain and cytoplasmic tail have been shown to be dispensable for HIV-1 infection by the use of truncated and glycophospholipid anchored CD4s (85).

Atomic structures of the human CD4 extracellular D1D2 fragment alone (156, 182) or bound to the gp120 core (100) have been solved by x-ray crystallography. A rat D3D4 structure at atomic resolution (27) and a lower resolution four domain human sCD4 structure (192) have been solved and allow for a complete picture of the

extracellular region of CD4. The sCD4 molecule forms an extended structure with each domain forming an immunoglobulin fold stacked on the next domain (192). The presumptive location of the transmembrane domain suggests that CD4 does not extend away from the membrane at a right angle, but at an angle of approximately 45° to the perpendicular (192). The sCD4 structure was solved in three different crystal forms which reveal a high degree of flexibility at the junction between the D1D2 and D3D4 portions (192). The region implicated in gp120 binding sits at the end of the extended molecule most distant from the membrane (100, 192). The gp120 binding site in CD4 forms a ridge on top of the D1 domain and is remarkable for the protrusion of the critical gp120 binding residue phenylalanine 43 away from the molecule, even in the absence of gp120 (100, 156, 182). In the CD4/gp120 cocrystal structure the D1D2 CD4 structure is not dramatically altered from that in the absence of gp120 (100). In the cocrystal structure, the gp120 binding ridge sits in the crevice between the inner and outer domains of gp120, and phenylalanine 43 assists in the formation of a large cavity in the interior of gp120, as discussed above (100).

HIV-1 isolates were initially recovered from PBMCs of infected individuals; however, in order to obtain high titer stocks, viruses were passaged through immortalized CD4+ cell lines of T- or B-cell origin (1, 75, 110). sCD4 blocks infection by these HIV-1 isolates *in vitro* , however it is inefficient at blocking infection by viruses passaged only briefly in PBMCs (primary isolates) (127). sCD4 induces shedding of gp120 from T-cell line adapted (TCLA) virions, but shedding from primary isolate virions is reduced (127). sCD4 binds to primary isolate virions with lower affinity than to TCLA virions (96, 143). All of these phenotypes are attributable to changes in the *env* gene. Work from this laboratory has shown that the increased affinity of TCLA virions for CD4 results in the ability to infect cells expressing low quantities of CD4, however primary isolates show a strong dependence on CD4 concentration for infection (90, 96, 143). Virion attachment is expected to be efficient even at low concentrations of CD4 (see Chapter 4), and this is

supported by experimental evidence (90, 141). Thus, these findings suggest that CD4 reversibly associates with adsorbed virions to form a virus-CD4 complex which is required for infection (by the same arguments applied for CCR5 in Chapter 4). Indeed, T-cell lines express reduced levels of CD4 compared to PBMC derived T-cells and studies of primary viruses passaged through T-cell lines expressing augmented amounts of CD4 suggest that increased CD4 affinity accounts for most, but not all, of the TCLA phenotype (141). Additional factors involved in T-cell line adaptation may be the lack of immune surveillance *in vitro*, and as yet unidentified cellular factors (141).

Coreceptors. Soon after the identification of CD4 as the primary receptor for HIV-1, several observations lead to the hypothesis that an additional factor is required for fusion of the viral and cellular membranes. First, expression of human CD4 in non-human and certain human cell types enables virus binding, but fusion does not occur (85). Heterokaryons between cells permissive for HIV-1 entry and nonpermissive cells that express human CD4 are permissive for fusion with HIV-1 virions (85). These results suggest the presence of a positive factor in permissive cells which promotes fusion after binding of the virus to CD4.

Additionally, the tropism of HIV-1 isolates for distinct subsets of CD4+ cells maps to the *env* gene suggesting the presence of cellular cofactors mediating this effect (85). HIV-1 isolates from different individuals or from the same individual at different times after infection replicate differently in cell culture systems (64). Viruses are defined as T-cell-tropic (T-tropic) or macrophage-tropic (M-tropic) (64). T-tropic viruses are those which can be propagated in immortalized T-cell lines as well as peripheral blood mononuclear cells (PBMC), but lack the ability to efficiently replicate in enriched populations of monocytes or macrophages (64). However, as noted above, propagation of primary T-tropic viruses through T-cell lines results in *env* mediated changes in phenotype termed lab adaptation (90, 141). M-tropic viruses efficiently replicate in CD4+ T-cells and monocytes/macrophages, but not in T-cell lines (64). These cellular

tropisms map to the V3 loop of gp120, and exchange of V3 loops between M-tropic and T-tropic viruses is typically sufficient to correspondingly alter the phenotype (64). M-tropic viruses dominate those found at early times after infection and T-tropic viruses typically arise after several years of infection with a time course correlated to CD4+ T-cell decline and immunodeficiency (17). A final clue as to the identity of the coreceptors came with the discovery of an HIV-1 suppressive factor in the supernatants of cultures of CD8+ cytotoxic T-cells (39). A major component of this factor was identified as the β-chemokines MIP1α, MIP1β, and RANTES (39). The ability of these chemokines to block HIV-1 replication is also dependent on the V3 loop of gp120 (40).

In May 1996 a report was published describing the expression cloning of the cDNA for a cofactor required for fusion of cells expressing a T-tropic lab adapted *env* gene with non-human cells expressing human CD4 (65). The cDNA encodes a protein with homology to the 7TM receptors for the α-chemokine IL-8, CXCR1 and CXCR2 (65). The identity of this protein as a coreceptor for T-tropic HIV-1 isolates was quickly confirmed (18). This HIV-1 coreceptor is now called CXCR4 as it has been shown to act as the receptor for the α-chemokine SDF-1 (24, 133). The similarity of this coreceptor to chemokine receptors, along with the identification of the β-chemokines MIP1α, MIP1β, and RANTES as HIV-1 suppressive factors lead to the identification of a β-chemokine receptor (CCR5) with this ligand specificity as a receptor for M-tropic HIV-1 isolates (3, 38, 50, 53, 54) as soon as it was cloned (150, 157).

The cloning of the coreceptors CXCR4 and CCR5 has explained many observations about HIV-1 *env* gene phenotypes. First, it is clear that most tropic effects are determined by coreceptor usage. Viruses previously designated as T-tropic predominantly use CXCR4 for entry, and likewise M-tropic viruses predominantly use CCR5 (107). Therefore, the older terminology has been replaced with a terminology based on the molecular basis of tropism and viruses are now referred to as X4 (for CXCR4 dependent), R5 (for CCR5 dependent), and X4R5 (for viruses which can use

both coreceptors) (16). Viruses are referred to as TCLA (for T-cell line adapted) when they have been passaged in T-cell lines (16). TCLA viruses are almost exclusively X4 or R5X4 viruses, because CCR5 is not expressed or expressed at undetectable levels in most T-cell lines (107). Lab adaptation has been attributed mainly to increased affinity of virions for CD4 (90, 141), and the inability of R5 viruses to replicate in T-cell lines can be explained by the lack of sufficient CCR5 in these cell types (107). However, the inability of X4 viruses to grow in primary monocytes and monocyte derived macrophages cannot be attributed to the lack of CXCR4 in these cells (107). Recent studies have suggested that, although the inability of X4 viruses to replicate in macrophages maps to the *env* gene and correlates with coreceptor usage, the X4 viruses are restricted at a post-entry early step of infection (i.e., uncoating or reverse transcription) (162). Additional studies will be required to fully clarify the basis for differential cell tropism by HIV-1 isolates.

Studies of rhesus macaques experimentally infected with pathogenic SIV/HIV-1 hybrids containing R5 or X4 HIV-1 *env* genes suggest that that the switch to CXCR4 coreceptor usage may cause increased pathogenicity and immunodeficiency *in vivo* (78). Similarly, studies of X4 and R5 virus replication in *ex vivo* lymphoid tissue suggest that, in contrast to CCR5 use, CXCR4 use causes rapid depletion of CD4+ cells, perhaps because CCR5+ cells represent a lower percentage of total CD4+ cells (74, 137). However, immunodeficiency can occur in humans infected with HIV-1 who do not develop X4 viruses, perhaps by overcoming the inhibitory effect of the natural CCR5 ligands (160). Thus, clarification of the role of the coreceptor phenotype in disease progression will also require additional studies. What is clear about the consequences of the coreceptor phenotype of HIV-1 isolates is that R5 viruses are those which are most commonly horizontally transmitted (107). There is a naturally occurring allele of CCR5 present in approximately 10% of the North American Caucasian population, with lower frequencies in other ethnic groups, which has a 32 bp deletion (ccr5Δ32 allele) resulting

in a frameshift and premature truncation in the second extracellular loop (48, 83, 108, 158). The gene product is undetectable on cell surfaces and epidemiological studies have indicated that individuals homozygous for this defect are resistant to horizontal transmission (48, 83, 108, 158). Additionally, heterozygotes have a delayed onset of AIDS by 2 to 4 years compared to populations homozygous for the wild-type allele (48, 83, 108, 158). This finding underscores the importance of coreceptors, and particularly CCR5, in HIV-1 infection and AIDS.

With the cloning of CXCR4 and CCR5 came the identification of numerous 7TM receptors which are expressed in potential HIV-1 target cell types and can act in some *in vitro* systems as coreceptors for some HIV-1 isolates (107). Other chemokine receptors, including CCR2, CCR3, and CCR8, have been shown to act as coreceptors for some HIV-1 isolates in transfected cells (107). Some 7TM receptors with homology to chemokine receptors, including Bonzo/STRL33 and BOB/GPR15, whose ligand specificities are unknown, can act as coreceptors *in vitro* (107). CXCR4 and CCR5 are clearly the major coreceptors for HIV-1. All HIV-1 isolates whose coreceptor usage has been described to date can use either CCR5 or CXCR4 (107). In addition, R5 viruses which show the ability to use the alternate coreceptors Bonzo or CCR3 in transfected cells are unable to replicate in PBMC derived from ccr5Δ32 homozygous individuals, suggesting that expanded coreceptor use in transfected cells does not correlate with the ability to replicate in the relevant cell types (149, 202). An R5X4 virus which also shows the ability to use Bonzo for entry was unable to replicate efficiently in ccr5Δ32 PBMCs in the presence of a potent inhibitor of CXCR4 coreceptor activity (202). These results suggest that CCR5 and CXCR4 are the most important coreceptors *in vivo*. CCR5 is also used by virtually all known strains of viruses from the SIV_{smm}/HIV-2 family, and other SIV families. The strength of the *in vitro* coreceptor activity of Bonzo and BOB for some SIV strains suggest that these orphan receptors may also be important *in vivo* (107). Interestingly, CXCR4 use in non-human primates is rare (107).

In addition to the ccr5Δ32 mutation, other genetic factors related to coreceptor usage have been shown to alter the course of HIV-1 disease (173). A less common CCR5 null allele (CCR5-m303) has similar effects to the ccr5Δ32 allele (173). Heterozygosity for an allele of CCR2 with a single conservative amino acid change which has a similar frequency to ccr5Δ32 (CCR2-V64I) has been linked to a 2 to 4 year delay in disease progression in HIV-1 infected cohorts (173). CCR2 is not thought to be an important coreceptor *in vivo* and because CCR2 is closely linked to the CCR5 gene, it has been proposed that this allele is in linkage disequilibrium with a CCR5 mutation (173). The CCR5 coding region linked to the CCR2-V64I allele is wild-type, but CCR5 promoter mutations have been shown to be linked to this allele, although differences in the CCR5 expression levels due to these mutations have not yet been demonstrated (173). A mutation in the 3' untranslated region of the SDF-1 gene has been linked to a significant delay in the onset of AIDS (173). This mutation has been proposed to increase the levels of circulating SDF-1, which is the ligand for CXCR4 and can block X4 virus infection, but this effect has yet to be demonstrated (173). Taken together, the mounting genetic evidence underscores the importance of chemokine receptors in HIV-1 replication and suggests that coreceptor based therapies hold a great deal of promise for the treatment of HIV-1 infections.

Biology of CCR5

Chemokines and chemokine receptors. Chemokines are 70-100 amino acid proteins, and are typically classified as α- or β-chemokines based on the structural motif of the first two cysteines in the protein (136). These cysteines are separated by an intervening amino acid in α-chemokines, and are adjacent in β-chemokines (136). Chemokine receptors couple to heterotrimeric G-proteins (136). They have seven transmembrane domains, with the amino-terminal domain (NT) on the extracellular side of the membrane and the carboxyl-terminus (CT) on the intracellular side (see Fig 1-2) (136). This topology gives three each of extracellular and intracellular loops (ECLs and ICLs, respectively) (136). Many chemokine receptors are modified by N-linked glycosylation (136). Chemokine receptors have four conserved cysteines, one in each of the extracellular domains, which form two disulfide bonds (136). The NT is linked to ECL3, and ECL1 is disulfide bonded to ECL2 (136). There are nine known β-chemokine receptors (CCRs) and five known α-chemokine receptors (CXCRs) which have overlapping ligand specificities within their chemokine families (136). The overlapping ligand specificity may allow for some redundancy in the chemokine signaling pathways, which could explain why individuals homozygous for the ccr5Δ32 allele are healthy (136).

Molecular and cell biology of CCR5. CCR5 is a receptor for the chemokines MIP1α, MIP1β, and RANTES, which are involved in chemotaxis of T-cells and monocytes/macrophages to sites of inflammation (136). In addition to these cells, CCR5 is highly expressed in circulating dendritic cells (104). Expression levels of CCR5 have been determined in PBMC subsets by a quantitative FACS approach, and vary widely in different cell types and after treatment with different cytokines, with maximal expression of approximately 50,000 molecules/cell in differentiated macrophages and mature dendritic cells (104).

Human CCR5 is 352 amino acids in length and contains the four conserved cysteines described above (150, 157). These cysteines have been reported to be necessary for ligand binding, most likely because the disulfide bonds support the normal extracellular conformation of CCR5 (23). Mutation of the cysteines reduces, but does not fully eliminate HIV-1 coreceptor function suggesting that the conformation of the extracellular domains imparted by the disulfide bonds is also somewhat important for normal interaction with gp120 (23). CCR5 is not modified by N-linked glycosylation, however it is modified by O-linked glycosylation (62). The modified residues have not been elucidated, nor has any role of O-linked glycosylation in HIV-1 infection been demonstrated (62). CCR5 is also modified by tyrosine sulfation of four tyrosines: Y3, Y10, Y14, and Y15 in the NT region (62). Sulfation of these tyrosines is important for both ligand binding and HIV-1 coreceptor activity (62). An additional post-translational modification, which is discussed further below, is the phosphorylation of serines in the CT region, which occurs in response to activation by chemokine ligands (134).

Most signal transduction through chemokine receptors is mediated by heterotrimeric G-proteins (145). Chemokine receptors are thought to couple to G_i family members which results in activation of phospholipase Cβ2, generation of inositol trisphosphate, and calcium mobilization (145). Chemotaxis eventually results from rearrangements of the cytoskeleton, which are mediated by these effectors, and by activation of the small G-proteins Rac and Rho through pathways that have not yet been elucidated (145). The details of the events involved in chemotaxis are poorly understood and certain to be the focus of future research (145). In addition to chemotaxis, chemokines can also stimulate differentiation and proliferation under some conditions, and these effects are mediated through the MAP kinase pathways and initiated by an unidentified tyrosine kinase (145). The possibility of heterotrimeric G-protein signaling through chemokine receptors in response to HIV-1 binding has been investigated with varying results. It was initially reported that gp120s from R5 strains of HIV-1 could

mobilize calcium in some CD4+ cell types, including T-cells (191). However, other groups failed to see a calcium flux in T-cells, but did see activation of Pyk2, a tyrosine kinase downstream of calcium mobilization (47). A highly sensitive system which could detect G_i activation in *Xenopus* oocytes in response to chemokines failed to detect a response with gp120s, although a specific antagonism of chemokine signaling by gp120 was observed (112). This result suggests that signaling in response to HIV-1 binding is probably different from the normal response to chemokines (154). As yet the pathway and function of chemokine receptor mediated signal transduction in response to virus binding is unknown. CCR5 mutants which are deficient in heterotrimeric G-protein signaling are competent for infection (154).

In response to ligand binding and activation of heterotrimeric G-protein signaling, CCR5 is phosphorylated on four serine residues near the carboxyl-terminus: S336, S337, S342, and S349 (134). This phosphorylation is thought to be mediated by G-protein coupled receptor kinases (GRKs) (134, 136). GRK2 and GRK3 are expressed in T-cells and monocytes and phosphorylate CCR5 when the GRKs are overexpressed in cultured cells, and thus are thought to mediate the phosphorylation of CCR5 *in vivo* (134). Phosphorylation results in endocytosis of CCR5 to an early endosomal compartment, an effect most likely mediated by non-visual arrestins and clathrin coated vesicles (134, 136). After removal of the ligand, CCR5 is recycled to the cell surface (136). The ability of an agonist to stimulate CCR5 endocytosis correlates with the potency of the agonist (134, 136). Interestingly, an amino-terminal modified aminooxypentane derivative of RANTES (AOP-RANTES) is a very potent agonist and induces endocytosis of CCR5, but appears to inhibit recycling of the endocytosed receptor (134, 136). AOP-RANTES is also the most effective chemokine derivative for the inhibition of R5 HIV-1 infection, suggesting that endocytosis is important for the chemokine mediated blockade of HIV-1 infection (134, 136). Indeed, CCR5 lacking the CT domain fails to undergo ligand induced endocytosis, and HIV-1 infection mediated by this receptor is poorly inhibited by

chemokines (136). Thus, chemokines may impair HIV-1 infection primarily through decreased surface expression of the coreceptors, whereas small molecules which act as CXCR4 and CCR5 antagonists may directly block the interaction of HIV-1 virions with the coreceptor (8, 136).

Potential of coreceptor based therapies. As mentioned above, the importance of CCR5 in AIDS has been underscored by the discovery of a null allele, ccr5Δ32, which confers near total resistance to HIV-1 infection (48, 83, 108, 158). Persons heterozygous for the ccr5Δ32 allele have reduced expression of CCR5 on T-cell surfaces, and a statistically significant delayed onset of AIDS after HIV-1 infection by 2 to 4 years (48, 83, 108, 158). A few exceptional cases of transmission of HIV-1 to ccr5Δ32 homozygotes have been reported, and the viruses in these individuals have an X4 tropism (173). These results suggest that there might be limits to the replication of X4 viruses in newly infected individuals, possibly the absence of susceptible target cells at typical sites of infection, or an increased susceptibility of these viruses to inactivation by the immune system (17). Lack of CCR5 expression in ccr5Δ32 homozygotes does not have any known negative effects (48, 83, 108, 158). CXCR4 knock-out mice, in contrast, do not survive to birth due to defects in development (109). It is not certain that inhibition of CXCR4 function in adults would have negative effects, or that inhibition of CCR5 function in adults which have developed with normal CCR5 would not. However, based on current knowledge, CCR5 is the most attractive target for coreceptor based chemotheraputic intervention in HIV-1 infected people. Assuming effective agents can be found, inhibition of CCR5 dependent replication may not be sufficient to block HIV-1 replication, and targeting CCR5 may drive the virus to adapt to alternative coreceptors, or drive the emergence of highly pathogenic X4 viruses sooner than normal (202). These issues have yet to be thoroughly addressed. One possible route that might be effective are chemokine derivatives, such as the highly effective AOP-RANTES (see above), however bioavailability and unwanted signaling through CCR5 may hamper their use.

However, a small molecule antagonist of CCR5 which has potent anti-HIV-1 activity has been reported, and should aid understanding of the potential of a small molecule approach (8).

Figures

Figure 1-1. Primary structure of HIV-1 gp120 from the prototype IIIB strain.

The amino acid sequence of IIIB gp120 is depicted in schematic form. Disulfide bonds are represented by solid lines connecting cysteine residues. Asparagines which are modified by N-linked glycosylation are marked with asterisks. The hypervariable regions discussed in the text are boxed. Figure was adapted from Leonard *et al* (105).

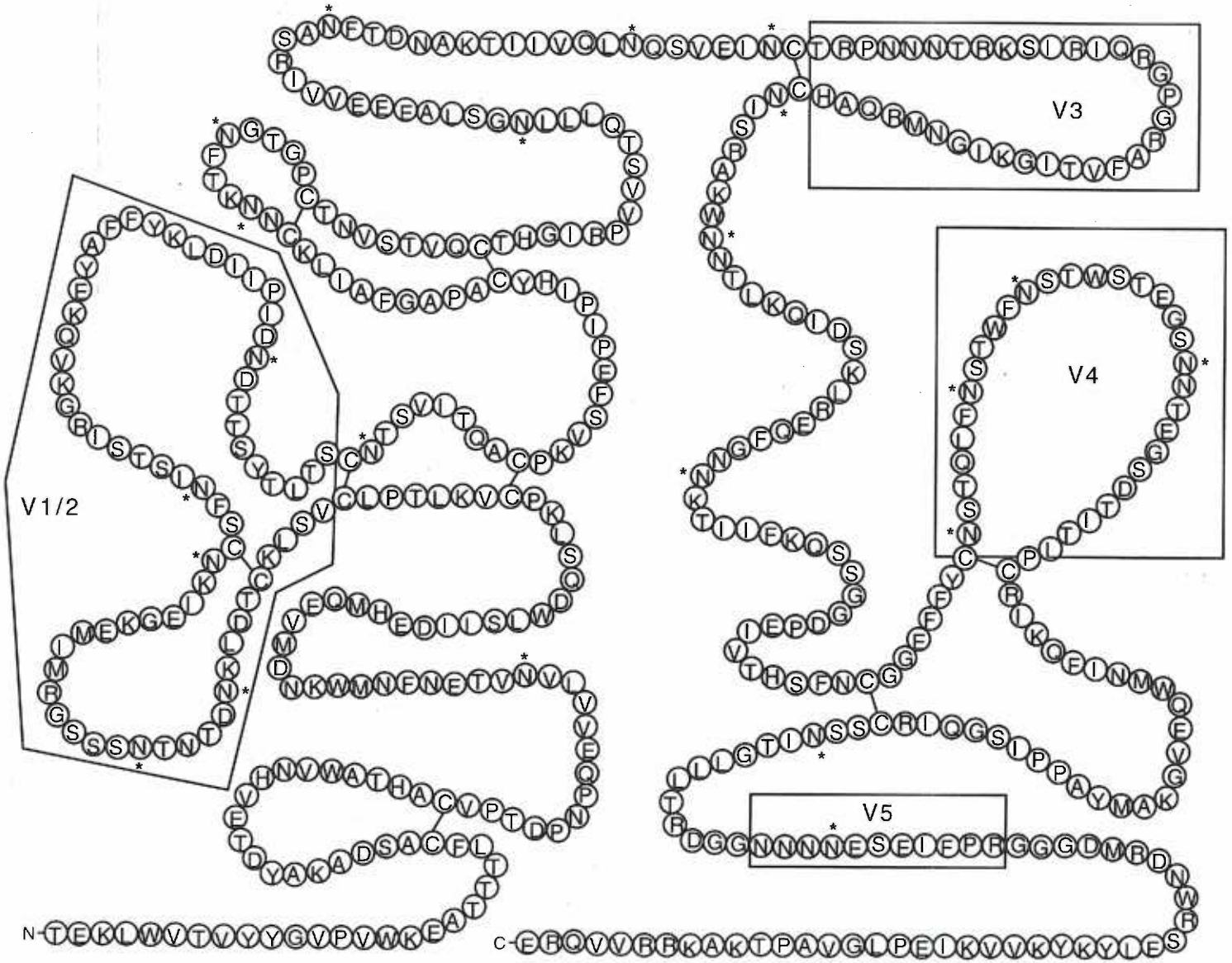
V1/2
V3
V4
V5
N
C

Figure 1-2. Primary structure of human CCR5.

The putative transmembrane topology of human CCR5 is depicted in schematic form. The four extracellular domains are denoted using the terminology from the text (NT=amino terminus, ECL=extracellular loop). The disulfide bond between ECL1 and ECL2 is depicted by a solid line connecting the two cysteines. The cysteines in the NT and ECL3 domains which form the other disulfide bond described in the text are also marked with solid lines; however, they are not connected in the figure for clarity. The tyrosines in the NT domain which are modified by sulfation (see text) are shaded.

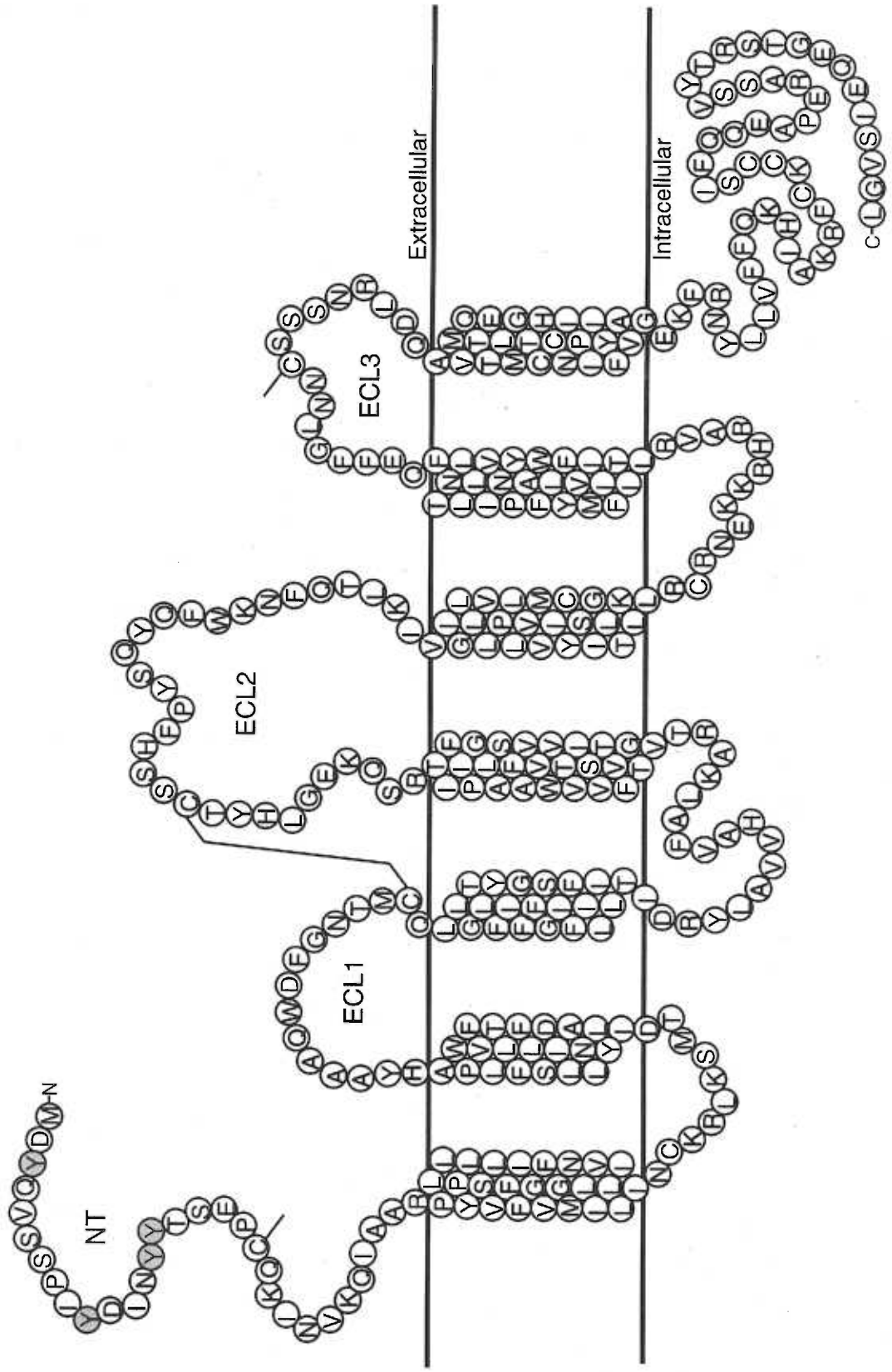
Extracellular
Intracellular
NT
ECL1
ECL2
ECL3
N
C

Chapter 2. Polymorphisms in the CCR5 Genes of African Green Monkeys and Mice Implicate Specific Amino Acids in Infections by Simian and Human Immunodeficiency Viruses

Shawn E. Kuhmann, Emily J. Platt, Susan L. Kozak, and David Kabat*

Running Title: Active Sites in the CCR5 Coreceptor

*With whom to correspond:

Department of Biochemistry and Molecular Biology

Oregon Health Sciences University

Portland, Oregon 97201-3098

Tel: (503) 494-8442

Fax: (503) 494-8393

Abstract

CCR5, a receptor for the CC-chemokines RANTES, MIP1α, and MIP1β, has been identified as a coreceptor for infections by macrophage-tropic isolates of human immunodeficiency virus type 1 (HIV-1). To study its structure and function, we isolated cDNA clones of human, African green monkey (AGM), and NIH/Swiss mouse CCR5, and we quantitatively analyzed infections by macrophage-tropic HIV-1 and SIV_{mac251} after transfecting human HeLa-CD4 cells with the CCR5 expression vectors. The AGM and NIH/Swiss mouse CCR5 proteins are 97.7% to 98.3% and 79.8% identical to the human protein, respectively. In addition, we analyzed site-directed mutants and chimeras of these CCR5s. Cell surface expression of CCR5 proteins was monitored using a specific rabbit antiserum and by binding the chemokine [^{125}I]MIP1β. Our major results were as follows: (i) Two distinct AGM CCR5 sequences were reproducibly found in DNA from CV-1 cells. The AGM(Y14N,L352F) CCR5 protein differs from the wild-type AGM CCR5 by two substitutions, Y14N in the amino terminal extracellular region and L352F at the carboxyl terminus. Interestingly, AGM(Y14N,L352F) CCR5 was inactive as a coreceptor for all tested macrophage-tropic isolates of HIV-1, whereas wild-type AGM CCR5 was active. As shown by chimera studies and site directed mutagenesis, the Y14N substitution in AGM(Y14N,L352F) CCR5 was solely responsible for blocking HIV-1 infections. In contrast, both AGM CCR5s were active coreceptors for SIV_{mac251}. Studies of DNA samples from other AGMs indicated frequent additional CCR5 polymorphisms, and we cloned an AGM CCR5 variant with a Q93R substitution in the extracellular loop 1 from one heterozygote. This variant CCR5 was active as a coreceptor for SIV_{mac251}, but was only weakly active for macrophage-tropic isolates of HIV-1. In addition, SIV_{mac251} appeared to be dependent on the extracellular amino terminus and loop 2 regions of human CCR5 for maximal infection. Our results suggest major differences in the interactions of SIV_{mac251} and macrophage-tropic HIV-1 isolates with I9, N13, and Y14 in the amino terminus, with Q93 in extracellular loop 1, and with extracellular loop 2 of

human CCR5. (ii) The NIH/Swiss mouse CCR5 protein differs at multiple positions from sequences recently reported for other inbred strains of mice. This CCR5 was inactive as a coreceptor for HIV-1 and SIV_{mac251}. Studies of chimeras that contained different portions of NIH/Swiss mouse CCR5 substituted into human CCR5, as well as the reciprocal chimeras, indicated that the amino terminal region and extracellular loops 1 and 2 of human CCR5 contribute to its coreceptor activity for macrophage-tropic isolates of HIV-1. Specific differences with previous CCR5 chimera results occurred because the NIH/Swiss mouse CCR5 contains a unique substitution corresponding to P183L in extracellular loop 2 that is nonpermissive for coreceptor activity. We conclude that diverse CCR5 sequences occur in AGMs and mice, that SIV_{mac251} and macrophage-tropic HIV-1 isolates interact differently with specific CCR5 amino acids, and that multiple regions of human CCR5 contribute to its coreceptor functions. In addition, we have identified naturally occurring amino acid polymorphisms in three extracellular regions of CCR5 (Y14N, Q93R, and P183L) that do not interfere with cell surface expression or MIP1β binding, but prevent infections by macrophage-tropic isolates of HIV-1. In contrast to previous evidence, these results suggest that CCR5 contains critical sites that are essential for HIV-1 infections.

reference proteins used in the chimera constructions were able to contribute to the coreceptor activities that were observed. To address these issues, we isolated CCR5 cDNAs from human, AGM, and NIH/Swiss mouse cells and we quantitatively analyzed their coreceptor activities in infections of human HeLa-CD4 cells by macrophage-tropic isolates of HIV-1 and by the simian immunodeficiency virus SIV_{mac251}. In addition, we analyzed coreceptor activities and cell surface expression levels of CCR5 site-directed mutants and interspecies chimeras. We found a surprising diversity of CCR5 sequences in DNA samples from different AGMs. Studies of these CCR5 clones suggested that SIV_{mac251} interacts differently than all tested macrophage-tropic HIV-1 isolates with position 14 in the amino terminus of CCR5, with position 93 in extracellular loop 1, and with extracellular loop 2. Our chimera results differ in several respects from independent studies (6, 21, 139, 155), in part because the NIH/Swiss mouse CCR5 contains a unique amino acid substitution in extracellular loop 2 that is nonpermissive for HIV-1 infections. We have identified amino acids in three extracellular regions of CCR5 that appear to be critical for HIV-1 coreceptor function.

Materials and Methods

Cells and viruses. HeLa and HeLa-CD4 cells (clone HI-J) were described previously (90). AGM cell lines CV-1, BS-C-1, Vero, and COS-7 as well as NIH/Swiss mouse NIH/3T3 fibroblasts were from the American Type Culture Collection (ATCC, Rockville, MD). HeLa, HeLa-CD4, CV-1, and NIH/3T3 cells were maintained in Dulbecco's modified Eagle medium (DMEM) with 10% fetal bovine serum (FBS). COS-7 cells were maintained in the same medium supplemented with glucose (4.5 g/L). BS-C-1 and Vero cells were maintained in minimum essential medium with 10% FBS and 0.1 mM MEM non-essential amino acids (Life Technologies, Inc., Grand Island, NY). The macrophage-tropic SF162, JR-FL, ADA, and Ba-L isolates of HIV-1 were obtained from the AIDS Research and Reference Reagent Program, Division of AIDS, NIAID, NIH: contributed by Dr. Jay Levy, by Dr. Irvin Chen, by Dr. Howard Gendelman, and by Drs. Suzanne Gartner, Mikulas Popovic, and Robert Gallo, respectively. HIV-1 viruses were passaged in phytohemagglutinin-stimulated human peripheral blood mononuclear cells (PBMCs). The medium was harvested at times of peak reverse transcriptase release, passed through a 0.45 μm pore size filter, aliquoted, and stored at -80°C. SIV_{mac251}, which was generously donated by Dr. Jay Nelson, was propagated in CEMX174 cells and was titered in sMAGI cells as described previously (32).

PCR cloning of CCR5 genes from human, AGM, and NIH/Swiss mouse cells. All custom oligonucleotides were synthesized by Oligos, etc. (Stamford, CT), and all restriction enzymes were obtained from New England Biolabs (Beverly, MA). Genomic DNA from human HeLa, AGM cell lines CV-1, BS-C-1, and Vero, and NIH/Swiss mouse NIH/3T3 cells was prepared as described (7). In addition, genomic DNA was prepared from the liver, spleen, and kidneys of a C57BL/6 mouse by standard methods (7). Two DNA samples, one from a vervet AGM and the other from a sabaeus AGM, were generously donated by Dr. Jon Allan (Department of Virology and Immunology,

Southwest Foundation for Biomedical Research, San Antonio, TX). Polymerase Chain Reaction (PCR) was performed with cloned Pfu polymerase (Stratagene, La Jolla, CA) according to the manufacturer's instructions. Reactions were performed in a 100 µl volume containing 1 x cloned Pfu buffer, 0.1 mM each dNTP, 0.5 to 1.5 µg genomic DNA, 50 pmol each of forward and reverse primer, and 5 U cloned Pfu polymerase. Thermal cycling was performed by heating to 94°C for 45 s, followed by 25 cycles of 94°C for 45 s, 55°C for 45 s, and 72°C for 2 min 30 s, followed by a final extension step of 72°C for 10 min. The primers used for human and AGM CV-1 DNA were forward: CKR5/5' (5' GGGGATCCGGTGGAACAAGATGGAT 3') and reverse: CKR5/3' (5' CCCTCGAGCCACTTGAGTCCGTGTCACA 3'). The primers used for NIH/Swiss and C57BL/6 mouse DNA were forward: MC5/5' (5' CCGGATCCCAGGATGGATTTTCAAGGG 3') and reverse: MC5/3' (5' GGCGCTCGAGTCAACCAGGTCATAAACCAGT 3'). Design of the primers was based on the reported sequences of human and mouse CCR5 (26, 150). The primers overlap the presumed start and stop codons of these genes (underlined). The ~1.1 kbp specific amplification products were subcloned into pBluescriptII(KS+) (Stratagene) using the *Bam* HI and *Xho* I restriction sites engineered into the primers, and in the plasmid multiple cloning site. The inserts were sequenced by fluorescent DNA sequence determination which was performed by the MMI Core Facility on the PE/ABD 377 DNA Sequencer using dye-terminator cycle sequencing chemistry (PE Applied Biosystems, Foster City, CA). Primers for sequencing were: M13 universal (-20) and M13 reverse primers (United States Biochemical Corporation, Cleveland, OH) which anneal to the vector 5' and 3' of the insert respectively, and the internal primers CKR1 (5' TCATCATCCTCCTGACAATCG 3') for human and AGM CV-1 clones, and CKR2 (5' CTTCTTCATTATCCTCCTGAC 3') for NIH/Swiss mouse. The human sequence agreed with the reported sequence (150). Although the NIH/Swiss mouse sequence differed from the reported mouse sequences (21, 26, 120), sequencing of multiple PCR

products confirmed that our sequence was correct. The sequence of the C57BL/6 mouse CCR5 differed from the reported sequence for strain 129/SvJ at one nucleotide resulting in a coding change at the equivalent of human codon 206. The reported sequence has Ser at this position (26), whereas our newly cloned sequence codes for Pro. Since this residue is Pro in the human, AGM, and NIH/Swiss mouse CCR5s, and since this change lies outside the extracellular loop 2 region which was of interest for this study, we used the cloned sequence in our study. Two different sequences of AGM CCR5 were obtained. These differ from each other in 3 nucleotides, two of which result in coding changes: AGM(Y14N,L352F) has an Asn residue at position 14, whereas wild-type AGM has a Tyr, and AGM(Y14N,L352F) has a Phe at position 352, whereas wild-type has Leu. Both sequences were isolated from multiple PCR reactions, suggesting that both are present in the genomic DNA of CV-1 cells. The *Bam* HI to *Xho* I fragments were then subcloned into pcDNA3 (Invitrogen Corp., San Diego, CA) cut with the same enzymes.

The primers used for vervet AGM, sabaeus AGM, BS-C-1, and Vero DNA were forward: AGMF (5' GGGTGGAACAAGATGGATTATC 3') and reverse: AGMR (5' ACTGTATGGAAAATGAGAGCTGC 3'). The 567 bp PCR products were sequenced directly using the AGMF primer. The 567 bp PCR product from the sabaeus AGM was digested with *Cla* I and subcloned into the same sites of the wild-type AGM expression vector to give the AGM(Q93R) expression construct.

Construction of chimeric and mutant CCR5. The human/mouse chimeras, MMHH, HMMM, MHMM, MMHM, MMMH, HHMM, MHHH, HMHH, HHMH and HHHM were created using conserved sites for the restriction endonucleases *Msc* I, *Bgl* II, and *Eco* RI (see Figs 2-1 and 2-2). They were constructed in pBluescriptII(KS+) except HHHM, which was constructed in pcDNA3. The human or NIH/Swiss mouse *Bgl* II to *Bsa* BI fragments, containing the CCR5 second extracellular loop, were cloned into the wild type human CCR5, wild type mouse CCR5 or HMMM chimera to produce

HHHHloop2M, MMMMloop2H, and HMMMloop2H. The HHHHloop2M(L183P) CCR5 was made by subcloning the *Bgl* II to *Bsa* BI fragment from C57BL/6 mouse CCR5 into the same sites in the human CCR5 cDNA. In the extracellular loop 2 region, NIH/Swiss and C57BL/6 mouse CCR5s differ only at the equivalent of codon 183 in human CCR5; thus this construct differs from HHHHloop2M by the change of codon 183 from Leu to Pro.

The AGM/human chimeras were constructed in pBluescriptII(KS+) using the conserved *Bgl* II site. Both plasmids were digested with either *Bgl* II and *Bam* HI or *Bgl* II and *Xho* I. The fragments from AGM(Y14N,L352F) CCR5 were then ligated into the vector containing human CCR5 digested with the same enzymes. A chimera was constructed using the amino terminal half of AGM(Y14N,L352F) CCR5 and the carboxyl terminal half of wild-type AGM CCR5. The result is a CCR5 which is identical to wild-type AGM except for the Y14N mutation in the amino terminal extracellular region. This chimera is referred to as AGM(Y14N). All CCR5 chimeras constructed in pBluescriptII(KS+) were excised with *Bam* HI and *Xho* I and subcloned into the pcDNA3 expression vector.

Site directed mutagenesis was performed with the Chameleon™ double-stranded site-directed mutagenesis kit (Stratagene) according to the manufacturer's instructions. The mutagenesis was performed on AGM or human CCR5 in pBluescriptII(KS+) using the mutagenic primers T9I (5' GTCAAGTCCAA<u>T</u>CTATGACATCG 3'), D13N (5' CCAACCTATGACATC<u>A</u>ATTATTATACATCGGAGCC 3'), and Y14N (5' CCAATCTATGACATCAAT<u>A</u>ATTATACATCGGAGCCC 3'). The T9I mutagenic primer introduces a C to T mutation (underlined) which mutates codon 9 of the AGM clone 2 CCR5 from Thr (ACC) to Ile (ATC). Likewise, the D13N primer mutates codon 13 of AGM clone 2 CCR5 from Asp (GAT) to Asn (AAT), and the Y14N primer mutates codon 14 of human CCR5 from Tyr (TAT) to Asn (AAT). The mutations were

confirmed by sequencing, and the mutated CCR5s were then excised with *Bam* HI and *Xho* I and ligated into pcDNA3 cut with the same enzymes.

Assay for coreceptor function. Coreceptors were transiently expressed in HeLa-CD4 (clone HI-J) cells by the calcium phosphate transfection method (7) using 20 μg pcDNA3-CCR5 plasmid DNA per 25 cm^2 flask seeded 24 h previously with $5x10^5$ cells. 48 h post-transfection the cultures were trypsinized and plated at $1.5x10^4$ to $2x10^4$ cells per 2 cm^2 well of a 24 well cluster plate for HIV-1 infection. Infectivities by macrophage tropic HIV-1 isolates were determined by the focal infectivity assay as described previously (96). Briefly, 72 h post-transfection cells were pre-treated with DEAE-dextran (8 μg/ml) in serum free DMEM at 37°C for 20 min. The cells were washed with serum free DMEM, then incubated with 0.2 ml of virus diluted in DMEM + 0.1% FBS at 37°C. After 2 h the cells were fed with 1 ml DMEM + 10% FBS and incubated at 37°C for 3 days. The cells were then fixed in ethanol and infected foci were visualized by an immunoperoxidase assay (37). For this purpose, the 0.45 μm filtered supernatant from the anti-p24 hybridoma 183-H12-5C (AIDS Research and Reference Reagent Program, Division of AIDS, NIAID, NIH: contributed by Dr. Bruce Chesebro and Dr. Hardy Chen) was used at 1:5 dilution. Staining of cells infected with SIV_{mac251} was done using a monoclonal antibody to the viral p27 protein that was generously donated by Dr. Jay Nelson and was purchased from Immunodiagnostics (Boston, MA). The cells were then sequentially incubated with 1:400 peroxidase conjugated goat anti-mouse IgG serum (Organon Teknika Corp., Durham, NC), and a substrate solution of 3-amino-9-ethyl-carbazole (Sigma, St. Louis, MO).

Anti-CCR5 antibody production. A synthetic peptide corresponding to the amino terminal 26 amino acids of human CCR5 (NH_4^+-MDYQVSSPIYDINYYTSEPCQKINVK-CO_2^-) (Microchemical Facility, Emory University, Atlanta, GA) was coupled to soluble keyhole limpet hemocyanin (KLH) (Sigma) via the free Cys residue using *m*-maleimidobenzoyl-N-hydroxysuccinimide ester

(Sigma) by standard methods (77). It was determined that 4.2 mg of peptide was coupled to 5 mg of KLH to give an estimate of ~108 peptides coupled per Mr~400,000 KLH monomer. 460 μg KLH-peptide conjugate was injected per rabbit per injection. Rabbits were initially injected with the coupled peptide in 50% complete Freund's adjuvant (Life Technologies Inc.), then boosted 14 days later with the conjugate in 50% incomplete Freund's adjuvant (Life Technologies Inc.). Subsequent boosts were ~28 days apart and in phosphate buffered saline (PBS) [0.14 M NaCl, 8 mM $Na_2HPO_4 \cdot 7H_2O$, 1.5 mM KH_2PO_4, 2.6 mM KCl] only. Test bleeds were taken, and serum prepared, 12-14 days after each boost. After the second boost, the serum of one of three rabbits was positive as demonstrated by Western immunoblotting of COS-7 cell membranes expressing human CCR5. The bleed following the third boost was used in this project.

Membrane isolation and Western immunoblotting. Total cellular membranes were isolated from ~$1x10^6$ COS-7 cells 48 h after being transfected (using the DEAE-Dextran method (7)) with pcDNA3 (mock) or pcDNA3-CCR5 DNA constructs. Monolayer cells were washed twice with PBS and scraped into 10 ml PBS. The cells were pelleted at 150xg for 5 min and resuspended in 4 ml swelling buffer [20 mM Hepes pH 7.2, 5 mM KCl, 1 mM $MgCl_2$, 1 mM phenylmethylsulfonyl fluoride (Sigma) added fresh] and swelled on ice for 10 min. Cells were homogenized in a dounce homogenizer to ~90% breakage. Nuclei were pelleted at 250xg for 10 min. The membranes were pelleted from the supernatant at ~27000xg for 15 min (20 krpm in Beckman Type 70.1 Ti rotor) and stored at -20°C. The solubilized membrane proteins were separated by 10% SDS-PAGE as described (7) and transferred to NitroPure nitrocellulose membranes (Micron Separations, Inc., Westboro, MA). Membranes were sequentially incubated with the anti-CCR5 serum, used at a 1:250 dilution, and then with protein A-HRP conjugate (Bio-Rad) at 1:10,000 dilution. Membranes were washed and HRP was visualized with chemiluminescence reagents (Dupont NEN Research Products, Boston MA) used according to the manufacturer's instructions.

Cell surface expression of CCR5s. Cells were plated in 4 well chamber slides (Nunc, Inc., Naperville, IL) 24 h prior to assaying for CCR5 expression by immunofluorescence. Viable cells were incubated with anti-CCR5 serum diluted at 1:25 to 1:50 in complete medium (DMEM + 10% FBS) for 1 h at 37°C. After washing with complete medium, the cells were incubated for 1 h at 37 °C with FITC-conjugated affinity purified antibody to rabbit IgG (Organon Teknika Corp., West Chester, PA) diluted at 1:100 in complete medium. Cells were then washed in complete medium, rinsed with PBS, fixed with cold methanol for 5 min, mounted over drops of 50% glycerol in PBS, and slides were viewed by fluorescence microscopy. A similar procedure was used to measure relative quantities of CCR5 antibody bound to the cells, except that the cells were incubated in 0.2 ml complete medium with [^{125}I]protein A (0.4 μCi/ml, 2 to 10 μCi/μg; DuPont NEN Research Products) instead of the FITC conjugated secondary antibody and the cells were plated in 24 well cluster plates. The cells were washed, solubilized in 0.1 N NaOH, counted in a gamma counter and the protein concentrations determined by the Coomassie dye method (Bio-Rad Laboratories). In addition, expression of CCR5 proteins on cell surfaces was analyzed by binding 0.5 nM [^{125}I]MIP1β (2200 Ci/mmol, DuPont NEN Research Products) for 2 h at 37°C. The cells were washed, solubilized, counted and protein levels determined as described above. Table 2-1 summarizes the abbreviations, structures, and evidence for cell surface expression of CCR5 proteins used in this investigation. As discussed below, several additional CCR5 proteins were analyzed and appeared to be negative for cell surface expression and for coreceptor activity [HHMM, HHHM, MHMM, MHMMloop2H, and MHMM(L183P). They are not shown in Table 2-1 because they were not informative.

Nucleotide sequence accession numbers. The GenBank accession numbers for the AGM(Y14N,L352F), AGM clone 2, human, NIH/Swiss mouse, and C57BL/6 mouse CCR5 nucleotide sequences are U83324, U83325, U83326, U83327, and AF022990 respectively.

Results

Structures of human, AGM, and NIH/Swiss mouse CCR5s and construction of their chimeras and site-directed mutants. Because the CCR5 DNA coding sequence lacks introns (150), we were able to isolate these sequences by a DNA-PCR method (see Materials and Methods). Fig 2-1 shows a comparison of the amino acid sequences of human, AGM, and NIH/Swiss mouse CCR5 proteins. Two AGM CCR5 sequences were reproducibly isolated from the DNA of CV-1 cells. The AGM and mouse CCR5 sequences are 97.7% to 98.3% and 79.8% identical to the human sequence, respectively. The AGM(Y14N,L352F) sequence differs from the wild-type AGM sequence by only two substitutions, Y14N that creates an NYT consensus site for potential asparagine-linked glycosylation and L352F at the carboxyl terminus. The NIH/Swiss mouse CCR5 amino acid sequence differs at multiple positions from recently described sequences isolated from 129/SvJ (26), B6CBA (120), and Balb/c (21) strains of mice. These four mouse CCR5 sequences differ from each other at a total of 14 positions, and all contain a two amino acid insertion in the amino terminus compared to human CCR5 (all amino acid numbering in this chapter is for the human CCR5). Fig 2-1 also indicates the locations of the 7 presumptive transmembrane sequences A-G. Fig 2-2 shows a topological model of human CCR5 that highlights the positions of amino acids that differ among the human, AGM, and mouse proteins. It is important to note that extracellular loop 3 is identical in these CCR5s; thus our studies were not informative about the potential role of this region in coreceptor function. In addition, this model shows the locations in the coding region of the *Msc* I, *Bgl* II, and *Eco* RI restriction enzyme cleavage sites in the DNA sequences that were used to construct most of the interspecies CCR5 chimeras, as well as the *Bsa* BI site that was used to construct additional chimeras (see below).

It was unclear from the above results whether the diversity of AGM CCR5 sequences was unique to CV-1 cells. To address this issue, two DNA samples were

analyzed that had been prepared from PBMCs of different AGMs. Investigation of a vervet AGM DNA suggested that this monkey was heterozygous for a D13N substitution in the wild-type AGM CCR5 sequence. Similarly, sequence analysis of the DNA sample from a sabaeus AGM suggested heterozygosity for a Q93R substitution in the wild-type AGM sequence (see Fig 2-3A). In this case the mutation generated a novel *Nci* I restriction enzyme cleavage site in the CCR5 gene. Reproducibly, PCR amplification of CCR5 sequences from this DNA revealed the presence of this *Nci* I site in the product (see Fig 2-3B). A *Cla* I fragment from the PCR product encoding this Q93R substitution was cloned and used to prepare a pcDNA3-AGM(Q93R) expression vector for functional analysis (see below). Southern blot studies of AGM DNA samples suggested the presence of a single CCR5 gene with multiple alleles and the absence of a CCR5 pseudogene (results not shown). Based on these results, we examined portions of the CCR5 sequences amplified from the AGM cell lines Vero and BS-C-1. Analysis of the Vero DNA sequence was consistent with homozygosity for the wild-type AGM allele. In contrast, analysis of the BS-C-1 DNA from a grivet AGM (161) suggested heterozygosity for an AGM(Q93K) allele (see appendix A). Thus, among five AGM DNA samples that we have examined, four appeared to have derived from heterozygotes with variant CCR5 alleles.

Studies of human CCR5 structure and expression using a rabbit antiserum specific for the amino terminal extracellular sequence. The antiserum made to the amino terminal hydrophilic region of human CCR5 (amino acids 1-26) showed a strong specific reactivity with surfaces of viable HeLa-CD4 cells that stably express human CCR5 (see Fig 2-4). The background immunofluorescence was negligible for control HeLa cells or for cells incubated with preimmune serum rather than antiserum. The patching of CCR5 seen in Fig 2-4 occurred when the antibody bound to the surfaces of viable cells at 37°C, whereas uniform immunofluorescence occurred when the cells were fixed with 3.7% paraformaldehyde prior to addition of the antiserum (results not shown). This suggests

that CCR5 is able to diffuse in the cell surface membrane. Although this antiserum did not react with cells that expressed NIH/Swiss mouse CCR5, substantial immunofluorescence was observed with cells that expressed AGM CCR5. In addition, strong specific radioactive labeling with very low backgrounds occurred when [^{125}I]protein A was incubated with the cells instead of the FITC-conjugated secondary antibody (see Table 2-1).

The rabbit antiserum was also active in Western immunoblotting as seen by specific reactivity with a Mr~40,000 protein that occurred in membranes from COS-7 cells that had been transfected with pcDNA3-CCR5, but not in membranes from mock transfected cells (see Fig 2-5). A strong specific component of this size was also seen when we used membranes from HeLa-CD4/CCR5 cells that stably synthesize human CCR5 or membranes from *Xenopus laevis* oocytes that had been injected with a synthetic mRNA that encodes CCR5 (results not shown). The size of human CCR5 as revealed by our antiserum to the native receptor appears to be compatible with a previous study that used epitope-tagged CCR5 (155). Also in agreement with the latter study, we found that the native human CCR5 protein lacks asparagine-linked oligosaccharides susceptible to cleavage with peptide-N-glycosidase F.

Coreceptor activities of human, AGM, and NIH/Swiss mouse CCR5 proteins for SIV_{mac251} and macrophage-tropic isolates of HIV-1. The coreceptor activities and cell surface expression levels of the human, AGM and AGM(Y14N,L352F), and mouse CCR5 proteins were assayed after transient transfection of HeLa-CD4 cells (clone HI-J) with the pcDNA3-CCR5 expression vectors (Fig 2-6). Cultures were infected with either SIV_{mac251} or macrophage-tropic HIV-1, and the foci of infected cells were stained 48-72 hours later using antibodies to viral proteins and peroxidase conjugated secondary antibodies (37). Because no foci occurred in the absence of exogenous CCR5 expression, we could distinguish between low level activity and inactivity of any CCR5 protein with a high degree of confidence. This is an advantage compared to nonfocal or syncytial

assays that have been used to study coreceptors. Moreover, we believe that this assay method is as reproducible as other quantitative methods that require transient transfection of cells. In five independent transfection and infection assays using the expression vector for human CCR5, the foci/well seen with the HIV-1 isolates SF162, JR-FL, Ba-L, and ADA had standard deviations of 16.6%, 32.5%, 10.4%, and 23.7% respectively. Generally the titers observed in our transient transfection assays (c.a. 500-1000 foci/well for cells expressing human CCR5) were approximately 10% as large as the total virus titers assayed in HeLa-CD4/CCR5 cells that stably express CCR5 in all of the cells. This corresponded approximately with our efficiencies of transient transfection (see Table 2-1). Moreover, the titers measured in our clones of HeLa-CD4/CCR5 cells were as large as the tissue culture infectious doses measured in cultures of human PBMCs (144).

As shown in Fig 2-6B, the SIV_{mac251} virus was highly infectious for HeLa-CD4 cells that had been transfected with expression vectors for human, AGM, and AGM(Y14N,L352F) CCR5s, but was noninfectious for cells that expressed NIH/Swiss mouse CCR5. Infectivity for cells that expressed AGM(Y14N,L352F) was approximately three-fold lower than for cells expressing AGM CCR5 and this difference was highly significant as indicated by the paired-comparison t-test ($P \leq 0.001$; N=4). In contrast to SIV_{mac251}, all of the macrophage-tropic HIV-1 isolates that we tested were infectious for cells that expressed human or wild-type AGM CCR5, but were completely non-infectious for cells that expressed AGM(Y14N,L352F) CCR5. This was verified in four independent assays, each using four different isolates of macrophage-tropic HIV-1 (i.e., SF162, JR-FL, Ba-L and ADA), and was further substantiated by the experiments described below. Thus, the SIV_{mac251} and HIV-1 viruses were differently affected by the amino acid substitutions that distinguish the AGM(Y14N,L352F) and wild-type AGM CCR5 proteins. Studies were also done using the AGM(Q93R) CCR5 variant that was cloned from a sabaeus AGM DNA sample. This CCR5 was highly expressed on cell surfaces as determined by immunoassays and by binding of [^{125}I]MIP1β (see Table 2-1).

As shown in Fig 2-6, it was almost completely inactive as a coreceptor for macrophage-tropic isolates of HIV-1, but was highly active for SIV_{mac251}. Specifically, in six independent assays, the titers of the SF162, JR-FL, Ba-L and ADA HIV-1 isolates were reduced by 88.2±2.2% for cells with the Q93R variant compared with the wild-type AGM CCR5 protein. In contrast, in four independent assays, the Q93R variant was 110±18% as active as wild-type AGM for infections by SIV_{mac251}. Interestingly, the AGM and AGM(Q93R) CCR5s were as active as human CCR5 for SIV_{mac251} infections. In contrast, AGM clone 2 CCR5 was much less active (c.a., 20%) than human CCR5 for infections by HIV-1 ($P<0.001$; N=22). Thus, AGM clone 2 CCR5 is only partially active as a coreceptor for HIV-1.

Coreceptor activities of human and AGM CCR5s analyzed using chimeras and site-directed mutants. To learn which of the amino acid substitutions in AGM(Y14N,L352F) CCR5 are responsible for its inability to mediate infections by macrophage-tropic isolates of HIV-1, we analyzed human/AGM CCR5 chimeras for their coreceptor activities in HIV-1 infections. As shown in Fig 2-7, the AGM(Y14N)/human CCR5 chimera with the AGM(Y14N,L352F) amino terminus was inactive in HIV-1 infections, whereas the reciprocal human/AGM(L352F) chimera was fully active. This suggested that the Y14N substitution was fully responsible for the lack of HIV-1 coreceptor activity of AGM(Y14N,L352F) CCR5 and that the L352F substitution had no significant effect. This conclusion was substantiated by studies of the human(Y14N) CCR5 mutant and the AGM(Y14N) CCR5 mutant. In both cases, the single Y14N mutations eliminated coreceptor activity for macrophage-tropic isolates of HIV-1 (see Fig 2-7). Thus, the Y14N mutations eliminated coreceptor activity for macrophage-tropic isolates of HIV-1 not only in the context of AGM CCR5, but also in the context of human CCR5. In addition, the AGM(Q93R) variant CCR5 was almost completely inactive as a coreceptor for all tested isolates of HIV-1 (see Fig 2-6). As described in Table 2-1, all of the CCR5s analyzed in Figs 2-6 and 2-7 were well expressed on cell surfaces as indicated

by three assay methods. These results suggest that different macrophage-tropic isolates of HIV-1 are highly dependent on amino acids at positions 14 and 93 of CCR5. In contrast, SIV_{mac251} infections are much less impaired by the Y14N mutation, and not significantly affected by the Q93R mutation. As mentioned above, wild-type AGM CCR5 is only approximately 20% as active for HIV-1 infections as human CCR5. In contrast, the human/AGM(L352F) chimera is fully as active as human CCR5 (see Fig 2-7) and similar results were obtained using a human/AGM chimera (results not shown). This suggests that sequences in the amino terminal half of AGM CCR5 inhibit, but do not prevent HIV-1 infections. The only amino acid substitutions on the extracellular surface in this region that distinguish the human and AGM CCR5 proteins are I9T and N13D (see Fig 2-1). This raised the possibility that HIV-1 infections may be partially inhibited by the I9T or N13D substitutions. To test this hypothesis, we constructed the T9I and D13N mutations in the wild-type AGM CCR5 context. As shown in Fig 2-7, these substitutions both appeared to increase the efficiencies of infections by macrophage-tropic isolates of HIV-1 by approximately 2-fold. However, the increases varied among the HIV-1 isolates, and the ADA isolate appeared to be unaffected by the T9I substitution. These results suggest that these sequence differences contribute significantly to the reduced coreceptor activity of AGM clone 2 CCR5 compared to human CCR5 for HIV-1 infections.

Coreceptor activities of human/mouse CCR5 chimeras in infections by macrophage-tropic HIV-1. In parallel with the above investigations, we used our human and NIH/Swiss mouse CCR5 clones to construct and analyze human/mouse CCR5 chimeras. For this purpose we initially analyzed chimeras constructed using the *Msc* I, *Bgl* II, and *Eco* RI sites (see Fig 2-2). Chimeras were made by substituting mouse sequences into human CCR5 (to give MMHH, HHMM, MHHH, HMHH, HHMH, and HHHM) as well as the reciprocal substitutions of human sequences into mouse CCR5 (to give HMMM, MHMM, MMHM, and MMMH). In addition, we made the

HHHHloop2M chimera by using the *Bgl* II and *Bsa* BI sites to specifically substitute only the extracellular loop 2 sequence of NIH/Swiss mouse CCR5 into the human protein (see Fig 2-2). MMMMloop2H and HMMMloop2H chimeras were made by substituting the coding sequence for extracellular loop 2 from human CCR5 into NIH/Swiss mouse CCR5, or the HMMM chimera respectively (see Fig 2-2, and schematic diagrams in Table 2-1). After transfecting the HeLa-CD4 cultures with the pcDNA3-CCR5 plasmids, multiple subcultures were prepared for analyzing cell surface expression of each CCR5 protein, and infections by four macrophage-tropic isolates of HIV-1. These CCR5 constructs and viruses were analyzed together in three to five independent experiments that fully supported the same conclusions (see Fig 2-8A).

In considering these results, it is important to understand the three methods that were used to detect cell surface expression of CCR5 proteins (see Materials and Methods). The first method employed our rabbit antiserum that detects the amino terminus of human CCR5 but not of mouse CCR5 to measure the percentage of transfected cells that immunofluoresce (see Fig 2-4). The second method used this same antiserum followed by binding of [^{125}I]protein A to quantitatively measure the relative levels of antibody adsorbed onto the cell surfaces. The third method analyzed the binding of 0.5 nM [^{125}I]MIP1β onto the cells and was capable of detecting all of the CCR5 proteins on cell surfaces that could bind this chemokine. Because 0.5 nM MIP1β is below the K_D for binding this chemokine to CCR5 proteins (150), because the K_D values differ for the CCR5 proteins used in this study (see below), and because slight variations in the K_D of different CCR5 proteins would result in large differences in binding of 0.5 nM MIP1β, the results obtained with this method provided only a qualitative indication of cell surface expression of the CCR5s. Saturating the receptors by using very high concentrations of [^{125}I]MIP1β was impractical due to limitations in our resources and because this would have lowered the ratio of specific saturable labeling in comparison to the negative controls. Complete MIP1β binding analyses were done using

a competition method (150) for the CCR5s of humans, AGMs, and mice. These assays confirmed that the CCR5s had distinct apparent affinities for human MIP1β and indicated that the IC_{50} for human CCR5 in HeLa-CD4 cells was approximately 17 nM (results not shown). A previous analysis indicated an apparent IC_{50} of 7.4 nM for human CCR5 expressed in human 293T cells using a competitive binding assay (150).

Three of our CCR5 chimeras (HHMM, HHHM, and MHMM) did not appear to be expressed on HeLa-CD4 cell surfaces as determined by our assays. Consequently, their inabilities to function as coreceptors were not informative and they are not shown in Table 2-1 or Fig 2-8. Similarly, derivatives of MHMM that contain the second extracellular loop of human CCR5 or C57BL/6 mouse CCR5 [i.e. MHMMloop2H and MHMM(L183P)] were not expressed on cell surfaces. Interestingly, these results are perfectly concordant with recent data of Bieniasz et al that chimeras with human sequences in the second region and mouse sequences in the fourth are incompatible with expression on cell surfaces (21). This supports the validity of our methods. The HHMH chimera was weakly expressed on cell surfaces, but the HHHHloop2M chimera that supported the same conclusions was highly expressed. Surprisingly, several of the chimeras that were well expressed as detected by our antiserum did not significantly bind [^{125}I]MIP1β or bound only a low level of this chemokine (e.g., HMMM, HMHH, HHMH, and HHHHloop2M). Presumably, these chimeric CCR5s must fold into a conformation with a lower affinity for MIP1β than other CCR5s tested. Since HMHH is an active coreceptor (see Fig 2-8), ability to bind MIP1β with a high affinity is not a prerequisite for coreceptor function. Studies of G protein-coupled receptors have indicated that minor changes in folding can have large effects on affinities for agonists or antagonists (31, 68, 181).

The results in Fig 2-8A indicate that the MHHH and HMHH chimeras were partially active as coreceptors for macrophage-tropic isolates of HIV-1. This is intriguing because both of these mouse substitutions caused many nonconservative changes in the

protein. In contrast, the MMHH chimera was completely inactive as a coreceptor although it was expressed on cell surfaces as determined by [^{125}I]MIP1β binding. Comparison of the MHHH and HMHH chimeras which are active coreceptors with MMHH which is inactive implies that the amino terminal and extracellular loop 1 regions of human CCR5 both contribute to coreceptor function. The fact that the MHHH and HMHH chimeras are significantly less active than human CCR5 for all tested isolates of HIV-1 ($P<0.001$; $N=20$) also suggests that human sequences in these substituted regions contribute to coreceptor activity. Interestingly, the titers of SF162 were reduced by approximately 65% on cells expressing HMHH compared to cells expressing MHHH (see Fig 2-8) and this difference was highly significant ($P\leq0.002$; $N=5$). Additionally, Ba-L titers were reduced by approximately 30% on HMHH compared to MHHH. While this difference is less striking, it is also statistically significant ($P\leq0.006$; $N=5$). The titers of JR-FL and ADA were not significantly different on HMHH compared to MHHH when analyzed by the paired comparison t-test. Taken together, these results suggest that the contributions to coreceptor activity of the amino terminus and extracellular loop 1 of CCR5 may differ depending on the HIV-1 strain.

In addition, the results in Fig 2-8 clearly indicate that the HHMH and HHHHloop2M chimeras are completely inactive as coreceptors for HIV-1. These results could imply that extracellular loop 2 of human CCR5 is essential for coreceptor activity and/or that loop 2 of NIH/Swiss mouse CCR5 is nonpermissive for HIV-1 infections. Either of these interpretations would be compatible with the fact that our HMMM and MMMH chimeras were also inactive. In addition, the MMHM and MMMMloop2H chimeras were inactive as coreceptors for HIV-1 isolates, suggesting that the second extracellular loop of human CCR5 is insufficient for coreceptor function in the context of the NIH/Swiss mouse protein. In contrast, the MMMMloop2H chimera was partially active as a coreceptor for SIV_{mac251} (see below). The inactivity of HHHHloop2M as a coreceptor for HIV-1 was surprising because Atchison et al recently presented evidence

coreceptors for SIV_{mac251} (see Fig 2-8B). The MMMMloop2H and MMHH chimeras are weakly active (approximately 6% and 11% of human CCR5 respectively), suggesting that extracellular loop 2 of the human CCR5 protein contributes to infections by SIV_{mac251}, but that it is insufficient for full activity. These low levels of coreceptor activity are significant because our assay has zero background in mock transfected cells. Additionally, the coreceptor activity of the MHHH chimera was similar to the MMMMloop2H and MMHH chimeras, suggesting that addition of the human extracellular loop 1 sequence did not substantially increase coreceptor activity. In contrast to these chimeras, the HMHH chimera was approximately two-fold more active than the human CCR5 protein for SIV_{mac251}. Additionally, the HMMMloop2H chimera, which has the same presumptive extracellular surface as the HMHH chimera, was approximately as active as human CCR5 in mediating infection of HeLa-CD4 cells by SIV_{mac251}. These results suggest that the amino acid residues in the amino terminus and extracellular loop 2 regions of human CCR5 that differ from NIH/Swiss mouse CCR5 are important in coreceptor function for SIV_{mac251}. Finally, the HHHHloop2M chimera was only about 2% as active as the human CCR5, suggesting that while extracellular loop 2 from a species compatible with infection is not sufficient for full SIV_{mac251} coreceptor activity (i.e., MMHH and MMMMloop2H), it is probably required.

Discussion

Functional diversity of CCR5 sequences in AGMs. We reproducibly cloned two CCR5 sequences from the DNA of the AGM cell line CV-1 (see Fig 2-1). The AGM(Y14N,L352F) protein contains Y14N and L352F in positions that are otherwise conserved in the human, wild-type AGM, and mouse CCR5 proteins. These AGM CCR5 proteins differ dramatically in their coreceptor activities. Both are active coreceptors for SIV_{mac251}, but only wild-type AGM protein is active for macrophage-tropic isolates of HIV-1 including SF162, JR-FL, Ba-L, and ADA (see Fig 2-6 and 2-7). By using chimera constructions and site-directed mutagenesis, we found that the inability of AGM(Y14N,L352F) CCR5 to function as a coreceptor for HIV-1 is solely due to the Y14N substitution and that the human(Y14N) mutant CCR5 is also inactive (see Fig 2-7). Thus, the Y14N mutation prevents infections by macrophage-tropic isolates of HIV-1 but does not block infections by SIV_{mac251}. Similarly, the AGM(Q93R) variant that we isolated from a sabaeus AGM DNA sample was fully active as a coreceptor for SIV_{mac251}, but was only weakly active for all tested isolates of macrophage-tropic HIV-1 (see Fig 2-6). Studies using human/NIH/Swiss mouse CCR5 chimeras also indicated that SIV_{mac251} could weakly use MMMMloop2H (this contains only the human extracellular loop 2 in a NIH/Swiss mouse background), whereas this chimera was unable to mediate infections by macrophage-tropic isolates of HIV-1 (see Fig 2-8). However, SIV_{mac251} uses HMMMloop2H much more efficiently than MMMMloop2H, suggesting that SIV_{mac251} also requires sequences in the amino terminal region of human CCR5 for maximal infectivity. These results suggest that the HIV-1 isolates are more dependent than SIV_{mac251} on Y14 and Q93 sites in human CCR5, whereas SIV_{mac251} is more reliant on extracellular loop 2. Moreover, we found that HIV-1 isolates use human CCR5 approximately 5 times more efficiently than the wild-type AGM CCR5, whereas SIV_{mac251} uses these CCR5s equally well. This reduction in HIV-1 infections is at least partially caused by the I9T and N13D substitutions in AGM clone 2 compared to human CCR5

(see Figs 2-1 and 2-7). Recent studies by Edinger et al were consistent with these conclusions (56).

To learn whether the Y14N mutation is common in AGMs or unique to the CV-1 cell line, we initially examined the first ~560 coding base pairs of two DNA samples that had been prepared from PBMCs of AGMs. Our investigation of a vervet AGM DNA sample suggested that it contained two distinct CCR5 sequences, one with a D13N mutation, and one that appeared identical in the predicted amino acid sequence of the wild-type AGM CCR5. The D13N mutation in the AGM context enhanced infections by macrophage-tropic isolates of HIV-1 approximately 2-fold, in accordance with the presence of Asn at position 13 in human CCR5 (see Fig 2-7). The sabaeus AGM DNA sample also appeared to have derived from a CCR5 heterozygote, and in this case one allele encoded a variant with a Q93R substitution in extracellular loop 1. This mutation added a novel *Nci* I restriction enzyme cleavage site that was reproducibly detected in CCR5 DNA amplified from this monkey, but not in DNA amplified from CV-1 cells (see Fig 2-3). As mentioned above, this AGM(Q93R) protein was almost completely inactive as a coreceptor for multiple isolates of macrophage-tropic HIV-1, but was fully active for SIV_{mac251} (see Fig 2-6). Based on these results, we analyzed the DNAs from the two AGM cell lines Vero and BS-C-1. The Vero analysis was consistent with homozygosity for the wild-type AGM CCR5 sequence. In contrast, sequencing analysis of CCR5 amplified from BS-C-1 cells, which were derived from a grivet AGM (161), suggested that this cell line is heterozygous in the coding sequence of its genomic DNA for a novel point mutation which encodes a Q93K substitution in the AGM CCR5 protein. Thus among five AGM DNA samples that we have examined, four appeared to have derived from CCR5 heterozygotes and all of the amino acid changes were distinct. This frequent heterozygosity implies that substantial CCR5 polymorphism must occur within single breeding populations of different AGM subspecies. In contrast, approximately 10% of North American Caucasians encode a CCR5 variant with a 32 base deletion (5, 108, 158).

The frequency of polymorphisms is substantially lower in other races (5, 108, 158). We conclude that AGMs have a higher prevalence of CCR5 polymorphisms than humans.

There is evidence that AGMs have been infected with SIV_{agm} since ancient times and that SIV_{agm} viruses have become highly diverse (4, 20, 88, 89, 99, 128). Indeed AGMs have been classified into four geographically distinct subspecies termed vervets (*Chlorocebus pygerythrus*), tantalus (*C. tantalus*), grivets (*C. aethiops*), and sabaeus (*C. sabaeus*), and each subspecies is naturally infected at a very high prevalence by a distinct strain of SIV_{agm} without apparent immunodeficiency (4, 20, 128, 132). Moreover, SIV_{agm} isolates are approximately equally divergent from SIV_{mac251} and from HIV-1 (88, 89). This evidence has implied that AGMs and SIV_{agm} viruses have coevolved since a time preceding divergences of AGM subspecies. These considerations suggest that extensive CCR5 polymorphism in AGMs might have been selected by their prolonged exposure to a large reservoir of SIV_{agm} viruses and that the polymorphisms in AGM CCR5 might limit pathogenesis or inhibit emergence of more pathogenic SIV_{agm} variants. If this were correct, the specific amino acid polymorphisms in AGM CCR5s would often occur at sites that are important for viral infection and pathogenesis. In agreement with this hypothesis, four of the amino acid substitutions that we have detected in AGM CCR5s are clustered at two sites on the extracellular surface (D13N, Y14N; and Q93R, Q93K) that appear to be important for infections by macrophage-tropic HIV-1. In contrast these same amino terminal and extracellular loop 1 regions of mouse CCR5 contain many nonconservative differences from human CCR5, yet the MHHH and HMHH chimeric proteins are relatively active coreceptors for HIV-1 (see Figs 2-1 and 2-8). In addition, polymorphisms in human CCR5 are infrequent and are dispersed throughout the protein (5). Further evidence about these issues will require analyses of additional AGM CCR5 genes and studies of multiple SIV_{agm} isolates using suitable focal infectivity assays (see Appendix A). As more AGM CCR5 variants are identified, it will also be important to analyze their chemokine receptor activities. Currently, we are investigating these issues

using novel and sensitive assays for chemokine receptor signaling in Xenopus oocytes and in mammalian cells (results not shown).

CCR5 polymorphisms in mice and analyses of human/NIH/Swiss mouse CCR5 chimeras. CCR5 of NIH/Swiss mice differs at a total of 10, 8, and 14 positions from the recently described sequences of 129/SvJ (26), B6CBA (120), and Balb/c (21) mice, respectively. The NIH/Swiss mouse CCR5 protein is 79.8% identical to human CCR5 (see Fig 2-1) but is completely inactive as a coreceptor for SIV_{mac251} or macrophage-tropic HIV-1. Consequently, to identify regions of human CCR5 that are important for interactions with HIV-1 but are absent from NIH/Swiss mouse CCR5, we employed human/mouse CCR5 chimeras. After this work was substantially initiated, Atchison et al described an independent study using the 129/SvJ mouse sequence as the reference for their chimera constructions (6), and analyses of human/CCR2b chimeras were also reported (6, 56, 155). A study of human/Balb/c mouse CCR5 chimeras was also reported during revision of this manuscript (21). Although our conclusions are compatible with these other studies (see below), the chimeras that we made and the results that supported our conclusions were somewhat different. A major difference derived from the presence in the NIH/Swiss mouse CCR5 of a P183L substitution (using the human CCR5 numbering system) at a site in extracellular loop 2 that is otherwise conserved in all CCR5 proteins that are known to function as coreceptors for human or simian immunodeficiency viruses. This substitution did not prevent cell surface expression or MIP1β binding, but was nonpermissive for infections. Accordingly, all chimeras with this sequence were inactive in our coreceptor assays (see Fig 2-8). In contrast, the HHHHloop2M(L183P) chimera which contains a Pro residue at position 183 was an active coreceptor for HIV-1 (see Fig 2-8).

The MHHH and HMHH chimeras were partially active as coreceptors for macrophage-tropic isolates of HIV-1, whereas MMHH was inactive although it was expressed on cell surfaces (see Fig 2-8). Comparison of these active MHHH and HMHH

coreceptors with MMHH suggests that the extracellular loop 1 and amino terminal regions of human CCR5 both contribute positively to coreceptor function. The fact that the MHHH and HMHH chimeras are significantly less active than the human CCR5s ($P \leq 0.02$; N=5) also supports this conclusion. In contrast, the HHMH and HHHHloop2M chimeras were inactive as coreceptors as were all other CCR5 chimeras that contained the NIH/Swiss mouse loop 2 sequence. This suggested that the human loop 2 sequence was essential and/or that the NIH/Swiss mouse sequence was nonpermissive for infections. In either case, this would imply that HIV-1 interacts closely with CCR5 loop 2. The fact that our MMHM, MMHH, and MMMMloop2H chimeras were inactive as coreceptors for HIV-1 suggested that the human loop 2 sequence was insufficient for coreceptor function in the context of the NIH/Swiss mouse CCR5 protein. In contrast, SIV_{mac251} was able to use MMHH and MMMMloop2H as coreceptors at low efficiencies, and addition of the human amino terminus (i.e., HMMMloop2H and HMHH chimeras) restored full activity (see Fig 2-8B). Because other evidence clearly indicated that the human loop 2 sequence is not essential for coreceptor activity in the context of chimeras made with the 129/SvJ CCR5 or human CCR2b proteins (6, 21, 155), we inferred that the NIH/Swiss mouse CCR5 loop 2 must be nonpermissive for infections, and we observed that it differs from the permissive 129/SvJ sequence only by a nonconservative P183L substitution. To test this idea we cloned the CCR5 coding sequence from a C57BL/6 mouse and we made the HHHHloop2M(L183P) chimera that contained this sequence. This chimera was active as a coreceptor for HIV-1, in contrast to the identical chimera that has a Leu residue at position 183 (see Fig 2-8). This evidence suggests that the P183L substitution that occurs in NIH/Swiss mice causes an absolute block in infections by all tested macrophage-tropic isolates of HIV-1 in the context of the HHHHloop2M chimera.

We believe that our analyses of human/NIH/Swiss mouse CCR5 chimeras are fully compatible with related evidence from other laboratories which have also implicated the amino terminus and extracellular loops 1 and 2 of human CCR5 in

infections by macrophage-tropic HIV-1 (6, 21, 139, 155). However, as discussed elsewhere (21, 139), the earlier studies did not give identical results, presumably because the reference proteins, viruses, cell lines, assay methods, and chimera splice sites were distinct. For example, several of these studies used syncytium rather than infection assays, epitope-tagged rather than native CCR5s, or coreceptor overexpression in COS-7 cells.

Based on our results, we believe that a major source of error in chimera analyses derives from the assumption that the reference protein sequences used in the chimeras have neutral rather than positive or negative effects on the activity being measured. As mentioned by Bieniasz et al (21), this assumption of neutrality is unlikely to be valid for coreceptors because the reference proteins that have been used were all closely related to human CCR5 and because many HIV-1 isolates can promiscuously employ different chemokine receptors such as CCR2b and CCR3 (38, 53, 155). Such promiscuity implies that substantial variations in coreceptor sequences are compatible with productive interactions with HIV-1. Our evidence clearly demonstrates that the assumption of neutrality is incorrect for the NIH/Swiss mouse loop 2 sequence, which is nonpermissive for coreceptor activity. One possible interpretation is that the P183 residue in human CCR5 and at the corresponding positions in the reference proteins used in previous chimera studies contributed positively to the coreceptor activities that were observed. Alternatively, the Leu residue at this site in NIH/Swiss mouse CCR5 might prevent infections, perhaps by a steric mechanism. In either case, effects of reference protein sequences are clearly very difficult to detect or to control for, yet they can profoundly influence results of chimera analyses.

Evidence for active sites in human CCR5. In addition to the chimera approach, which has a limited resolution and is complicated by certain assumptions as described above, we have employed an alternative method to identify active sites in CCR5. Specifically, we have compared closely related CCR5 proteins that differ only in several

amino acids yet have substantial differences in their coreceptor activities. This approach has proven to be advantageous because it does not require assumptions about the ability of HIV-1 to interact with a reference protein and because it has enabled us to rapidly identify specific CCR5 amino acids that are important for HIV-1 infections. By studying CCR5 polymorphisms in AGMs and mice, we have found that the Y14N, Q93R, and P183L substitutions severely inhibit infections by macrophage-tropic isolates of HIV-1 (see Figs 2-6, 2-7, and 2-8). Similarly, by comparing the coreceptor activities of the closely related human and AGM proteins, we obtained evidence that I9T and N13D substitutions significantly reduce, but do not prevent HIV-1 infections (see Fig 2-7).

To the best of our knowledge, Y14N, Q93R, and P183L are the first amino acid substitutions on the extracellular surface of CCR5 that allow processing to cell surfaces and chemokine binding, but appear to block HIV-1 infections. Additional mutagenesis studies of the Y14, Q93, and P183 amino acids are in progress and may help to more precisely determine the roles of these residues in HIV-1 infections. In contrast, chimera studies have indicated that many nonconservative substitutions and deletions at nearby positions are compatible with CCR5 coreceptor activity. Based on these considerations, we propose that macrophage-tropic HIV-1 isolates interact broadly with different regions of CCR5 but that certain amino acids in these regions are nevertheless critical for infections by independent isolates of macrophage-tropic HIV-1. These key amino acids might be important for conformations of the contact regions or they might directly comprise the contact sites. As discussed above, the existence of critical sites in CCR5 was unexpected because of earlier evidence that all regions of human CCR5 may be expendable for infections by macrophage-tropic HIV-1 in the context of specific chimera structures (6, 21, 139, 155). The finding of sites in CCR5 that are critical for infections by all tested isolates of macrophage-tropic HIV-1 has the important corollary that targeting these sites with monoclonal antibodies or drugs might reduce transmission or be clinically beneficial to infected individuals.

Acknowledgments

This research was supported by NIH Grant CA67358. E.J.P. was supported by an NRSA postdoctoral fellowship (number IF32AID9735-01) from the NIH. S.E.K. was supported in part by the N.L. Tartar Research Fund from the Oregon Health Sciences Foundation.

We are grateful to Dr. Jon Allan (Department of Virology and Immunology, Southwest Foundation for Biomedical Research, San Antonio, TX) for generously donating the AGM DNA samples and to Dr. Jay Nelson for generously providing SIV_{mac251} and the anti-p27 monoclonal antibody. We are additionally grateful to Dr. Paul Bieniasz and colleagues for sending us their accepted manuscript before it was published. We are very grateful to our coworkers and colleagues Navid Madani, Chetankumar Tailor, Roger Cone, and Philip Stork for encouragement and helpful advice.

Table and Figures

TABLE 2-1. Properties of CCR5 proteins.

[a]For immunofluorescence (see Fig 2-4), the percent of positive cells were counted. The results shown are average values for independent experiments. For human CCR5, the average transfection effeciency as determined by this method was 15% (N=9). The symbol --- indicates that the CCR5 protein could not be detected by the antiserum due to the presence of the NIH/Swiss mouse N-terminus.

[b]For [^{125}I] protein A immunoassay, the average background in mock transfected cells was 7.1 cpm/μg protein (N=9). Each assay was done in duplicate and the cpm/μg protein above background was recorded. The results are averages of multiple assays. The average protein value for the samples was approximately 50 to 100 μg in independent assays. The symbol --- indicates that the CCR5 protein could not be detected by the antiserum due to the presence of the NIH/Swiss mouse N-terminus. ND indicates the assay was not performed for this CCR5 construct.

[c]The [^{125}I]Mip1β binding assays were done in triplicate using 0.5 nM [^{125}I]Mip1β at 37°C for 2 h and the data are recorded as the average cpm/μg protein above background. The average backgrounds in the assays were 6.7 cpm/μg protein (N=7). The average protein value for the samples was approximately 50 to 100 μg in independent assays.

[d]The [^{125}I]Mip1β binding data for Human(Y14N), HMMM, HMHH, HHMH, HHHHloop2M, HMMMloop2H, and HHHHloop2M(L183P) were not significantly above the backgrounds. However, all of these CCR5 proteins were highly expressed on cell surfaces as detected by the antibody methods.

TABLE 3-1. Properties of CCR5 proteins used in this investigation

CCR5	Structure	Immunofluorescence % positive[a]	Immunoassay [125I]protein A (cpm/μg protein)[b]	[125I]MIP1β Binding (cpm/μg protein)[c]
Human	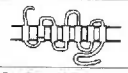	15	125	15
AGM (Y14N,L352F)	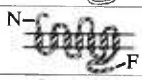	9.8	21	61
AGM	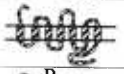	6.6	10	111
AGM(Q93R)	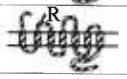	9.9	21	94
NIH/Swiss Mouse	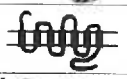	---	---	28
AGM(Y14N)	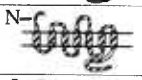	22	40	60
AGM(T9I)	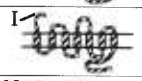	13	ND	22
AGM(D13N)	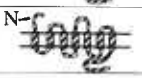	7.6	ND	16
AGM(Y14N)/ Human	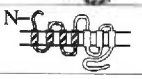	20	67	67
Human/ AGM(L352F)		24	134	15
Human(Y14N)	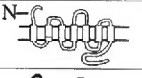	12	33	1.6[d]
MMHH		---	---	15
HMMM		18	57	0[d]
MMHM		---	---	31
MMMH		---	---	28
MHHH	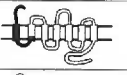	---	---	131
HMHH	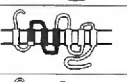	17	111	7.3[d]
HHMH	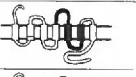	5.0	13	2.1[d]
HHHHloop2M	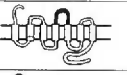	19	100	0[d]
MMMMloop2H		---	---	16
HMMMloop2H		9.6	47	4.5[d]
HHHHloop2M (L183P)	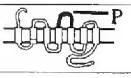	15	ND	0[d]

Figure 2-1. Sequence alignment of human, AGM, and NIH/Swiss mouse CCR5 proteins.

Several clones were isolated from each PCR reaction and were sequenced to ensure reproducibility and accuracy for the cloning. The two distinct AGM clones contained three nucleotide substitutions that resulted in substitutions of two amino acids. The AGM sequence designated as wild-type is more homologous to the CCR5 sequences of other species and most commonly found in AGMs (see Results) and is therefore considered to represent the main evolutionary lineage. The NIH/Swiss mouse sequence differs from previously reported sequences from the C57BL/6 (26), CD-1 (120), and Balb/c (21) strains by multiple amino acid substitutions. The lines A-G show the seven presumptive transmembrane regions. The restriction enzymes written over the sequences indicate the common restriction enzyme cleavage sites that were used to generate chimeric CCR5 proteins.


A
Msc I
B
C
D
Bgl II
Bsa BI
E
F
Eco RI
G
Human
AGM(Y14N,L352F)
AGM
NIH/Swiss Mouse
MDYQVSSP..IYDINYYTSEPCQKINVKQIAARLLPPLYSLVFIFGFVGNMLVILILINCKRLKS 63
MDYQVSSP..TYDIDNYTSEPCQKINVKQIAARLLPPLYSLVFIFGFVGNILVVLILINCKRLKS 63
MDYQVSSP..TYDIDYYTSEPCQKINVKQIAARLLPPLYSLVFIFGFVGNILVVLILINCKRLKS 63
MDFQGSVPTYIYDIDYGMSAPCQKINVKQIAAQLLPPLYSLVFIFGFVGNMMVFLILISCKRLKS 65
MTDIYLLNLAISDLFFLLTVPFWAHYAAAQWDFGNTMCQLLTGLYFIGFFSGIFFIILLTIDRYL 128
MTDIYLLNLAISDLLFLLTVPFWAHYAAAQWDFGNTMCQLLTGLYFIGFFSGIFFIILLTIDRYL 128
MTDIYLLNLAISDLLFLLTVPFWAHYAAAQWDFGNTMCQLLTGLYFIGFFSGIFFIILLTIDRYL 128
MTDIYLLNLAISDLLFLLTLPFWAHYAANEWVFGNIMCKVFTGVYHIGYFGGIFFIILLTIDRYL 130
AVVHAVFALKARTVTFGVVTSVITWVVAVFASLPGIIFTRSQKEGLHYTCSSHFPYSQYQFWKNF 193
AIVHAVFALKARTVTFGVVTSVITWVVAVFASLPRIIFTRSQREGLHYTCSSHFPYSQYQFWKNF 193
AIVHAVFALKARTVTFGVVTSVITWVVAVFASLPRIIFTRSQREGLHYTCSSHFPYSQYQFWKNF 193
AIVHAVFALKVRTVNFGVITSVVTWVVAVSASLPEIIFTRSQKEGFHYTCSPHFLHTQYHFWKSF 195
QTLKIVILGLVLPLLVMVICYSGILKTLLRCRNEKKRHRAVRLIFTIMIVYFLFWAPYNIVLLLN 258
QTLKIVILGLVLPLLVMVICYSGILKTLLRCRNEKKRHRAVRLIFTIMIVYFLFWAPYNIVLLLN 258
QTLKIVILGLVLPLLVMVICYSGILKTLLRCRNEKKRHRAVRLIFTIMIVYFLFWAPYNIVLLLN 258
QTLKMVILSLILPLLVMIICYSGILHTLFRCRNEKKRHRAVRLIFAIMIVYFLFWTPYNIVLLLT 260
TFQEFFGLNNCSSSNRLDQAMQVTETLGMTHCCINPIIYAFVGEKFRNYLLVFFQKHIAKRFCKC 323
TFQEFFGLNNCSSSNRLDQAMQVTETLGMTHCCINPIIYAFVGEKFRNYLLVFFQKHIAKRFCKC 323
TFQEFFGLNNCSSSNRLDQAMQVTETLGMTHCCINPIIYAFVGEKFRNYLLVFFQKHIAKRFCKC 323
TFQEFFGLNNCSSSNRLDQAMQATETLGMTHCCLNPVIYAFVGEKFRSYLSVFFRKHIVKRFCKR 325
CSIFQQEAPERASSVYTRSTGEQEISVGL 352
CSIFQQEAPERASSVYTRSTGEQETSVGF 352
CSIFQQEAPERASSVYTRSTGEQETSVGL 352
CSIFQQDNPDRASSVYTRSTGEHEVSTGL 354

Figure 2-2. Topological model of human CCR5 in the membrane.

The extracellular membrane face is above the membrane which is indicated by solid parallel lines, whereas the intracellular face is below. The splice sites used to make CCR5 chimeras are indicated by arrows with the names of the restriction enzymes that were employed. The shaded amino acids are positions that differ among the human, AGM, and NIH/Swiss mouse CCR5 proteins (see Fig 2-1). The asterisks at Y14, Q93, and P183 indicate sites that appear to be critical for infections by macrophage-tropic isolates of HIV-1.

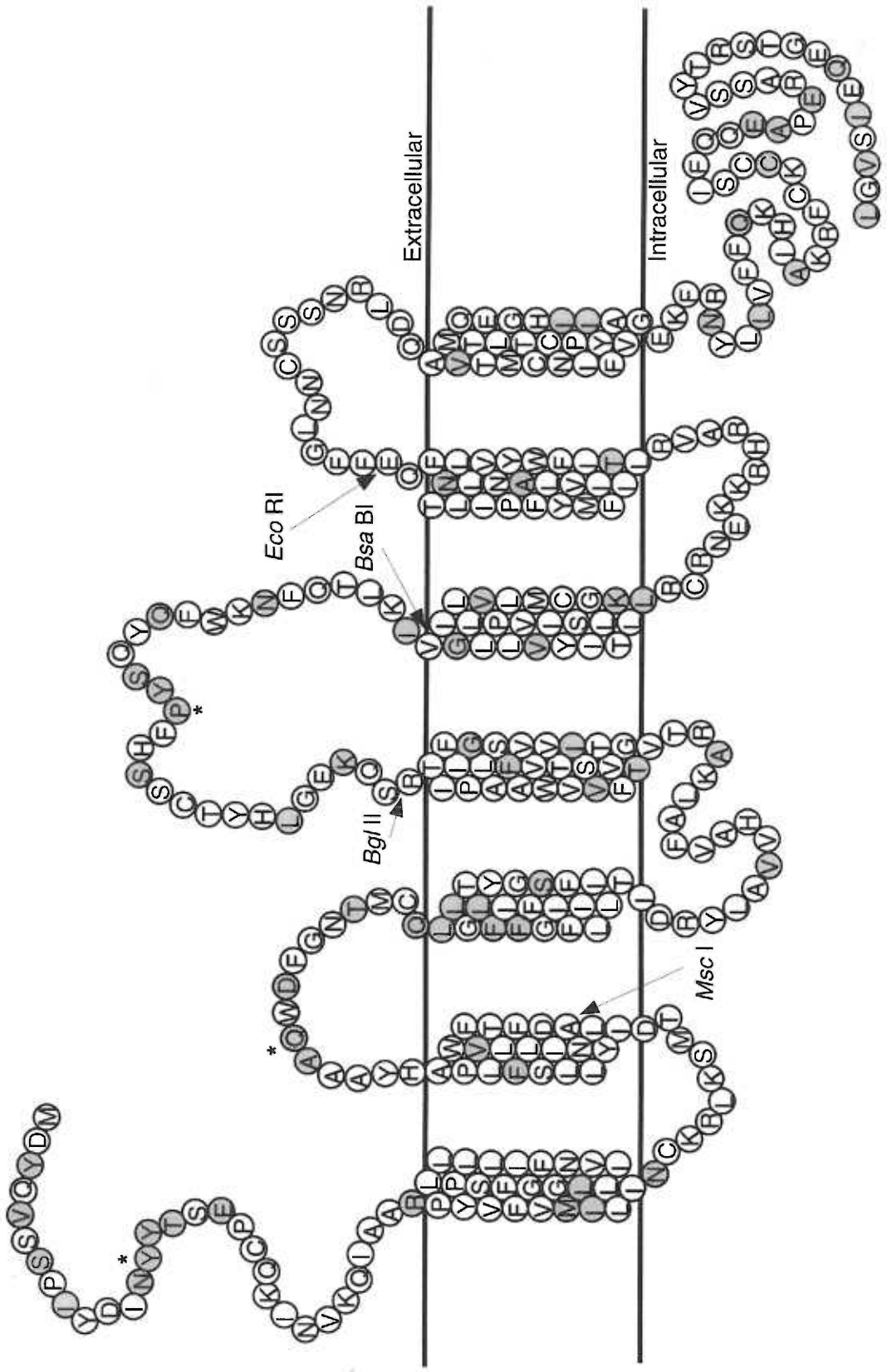
Extracellular
Intracellular
Eco RI
Bsa BI
Bgl II
Msc I

Figure 2-3. Identification of a CCR5 polymorphism in the DNA of a sabaeus AGM.

Panel A shows electropherograms from automated thermal cycle sequencing analysis of DNA samples amplified from the CCR5 genes of the sabaeus monkey (lower section) compared with the corresponding sequence from the AGM CV-1 cell line. The control CV-1 sample contains a homogeneous sequence in this region, with an A at position 290 (numbered from the first base of the PCR primer AGMF (see Materials and Methods)). In contrast, the sabaeus AGM sequence was identical except for an ambiguity (R = A or G) at this position. This change was seen in CCR5 sequences that were independently amplified from the sabaeus AGM DNA sample. Panel B shows a restriction enzyme digestion analysis of CCR5 DNAs that were obtained in an independent PCR amplification reaction using the CV-1 and sabaeus DNA preparations. Restriction fragments generated by digestion with *Nci* I were separated on a 2% agarose gel. The mutation implicated in the sabaeus CCR5 gene by the A290G substitution (see Panel A) adds a novel *Nci* I restriction enzyme cleavage site that reproducibly cleaves a fraction of the 567 bp sabaeus PCR amplification product to give fragments of predicted sizes 279 and 288 bp which are not resolved on this gel (lane 1). Digests of the CV-1 DNA amplification product show no cleavage fragments (lane 2). The 567 bp fragment is only partially cleaved in lane 1 because the sabaeus monkey was heterozygous (see panel A). The PCR product containing the mutant sabaeus CCR5 sequence was cut with *Cla* I, and the fragment spanning codons 12 through 124 of the AGM clone 2 coding sequence was cloned into the pcDNA3-AGM clone 2 plasmid that had also been cut with *Cla* I as described in Materials and Methods. In lane 3 the full coding sequence of the AGM(Q93R) mutant CCR5 (1087 bp excised from the pcDNA3-AGM(Q93R) plasmid with *Bam* HI and *Xho* I) was digested with *Nci* I, showing that the mutant also gives the predicted 288 bp fragment as well as a fragment with a predicted size of 799 bp. The wild-type AGM sequence is not digested with *Nci* I (results not shown).

A.

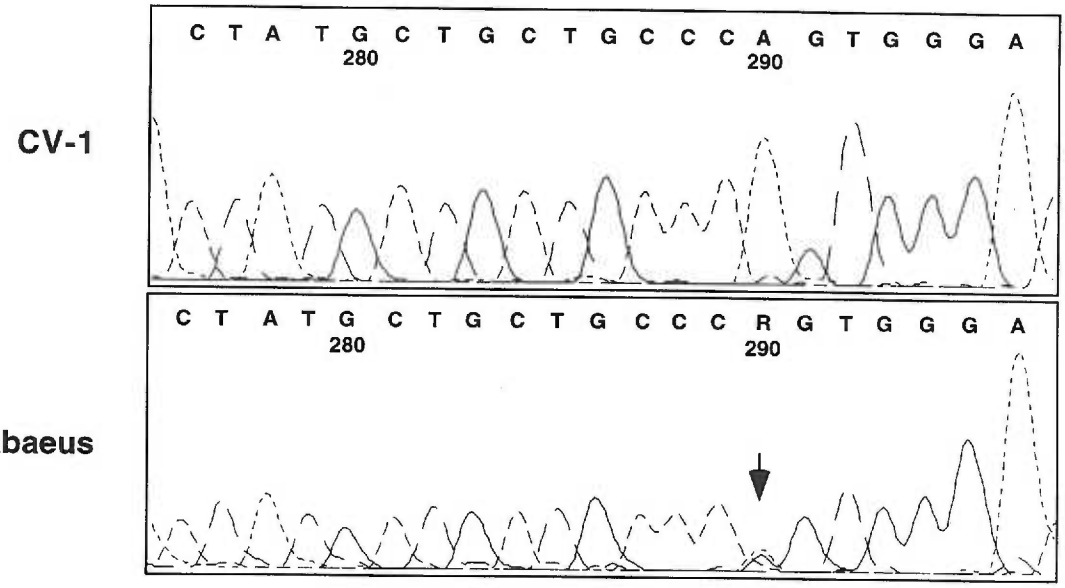
CV-1
C T A T G C T G C T G C C C A G T G G G A
280
290
sabaeus
C T A T G C T G C T G C C C R G T G G G A
280
290

B.

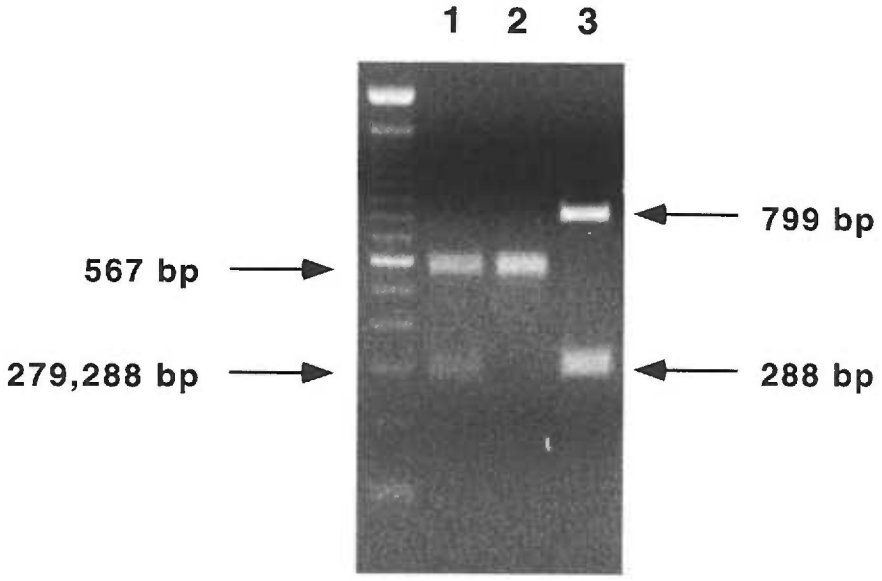
1 2 3
799 bp
567 bp
279,288 bp
288 bp

Figure 2-4. Detection of human CCR5 on surfaces of viable cells by immunofluorescence microscopy.

Each panel shows photomicrographs of the same fields taken with phase contrast (top) and fluorescent imaging (bottom). The cells in the left-hand panel are control HeLa cells, and those in the center and right-hand panels are a clone of the HeLa-CD4 cell line HI-J which stably expresses human CCR5 encoded by the retroviral expression vector pSFF-CCR5 (96, 144) in all of the cells. The primary antiserum used in the left-hand and center panels was the rabbit anti-CCR5 serum, whereas in the right-hand panel the preimmune serum from the same rabbit was used. The patching of fluorescence is caused by antibody-induced crosslinking of the cell-surface CCR5. Labeling only occurs when the specific antibody binds to cells that express CCR5, and not with preimmune serum or with HeLa cells that lack CCR5.

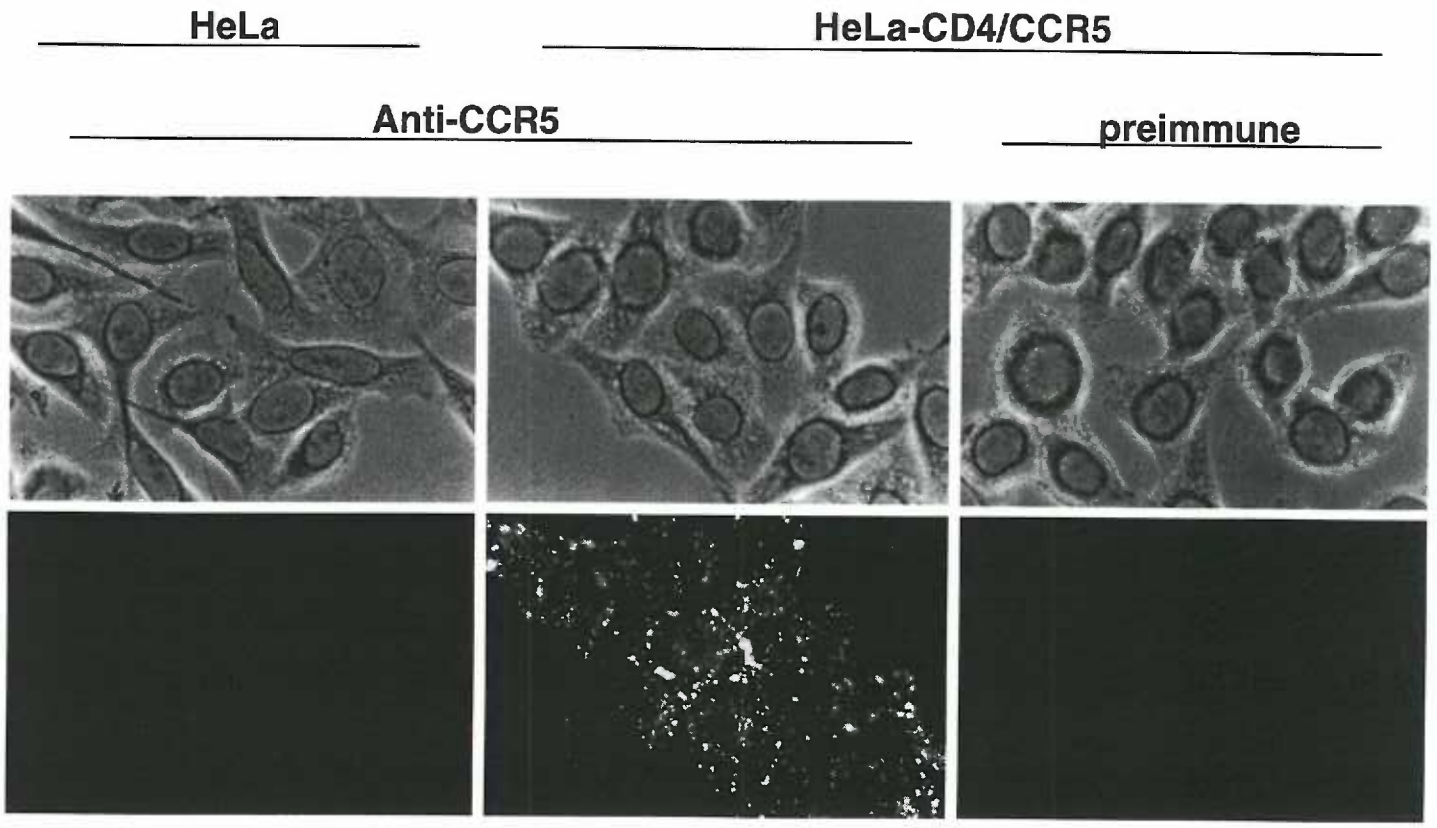
HeLa
HeLa-CD4/CCR5
Anti-CCR5
preimmune

Figure 2-5. Protein immunoblot (Western) analysis of human CCR5 in membrane preparations from COS-7 cells that express this chemokine receptor.

Membrane preparations from COS-7 cells transfected with the pcDNA3-CCR5 expression construct (lanes 2 and 4) or with pcDNA3 alone (lanes 1 and 3) were separated on a 10% SDS-PAGE gel and transferred to nitrocellulose. Transferred proteins were then blotted with the anti-CCR5 antibody prepared as described in the text (lanes 1 and 2), or with the preimmune serum from the same rabbit (lanes 3 and 4). Bound rabbit IgG was detected by standard chemiluminescent western blotting techniques. The molecular weights of the SDS-PAGE size standards (lanes M) are indicated in the left-hand column. The band at Mr~40,000 (arrow) is detected only in CCR5 transfected cells with the serum from the immunized rabbit. The intense bands near the top of the gel represent non-specific cross reaction with one of the chemiluminescence reagents, since they were absent when westerns were visualized with [^{125}I]protein A.

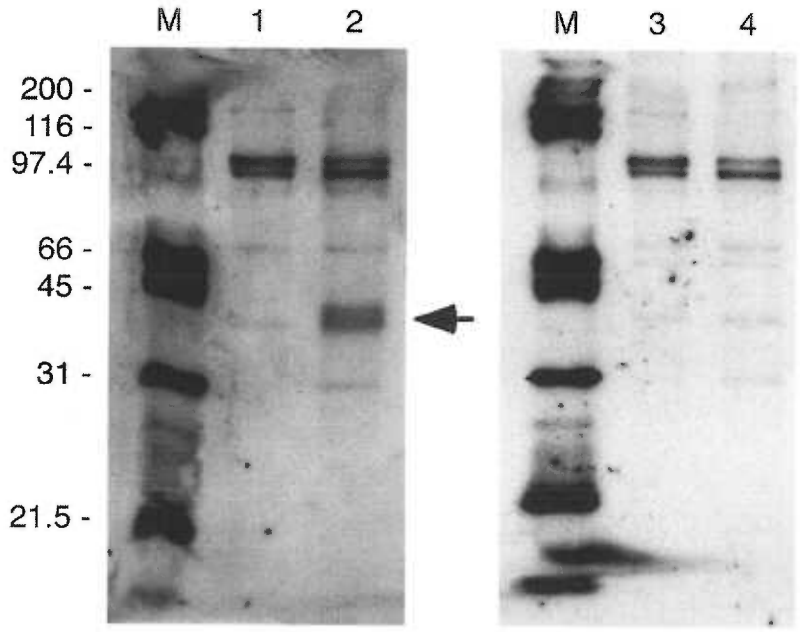
M
1
2
M
3
4
200 -
116 -
97.4 -
66 -
45 -
31 -
21.5 -

Figure 2-6. Coreceptor activities of naturally occurring CCR5 proteins encoded by humans, AGMs, and mice.

The coreceptor activities were all normalized relative to the activity of human CCR5 in the same experiment. Panel A shows the activities of each CCR5 for infections by the macrophage-tropic HIV-1 isolates SF162, JR-FL, ADA, and Ba-L, whereas panel B shows the activities for infection by SIV_{mac251}. The error bars are the S.E.M. values except where N=2, where they represent the range of values obtained. In panel A, N=4 for all CCR5 constructs with the JR-FL isolate, except AGM where N=6; N=2 for all CCR5 constructs with the ADA isolate, except AGM where N=4; N=6 for all CCR5 constructs with the SF162 and Ba-L isolates with the exception of AGM(Q93R) constructs where N=7, and AGM where N=8. In panel B, N=3 for all CCR5 constructs except AGM(Q93R) where N=4.

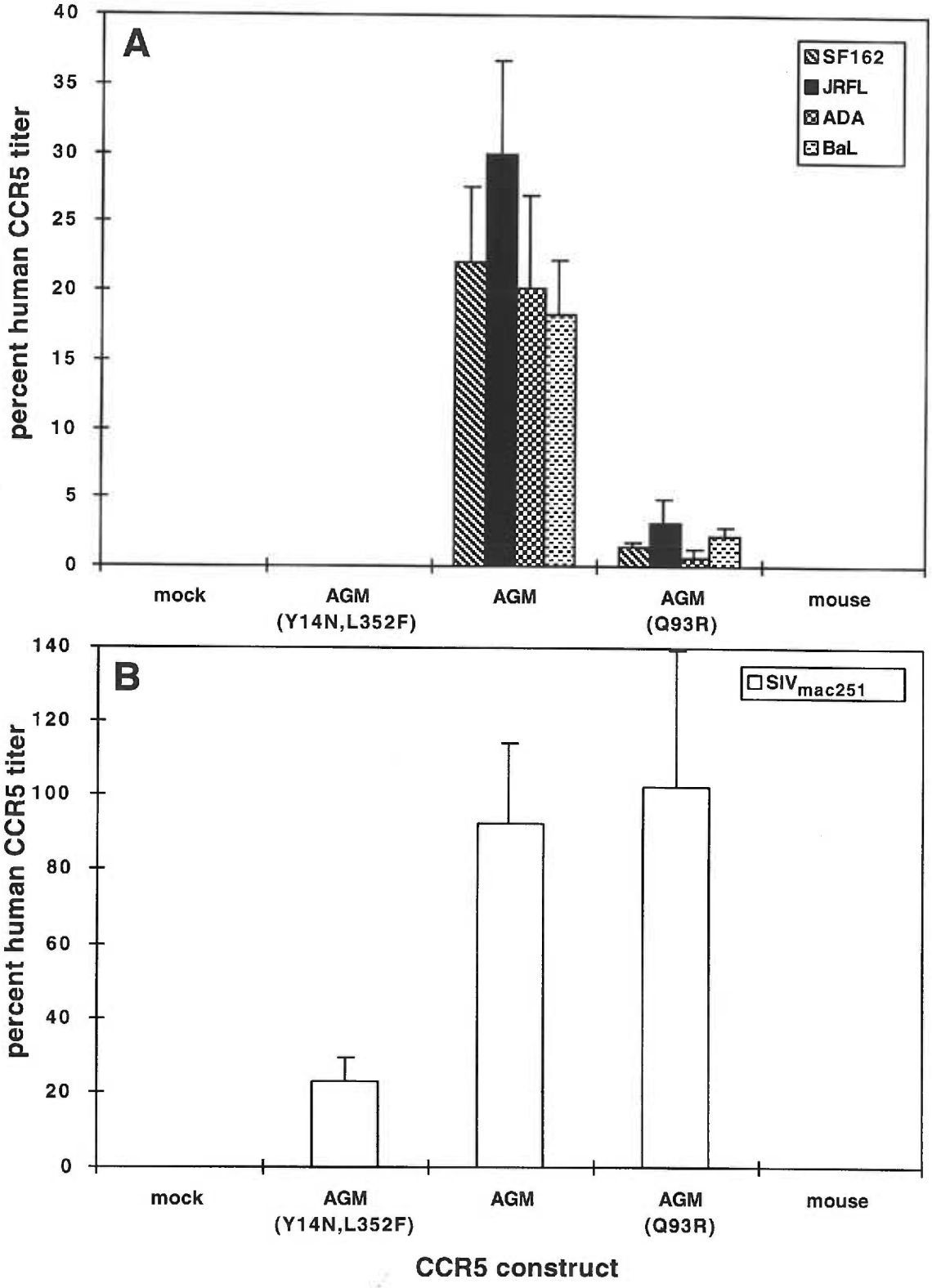
A
percent human CCR5 titer
40
35
30
25
20
15
10
5
0
SF162
JRFL
ADA
BaL
mock
AGM (Y14N,L352F)
AGM
AGM (Q93R)
mouse
B
percent human CCR5 titer
140
120
100
80
60
40
20
0
SIVmac251
mock
AGM (Y14N,L352F)
AGM
AGM (Q93R)
mouse
CCR5 construct

Figure 2-7. Coreceptor activities of human/AGM CCR5 chimeras and of human(Y14N), AGM(Y14N), AGM(T9I), and AGM(D13N) mutants.

The coreceptor activities were all normalized relative to the activity of human CCR5 in the same experiment, using the macrophage-tropic HIV-1 isolates SF162, JR-FL, ADA, and Ba-L. The error bars are the S.E.M. values except where N=2, where they represent the range of values obtained. N=2 for all HIV-1 isolates using the AGM(Y14N)/human, human/AGM(L352F), and AGM(Y14N) CCR5 constructs. N=4 for all HIV-1 isolates using the human(Y14N) CCR5 construct. N=6 for the SF162 and Ba-L isolates using the AGM(Y14N,L352F) CCR5 construct, and N=8 using the AGM construct with these isolates. N=4 for the JR-FL isolate and N=2 for the ADA isolate using the AGM(Y14N,L352F) construct. N=6 for the JR-FL isolate and N=4 for the ADA isolate using the AGM construct. N=4 for all isolates for the AGM(T9I) and AGM(D13N) CCR5 constructs.

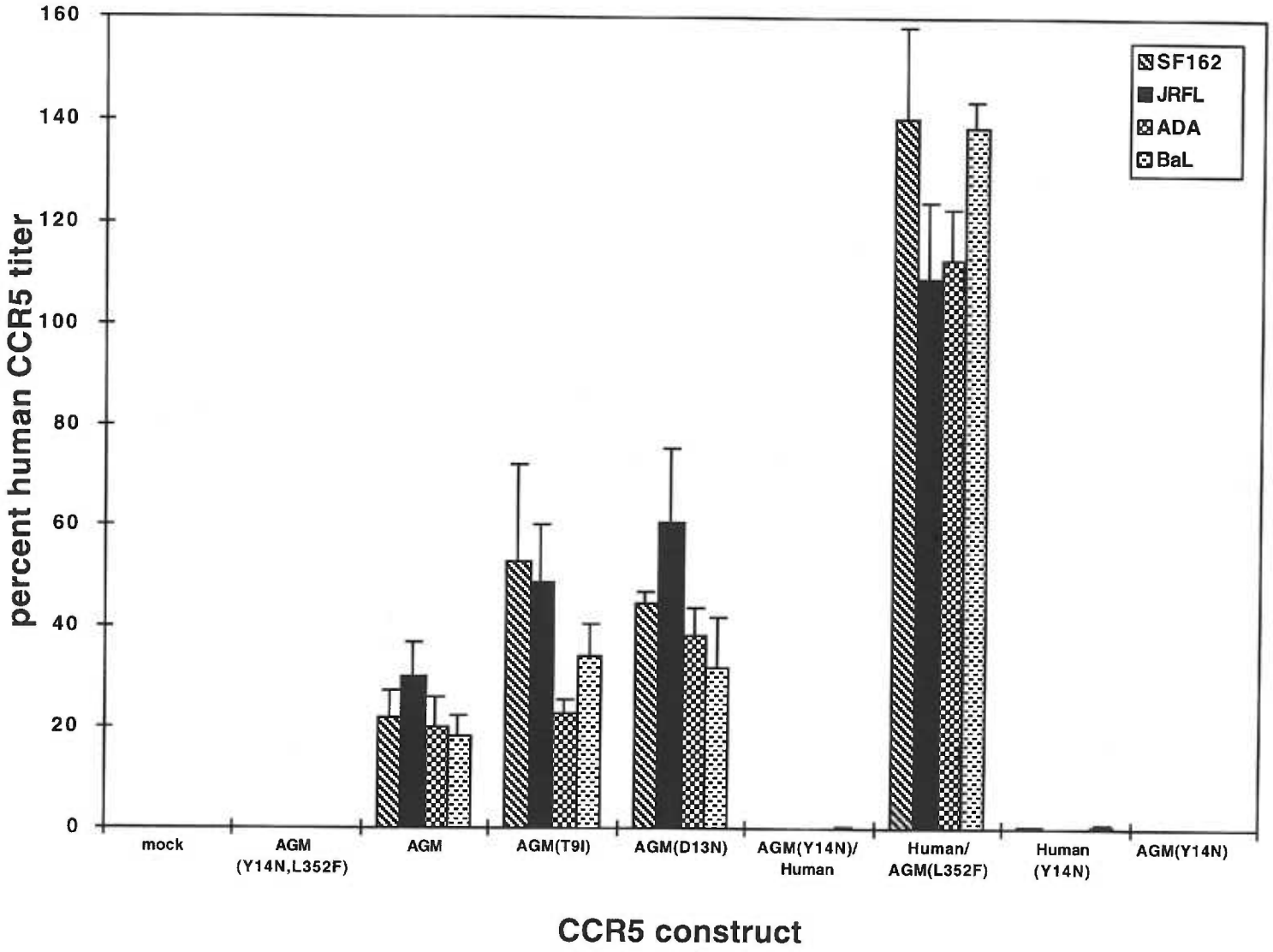
160
140
120
100
80
60
40
20
0
percent human CCR5 titer
SF162
JRFL
ADA
BaL
mock
AGM (Y14N,L352F)
AGM
AGM(T9I)
AGM(D13N)
AGM(Y14N)/ Human
Human/ AGM(L352F)
Human (Y14N)
AGM(Y14N)
CCR5 construct

Figure 2-8. Coreceptor activities of human/NIH/Swiss mouse CCR5 chimeras for infections of macrophage-tropic HIV-1 (panel A) or SIV_{mac251} (panel B).

The coreceptor activities were all normalized relative to the activity of human CCR5 in the same experiment. The error bars are the S.E.M. values except where N=2, where they represent the range of values obtained. In panel A, N=5 for all coreceptors with all HIV-1 isolates, except HMMM, MMMH, and HHMH where N=3 for all HIV-1 isolates, and the HHHHLoop2M(L183P) construct where N=4 for the SF162, ADA, and Ba-L isolates and N=3 for the JR-FL isolate. In panel B, N=3 for the mock, mouse, MMMMloop2H, and HMMMloop2H CCR5 constructs, and N=2 for the MMHH, MHHH, HMHH, and HHHHloop2M CCR5 constructs.

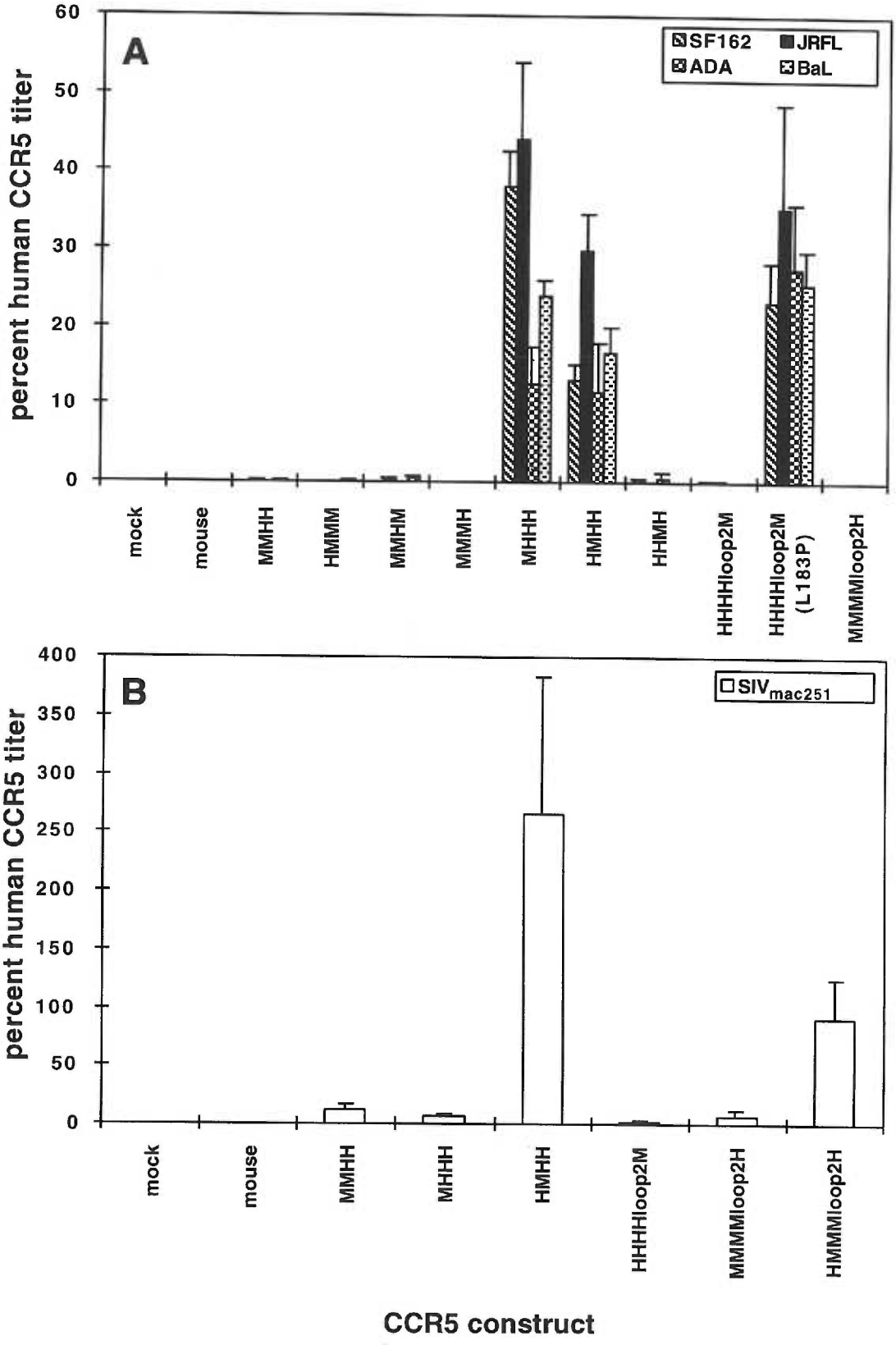
A
SF162
JRFL
ADA
BaL
percent human CCR5 titer
60
50
40
30
20
10
0
mock
mouse
MMHH
HMMM
MMHM
MMMH
MHHH
HMHH
HHMH
HHHHloop2M
HHHHloop2M (L183P)
MMMMloop2H
B
SIVmac251
percent human CCR5 titer
400
350
300
250
200
150
100
50
0
mock
mouse
MMHH
MHHH
HMHH
HHHHloop2M
MMMMloop2H
HMMMloop2H
CCR5 construct

Chapter 3. A Critical Site in the Core of the CCR5 Chemokine Receptor Required for Binding and Infectivity of Human Immunodeficiency Virus Type 1

Salvatore J. Siciliano[‡§], Shawn E. Kuhmann[†§], Youmin Weng[‡], Navid Madani[†], Martin S. Springer[‡], Janet E. Lineberger[††], Renee Danzeisen[††], Michael D. Miller[††], Michael P. Kavanaugh[Δ], Julie A. DeMartino[‡§§], and David Kabat[†§§*]

[‡]Merck Research Laboratories, Immunology and Rheumatology

Rahway, NJ 07065

[††]Merck Research Laboratories, Antiviral Research

West Point, PA 19486

[†]Department of Biochemistry and Molecular Biology and [Δ]Vollum Institute

Oregon Health Sciences University

Portland, OR 97201

Running Title: An Active Site in the Core of the HIV-1 Coreceptor CCR5

[§,§§]These authors contributed equally to this work.

[*]With whom to correspond:

Department of Biochemistry and Molecular Biology

Oregon Health Sciences University

Portland, Oregon 97201-3098

Tel: (503) 494-8442

Fax: (503) 494-8393

Abstract

Like the CCR5 chemokine receptors of humans and rhesus macaques, the very homologous (c.a. 98-99% identical) CCR5 of African green monkeys (AGMs) avidly binds β-chemokines and functions as a coreceptor for simian immunodeficiency viruses. However, AGM CCR5 is a weak coreceptor for tested macrophagetropic (R5) isolates of human immunodeficiency virus type 1 (HIV-1). Correspondingly, gp120 envelope glycoproteins derived from R5 isolates of HIV-1 bind poorly to AGM CCR5. We focused on a unique extracellular amino acid substitution at the juncture of transmembrane helix 4 (TM4) and extracellular loop 2 (ECL2) [Arg for Gly at amino acid 163 (G163R)] as the likely source of the weak R5 gp120 binding and HIV-1 coreceptor properties of AGM CCR5. Accordingly, a G163R mutant of human CCR5 was severely attenuated in its ability to bind R5 gp120s and to mediate infection by R5 HIV-1 isolates. Conversely, the R163G mutant of AGM CCR5 was substantially strengthened as a coreceptor for HIV-1 and had improved R5 gp120 binding affinity relative to the wild-type AGM CCR5. These substitutions at amino acid position 163 had no effect on chemokine binding or signal transduction, suggesting the absence of structural alterations. The 2D7 monoclonal antibody has been reported to bind to ECL2 and to block HIV-1 binding and infection. Whereas 2D7 antibody binding to CCR5 was unaffected by the G163R mutation, it was prevented by a conservative ECL2 substitution (K171R), shared between rhesus and AGM CCR5s. Thus, it appears that the 2D7 antibody binds to an epitope that includes K171, and may block HIV-1 infection mediated by CCR5 by occluding an HIV-1 binding site in the vicinity of G163. In summary, our results identify a site for gp120 interaction that is critical for R5 isolates of HIV-1 in the central core of human CCR5, and we propose that this site collaborates with a previously identified region in the CCR5 amino terminus to enable gp120 binding and HIV-1 infections.

Introduction

Infection by human immunodeficiency virus type 1 (HIV-1) involves adsorption onto cell surface CD4, followed by interaction of the viral gp120·gp41 envelope glycoprotein complexes with a coreceptor (3, 38, 50, 53, 54, 65). Association of gp120 with CD4 induces a conformational change that exposes previously buried epitopes in gp120 and gp41 (159, 176, 197), including a site for gp120 interaction with the coreceptor (101, 151, 177, 193). The latter interaction is thought to cause an additional conformational change that facilitates fusion of the viral and cellular membranes, resulting in transfer of the viral cores into the cytosol (100). The known coreceptors are all G protein-coupled receptors with seven transmembrane domains (TM) that normally signal in response to cognate chemokine ligands (129). The major coreceptor for macrophagetropic (R5) isolates of HIV-1 is CCR5, a receptor for the β-chemokines MIP1α, MIP1β, and RANTES (3, 38, 50, 53, 54, 150). The coreceptor for T-celltropic (X4) HIV-1 isolates is CXCR4, a receptor for the α-chemokine SDF (18, 24, 65). R5 isolates are generally responsible for initial infection of individuals and predominate during the relatively early stages of disease, whereas X4 and R5X4 viruses accumulate in the late stages of immune system demise (42, 48, 108, 158, 163, 203).

Previous investigations have demonstrated that multiple extracellular regions of CCR5 may be important for infection by R5 isolates of HIV-1 (6, 21, 98, 139, 153, 155, 194). Studies using receptor chimeras (fusions between CCR5 and chemokine receptors unable to support HIV-1 infection) initially highlighted the contributions to infection of the amino terminal region of CCR5 and extracellular loops (ECLs) 1 and 2 (6, 21, 98, 139, 153, 155). Residues of the amino terminus of CCR5 critical to gp120 binding and infection (Y^{10}DINYY^{15}) have since been more precisely defined by other approaches including site-directed mutagenesis (55, 61, 81, 98, 117, 148, 153), whereas a potential role of ECL2 in mediating HIV-1 viral infectivity has been strengthened by a report by Wu and coworkers that a monoclonal antibody whose epitope maps to a peptide derived

from this domain (2D7) inhibits both infection and [^{125}I]gp120 binding (194). However, it is not known if 2D7 exerts its inhibitory effects by attaching to a site on CCR5 required for HIV-1 binding, or if its binding globally alters CCR5 conformation or sterically interferes with gp120 interaction with another region of the receptor. Therefore, outside of an interaction with the receptor's amino terminus, other interactions between HIV-1 and CCR5 critical to viral infection are incompletely delineated.

Recently, we found a high frequency of heterozygosity for CCR5 substitution polymorphisms in African green monkeys (AGMs), a group of primate species believed to have been infected by immunodeficiency viruses since ancient times (98). These initially identified substitutions predominantly cluster in the amino terminus (D13N, Y14N) and in ECL1 (Q93R, Q93K) and they partially inhibit infections by SIV_{agm} isolates (see Appendix A). Infectivities of R5 HIV-1 isolates were also inhibited by the Y14N, and Q93R substitutions in the context of the wild-type AGM CCR5 and by Y14N in the context of human CCR5 (98). However, although wild-type AGM CCR5 is a strong coreceptor for SIV isolates, it is a relatively weak coreceptor for R5 HIV-1 isolates (98). This observation was surprising because rhesus macaque CCR5 is a strong coreceptor for R5 HIV-1 isolates (36), but differs from AGM CCR5 in only three amino acids. Indeed, the only extracellular amino acid substitution that is unique to AGM CCR5 and absent from rhesus and human CCR5s is G163R, which occurs at the juncture of TM4 and ECL2. We now describe evidence that this site is critical for gp120 binding and for infections by all tested R5 isolates of HIV-1.

Materials and Methods

Cells and viruses. HeLa and HEK293T cells were from the American Type Culture Collection (ATCC, Rockville, MD). HeLa-CD4 (clone HI-J), and HeLa-CD4-CCR5 (clone JC.37) cells were described previously (90, 144). HeLa and HeLa-derived cells were maintained in Dulbecco's modified Eagle medium (DMEM) with 10% fetal bovine serum (FBS). HEK293T cells were maintained in the same medium supplemented with glucose (4.5 g/L). The SF162, JRFL, ADA, and BaL R5 isolates of HIV-1 were obtained from the AIDS Research and Reference Reagent Program, Division of AIDS, NIAID, NIH. HIV-1 viruses were passaged in phytohemagglutinin-stimulated human peripheral blood mononuclear cells. Medium was harvested at times of peak reverse transcriptase release, passed through a 0.45 μm pore size filter, aliquoted, and stored at -80°C. The JRCSF isolate was obtained as an infectious molecular clone, pYK-JRCSF, from the AIDS Research and Reference Reagent Program, Division of AIDS, NIAID, NIH and transfected into HeLa cells. Culture medium was harvested after 72 h, and used to infect HeLa-CD4-CCR5 cells (clone JC.37). Viral supernatants were harvested and filtered as above and the supernatant from day 3 after infection was used in this study.

CCR5 constructs and mutagenesis. The rhesus macaque CCR5 expression plasmid was the generous gift of Zhiwei Chen and Preston Marx (Aaron Diamond AIDS Research Center) (36). Constructs containing human and AGM CCR5 were previously described (98). For some experiments, the human and AGM CCR5 plasmids were mutagenized to create the AGM (R163G) and human (G163R) CCR5s by the QuickChange mutagenesis kit (Stratagene, La Jolla, CA) as directed by the manufacturer, for the remaining experiments, mutants with identical coding sequences were created by swapping the *Bcl* I to *Bgl* II restriction fragment between AGM and human CCR5s. In either case, the entire coding sequence of CCR5 was sequenced to confirm that only the desired mutation was introduced. The chimeric CCR5s were created by splicing AGM

and human CCR5 at either the *Bcl* I or *Bgl* II restriction site as described (98). The human (Y14N) site-directed mutant was described and characterized previously (98).

gp120 expression and purification. The molecular clone pYU2 was obtained from the AIDS Research and Reference Reagent Program, Division of AIDS, NIAID, NIH, and the molecular clone SF162 from Cecelia Chang-Meyer. The expression and purification of YU2 gp120 are described, with similar procedures used for expression and purification of SF162 gp120. Briefly, the YU2 envelope glycoprotein gp120 was PCR amplified from proviral DNA using synthetic oligonucleotides designed according to the published sequence. The resulting PCR product was ligated into pSC11 (106), modified to contain a multilinker sequence, to generate pJL23, and was sequence verified. The 3' antisense primer design appended a FLAG (Eastman Kodak Co., New Haven, CT) epitope to the gp120 viral envelope protein following position R498.

Plasmid pJL23 was used to generate recombinant vaccinia virus Venv-4 using standard techniques (43) for large scale expression of soluble gp120-FLAG. 16 T-225 flasks of CV-1 cells were seeded to contain approximately 1-2x10^7 cells/flask on the day of infection. Cells were infected with Venv-4 at an MOI of 5 for 2 hours in 0.1% BSA in PBS. After infection, cell monolayers were washed 2X with PBS and refed with 50 ml OptiMEM (Life Technologies, Gaithersburg, MD) per flask. After approximately 68 hours, supernatants were harvested by centrifugation at 6000 rpm for 30 min at 4°C. Clarified supernatants were supplemented with Triton X-100 (Boehringer Mannheim Corp., Indianapolis, IN) to 0.5%, quick-frozen in liquid nitrogen, and stored at -70°C.

Soluble gp120-FLAG proteins were purified by FPLC affinity chromatography using M2-anti-FLAG affinity gel (Eastman Kodak Co.) in an HR5/5 column (Amersham Pharmacia Biotech, Piscataway, NJ; bed volume ~1ml) equilibrated in TBS [50mM Tris-HCl (pH 8.0), 150mM NaCl]. Culture supernatants (500 to 1000 ml) were thawed at 37°C, supplemented to 10 μg/ml each aprotinin and leupeptin (Boehringer Mannheim Corp.), filtered through a 0.22 μm filter, and then passed continuously over the M2

column at 1ml/min at 4°C for 24 to 28 h. The resin was washed extensively with TBS and bound proteins were eluted with 100 μM synthetic FLAG peptide (Eastman Kodak Co.) in TBS. Fractions (1ml) containing gp120-FLAG were identified by Colloidal Blue staining of 10% SDS-PAGE gels (Novex, San Diego, CA). Peak fractions were pooled, snap-frozen in liquid nitrogen, and stored at -70°C.

Pooled fractions were separated from synthetic FLAG peptide and TBS by C4 reverse phase chromatography. Samples were loaded onto a 5 cm Vydac C4 analytical column at 1 ml/min in 10% acetonitrile, 0.1% TFA. Using a 25-50% gradient, gp120 eluted at approximately 36-38% acetonitrile. Samples were collected on dry ice and immediately lyophilized. Dried samples were resuspended in PBS. Relative protein concentration determinations were made using a modified gp120 capture ELISA (Intracel, Issaquah, WA) using anti-gp120 monoclonal antibody A32 from James Robinson at Tulane. Fractions with peak activity according to ELISA were subjected to amino acid analysis for final concentration determinations.

BaL gp120 was purified as previously described from the culture medium of Schneider 2 drosophila cells that were generously donated by Dr. Raymond Sweet (Smith-Kline Beecham Pharmaceuticals, King of Prussia, PA) (86).

Binding assays. [^{125}I]MIP1α 2200 μCi/mmol) was purchased from DuPont NEN Research Products, Boston MA. Conditions for competition binding assays using chemokines are similar to those described previously (179).

YU2 gp120 was iodinated by the chloramine-T method according to the procedure of Rollins et al. (152). Assay conditions for measurement of direct binding of [^{125}I]YU2 gp120 to CCR5 expressing cells, in the presence of 10 nM soluble CD4, and inhibition of binding of [^{125}I]MIP1α to CCR5 expressing cells by YU2gp120·sCD4 complexes have also been described previously (165, 193).

For gp120 binding assays done using cells expressing transmembrane bound CD4, pcDNA3 expression vectors for CD4 and CCR5 were cotransfected into HEK293T

cells by the standard DEAE-dextran/chloroquine method (35), except that the cells were plated in flasks that were treated with 0.1 mg/ml poly-L-lysine (Sigma, St. Louis, MO) for 30 min and no DMSO shock was used. Cells were seeded 48 h after transfection at 2x105 cells/well in poly-L-lysine treated 24 well tissue culture cluster plates. 24 h later cells were incubated with the indicated concentration of BaL gp120 in DMEM, 10% FBS for 30 min at 37°C. [^{125}I]MIP1β (2200 μCi/mmol, DuPont NEN Research Products, Boston MA) was added to a final concentration of 0.5 nM, and cells were incubated for an additional 30 min. The cells were washed, solubilized in 0.1 N NaOH, and counted in a gamma counter. Background counts were determined on vector-transfected cells and subtracted from the values obtained on CCR5-transfected cells. Counts were then expressed as percent binding by normalizing to values obtained with no added gp120.

Coreceptor activity assays. The assay to determine infectivities by R5 HIV-1 isolates was performed as previously described (98). Briefly, coreceptors were transiently expressed in HeLa-CD4 (clone HI-J) cells by the calcium phosphate transfection method (35). 48 h post-transfection the cultures were trypsinized and plated at $1.5x10^4$ cells/well of a 24 well cluster plate for HIV-1 infection. 72 h post-transfection cells were pre-treated with DEAE-dextran (8 μg/ml) at 37°C for 20 min, then incubated with 0.2 ml of virus diluted in DMEM, 0.1% FBS at 37°C. After 2 h the cells were fed with 1 ml DMEM, 10% FBS and incubated at 37°C for 3 days. The cells were then fixed in ethanol and infected foci were visualized by an immunoperoxidase assay (37), using as primary antibody the 0.45 μm filtered supernatant from the anti-p24 hybridoma 183-H12-5C (AIDS Research and Reference Reagent Program, Division of AIDS, NIAID, NIH). Stained foci were counted with a dissecting microscope under diffuse illumination, and values were normalized to those obtained using the same virus stock in the same experiment on cells transfected with wild-type human CCR5.

Signal transduction. *Xenopus laevis* oocytes were collected and prepared as previously described (112). CCR5 cDNAs were subcloned into the oocyte expression

CCR5 expressing cells even at concentrations of gp120 as high as 500 nM. In contrast, the IC_{50} values of sCD4 complexed gp120s in displacing MIP1α from human and rhesus receptors was between 5 and 10 nM (Fig 3-3A). The failure of [^{125}I]MIP1α to be displaced from AGM CCR5 in these experiments could be explained if [^{125}I]MIP1α and R5 gp120·sCD4 complexes bind simultaneously but noncompetitively to AGM CCR5. Alternatively, it is possible that the affinity of gp120·sCD4 for AGM CCR5 is sufficiently low so as not to be able to displace the radiolabeled chemokine.

To address this issue directly, we analyzed the binding of [^{125}I]YU2 gp120·sCD4 complexes to the receptor bearing cells. As shown in Fig 3-3B, despite the fact that cells expressing AGM CCR5 were competent to bind [^{125}I]MIP1α (Fig 3-3A), complexes of [^{125}I]YU2 gp120·sCD4 bound specifically only to cells expressing human or rhesus CCR5s, but not to cells expressing AGM CCR5.

Role of G163 in binding and infection of R5 isolates of HIV-1. The above results suggested that AGM CCR5 functions as an attenuated coreceptor for R5 HIV-1 isolates and that it binds with relatively poor affinity to the viral gp120 envelope glycoproteins. To determine if the G163R substitution unique to the extracellular surface of AGM CCR5 was responsible for its deficits in HIV gp120 binding and coreceptor function, we constructed and analyzed the human (G163R) and AGM (R163G) CCR5 mutants.

Fig 3-4 shows analyses of the coreceptor activities of the wild-type and mutant CCR5s in mediating infections by five different R5 isolates of HIV-1. Equivalent levels of surface expression of receptor on transfected HeLa-CD4 cells were indicated by binding of [^{125}I]MIP1β and/or antibodies directed against the human receptor (see Fig 3-4 legend, and data not shown). Infections were quantitated by a focal assay on HeLa-CD4 cells transfected with the corresponding pcDNA3-CCR5 expression vectors (98), and data normalized relative to the activity of wild-type human CCR5 in each assay. From this figure it is clear that as compared to human CCR5, AGM CCR5 is a much weaker coreceptor for all examined HIV-1 isolates. However, the AGM (R163G) substitution

restores the efficiency with which the mutant AGM receptor is able to mediate viral infection almost to wild-type human CCR5 levels. Reciprocally, the human (G163R) substitution reduces the coreceptor activity of the mutant human receptor to the level of wild-type AGM CCR5.

We also analyzed the binding of β-chemokines and of YU2 and SF162 gp120·sCD4 complexes to these wild-type and mutant CCR5s. As shown in Fig 3-5 (C and D), the substitutions at amino acid 163 had no significant effect on the affinities of MIP1α for the different CCR5s. Likewise, these substitutions had no effect on the affinities of human or AGM CCR5s for MIP1β (see below). However, YU2 gp120·sCD4 complexes were able to displace [^{125}I]MIP1α much more readily from human CCR5 than from the human CCR5 (G163R) mutant (Fig 3-5A). Similarly, YU2 gp120·sCD4 complexes displaced chemokine more efficiently from the AGM (R163G) mutant than from wild-type AGM CCR5 (Fig 3-5B). These results suggest that the G163R amino acid substitution found in AGM CCR5 reduces its affinity for gp120s derived from R5 isolates of HIV-1.

We substantiated this conclusion by directly analyzing the binding of [^{125}I]YU2 gp120·sCD4 complexes to cell surface CCR5. As shown in Fig 3-6, the binding of [^{125}I]YU2 gp120·sCD4 complexes to cells transfected with human CCR5 was substantially attenuated by the G163R mutation, whereas the ability to bind to AGM CCR5 was restored by the reciprocal R163G mutation. Results similar to those in Figs 3-4 and 3-5 were also obtained using gp120 derived from the R5 isolate SF162 (data not shown).

The previous results were derived by measuring the binding of cell surface CCR5 to soluble complexes of monomeric gp120 and CD4. In contrast, HIV-1 infections involve coooperative viral attachment onto cell surface CD4 followed by interactions with a coreceptor in the same membrane. Presumably, these alternative pathways for gp120 interaction with CCR5 would differ energetically, in part because the gp120 of

virus adsorbed onto cell surface CD4 would be confined in a small space at a relatively high concentration. For these reasons, we co-expressed full length human CD4 with the CCR5s in HEK293T cells, and analyzed the displacement of [^{125}I]MIP1β by gp120 derived from an R5 HIV-1 isolate (BaL). [^{125}I]MIP1β was used for this analysis because it binds with equivalent affinity to all of the CCR5s being tested, with IC_{50} values, derived using unlabeled MIP1β to displace [^{125}I]MIP1β from CCR5 bearing cells, of 6.9±1.3 nM, 3.9±0.8 nM, 5.8±1.5 nM, and 4.4±0.9 nM for human, AGM, human (G163R), and AGM (R163G) CCR5s, respectively (data not shown). As shown in Fig 3-7, the resulting [^{125}I]MIP1β displacement data were qualitatively similar to the previous results obtained using YU2 or SF162 gp120·sCD4 complexes (i.e., Figs 3-5A and B). Importantly, these data corroborate our original findings by demonstrating that gp120·CD4 complexes on cell surfaces bind more avidly to human CCR5 than to the human (G163R) CCR5 mutant, and more avidly to AGM (R163G) CCR5 than to wild-type AGM CCR5.

Signal transduction by wild-type and mutant AGM and human CCR5s. To further learn if mutations at position 163 cause major disruption of CCR5 structure or function, we quantitatively analyzed the signal transducing properties of these receptors in response to MIP1α, MIP1β, and RANTES (see Materials and Methods). As illustrated by the representative results in Fig 3-8, human and AGM CCR5s were highly responsive to β-chemokines and the signalling was not significantly affected by the substitutions at position 163. As shown previously, continued exposure to chemokines in this system is followed by down-modulation of signalling responses (112). The extents of down-modulation and the time constants for desensitization of the responses were also not signifcantly altered by the G163R mutation in human CCR5 (results not shown).

Binding of the 2D7 monoclonal antibody to CCR5 extracellular loop 2. It has previously been reported that murine monoclonal antibody, 2D7, binds to a peptide corresponding to ECL2 of human CCR5 and neutralizes chemokine interaction with

CCR5 as well as HIV-1 infections by R5 isolates (194). Indeed, we found that when HeLa-CD4 cells transfected with human CCR5 were pretreated for 30 min with 2.5 μg/ml, 5 μg/ml, 12.5 μg/ml, and 25 μg/ml of 2D7, infections by the R5 isolate JRCSF were inhibited by 24%, 58%, 77%, and 93%, respectively (data not shown). These results suggested that R5 gp120s may interact with CCR5 ECL2. Since the G163R AGM substitution is at the juncture of TM4 and ECL2 in CCR5, we analyzed the binding of 2D7 antibody to wild type and mutant human and AGM CCR5s. We found that while 2D7 bound to human CCR5 expressed in HEK293T cells (Table 3-2), it did not bind to AGM CCR5 when expressed in these cells (Table 3-2) or in HeLa/CD4 cells (data not shown). We also analyzed binding of 2D7 antibody to mutants and chimeras (see Materials and Methods) of human and AGM CCR5. The results shown in Table 3-2 suggest that both G and R at position 163 are compatible with binding of 2D7. For example, both human CCR5 and human (G163R) CCR5 bound 2D7 antibody. In addition, amino acids 1 through 168 of CCR5 site did not contribute to 2D7 binding as both human CCR5 and the AGM/human CCR5 chimera spliced at this site bound 2D7 antibody. However, a highly conservative K171R substitution present in ECL2 of both AGM and rhesus CCR5 receptors destroyed the 2D7 epitope, as evidence by the absence of 2D7 binding to a human/AGM chimera spliced at position 168. Interestingly the K171R mutation does not significantly interfere with HIV-1 infections, as this chimera is an active coreceptor (98). Taken together, our results suggest that 2D7 binds to a region of ECL2 in human CCR5 that encompasses K171, and imply that the interaction of 2D7 with this portion of ECL2 may inhibit HIV-1 interaction with a nearby site, which presumably includes or whose conformation is influenced by G163.

Discussion

Importance of the G163 region of human CCR5 for binding and infectivity of R5 strains of HIV-1. In this investigation, we analyzed differences in the R5 gp120 binding affinities and coreceptor activities of closely homologous human and non-human primate CCR5 proteins. In particular, we found that R5 gp120·sCD4 complexes bind well to human and rhesus macaque but not African green monkey (AGM) CCR5. In addition, as compared to human CCR5, AGM CCR5 is a poor coreceptor for R5 isolates of HIV-1 (e.g., see Fig 3-4), despite the fact that these CCR5s do not significantly differ in their coreceptor activities for SIV_{mac251} (36, 98) and SIV_{agm} isolates (see Appendix A). These observations were initially surprising because AGM CCR5 contains only two unique amino acid substitutions that are absent from either of these other CCR5 homologues (see Table 3-1 and Fig 3-1) and only one of these, G163R, is expected to occur in an extracellular domain of the receptor where it has the potential to interact with the viral glycoprotein. More specifically, the G163R substitution is predicted to lie at the juncture of TM4 and ECL2, a region that has not previously been unambiguously implicated in HIV-1 infections.

Using mutant human receptors, we demonstrated that the G163R substitution attenuates CCR5 binding to monomeric gp120s derived from R5 strains of HIV-1 (see Figs 3-3, 3-5, 3-6, and 3-7), and additionally is primarily responsible for lessened HIV-1 coreceptor activity (Fig 3-4). Thus, the human (G163R) CCR5 mutant binds gp120 less avidly than wild-type human CCR5 and is a poor coreceptor. Similarly, the reciprocal (R163G) CCR5 mutation of the AGM receptor enhances both gp120 binding and HIV-1 coreceptor activity. The effects of these substitutions were similar for five different R5 HIV-1 isolates and three different monomeric R5 gp120s examined, indicating that the virus interaction affected by this substitution may be universal to R5 HIV-1 strains. Furthermore, as measured by binding of [^{125}I]MIP1β, [^{125}I]MIP1α, or CCR5 specific antibodies (e.g., see Figs 3-2, 3-3, 3-5, and 3-7), the effects of the G163R substitution on

gp120 binding and HIV-1 infection are not the result of inhibition of surface expression of the receptor or of a global alteration in receptor structure. Moreover, the G163R substitution does not alter CCR5-mediated signal transduction responses to MIP1α, MIP1β, or RANTES or the kinetics or extents of CCR5 desensitization caused by prolonged exposures to MIP1α. Consequently, this substitution does not significantly perturb the binding of β-chemokines or the alternative CCR5 conformations involved in signal transduction or in receptor down-modulation.

We conclude therefore that the core region of CCR5 including G163 is critically involved in adsorption and infection of R5 HIV-1 isolates. Although we have not yet thoroughly analyzed this region by mutagenesis, we believe that it may overlap with an epitope in ECL2 defined by the 2D7 mouse monoclonal antibody that also is known to block gp120 binding and infectivity of R5 HIV-1 isolates (194). Our results suggest that 2D7 antibody binding is sensitive to a K171R substitution (see Table 3-2), a position which is close in linear sequence to G163 (see Fig 3-1).

The particular mechanistic role of G163 in viral interaction with CCR5, and the dimensions of the region within the receptor that it helps define remain unknown. However, as we have preliminary evidence suggesting that G163E and G163A human CCR5 mutants both bind R5 derived gp120s with high affinity, it is unlikely that the small, flexible nature of glycine at position 163 is required for effective interaction with the HIV-1 envelope glycoprotein. Instead, glycine, alanine, or glutamic acid at position 163 may all be permissive amino acids in the context of CCR5, with each able to play an indirect role in gp120 binding. In contrast, our data indicate that arginine at position 163 clearly is non-permissive to gp120 binding and HIV-1 infection. This may perhaps be due to the potentially positively charged, electrostatic nature of this amino acid, or alternatively to its unique ability to influence the conformation of a critically important receptor site that may be nearby. Further studies will be required to evaluate these possibilities.

Other regions of human CCR5 are also essential for gp120 binding and HIV-1 infectivity. While our results demonstrate that the G163R AGM CCR5 amino acid substitution plays a major role in inhibiting the binding of R5 gp120 glycoproteins to CCR5 and in impairing AGM CCR5's ability to mediate infection by R5 HIV-1 isolates, our data also suggest that other amino acid diffferences between human and AGM CCR5s may play a supporting role. Thus, AGM (R163G) CCR5 is only approximately 60-80% as active as human CCR5 in mediating HIV-1 infections (Fig 3-4), and binds more weakly to YU2 gp120·sCD4 complexes (Figs 3-5 and 3-6). Similarly, human (G163R) CCR5 binds YU2 gp120·sCD4 complexes much more avidly than AGM CCR5 which also contains Arg at position 163 (Figs 3-5 and 3-6). Residue substitutions outside of G163 in AGM CCR5 known to be inhibitory to HIV-1 infection and gp120 binding include I9T, N13D and Y14N, with the latter substitution having the most profound effects [(98), Fig 3-4]. Likewise, amino acids in the amino terminus of human CCR5, including amino acidsY^{10}DINYY^{15}, have been shown to be critical for R5 gp120 binding and HIV-1 infectivity (55, 61, 98, 117, 148, 153). Based on these considerations, it appears that infection by R5 strains of HIV-1 likely require binding interactions with two distinct regions of CCR5: the amino terminus of the receptor, and a region of the receptor outside of the amino terminus which encompasses the G163 region. While it may be that these two domains of CCR5 act independently in this regard, we cannot rule out the possibility that they may cooperate to form a single viral interaction site.

It is intriguing however that infections by R5 HIV-1 isolates require interactions with both the G163 and amino terminal regions of CCR5, because these regions have also been implicated in agonist binding to related receptors (167). Indeed, it has been proposed that agonists associate with chemokine receptors by a two step mechanism involving an initial interaction with the amino terminus followed by a conformational change that facilitates association with ECL 2 (125). Our results are compatible with a similar mechanism of HIV-1 binding to CCR5.

CCR5 coreceptor activities do not strictly correlate with their affinities for gp120s of R5 HIV-1 isolates. Although it has been known that gp120 binding to CCR5 is essential for infections by R5 strains of HIV-1, it has been difficult to measure gp120 affinities for CCR5 in a physiologically relevant manner. In part, this difficulty stems from the fact that infection involves trimeric gp120·gp41 complexes embedded in the virion membrane that associate with CD4 and then diffuse on cell surfaces to interact with the coreceptor (100, 144). In contrast, our binding assays employ purified soluble monomeric gp120s (Figs 3-3, 3-5, 3-6, and 3-7). While taking this caveat into consideration in the interpretation of our data, our results still strongly suggest that CCR5 coreceptor activities do not correlate precisely with their affinities for R5-derived monomeric gp120s. For example, gp120·sCD4 complexes bind with higher affinity to human (G163R) CCR5 than to AGM CCR5 (see Figs 3-5A and 3-6), yet these CCR5s have similar coreceptor activities (Fig 3-4). Furthermore, AGM CCR5 mediates infections by R5 HIV-1 isolates 10-20% as well as human CCR5 (see Fig 3-4) despite its exceedingly poor apparent affinity for gp120·sCD4 complexes. Therefore, it appears that HIV-1 infections may be surprisingly insensitive to factors that substantially decrease virus affinities for CCR5. This conclusion may have profound implications for the prospects of identifying CCR5 directed antivirals, as small molecule inhibitors of the interaction between gp120 and CCR5 which merely lower the affinity of gp120 for CCR5 may not then be able to ultimately block viral entry.

Acknowledgments

This research was partially supported by NIH grants CA67358 and CA54149 (to D.K.) and NS33270 (to M.P.K.). N.M. was partially supported by an NIH predoctoral fellowship in Molecular Hematology and Oncology (T32HL07781). The SF162, JRFL, ADA and BaL R5 isolates of HIV-1 were provided by the AIDS Research and Reference Reagent Program, Division of AIDS, NIAID, NIH: Contributed by Dr. Jay Levy, by Dr. Irvin Chen, by Dr. Howard Gendelman, and by Drs. Suzanne Gartner, Mikulas Popovic, and Robert Gallo, respectively. pYU2, pYK-JRCSF, and the anti-p24 hybridoma 183-H12-5C were also obtained from the AIDS Research and Reference Reagent Program, Division of AIDS, NIAID, NIH: contributed by Drs. Beatrice Hahn and George Shaw, by Drs. Irvin Chen and Yoshio Koyanagi, and by Drs. Bruce Chesebro and Hardy Chen respectively. Schneider 2 drosophila cells producing BaL gp120 were generously donated by Smith-Kline Beecham Pharmaceuticals, courtesy of Dr. Raymond Sweet. We are very grateful to our coworkers and colleagues Emily Platt, Susan Kozak, Chetankumar Tailor, and Ali Nouri for encouragement and helpful advice and to David Keller for assistance with preliminary studies.

Tables and Figures

TABLE 3-1. Sequence differences between primate CCR5s.

	amino acid and location[a]										
	9	13	49	52	78	123	130	163	171	198	348
CCR5[b]	NT	NT	TM1	TM1	TM2	ICL2	ICL2	ECL2	ECL2	ECL2	CT
human	I	N	M	I	F	T	V	G	K	I	I
chimp		D				S					
rhesus	T	D	I	V	L		I		R	M	
AGM	T	D	I	V	L		I	R	R		T

[a]The abbreviations used are: NT=amino terminus, TM=transmembrane sequence, ICL=intracellular loop, ECL=extracellular loop, and CT=carboxyl terminus.

[b]A blank space indicates that the sequence is identical to the reference human CCR5. The Genbank accession numbers for the CCR5 nucleotide sequences are: human, U54994; chimpanzee, AF005663; rhesus macaque, U73739; and African green monkey, U83325.

TABLE 3-2. Binding of monoclonal antibody 2D7 to human, AGM, mutant, and chimeric CCR5s.

CCR5	N-terminus	amino acid		ratio of 2D7 bound (CPM)
construct	aa 1 to 162	163	171	to MIP1β bound (CPM)
human	human	G	K	1.5±0.2
AGM	AGM	R	R	0
human (G163R)	human	R	K	0.6±0.1
AGM (R163G)	AGM	G	R	0
human/AGM (*Bgl* II)	human	G	R	0
AGM/human (*Bgl* II)	AGM	R	K	0.4±0.1
AGM/human (*Bcl* I)	AGM	G	K	0.6±0.1

Figure 3-1. Topology of human CCR5 highlighting sites of primate sequence variations.

The extracellular membrane face is above the membrane which is indicated by solid parallel lines, whereas the intracellular face is below. The splice sites used to make CCR5 chimeras are indicated by arrows with the names of the restriction enzymes that were employed. The highlighted amino acids are positions that differ among the human, AGM, rhesus macaque and chimpanzee CCR5 proteins (see Table 3-1).

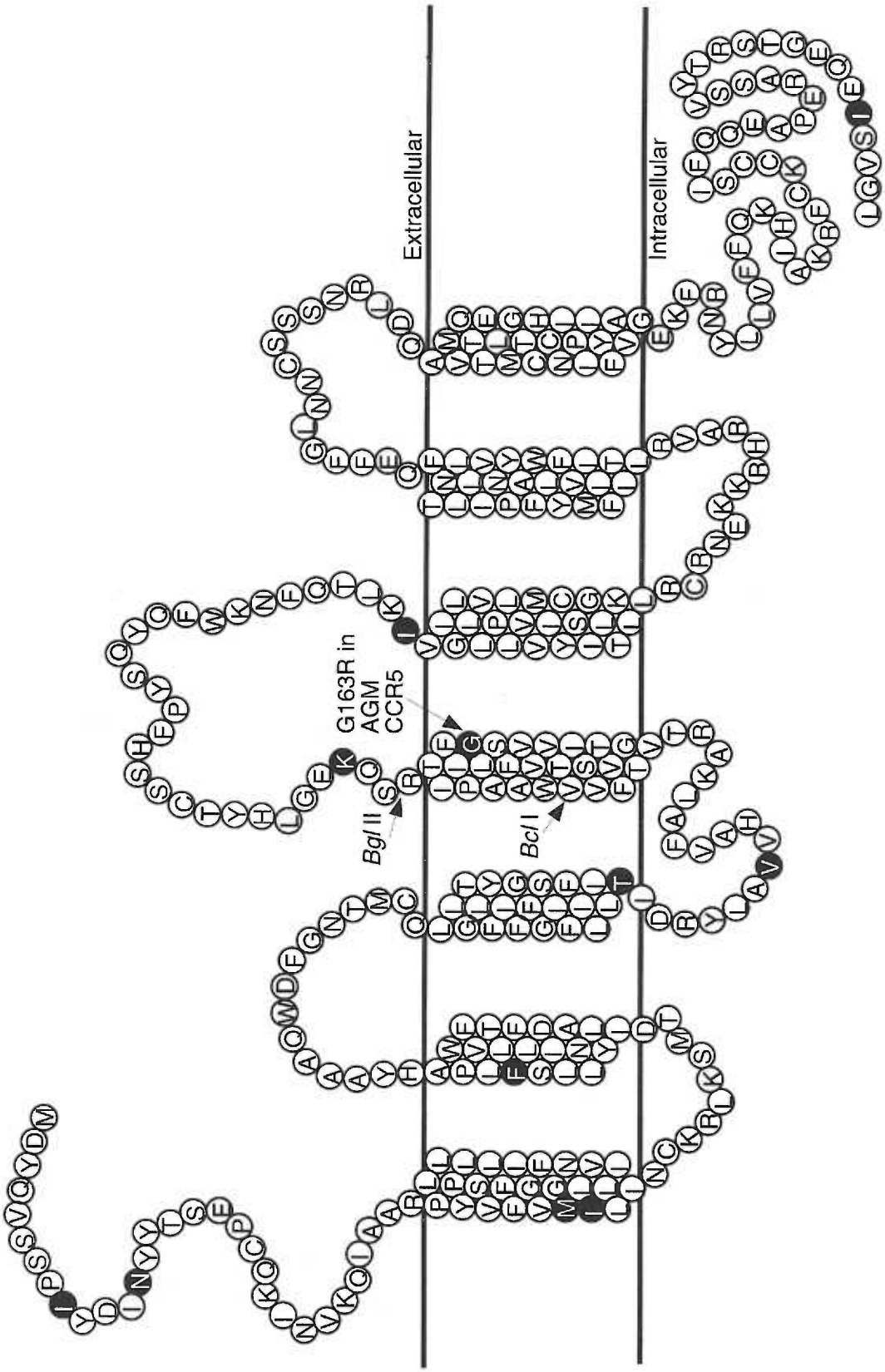
Extracellular
Intracellular
G163R in
AGM
CCR5
Bgl II
Bcl I

Figure 3-2. Human, AGM, and rhesus CCR5s bind MIP1α with high affinity.

Human (open circles), rhesus (open squares), and AGM (open diamonds) CCR5s were transiently expressed in HEK293T cells. Affinities were determined by competition binding between a fixed concentration of [^{125}I]MIP1α and increasing concentrations of unlabeled MIP1α. Results are the average of triplicate determinations from a single representative experiment. $3x10^5$ cells transfected with human or rhesus CCR5, or $7.5x10^4$ cells transfected with AGM CCR5 were used per determination.

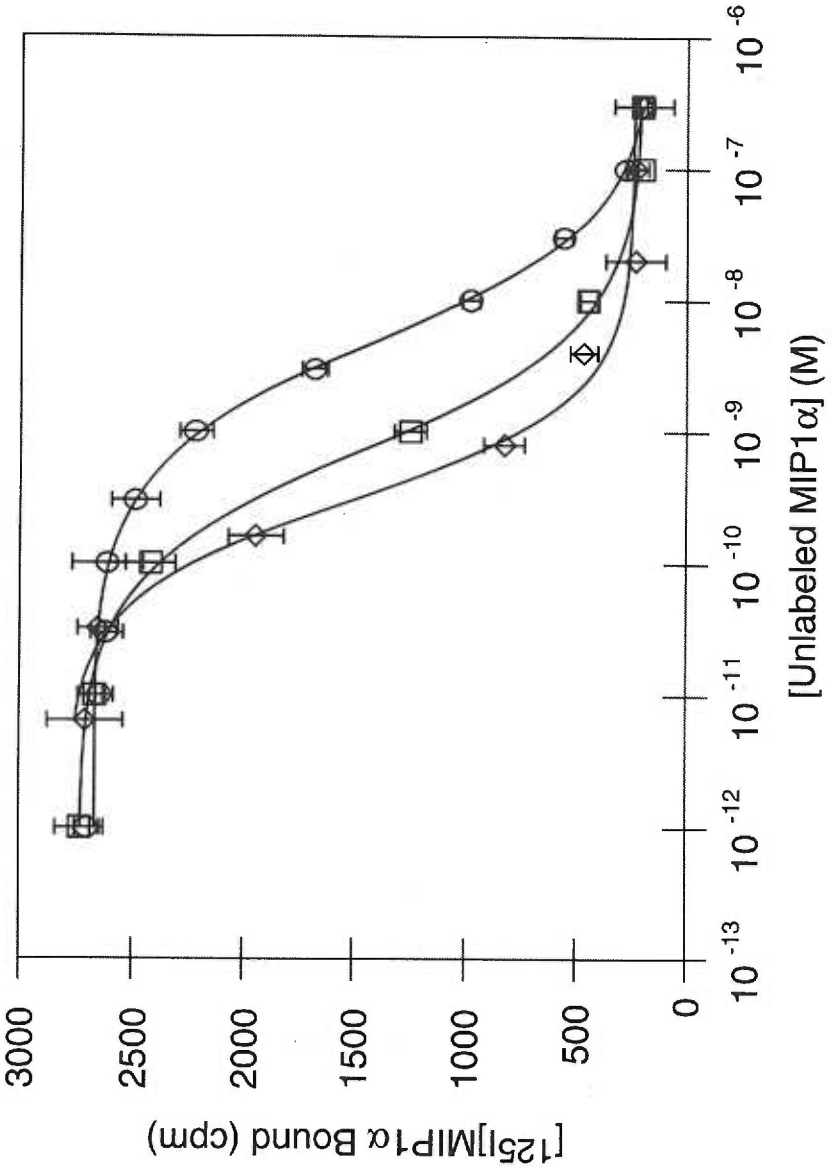
[125I]MIP1α Bound (cpm)
3000
2500
2000
1500
1000
500
0
10 -13
10 -12
10 -11
10 -10
10 -9
10 -8
10 -7
10 -6
[Unlabeled MIP1α] (M)

Figure 3-3. YU2 gp120·sCD4 complexes bind poorly to AGM CCR5.

Panel *A*: Competition binding between unlabeled YU2 gp120·sCD4 complexes and a fixed concentration of [^{125}I]MIP1α to HEK293T cells expressing human (filled triangles), rhesus (filled circles), or AGM (filled squares) CCR5s. Results are the average of triplicate determinations from a single representative experiment. $3x10^5$ cells transfected with human or rhesus CCR5, or $7.5x10^4$ cells transfected with AGM CCR5 were used per determination. Panel *B*: Direct binding of [^{125}I]YU2 gp120·sCD4 complexes to transiently transfected HEK293T cells expressing human, rhesus or AGM receptors as indicated (10^6 cells per determination). Results are the average of triplicate determinations from a single representative experiment.

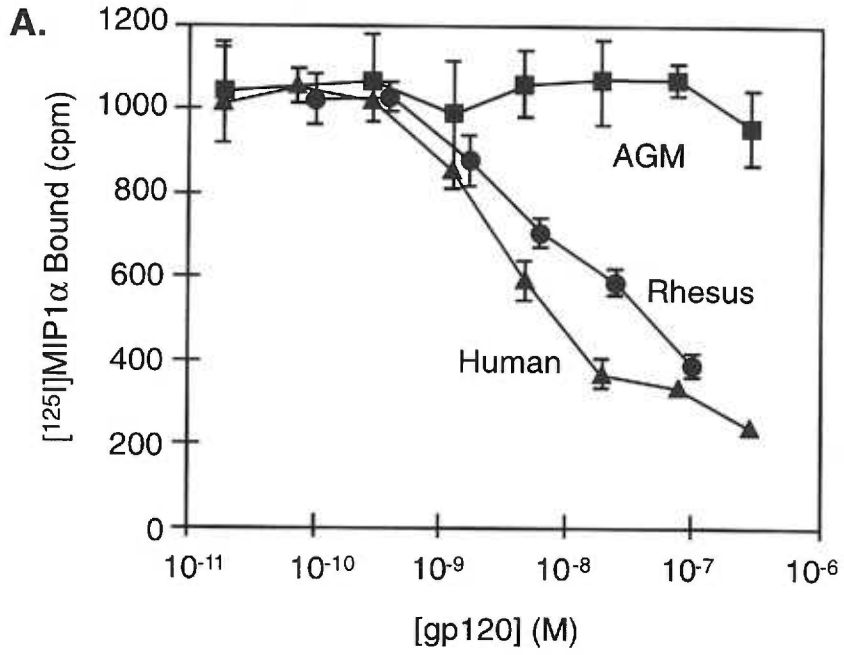
A.
1200
1000
800
600
400
200
0
[125]MIP1α Bound (cpm)
AGM
Rhesus
Human
10-11
10-10
10-9
10-8
10-7
10-6
[gp120] (M)

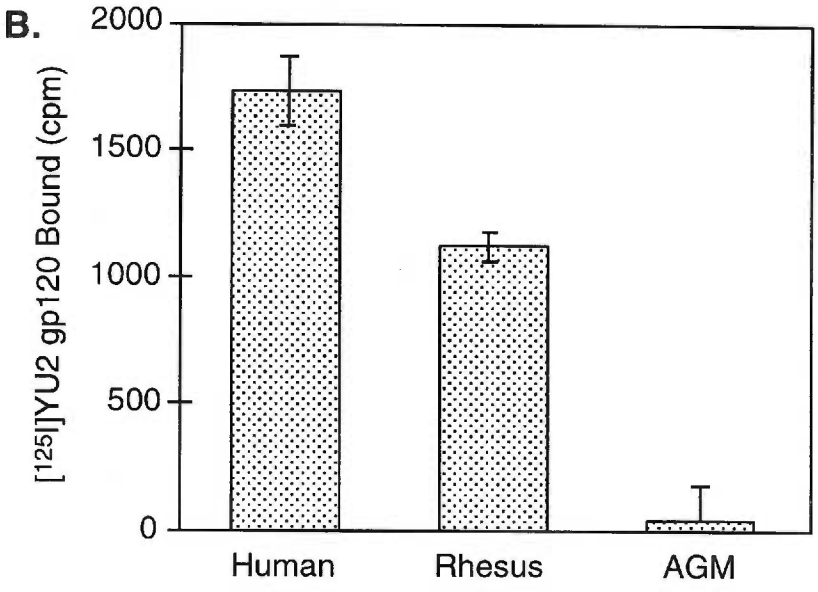
B.
2000
1500
1000
500
0
[125]YU2 gp120 Bound (cpm)
Human
Rhesus
AGM

Figure 3-4. Coreceptor activities of human, AGM, and mutant CCR5s.

Relative coreceptor activities of the CCR5 constructs was determined in HeLa-CD4 cells for each of the R5 HIV-1 isolates indicated. The coreceptor activities were normalized to the activity of human CCR5 in the same experiment. The values are the averages of two experiments and the error bars represent the range of values obtained. Mock transfected cells were transfected with pcDNA3 with no insert. The human derived coreceptors were expressed in the HeLa-CD4 cells as indicated by binding of rabbit anti-CCR5 serum as previously described (98). The values for binding from a representative experiment were: human, 15.0±0.9 CPM/μg protein; human (G163R), 8.4±2.3 CPM/μg protein; and human (Y14N), 5.0±1.6 CPM/μg protein. This antiserum does not efficiently recognize the AGM derived CCR5s, largely due to the N13D substitution in the amino terminus (97). Likewise, these coreceptors also bound the 2D7 monoclonal antibody: human, 33.3±1.0 CPM/μg protein; human (G163R), 11.6±0.7 CPM/μg protein; and human (Y14N), 26.2±0.7 CPM/μg protein. This antibody also does not efficiently recognize the AGM derived CCR5s, largely due to the K171R substitution in ECL2 (see Table 3-2). Thus, expression of AGM derived CCR5s was inferred from binding of MIP1α and MIP1β (see Figs 3-5 and 3-7, and data not shown).

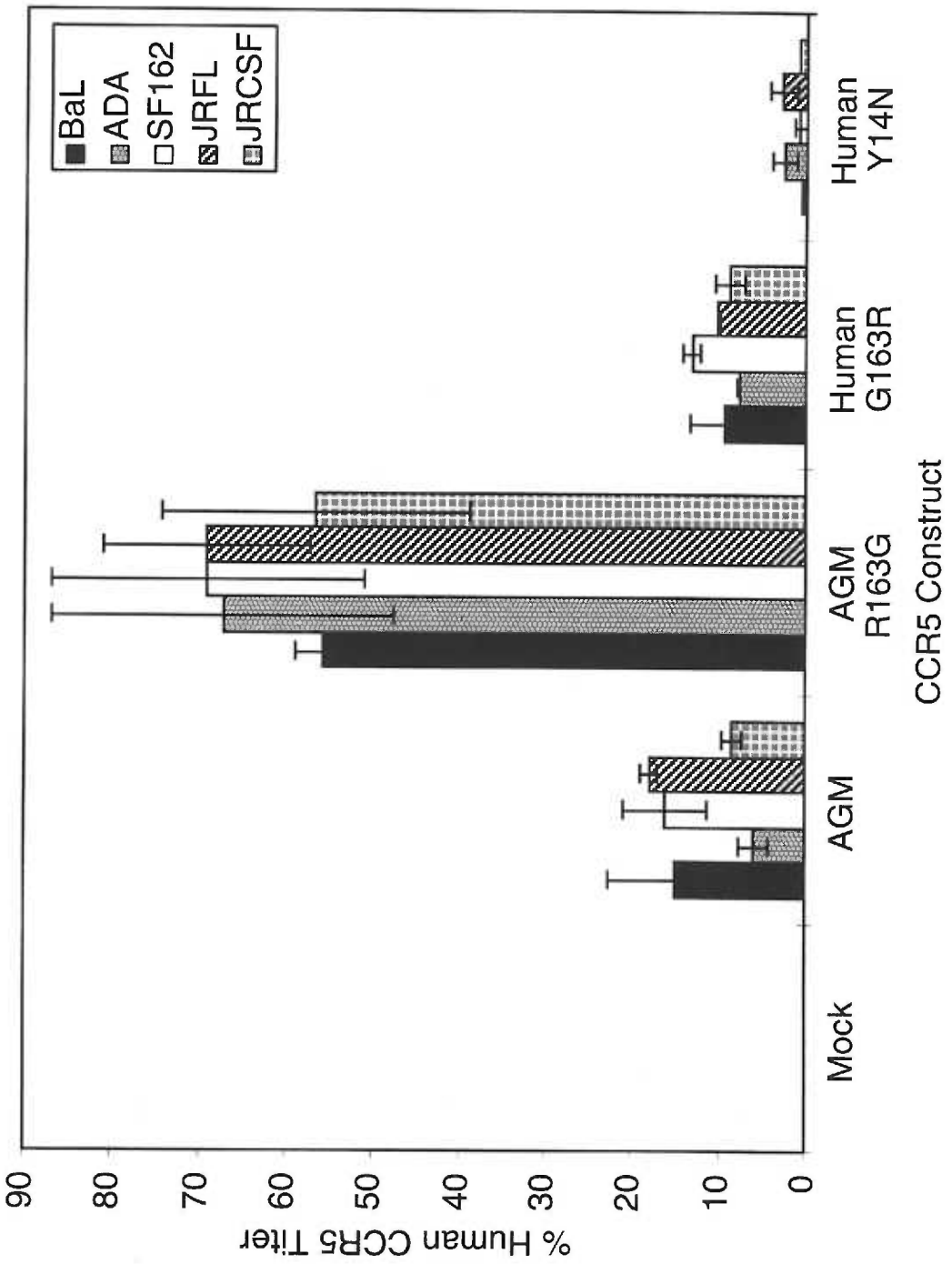
BaL
ADA
SF162
JRFL
JRCSF
% Human CCR5 Titer
0
10
20
30
40
50
60
70
80
90
Mock
AGM
AGM R163G
Human G163R
Human Y14N
CCR5 Construct

Figure 3-5. CCR5 substitutions at amino acid 163 alter the binding properties of YU2 gp120·sCD4 complexes, but not MIP1α.

For panels *A* and *B* , YU2 gp120·sCD4 complexes were used to compete for binding of [^{125}I]MIP1α to HEK293T cells. Results are the average of triplicate determinations from a single representative experiment using cells transfected with human CCR5 (open circles) or the human (G163R) receptor mutant (open squares) in panel *A*, or cells transfected with AGM CCR5 (open circles) or the AGM (R163G) receptor mutant (open squares) in panel *B*. For panels *C* and *D*, unlabeled MIP1α competes for the binding of [^{125}I]MIP1α to transiently transfected HEK293T cells expressing one of four CCR5 variants. In panel *C*, data are from cells transfected with human CCR5 (open circles) or the G163R human receptor mutant (open squares). In panel *D*, data are from cells transfected with AGM CCR5 (open circles) or the AGM (R163G) receptor mutant (open squares). In all cases, 10^5 cells were used per determination.

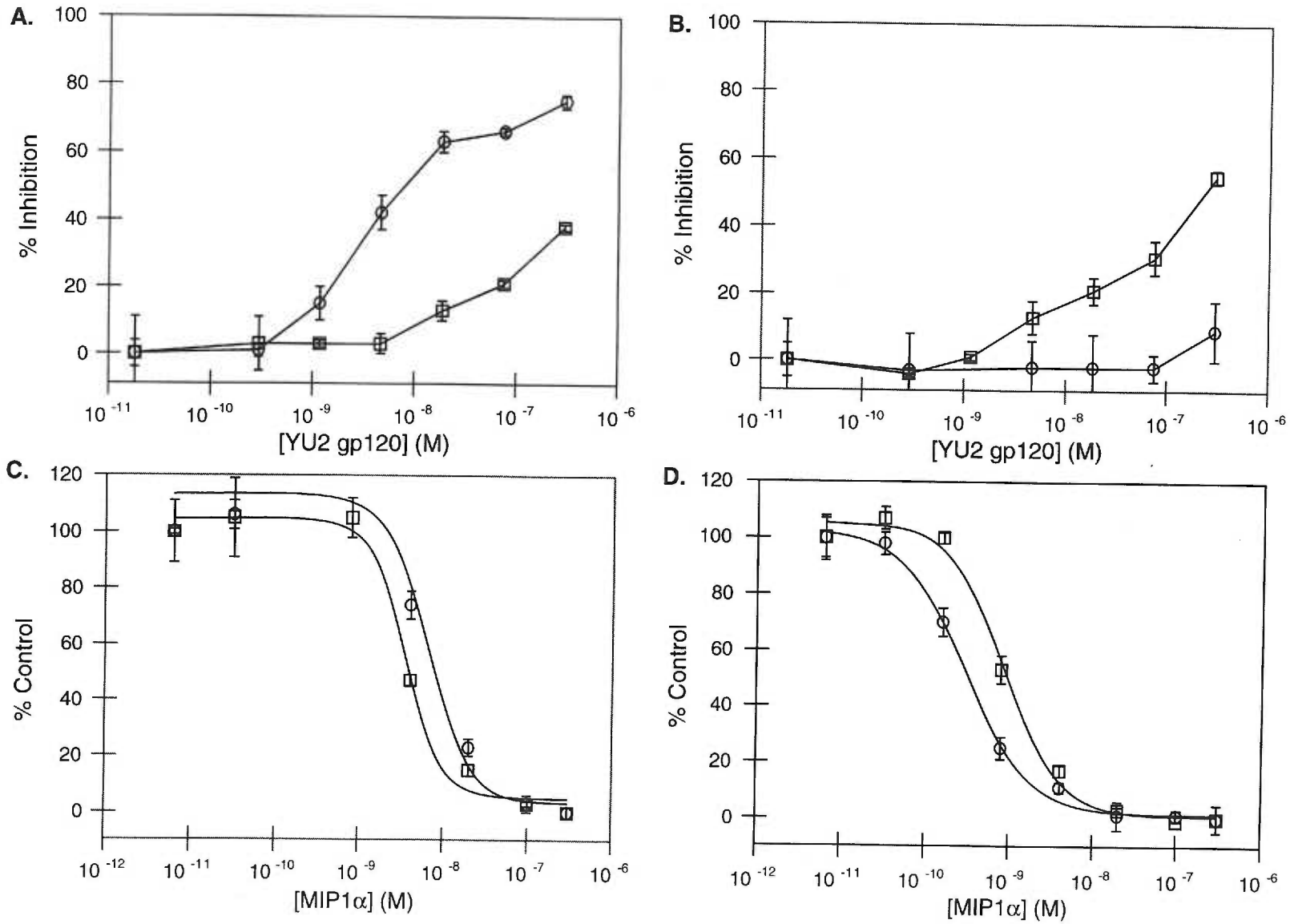
A.
100
80
60
40
20
0
% Inhibition
10 -11
10 -10
10 -9
10 -8
10 -7
10 -6
[YU2 gp120] (M)
B.
100
80
60
40
20
0
% Inhibition
10 -11
10 -10
10 -9
10 -8
10 -7
10 -6
[YU2 gp120] (M)
C.
120
100
80
60
40
20
0
% Control
10 -12
10 -11
10 -10
10 -9
10 -8
10 -7
10 -6
[MIP1α] (M)
D.
120
100
80
60
40
20
0
% Control
10 -12
10 -11
10 -10
10 -9
10 -8
10 -7
10 -6
[MIP1α] (M)

Figure 3-6. CCR5 substitutions at amino acid 163 alter the binding properties of [^{125}I]YU2 gp120·sCD4 complexes.

The direct binding of [^{125}I]gp120·sCD4 complexes was measured using transiently transfected HEK293T cells expressing human, human (G163R) mutant, AGM or AGM (R163G) mutant receptors as indicated. Results are the average of triplicate determinations from a single representative experiment, using 10^6 cells per determination.

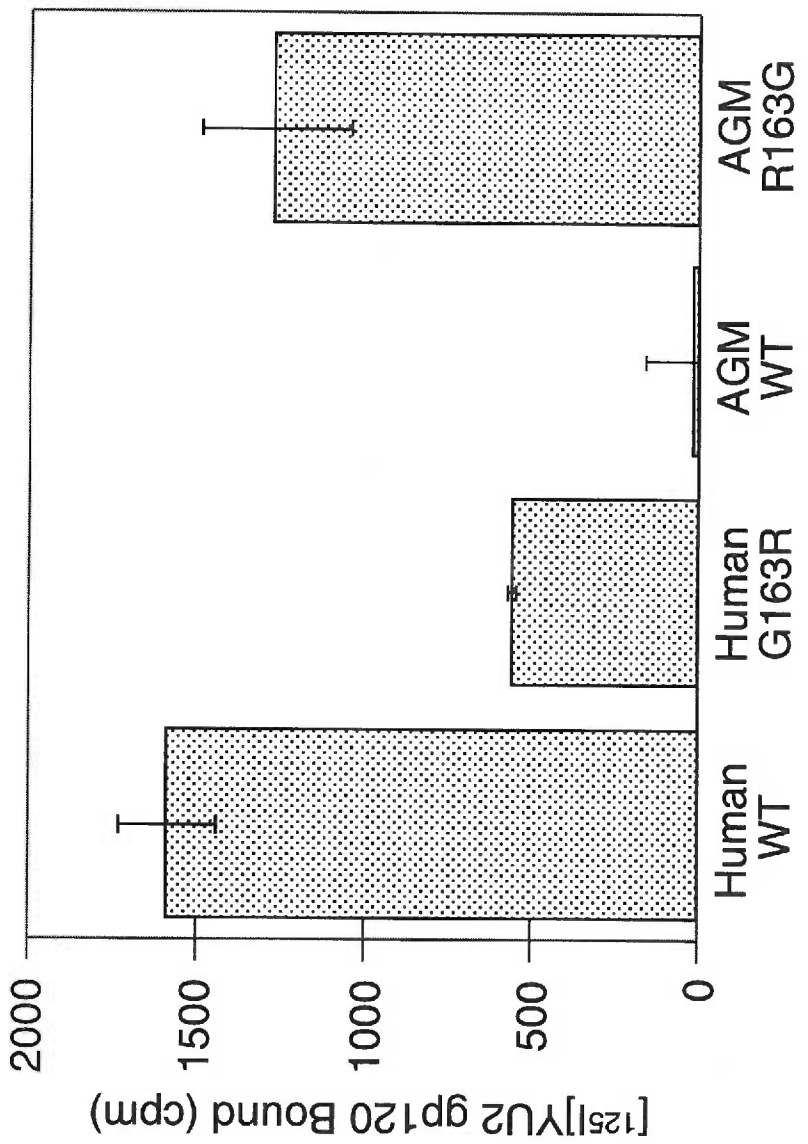
[125I]YU2 gp120 Bound (cpm)
2000
1500
1000
500
0
Human WT
Human G163R
AGM WT
AGM R163G

Figure 3-7. CCR5 substitutions at amino acid 163 alter the binding of BaL gp120 to cells coexpressing CD4 and CCR5.

BaL gp120 was used to compete for binding of [^{125}I]MIP1β to HEK293T cells cotransfected with CCR5 and CD4 expression plasmids. Panel *A*: [^{125}I]MIP1β binding to wild-type human CCR5 (open circles) and human (G163R) mutant CCR5 (open squares) in the presence of the indicated concentrations of BaL gp120. Each point is the average from 9 experiments. Panel *B*: [^{125}I]MIP1β binding to wild-type AGM CCR5 (open circles) and AGM (R163G) mutant CCR5 (open squares) in the presence of the indicated concentrations of BaL gp120. Each point is the average from 6 experiments. The error bars represent the SEM.

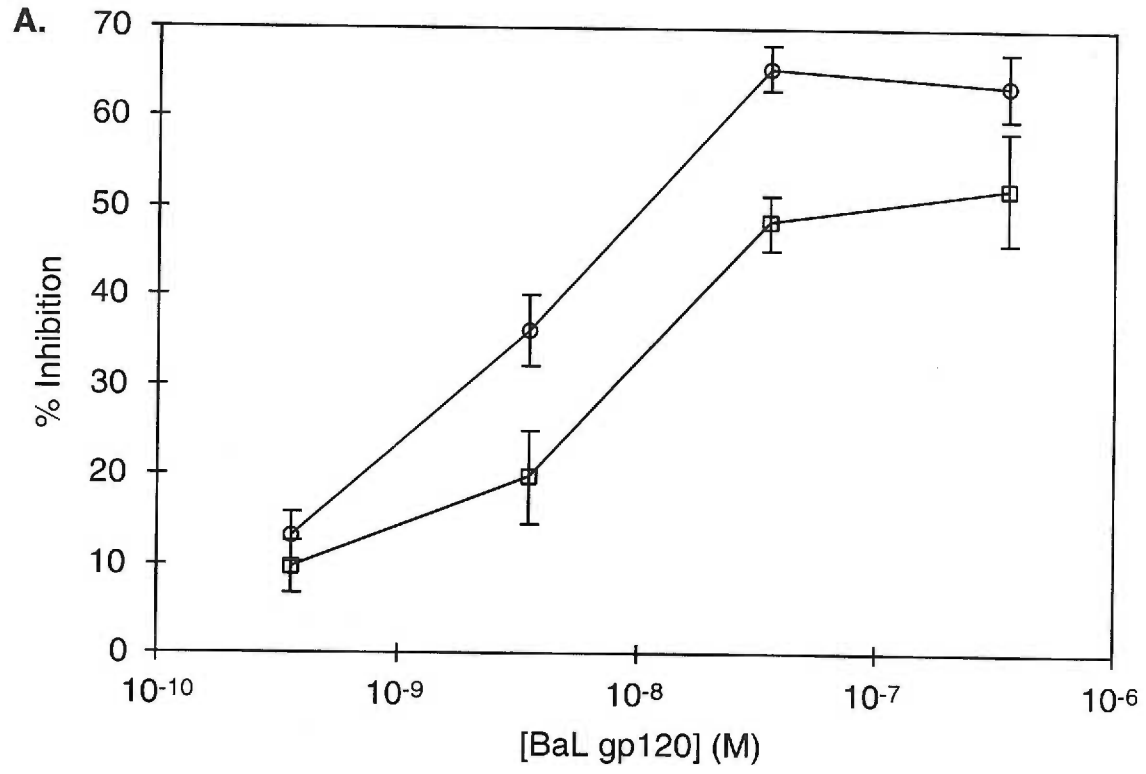
A.
70
60
50
40
30
20
10
0
% Inhibition
10-10
10-9
10-8
10-7
10-6
[BaL gp120] (M)

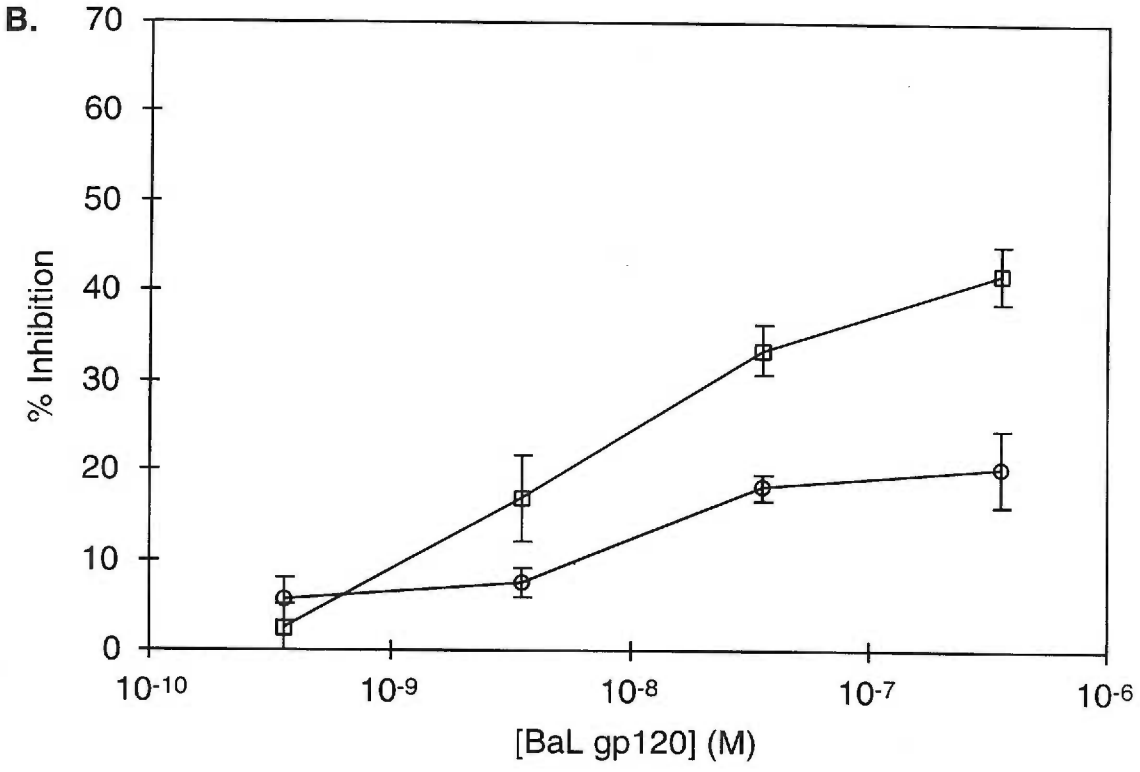
B.
70
60
50
40
30
20
10
0
% Inhibition
10-10
10-9
10-8
10-7
10-6
[BaL gp120] (M)

Figure 3-8. Effect of substitutions at amino acid 163 on activation of CCR5 by MIP1α.

Inward currents were measured by two-electrode voltage clamp in oocytes coexpressing CCR5 and Kir 3.1. In panel *A*, activation of human CCR5 (open circles) by MIP1α was compared to the corresponding activation of human (G163R) mutant CCR5 (open squares). In panel *B*, activation of AGM CCR5 (open circles) by MIP1α was compared to AGM (R163G) mutant CCR5 (open squares). Inward K^+ currents were measured at -80 mV during voltage pulses in 2 (*B*) or 3 (*A*) oocytes. Error bars in *A* represent the SEM. The EC_{50}s of activation were: human, 0.74±0.28 nM; human (G163R), 1.22±0.13 nM; AGM, 0.30±0.06 nM; and AGM (R163G), 0.30±0.01 nM

Chapter 4. Cooperation of Multiple CCR5 Coreceptors Required for Infections by Human Immunodeficiency Virus Type 1

Shawn E. Kuhmann, Emily J. Platt, Susan L. Kozak and David Kabat*

Department of Biochemistry and Molecular Biology

Oregon Health Sciences University

Portland, OR 97201-3098

Running Title: Quantitative Studies of the CCR5 Coreceptor

*With whom to correspond:

Telephone: (503) 494-8442

Fax: (503) 494-8393

E-mail: kabat@ohsu.edu

Abstract

In addition to the primary cell surface receptor CD4, CCR5 or another coreceptor is necessary for infections by human immunodeficiency virus type 1 (HIV-1), yet the mechanisms of coreceptor function and their stoichiometries in the infection pathway remain substantially unknown. To address these issues, we studied the effects of CCR5 concentrations on HIV-1 infections using wild-type CCR5 and two attenuated mutants, Y14N at a critical tyrosine sulfation site in the amino terminus and G163R in extracellular loop 2. The Y14N mutation converted a YYT sequence at positions 14-16 to an NYT consensus site for N-linked glycosylation, and the mutant protein was shown to be glycosylated at that position. The relationships between HIV-1 infectivities and CCR5 concentrations were sigmoid shaped curves that were dramatically altered in different ways by these mutations. Both mutations shifted the curves by factors of approximately 30-150-fold along the CCR5 concentration axis, consistent with evidence that they reduce affinities of virus for the coreceptor. In addition, the Y14N mutation specifically reduced the maximum efficiencies of infection that could be obtained at saturating CCR5 concentrations. The sigmoid shaped curves for all R5 HIV-1 isolates were quantitatively consistent with a simple mathematical model, implying that CCR5s reversibly associate with cell surface HIV-1 in a concentration dependent manner, that approximately 4-6 CCR5s assemble around the virus to form a complex needed for infection, that both mutations inhibit assembly of this complex but only Y14N also significantly reduces its activity, and that HIV-1 on cell surfaces is inactivated at a substantial rate that has a critical influence on HIV-1 infectivities. Thus, HIV-1 adsorbed onto cell surfaces is in a competitive race between inactivation and an infection pathway that requires virus association with multiple CCR5s to form a membrane fusion pore.

Introduction

Infections by human immunodeficiency virus type 1 (HIV-1) are initiated by virus binding followed by fusion of the viral membrane with the host cell plasma membrane. This process is dependent on "knobs" in the viral envelope that consist of gp41 integral membrane trimers and associated gp120 surface subunits (reviewed in reference 34). Binding of HIV-1 onto the primary receptor CD4 induces a conformational change in gp120 that exposes a previously buried site for association with a coreceptor (100, 101, 151, 177, 193). Although several chemokine receptors can function at least weakly as HIV-1 coreceptors, CCR5 and CXCR4 are believed to be most important *in vivo* (3, 38, 50, 53, 54, 65, 107, 202). Viruses (termed R5) that use CCR5 are involved in transmission between individuals, whereas variants that use CXCR4 (termed X4) often form during disease progression (42, 108, 158, 160). Following HIV-1 interaction with a coreceptor, a trimeric coiled coil is extended from the gp41 subunits into the cellular membrane (34). It is believed that membrane fusion is subsequently initiated by formation of a small pore (34).

Several extracellular regions of CCR5 have been implicated in its coreceptor function (6, 21, 98, 139, 153, 155). An amino terminal region containing sulfated tyrosines at Y3, Y10, Y14, and Y15 is critical for gp120 binding and infectivity (55, 61, 62, 98, 148). Previously, we identified a Y14N polymorphism in the CCR5 of African green monkeys (AGMs) that severely disrupts HIV-1 coreceptor activity (98). Another important region occurs in extracellular loop 2 (ECL2). Wild-type AGM CCR5 differs from human CCR5 by a G163R substitution that severely inhibits R5 gp120 binding and HIV-1 infections without affecting chemokine binding or signaling (166). Monoclonal antibody 2D7 recognizes a nearby epitope in ECL2 of CCR5 that includes K171 and E172 and it also inhibits R5 gp120 binding and HIV-1 infections (103, 135, 166, 194). Studies of CCR5 chimeras are also compatible with these conclusions (6, 21, 98, 155, 184).

Information concerning the effects of CCR5 cell surface concentrations on its coreceptor activity would potentially elucidate the dynamic cell surface interactions that control HIV-1 infections and disease. Although natural variation in CD4 and coreceptor concentrations and changes in their levels during activation and differentiation of T-lymphocytes and macrophages correlate with cellular susceptibilities to HIV-1 infections (130, 138, 178, 195), the basic mechanisms that underlie these effects have not been analyzed. Indeed, standard assays for coreceptors have employed transiently transfected cell populations that contain unknown and heterogeneous quantities of CD4, CCR5, and/or CXCR4 (6, 21, 23, 55, 61, 98, 139, 148, 153, 155, 166, 184). In this study, we quantitatively analyzed efficiencies of R5 HIV-1 infections of human HeLa-CD4 cells as functions of the cell surface concentrations of wild-type CCR5 or of mutants CCR5(Y14N) and CCR5(G163R), and we developed a mathematical model that quantitatively fits the data. Our results suggest that multiple CCR5s reversibly associate with HIV-1 on cell surfaces to form a complex that is essential for the membrane fusion step of infection.

Materials and Methods

Cells and viruses. 293T cells were from the American Type Culture Collection (Rockville, MD) and maintained in Dulbecco's modified Eagle medium (DMEM) supplemented with 10% fetal bovine serum (FBS) and 4.5 g/liter glucose. All other cells were maintained in DMEM with 10% FBS. HeLa-CD4 (clone HI-J), and HeLa-CD4/CCR5 (clones JC.53, and JC.10) cells were described previously (90, 144). HeLa-CD4-CCR5 cells expressing the Y14N and G163R variants of human CCR5 were obtained by ligating the BamHI and XhoI fragment from the pcDNA3 expression vectors for the mutant CCR5s (98, 166) into pSFF (19) cut with the same enzymes. The retroviral vector SFF-CCR5 was prepared and used to infect HI-J cells as previously described (144). Cell clones were isolated by limiting dilution. Clones were screened for expression and clonality by immunofluorescence microscopy, and expression levels were quantitated by radioimmunoassay and quantitative immunofluorescent flow cytometry as described below.

The R5 SF162, JRFL, ADA, and BaL isolates of HIV-1 were obtained from the AIDS Research and Reference Reagent Program, Division of AIDS, NIAID, NIH; contributed by Dr. Jay Levy, by Dr. Irvin Chen, by Dr. Howard Gendelman, and by Drs. Suzanne Gartner, Mikulas Popovic, and Robert Gallo, respectively. The JRCSF isolate was obtained as an infectious molecular clone, pYK-JRCSF, from the AIDS Research and Reference Reagent Program, Division of AIDS, NIAID, NIH, contributed by Drs. Irvin Chen and Yoshio Koyanagi. High titer stocks of these HIV-1 isolates were prepared as previously described (166).

Transient expression of CCR5s in HeLa-CD4. Single amino acid substitutions in human CCR5 were introduced in the pKS(+)-CCR5 vector (98) using the Quickchange site-directed mutagenesis kit (Stratagene, La Jolla, CA) as directed by the manufacturer. The coding region was sequenced to ensure that only the desired mutation was introduced, excised with BamHI and XhoI, and ligated into pcDNA3 (Invitrogen Corp.,

San Diego, CA). HI-J cells were transiently transfected with the pcDNA3-CCR5 expression vectors using the Superfect reagent (Qiagen Inc., Santa Clara, CA) according to the manufacturer's instructions. Expression of mutant CCR5s cells was confirmed after 48 h by immunofluorescent flow cytometry and coreceptor function was determined by focal infectivity assay as described below.

Focal infectivity assays. The focal infectivity assay (37) was used to titer preparations of R5 HIV-1. Briefly, cells were plated at $5x10^3$ cells/well in 48-well cluster plates. 24 h later the cells were pre-treated with DEAE-dextran (8 μg/ml) at 37°C for 20 min, then incubated with 0.1 ml of virus diluted 10, 100, or 1000 fold in DMEM, 0.1% FBS at 37°C. After 2 h the cells were fed with 1 ml DMEM, 10% FBS and incubated at 37°C for 72 h. The cells were then fixed in ethanol and infected foci were visualized by an immunoperoxidase assay (37), using as primary antibody the 0.45 μm filtered supernatant from the anti-p24 hybridoma 183-H12-5C (AIDS Research and Reference Reagent Program, Division of AIDS, NIAID, NIH; contributed by Drs. Bruce Chesebro and Hardy Chen). Titers on specific cell lines were determined by counting the stained foci in the well with the lowest dilution that contained less than 200 foci/well and multiplying by the dilution factor. Titers were normalized to those on JC.53 cells expressing high levels of CD4 and CCR5 where the titers of the concentrated stocks were approximately 10^6 ffu/ml for JRCSF and $5x10^5$ ffu/ml for BaL (or 100 and 50 foci/well at the 1000 fold dilution). The lower limit of detection was 100 ffu/ml or approximately 0.01 to 0.05 percent of the JC.53 titer. Syncytia were scored by microscopic examination of the foci in a given well for the presence of multinucleated cells as described (96).

Measurement of cell surface CCR5. To estimate the CCR5 antigen density on HeLa-CD4/CCR5 cells, the Dako Qifikit (Dako Corporation, Carpenteria, CA) for quantitative analysis of indirect immunofluorescence staining in flow cytometry was used according to the manufacturer's instructions. Cells were lifted in 8 mM EDTA, 0.9% w/v NaCl. Primary antibody staining was with 25 μg/ml of mouse anti-human CCR5

monoclonal 2D7 (PharMingen, San Diego, CA). The FACScalibur flow cytometry system (Becton Dickinson Immunocytometry Systems, San Jose, CA) was used to record all flow cytometry data. The results were processed according to the manufacturer's instructions. In addition to flow cytometry, a quantitative radioimmunoassay was used to quantitate cell surface CCR5. Anti-CCR5 monoclonal 2D7 (5 μg/ml) was incubated with cells seeded at $2x10^5$ cells/well in 24 well cluster plates for 1.5 h at 37°C. The cells were then sequentially incubated with 1:250 goat anti-mouse IgG serum (Organon Teknika, Durham, NC), and 1:250 [^{125}I]protein A (0.4 μCi/ml, 2 to 10 μCi/μg, NEN Life Science Products, Boston, MA) at 37°C for 1 h each. Cells were washed, lysed in 0.1 N NaOH, and counted in a gamma counter. Counts were normalized to the protein concentration determined by the Coomasie blue method (Bio-Rad Laboratories, Hercules, CA). In each experiment cell lines were assayed in duplicate wells, and multiple cell lines from the HeLa-CD4/CCR5 panel previously described (144) were assayed to ensure the colinearity of this assay with that previously described using a saturating concentration of a polyclonal rabbit anti-CCR5 serum (144).

[^{35}S]sulfate labeling, glycosidase treatment, and electrophoretic analysis of CCR5. $2x10^6$ 293T cells in 100 mm dishes were transfected with the appropriate pcDNA3-CCR5 construct using the Superfect reagent as instructed by the manufacturer, and labeling was performed 24 h later. Metabolic labeling with [^{35}S]sulfate was performed as described (62) with the following modifciations. Approximately 75% confluent cultures of transfected 293T cells or HeLa-CD4/CCR5 (clone JC.53) cells were incubated with 1 mCi [^{35}S]sulfate (NEN Life Science Products) for 16 h in 8 ml sulfate free minimum essential medium (MEM) with 5% FBS dialyzed against PBS. The MEM was prepared from the Selectamine kit (Life Technologies, Grand Island, NY) with a modified 10x Eagle's balanced salt solution with $MgCl_2$ substituted for $MgSO_4$. After labeling, the crude cellular membrane fraction was prepared as described (98). Membrane proteins were solubilized in lysis buffer (0.5% NP-40 in PBS with protease inhibitors) and

immunoprecipitated with 5C7 mouse-anti human CCR5 monoclonal antibody (AIDS Research and Reference Reagent Program, Division of AIDS, NIAID, NIH; contributed by LeukoSite, Inc.) followed by protein-A sepharose (Sigma, St. Louis, MO) as described (62). Alternatively, labeled cells were solubilized in lysis buffer, the nuclei were removed by centrifugation at 500xg for 20 min, and CCR5 was immunoprecipitated with 5C7. In both cases, the immunoprecipitated proteins were separated by 0.1% sodium dodecyl sulfate (SDS), 8% polyacrylamide gel electrophoresis, and separated proteins transferred to NitroPure nitrocellulose membranes (Micron Separations, Inc., Westboro, MA). The ^{35}S labeled proteins were detected by autoradiography of the nitrocellulose membrane. In other experiments, membrane fractions from unlabeled cells were electrophoresed, transferred to nitrocellulose, and CCR5 was detected by Western immunoblotting with rabbit anti-human CCR5 serum and chemiluminescence reagents as described (98). For experiments in which O-glycosidase treatment was required, CCR5 immunoprecipitates were resuspended in 30 µl of buffer (PBS, 1% Triton X-100, 0.5% SDS) and treated at 37°C for 2 h with a cocktail of glycosidases containing 50 mU neuraminidase, 3 mU O-glycosidase, 13 mU β-galactosidase, and 100 mU N-acetyl-β-D-glucosaminidase. N-glycosidase was performed by resuspending membrane preparations in 4 µl of 1% SDS in PBS, and denaturing by heating to 65°C for 10 min. 1 U of peptide N-glycosidase F was added in 40 µl of 1% NP-40 in PBS and incubated at 37°C for 4 h. All enzymes were from Roche Molecular Biochemicals, Indianapolis, IN.

gp120 and MIP1β binding. The competition of [^{125}I]MIP1β binding by BaL gp120 or by unlabeled MIP1β was performed essentially as previously described for 293T cells transiently transfected with CD4 and CCR5 (166). HeLa-CD4/CCR5 and HeLa-CD4/mutant CCR5 clones were seeded at $5x10^4$ cells per well of a 24 well cluster plate and incubated 24 h later with 3 nM [^{125}I]MIP1β (2200 µCi/mmol, NEN Life Science Products), with the addition of purified BaL gp120 (166) or unlabeled MIP1β (Peprotech,

Rocky Hill, NJ) as required, in DMEM with 10% FBS for 1 h at 37°C, washed three times, and lysed in 0.1 M NaOH. The lysates were analyzed in a gamma counter.

Mathematical analysis of the infectivity results. Our analysis is closely correspondent with our infectivity protocol, in which virus is adsorbed for 2 h onto cell clones that contain different amounts of CCR5 but a constant amount of CD4, and the foci of infection are counted after 72 h. Thus, we are measuring the integrated total quantity of infections that occur in these cultures rather than the rates of infection. This requires the integration of rate equations over the time period of our assays. When preparations of HIV-1 are incubated with HeLa-CD4 (clone HI-J) cells for 2 h at 37°C, a small fraction of the infectious virions adsorb onto the cells to form virus·$(CD4)_n$ complexes. Thus, removing the virus-containing medium onto a fresh culture results in the same titer on both culture dishes (90). These titers are directly proportional to the concentrations of virus, to the numbers of cells in the cultures and to the adsorption times (90). Consistent with evidence that coreceptor associations occur secondarily after CD4 interaction (100, 101, 151, 177, 193), the rate or extent of virus adsorption is unaffected by the presence or concentration of a coreceptor (95, 124, 144). Based on previous studies and theoretical considerations, it is likely that this adsorption would be essentially irreversible when the CD4 concentration is above a low trace threshold of approximately 10^3-10^4 CD4/cell (15, 72, 164), which is substantially below the level of 1.5×10^5 CD4/cell on the HI-J clone of HeLa-CD4 cells used in this investigation (90, 141). This irreversibility, which is not necessary to our model, occurs because the cells act as multivalent absorbers rather than as a dispersed solution of receptors (15, 72, 164). Our previous evidence was consistent with the hypothesis that the number n of CD4s in the virus·$(CD4)_n$ complexes is dependent on the cell surface concentration of CD4, and that the number of accessible binding sites for CCR5 is proportional to n (144), as expected (100, 101, 151, 177, 193). Thus, when the CD4 concentration was lowered, the number of binding sites for CCR5 was reduced and a higher concentration of CCR5 was required

for efficient infections by R5 HIV-1 isolates (144). The HI-J clone of HeLa-CD4 cells contains a high concentration of CD4 and therefore a trace concentration of wild-type CCR5 (c.a., 10^3 CCR5/cell) was adequate for efficient infections (144). These earlier results established that CCR5 interacts with the virus·$(CD4)_n$ complexes in a concentration dependent manner. Accordingly, we assume that the virions initially adsorb in equal numbers onto all of the HI-J-derived cell clones and that infection requires a cell surface interaction of the adsorbed virus (v) with CCR5 that can be approximated as follows:

$$v\cdot(CD4)_n + mCCR5 \rightleftarrows v\cdot(CD4)_n\cdot(CCR5)_m \longrightarrow \text{infection} \qquad 1.$$

Therefore the rate of infection at any instant is

$$\frac{di}{dt} = k_1\,[v\cdot(CD4)_n\cdot(CCR5)_m] \qquad 2.$$

where k_1 is the rate constant for the final reaction and di/dt is the rate of infection. By algebra from the equilibrium in equation 1 this yields the solution that

$$\frac{di}{dt} = \frac{k_1\,[v]\,[CCR5]^m}{K_d + [CCR5]^m} \qquad 3.$$

where K_d is the dissociation constant for the equilibrium in equation 1.

The concentration [v] of total infectious virus on the cell surfaces at any time *t* after initial adsorption declines due to infection and inactivation. Hence,

$$\frac{d[v]}{dt} = -\left(\frac{k_1\,[CCR5]^m}{K_d + [CCR5]^m} + k_2\right)[v] \qquad 4.$$

where k_2 is the rate constant for inactivation. Integration of equation 4 gives

$$[v] = [v]_0\, e^{-\left(\frac{k_1\,[CCR5]^m}{K_d + [CCR5]^m} + k_2\right)t} \qquad 5.$$

where $[v]_0$ is the concentration of infectious virus that is initially adsorbed onto the cell surfaces.

Substitution of equation 5 into equation 3 gives:

$$\frac{di}{dt} = \left(\frac{k_1 [v]_0 [CCR5]^m}{K_d + [CCR5]^m} \right) e^{-\left(\frac{k_1 [CCR5]^m}{K_d + [CCR5]^m} + k_2 \right) t} \quad 6.$$

Integrating equation 6 between the initial uninfected state at t=0 and the final state at t=∞ (we can assume that all of the viable virus has been removed from the cell surfaces long before the cultures are fixed at 72 h) gives the result

$$i_{total} = \frac{k_1 [v]_0 [CCR5]^m}{(k_1 + k_2) [CCR5]^m + k_2 K_d} \quad 7.$$

It is useful to define the term $E=k_1/(k_1+k_2)$. From equation 7 it follows that $i_{total}=[v]_0E$ at high levels of CCR5. Thus, E is the fraction of initially adsorbed virus that successfully infects the culture when the specific CCR5 is not limiting. We normalize the infectivity data for each assay relative to the infectivity obtained in the control culture (clone JC.53) that expresses a large amount of wild-type CCR5, thus where $i_{total}=[v]_0E_{wt}$. This gives:

$$i_{rel} = \frac{E_{rel} [CCR5]^m}{[CCR5]^m + \frac{k_2 K_d}{k_1 + k_2}} \quad 8.$$

where i_{rel} is the normalized infectivity for the assay and $E_{rel}=E/E_{wt}$. Thus E_{rel} is the asymptote of the sigmoid shaped plot of i_{rel} *versus* [CCR5] for the specific panel of cell clones being assayed. Taking the logarithm of equation 8 gives:

$$\log\left(\frac{i_{rel}}{E_{rel} - i_{rel}} \right) = \log\left(\frac{k_1 + k_2}{k_2 K_d} \right) + m \log[CCR5] \quad 9.$$

Consequently, the model predicts that a plot of $\log[i_{rel}/(E_{rel}-i_{rel})]$ *versus* log[CCR5] should give a straight line with a slope *m* and intercept of $\log[(k_1+k_2)/(k_2K_d)]$. It is important to realize that use of equations 8 and 9 is valid regardless of the time period used for virus adsorption. The 2 h adsorption time employed in our protocol could be considered to be the sum of multiple brief periods, each of which would yield the same i_{rel} *versus* [CCR5] plot. This occurs because the infectivity measurements are normalized relative to values obtained using highly susceptible JC.53 cells that express wild-type

CCR5 and because all of the cell clones including JC.53 adsorb the same quantities of HIV-1 (see above).

Although we have assumed in equation 4 that inactivation of cell surface-adsorbed virus affects all species of virus, it might alternatively be postulated that inactivation would be accelerated in the fusion–competetent assemblages. Indeed, such an assumption has been considered previously for influenza A virus (131). According to this idea, assembly of a fusion-competent complex destabilizes the virus and sensitizes it to either infection or inactivation. This hypothesis would predict that $i_{rel}=E_{rel}$ at all CCR5 concentrations. However, our results clearly show that i_{rel} values depend strongly on CCR5 concentrations (see Results). Hence, our results support the assumption inherent in equation 4.

It is notable that a kinetic analysis of the initial rates of infection could be done after a brief period of virus adsorption using equation 3. Normalizing such initial rates relative to the values observed with wild-type CCR5 (JC.53) cells would give $(di/dt)_{rel}=k_{1,rel}[CCR5]^m/(K_d+[CCR5]^m)$. It would be predicted that the asymptotes of the sigmoid shaped plots of $(di/dt)_{rel}$ *versus* [CCR5] would equal $k_{1,rel}$. Hence a plot of $\log\{(di/dt)_{rel}/[(di/dt)_{rel,max}-(di/dt)_{rel}]\}$ *versus* log[CCR5] would give a straight line with a slope *m* and intercept of $\log(1/K_d)$. This is strikingly similar to the analysis of the cumulative infection data as shown above in equation 9. This implies that the graphical methods used to analyze the sigmoid-shaped curves obtained from kinetic measurements or from cumulative infectivity data would be identical and would be expected to give the same estimates of *m*. The only difference in the graphical analysis would be the meaning of the intercepts. Although kinetic analyses would also be useful, they are more difficult because the infections would have to be synchronized and because estimates of di/dt require several infectivity assays. For these reasons, we used i_{rel} measurements and equation 9 for this initial investigation.

Results

Mutagenesis of CCR5 at positions Y14 and G163. We constructed several substitution mutants at the Y14 and G163 positions of CCR5, and we tested their coreceptor activities by a standard transient transfection-focal infectivity assay with HeLa-CD4 (clone HI-J) cells (90, 98). These mutant CCR5s were all expressed at similar levels on the cell surfaces (see Fig 4-1, legend). Fig 4-1 shows the normalized titers of infection mediated by these CCR5s relative to wild-type CCR5 for five different R5 isolates of HIV-1. In contrast to the relatively large functional differences revealed by the studies described below, most of these substitutions caused only slight 2-3-fold reductions in these assays. Similar assays of alanine-scanning mutants have previously also found only small effects except for several sites in the critical amino terminal region (23, 55, 71, 148). Despite the limitations of this methodology, the data in Fig 4-1A confirm the importance of CCR5 residues Y14 and G163 in R5 HIV-1 infections. Y14F eliminates the anionic sulfated hydroxyl group and causes significant attenuation, and further inhibitions are caused by A, Q, or N substitutions, whereas replacement with the alternative anionic amino acid E has the least effect. At position 163, the greatest inhibitions occur when G is replaced with the two largest amino acids assayed, R and W.

Properties of the CCR5(Y14N) and CCR5(G163R) proteins. As shown in Fig 4-2A and B, we have confirmed the sulfation of CCR5 by labeling cells with [^{35}S]sulfate followed by immunoprecipitation of the CCR5 and electrophoresis in the presence of 0.1% SDS. Consistent with previous evidence for tyrosine sulfation and O-linked glycosylation of CCR5 (62), the sulfate labeling of CCR5 was not reduced by enzymatic removal of O-linked oligosaccharides (e.g., see Fig 4-2B). Interestingly, CCR5(Y14N) is relatively heterogeneous in size, with approximately 60-70% of the molecules having larger apparent M_r than wild-type CCR5 or CCR5(G163R). Accordingly, this mutation converts the YYT sequence at positions 14-16 into an NYT consensus site for N-linked glycosylation, and endoglycosidase F converts the larger CCR5(Y14N) components into

the smaller-sized species (Fig 4-2C). As discussed below, N-linked glycosylation of CCR5(Y14N) may have a small effect on our assays using this mutant.

We also analyzed the effects of the G163R and Y14N mutations on interactions of CCR5 with MIP1β and with a previously characterized gp120 dervied from the BaL isolate of R5 HIV-1 (95, 166). Interestingly, MIP1β bound strongly and specifically onto cells that expressed these mutant CCR5s. Moreover, the apparent affinities of MIP1β for the wild-type and mutant CCR5s were identical as indicated by the displacement of [^{125}I]MIP1β caused by increasing concentrations of unlabeled MIP1β (see Fig 4-3B). However the maximum level of MIP1β binding relative to the total quantity of cell surface CCR5 was lower for CCR5(Y14N) than for wild-type CCR5 or CCR5(G163R). Thus, in a representative experiment as described in Fig 4-3 legend, the maximum binding of MIP1β normalized relative to the binding of 2D7 monoclonal antibody was 0.7 for wild-type CCR5, 0.7 for CCR5(G163R), and 0.3 for CCR5(Y14N). These data imply that, relative to wild-type CCR5 and CCR5(G163R), approximately 60% fewer of the CCR5(Y14N) molecules on the cell surfaces are able to interact with MIP1β, and we presume that these inactive molecules are the N-glycosylated components.

In agreement with previous reports (166, 177, 193), we also found that BaL gp120 was able to competitively displace [^{125}I]MIP1β from the surfaces of cells that contained CD4 and wild-type CCR5 (see Fig 4-3A). In contrast, the displacement of [^{125}I]MIP1β from CCR5(G163R) was highly attenuated in agreement with previous evidence (166), and we were unable to detect any significant gp120 induced displacement of this labeled chemokine from cells that expressed CCR5(Y14N). These results suggest that the Y14N and G163R mutations both reduce CCR5 affinity for R5 gp120.

Dependencies of R5 HIV-1 infections on cell surface concentrations of wild-type CCR5, CCR5(Y14N), and CCR5(G163R). Previously, we used the HI-J clone of HeLa-CD4 cells (c.a., 1.5x10^5 CD4/cell) to construct derivative clones that stably express discrete amounts of wild-type CCR5 over a broad range of concentrations (144); and we

have now employed these same methods to construct panels of HeLa-CD4/CCR5(Y14N) and HeLa-CD4/CCR5(G163R) cell clones. Table 4-1 shows the CCR5 expression levels on these cell clones, including data for two clones (JC.10 and JC.53) that express widely different amounts of wild-type CCR5.

We measured infectivities of the R5 HIV-1 isolates BaL and JRCSF using the cell clones listed in Table 4-1. Each cell clone was analyzed 3-8 times with each virus in parallel with identical assays in the JC.10 and JC.53 cells that express wild-type CCR5, and the infectivities were normalized relative to the titers of the same viruses in the JC.53 cells. As illustrated by the representative results in Fig 4-4A, the titers in the JC.53 and JC.10 control cells were not significantly different despite the 32-fold difference in their concentrations of CCR5, confirming our previous conclusion that a trace of wild-type CCR5 suffices for maximally efficient R5 HIV-1 infections (144). This is consistent with other evidence that all HI-J-derived clones initially adsorb equal amounts of HIV-1 and that wild-type CCR5 then functions efficiently even at low concentrations to facilitate the entry process (see Mathematical analysis in Materials and Methods). This is expected because HI-J cells have a high concentration of CD4 and therefore would be predicted to function as an efficient polyvalent trap for binding HIV-1 that diffuses into contact with the cell surfaces (15, 164) and because sites for binding CCR5 only become accessible after the virus has attached to cell surface CD4 (100, 101, 151, 177, 193). In contrast, efficient infections of these viruses in the CCR5(G163R) and CCR5(Y14N) panels required much higher concentrations of the coreceptor (see Fig 4-4), consistent with evidence in Fig 4-3 that these mutations reduce coreceptor affinities for R5 gp120. The infectivity curves were half-maximal when the cells expressed approximately $3x10^4$ CCR5(G163R)/cell, which is at least 30-times higher than the threshold concentration of wild-type CCR5 required for the same efficiency of infection (144). In the Y14N clonal panel, the midpoints of the infectivity curves (c.a., $1.3\text{-}1.7x10^5$ CCR5(Y14N)/cell) were shifted even further toward high concentrations. These functional differences between

the wild-type and mutant CCR5s are extremely large compared with the differences observed in Fig 4-1. In contrast to these results with R5 isolates of HIV-1, the presence or quantities of these CCR5s on the surfaces of the HI-J-derived cell clones had no effect on titers of the X4 control virus NL4-3 (144; also, data not shown).

Several other features of these results are notable. First, the plots appear to have sigmoid shapes (see Fig 4-4). This was confirmed by studies using other R5 HIV-1 viruses (see below). It implies that multiple CCR5 molecules may be required for R5 HIV-1 infections. Second, the sigmoid curves plateau at different efficiencies of infection. Third, as described in detail below, these results strongly imply that inactivation or dissociation of cell surface-adsorbed R5 HIV-1 must be a significant process that has major influence on the infectivity assays.

Microscopic analyses of the immunoperoxidase-stained foci of infection in these cultures suggested that the limiting step in utilization of the Y14N mutant CCR5 occurred at or before the membrane fusion step of infection (see Fig 4-5). Specifically, the foci of infection in the control cultures with wild-type CCR5 consisted mostly of large syncytia. In contrast, the infected foci in cultures with CCR5(Y14N) consisted of small syncytia or single cells. This was especially striking in the clones that contained low amounts of CCR5(Y14N), in which the foci were principally single infected cells. The sizes and frequencies of syncytia were also significantly correlated with cell surface concentrations of CCR5(G163R).

Quantitative evaluation of the infectivity data. The mathematical model that is rationalized and derived in Materials and Methods provides a simple quantitative approach for interpreting the infectivity results shown in Fig 4-4. This model predicts that a plot of $\log[i_{rel}/(E_{rel}-i_{rel})]$ *versus* log[CCR5] should give a straight line with a slope *m*, where i_{rel} is the titer of the virus in a cell clone divided by the titer in the control JC.53 cells that express wild-type CCR5, E_{rel} is the asymptote for each sigmoid-shaped curve in Fig 4-4, and *m* is the number of CCR5s required to mediate R5 HIV-1 infection.

The data for several infections of our clonal panels are plotted in this manner in Fig 4-6, and a compilation of the midpoints of the sigmoid-shaped curves (EC_{50} values) and of the estimated *m* values are shown in Table 4-2. Because the efficiencies of JRCSF virus infection in the majority of the CCR5(Y14N) cell clones were near or below the limit of detection (see Fig 4-4), these results were not analyzed in Fig 4-6. However, we isolated three adapted variants of the JRCSF virus that were better able to infect the CCR5(Y14N) clonal panel (142), and the data obtained using these adapted variants are included in Fig 4-6 and Table 4-2. Consistent with our model, the data points for different viruses in different clonal panels appear to fall on straight lines. Moreover, within experimental error these straight lines have the same slopes. This is a prediction of the model because the number *m* of CCR5s required to form a fusion-competent complex should be independent of the specific R5 isolates of HIV-1 or of the CCR5 that is analyzed.

Discussion

Importance of coreceptor concentrations in HIV-1 infections. In agreement with previous correlations observed in populations of human T-lymphocytes and macrophages (130, 138, 178, 195), our experiments provide strong evidence for the importance of CCR5 concentrations in controlling cellular susceptibilities to R5 HIV-1 infections. Moreover, the relationships between viral infectivities and cell surface CCR5 concentrations are nonlinear functions with sigmoid shapes that are altered in two distinct ways by CCR5 mutations (see Fig 4-4). Both Y14N and G163R mutations reduce the affinities of virus-CCR5 interactions and dramatically shift the infectivity curves toward higher CCR5 concentrations. In addition, the Y14N mutation substantially reduces the maximum infectivities that occur at very high CCR5 concentrations (i.e., the asymptotes in Fig 4-4).

Inactivation of HIV-1 critically influences coreceptor assays. Our results strongly suggest that inactivation or dissociation of cell surface-associated virus is a significant process that influences HIV-1 titers, especially in assays using low concentrations of weak coreceptors. Because natural R5 HIV-1 isolates bind first to CD4 and only secondarily to CCR5 (100, 101, 177, 193), and because all of the cell clones we used were derived from the HI-J clone of HeLa-CD4 cells that contains a large quantity of cell-surface CD4 (c.a., 1.5×10^5 CD4/cell) (90, 141), it is very likely that all of the cell clones incubated with aliquots of an HIV-1 preparation would initially adsorb the same quantity of virus. Indeed, the fact that R5 HIV-1 titers are identical in the JC.10 and JC.53 cells (see Fig 4-4) despite the enormous difference in their concentrations of CCR5 (see Table 4-1), supports this idea. This conclusion is also supported by previous studies of HIV-1 (90, 124) and other viruses (164) and by theoretical considerations (15, 72, 164). In essence, the HI-J cells function as polyvalent absorbers to efficiently bind HIV-1 that diffuses into contact with cell surfaces and CCR5 then influences a post-adsorption step of the infection pathway. Consequently, the inefficient infections of many cell

clones (see Fig 4-4) implies that inactivation or dissociation of cell surface-adsorbed virions must occur at a rate that significantly competes with infection. Although this conclusion does not depend on our mathematical modeling, the process of inactivation is also implicit in this model, which appears to be quantitatively compatible with out data. Thus, according to equation 8, i_{rel} values would equal 1 at all CCR5 concentrations if the rate constant (k_2) for virus inactivation were zero. Without a process of HIV-1 inactivation or dissociation, even cells with low concentrations of highly attenuated CCR5s would eventually be able to efficiently harvest the adsorbed infectious virions into the cell.

This analysis suggests that CCR5 mutations can reduce HIV-1 titers by two mechanisms. One involves a reduction in CCR5 affinity for the adsorbed virus, resulting in a lowered efficiency of assembling an intermediate that is required for membrane fusion. Secondly, mutations can drastically reduce the rates or efficiencies at which the fusion competent assemblages function. In this case, the competitive process of virus inactivation becomes more predominant. This inhibition of the apparent rate constant for fusion is severe in the case of CCR5(Y14N) and is slight in the case of CCR5(G163R), implying that the amino terminal sulfated region of CCR5 may be exceptionally important for this step of infection. It is also evident from the substantially different i_{rel} maxima for BaL and JRCSF viruses in the CCR5(Y14N) panel despite their similarity in the CCR5(G163R) panel that the reduction in the maximum efficiency of fusion is not a property of the mutant coreceptors *per se*, but is caused by an inefficient interaction between CCR5(Y14N) and the specific virus.

Stoichiometry of CCR5 in mediation of R5 HIV-1 infections. The infectivity curves (e.g., Fig 4-4) have sigmoid shapes and are quantitatively consistent with the simple mathematical analysis described in Materials and Methods and shown in Fig 4-6 and Table 4-2. In accordance with our model, the data points in Fig 4-6 for different viruses in different clonal panels appear to fall on straight lines that have the same slopes

within experimental error. In addition to the conclusions described above, this suggests that infections of R5 HIV-1 isolates require the concerted action of multiple CCR5 molecules. Moreover, our analyses imply that the required number *m* of CCR5s is probably in the range of 4-6 (see Table 4-2). Interestingly, this conclusion is consonant with studies of influenza A virus, which have suggested that the membrane fusion step of infection may require a collar of approximately 3-6 viral hemagglutinin-receptor complexes surrounding a membrane pore (14, 25, 46), and with evidence that multiple *env* trimers are necessary for HIV-1 infection (69, 102). In addition, receptor clustering may be required for infections by other retroviruses (168).

In part because of assumptions inherent in any process of mathematical modeling, we emphasize that the *m* values in Table 4-2 should be considered to be approximations. Furthermore, only a portion of the cell surface CCR5 may be available for HIV-1 infections, perhaps because of sequestration in different microenvironments (28, 103). This is especially likely in the case of CCR5(Y14N) because a fraction (c.a., 60-70%) of these molecules contain N-linked oligosaccharides (e.g., see Fig 4-2). This glycosylation appears to prevent interactions with MIP1β (see Fig 4-3) and it seems likely that such a large modification would also prevent interactions of R5 HIV-1 with this region of CCR5 that is known to be critical for coreceptor activity (55, 61, 62, 98, 148). Consequently, we believe that the CCR5(Y14N) molecules that lack N-linked oligosaccharides are responsible for the weak infectivity mediated by this mutant coreceptor. If the functionally relevant fraction of CCR5 were reduced by any mechanism, our estimated EC_{50} values would be correspondingly lowered, whereas our estimates of *m* would be unaltered (see equation 9). Similarly, this factor would not affect our estimates of the asymptotes in Fig 4-4. Consequently, this type of error would not affect any of our conclusions about infection mechanisms. However, there are indications that CCR5 may dimerize on cell surfaces (13), and we have observed CCR5 complexes in some of our electrophoresis studies (e.g., see Fig 4-2). If this is correct, our estimates of *m* would

imply that this number of dimers rather than monomers must associate with R5 HIV-1 to mediate infections. These uncertainties will require additional investigations.

We consider it likely that our *m* estimates are the minimum number of CCR5s required for R5 HIV-1 infections and that viral assemblages with larger numbers of CCR5 would also be competent to undergo the membrane fusion reaction, perhaps even at an accelerated rate. This factor would potentially result in sigmoid plots in which i_{rel} values would continue to increase somewhat at very high CCR5 concentrations and in corresponding deviations from linearity in the log-log plots (e.g., Fig 4-6). Our data have not provided clear indications concerning this matter.

We also emphasize that the sigmoid shaped plots of HIV-1 infectivity *versus* CCR5 concentration were obtained using mutant CCR5s. Because wild-type CCR5 functions efficiently even at barely detectable trace concentrations, it was not possible to resolve the low concentration region for this coreceptor (e.g., see Fig 4-4 and reference (144). Nevertheless, we believe that the cooperativity and stoichiometry of coreceptors in the infection pathway should be identical for all CCR5s and HIV-1 isolates, and our results are consistent with this hypothesis (see Fig 4-6 and Table 4-2).

General conclusions. These results provide strong evidence that CCR5 reversibly associates in a concentration dependent manner with R5 HIV-1 on the surfaces of CD4-positive cells to form a complex that is essential for infections, that this complex contains at least 3-6 CCR5 molecules, and that virus dissociation or inactivation occurs at a competitively significant rate that can substantially influence HIV-1 titers in cell culture assays. Since lymphocytes and macrophages also express widely different amounts of CD4 and coreceptors at distinct stages of activation and differentiation (104, 130, 178), it seems likely that similar HIV-1 inactivation processes may occur *in vivo*. Our results also reveal that mutations in CCR5 can strongly inhibit assembly of the essential complexes and/or the functional activities of the complexes. Similarly, distinct viruses can interact with CCR5 with different affinities and with different fusion efficiencies.

However, our results do not establish whether the number of CCR5 molecules necessary for infection must all coordinately interact with a single gp120-gp41 trimer or with distinct trimers. We favor the latter hypothesis because similar estimates have been made for the number of influenza A hemagglutinin trimers required to form a "fusion pore" (14, 25, 46), and because evidence suggests that the mechanisms for membrane fusion are highly concordant for these viruses (34). Consistent with these conclusions, it appears that multiple gp120-gp41 trimers are required for HIV-1 infections (69, 102).

Based on these results, we suggest that careful control of CD4 and coreceptor expression levels will be important for understanding the functions of these molecules and for evaluating drugs that may interfere with these early steps of infection. As illustrated by comparison of Figs 4-1 and 4-4, inhibitory effects of CCR5 mutations and their mechanistic implications can be severely underestimated at high expression levels or by using conventional coreceptor assays. In addition, because infectivity assays but not syncytial assays are sensitively affected by virus inactivation (see above) these methods should not be assumed to be correspondent. Finally, our data implies that the effectiveness of drugs targeted at CCR5 would likely depend on the cell surface concentrations of CD4 (144) and CCR5 in the specific cells. Drugs that inhibit affinities of coreceptors for HIV-1 would probably be less beneficial than drugs that also block the functional activities of the assembled coreceptor complexes.

Acknowledgements

This research was supported by NIH grant 2 RO1 CA67358. E.J.P. was supported in part by NRSA postdoctoral fellowship I F32 AI09735 from the NIH. We are grateful to our coworkers and colleagues Navid Madani, Chetankumar Tailor, Mariana Marin, and Jean-Michel Heard for encouragement and critical advice. We are additionally grateful to Antony Bakke and Randy Smith for their assistance with flow cytometry, and to Adriana Weissman for conducting preliminary experiments.

Tables and Figures

TABLE 4-1. CCR5 expressing clones derived from HI-J cells

Cell Line	CCR5 expression[a] (10^4 molecules/cell ± SEM)
CCR5(Y14N) clones	
JYN.8	4.2±0.5
JYN.5	5.6±0.4
JYN.4	6.0±0.4
JYN.15	8.3±0.1
YD2	9.4±0.6
JYN.2	10±0.7
JYN.3	10±0.2
JYN.14	13±0.6
JYN.2-19[b]	16±1.1
YB8[b]	17±1.4
JYN.2-15[b]	17±1.6
JYN.2-27[b]	25±3.9
CCR5(G163R) clones	
JGR.H5	1.8±0.3
JGR.H4	1.9±0.2
JGR.L2	2.3±0.3
JGR.H3	2.7±0.2
JGR.L10	3.2±0.2
JGR.L6	4.1±0.2
JGR.H7	5.7±0.2
JGR.H11[b]	9.8±1.7
wild-type CCR5 clones	
JC.10[b]	0.6±0.1
JC.53[b]	19±1.3

[a]Expression was determined by radioimmunoassay as described in Materials and Methods except where noted. The background binding was determined on HI-J cells which do not express CCR5 and was subtracted from the values shown. The background

was equivalent to values obtained when the anti-CCR5 monoclonal 2D7 was omitted and was approximately 15% of the binding measured on JC.10 cells. Cell lines on which the number of 2D7 antibody binding sites had been determined by quantitative flow cytometry were included in the same radioimmunoassay and used to generate a standard curve to convert the binding values to the equivalent number of antibody binding sites. Values represent the mean of 4 or 5 independent assays ± SEM.

[b]Expression of CCR5 in these clones was determined by quantitative flow cytometry as described in Materials and Methods. The background fluorescence was determined on HI-J cells which do not express CCR5 and was subtracted from the values shown. The background was equivalent to values obtained when the anti-CCR5 monoclonal 2D7 was omitted and was approximately 30% of the fluorescence measured on JC.10 cells. The values obtained were converted to the number of 2D7 antibody binding sites using a calibration curve generated by beads conjugated with known quantities of mouse IgG (see Materials and Methods). Values represent the mean of 3 to 7 independent assays ± SEM.

TABLE 4-2. Mathematical analysis of infectivity data

clonal panel	virus	R	m	EC_{50} (CCR5/cell)
CCR5(G163R)	JRCSF	0.91	5.4±1.1	$3.2x10^4±0.3x10^4$
	BaL	0.92	3.0±0.6	$3.0x10^4±0.2x10^4$
CCR5(Y14N)	JRCSF(YB8 adapted#1)	0.96	6.1±0.7	$1.4x10^5±0.1x10^5$
	JRCSF(YB8 adapted#2)	0.96	6.5±0.7	$1.3x10^5±0.1x10^5$
	JRCSF(JYN.4 adapted)	0.83	4.3±1.7	$6.4x10^4±0.7x10^4$
	BaL	0.96	6.6±0.7	$1.2x10^5±0.1x10^5$

Data plotted in Fig 4-6 were fit to equation 9 as given in Materials and Methods using Kaleidagraph (Synergy Software, Reading, PA). The calculated linear correlation coefficient is reported in the R column. The EC_{50} value (the CCR5 concentration where $i_{rel}=E_{rel}/2$) is calculated based on $EC_{50}{}^m=k_2K_d/(k_1+k_2)$. This allows the comparison of the midpoints of curves with different estimates of *m*. The EC_{50} and *m* values are reported ± the standard error as calculated by Kaleidagraph.

Figure 4-1. Infections of HeLa/CD4 (clone HI-J) cells transiently transfected with site-directed mutants of CCR5.

Site-directed mutants of CCR5 with alterations at Y14 and G163 in a mammalian expression vector were transiently transfected into HI-J cells. Titers of the 5 different R5 HIV-1 isolates indicated were determined after 48 h by a focal infectivity assay which uses $p24^{gag}$ immunoperoxidase staining to detect foci. The titers are normalized to those determined on cells transfected with the wild-type CCR5 expression vector in the same assay. The infection assay was repeated 3 or 4 times, with error bars representing the SEM. Expression was measured by immunofluorescent flow cytometry, using 2D7 as the primary antibody. The percent of transfected cells ranged from approximately 5% to 30% between assays, however values were similar for different constructs within a given assay. The transfection efficiencies for one representative assay were: wild-type, 8.9%; Y14A, 10.8%; Y14E, 9.0%; Y14F, 10.3%; Y14N, 10.1%; Y14Q, 10.0%; G163A, 7.0%; G163E, 10.1%; G163K, 8.3%; G163P, 7.0%; G163R, 7.2%; G163W, 7.3%. The mean expression level in transfected cells was approximately $6x10^4$ CCR5/cell, with values distributed over the range of $3x10^3$ CCR5/cell to $4x10^5$ CCR5/cell, and the mutations did not alter the expression levels (data not shown).

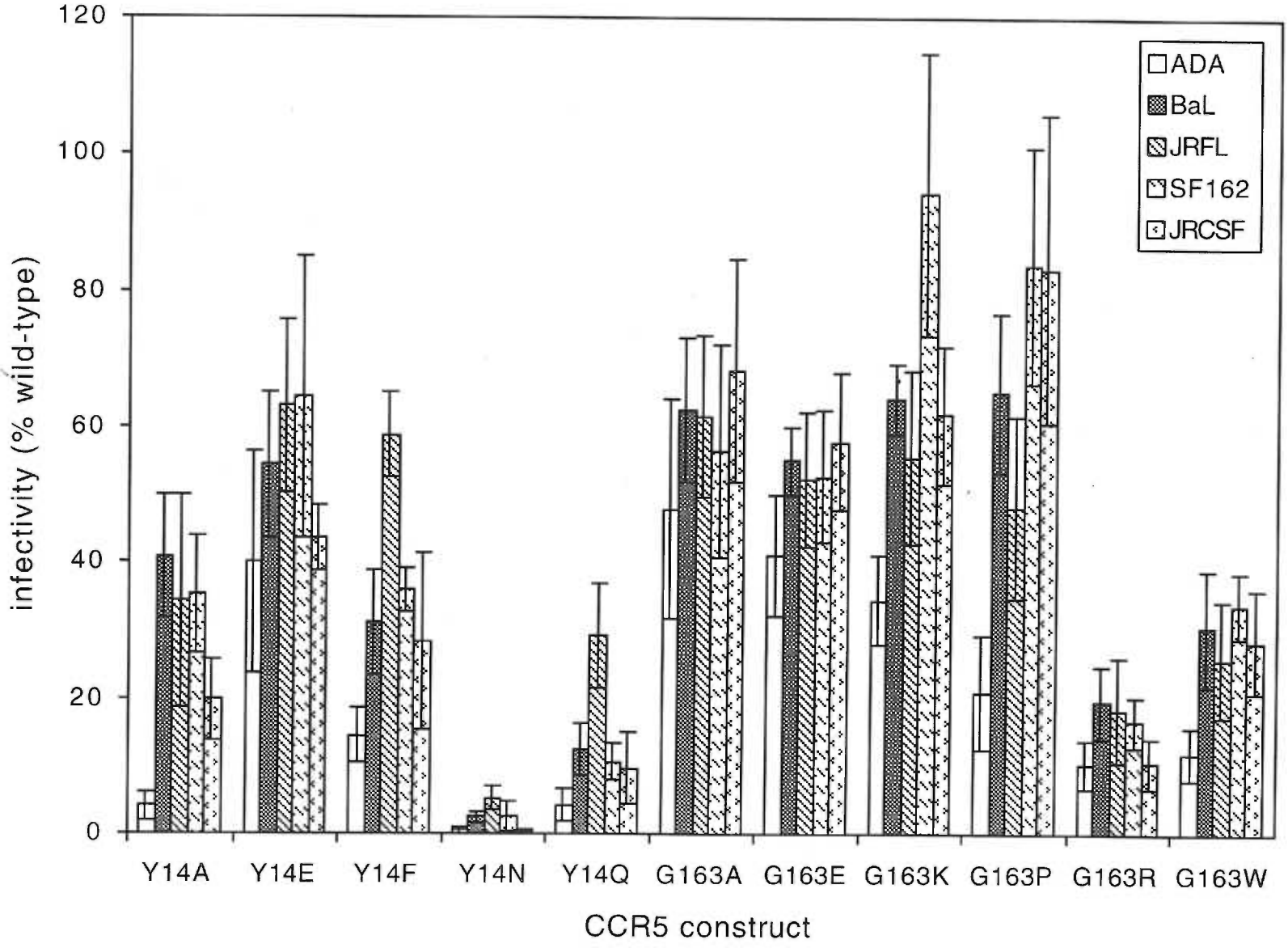
120
100
80
60
40
20
0
infectivity (% wild-type)
ADA
BaL
JRFL
SF162
JRCSF
Y14A
Y14E
Y14F
Y14N
Y14Q
G163A
G163E
G163K
G163P
G163R
G163W
CCR5 construct

Figure 4-2. Analysis of the sulfation of wild-type CCR5, CCR5(G163R), and CCR5(Y14N), and the N-glycosylation of CCR5(Y14N).

A) 293T cells transfected with the indicated CCR5 plasmids were metabolically labeled with [^{35}S]sulfate. CCR5 was immunoprecipitated from the crude membrane fraction with mouse anti-human CCR5 monoclonal 5C7, separated by 0.1% SDS, 8% polyacrylamide gel electrophoresis (SDS-PAGE), and transfered to a nitrocellulose membrane. ^{35}S labeled proteins were detected by autoradiography. Mock indicates cells transfected with vector alone. B) [^{35}S]sulfate labeled CCR5 from HeLa-CD4/CCR5 cells (clone JC.53) or transfected 293T cells were immunoprecipitated from whole-cell lysates and treated with an O-glycosidase cocktail or treated under the same conditions in the absence of enzyme as indicated (see Materials and Methods). The treated immunoprecipitates were separated by SDS-PAGE and labeled CCR5 detected by autoradiography. C) Membrane fractions from transfected 293T cells were separated by SDS-PAGE and analyzed by Western immunoblot with polyclonal rabbit anti-human CCR5 serum. Samples were treated prior to SDS-PAGE with peptide N-glycosidase F (see Materials and Methods) or mock treated as indicated. The polyclonal serum was raised against an amino terminal peptide including the Y14 region (98), and detects the N-glycosylated form of CCR5(Y14N) inefficiently. Indeed, the enzymatically deglycosylated form is readily detected (compare the two lanes on the right side). In all panels the mobility of protein standards with the indicated M_r (in thousands) are shown on the left of the panel.

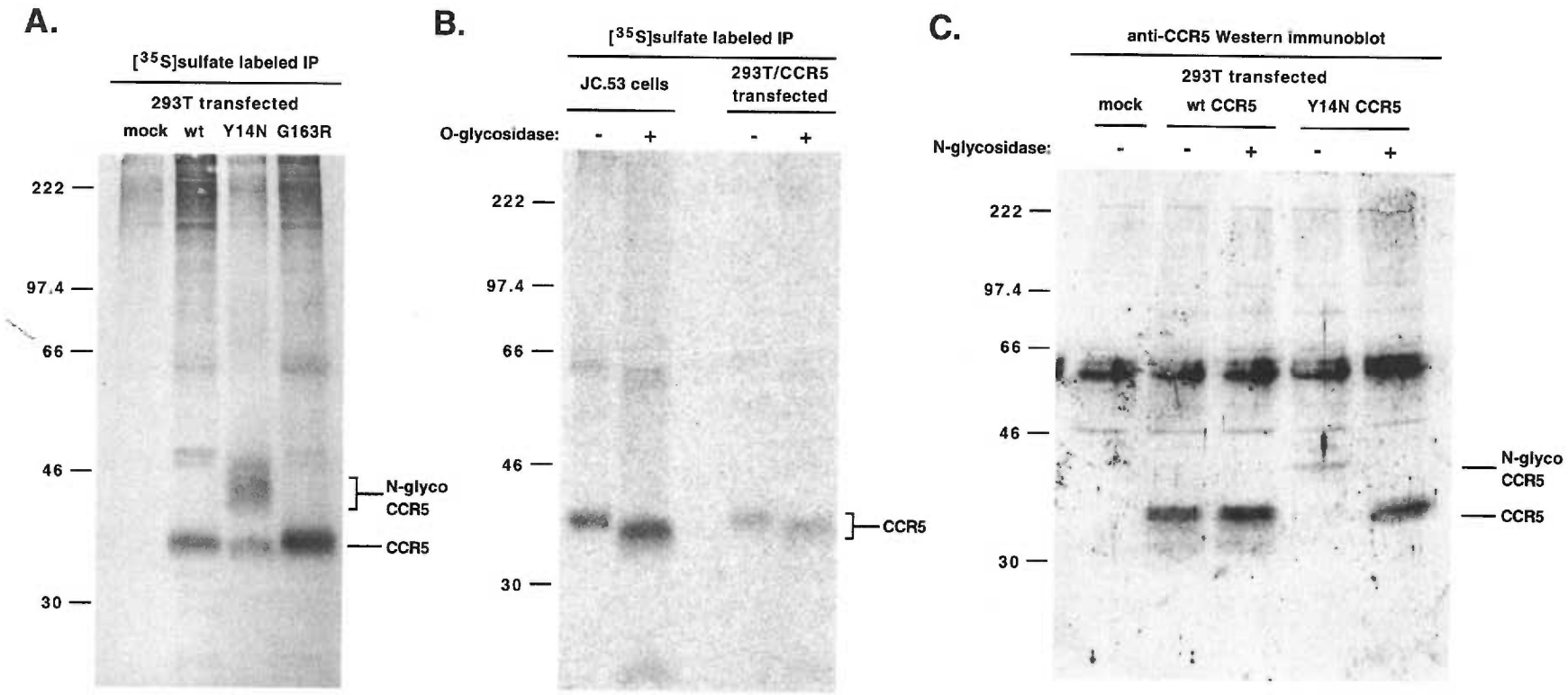
A.
[35S]sulfate labeled IP
293T transfected
mock
wt
Y14N
G163R
222
97.4
66
46
30
N-glyco CCR5
CCR5
B.
[35S]sulfate labeled IP
JC.53 cells
293T/CCR5 transfected
O-glycosidase:
-
+
-
+
222
97.4
66
46
30
CCR5
C.
anti-CCR5 Western immunoblot
293T transfected
mock
wt CCR5
Y14N CCR5
N-glycosidase:
-
-
+
-
+
222
97.4
66
46
30
N-glyco CCR5
CCR5

Figure 4-3. Binding of gp120 and MIP1β to wild-type, G163R, and Y14N CCR5 expressing HeLa-CD4 clones.

A) Cells were incubated with 3 nM [^{125}I]MIP1β in the presence of increasing concentrations of purified BaL gp120. The [^{125}I]MIP1β bound is plotted as a percent of the [^{125}I]MIP1β bound in the absence of gp120 ± the standard deviation. The cell lines used were JC.53 (wild-type CCR5), YB8 (CCR5(Y14N)), and JGR.H11 (CCR5(G163R)). For expression levels of CCR5 on these clones see Table 4-1. B) The same clones as in A) were incubated with 3 nM [^{125}I]MIP1β in the presence of increasing concentrations of unlabeled MIP1β, and bound [^{125}I]MIP1β is plotted as a percent of binding in the absence of unlabeled MIP1β ± the standard deviation. This data was analyzed by the Scatchard method as previously described (144) (analysis not shown). The estimates of the K_m and B_{max} values, respectively, for each cell line generated by this analysis are: 18±4 nM, $1.4x10^5$±$0.3x10^5$ MIP1β/cell for JC.53; 22±8 nM, $0.5x10^5$±$0.2x10^5$ MIP1β/cell for YB8; 8±2 nM, $0.7x10^5$±$0.2x10^5$ MIP1β/cell for JGR.H11.

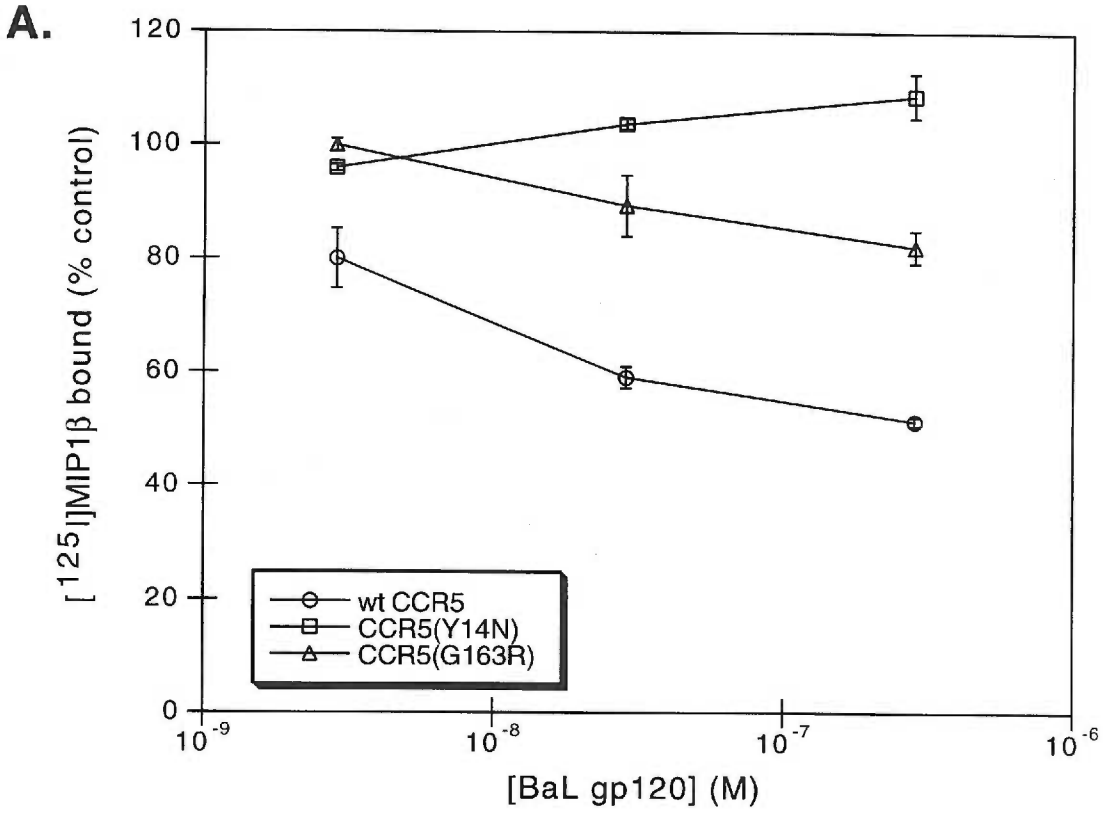
A.
120
100
80
60
40
20
0
[125I]MIP1β bound (% control)
wt CCR5
CCR5(Y14N)
CCR5(G163R)
10-9
10-8
10-7
10-6
[BaL gp120] (M)

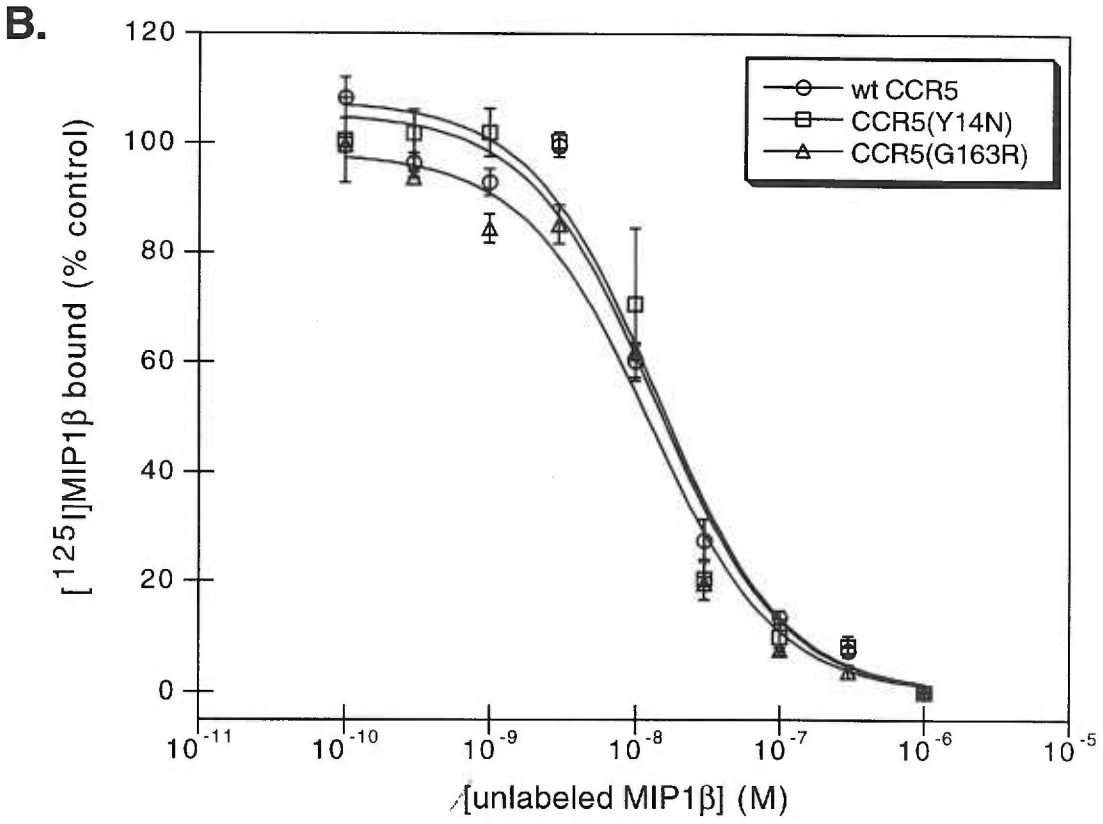
B.
120
100
80
60
40
20
0
[125I]MIP1β bound (% control)
wt CCR5
CCR5(Y14N)
CCR5(G163R)
10-11
10-10
10-9
10-8
10-7
10-6
10-5
[unlabeled MIP1β] (M)

Figure 4-4. Infections mediated by the CCR5(G163R) and CCR5(Y14N) cell lines.

A) Infections mediated by CCR5(G163R) expressing clonal cell lines. The curves with open symbols show the level of HIV-1 infections of HeLa-CD4/CCR5(G163R) cells as determined by a focal infectivity assay which uses $p24^{gag}$ immunoperoxidase staining to detect foci. The isolates used were JRCSF (squares) and BaL (diamonds). The titers were normalized to those determined on HeLa-CD4/CCR5 (clone JC.53, ca., $2x10^5$ CCR5/cell) with the same virus stocks in the same assay. Each point is the average of 5 or 7 experiments, the error bars represent the SEM. The closed symbols indicate infections of HeLa-CD4/CCR5 cells expressing wild-type CCR5 (clones JC.10 and JC.53, c.a., $6x10^3$ CCR5/cell and $2x10^5$ CCR5/cell, respectively). B) Infections mediated by CCR5(Y14N) expressing cell lines. The isolates used were JRCSF (squares) and BaL (diamonds). The titers were normalized as in A. Each point is the average of 3 to 8 experiments, the error bars represent SEM.

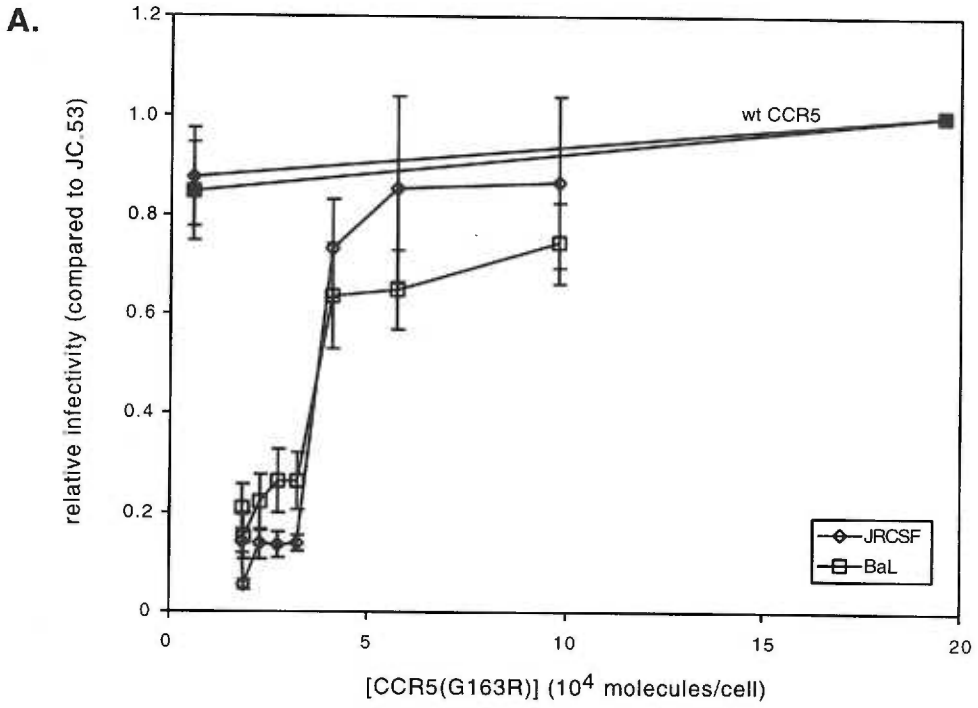
A.
1.2
1.0
0.8
0.6
0.4
0.2
0
relative infectivity (compared to JC.53)
wt CCR5
JRCSF
BaL
0
5
10
15
20
[CCR5(G163R)] (10^4 molecules/cell)

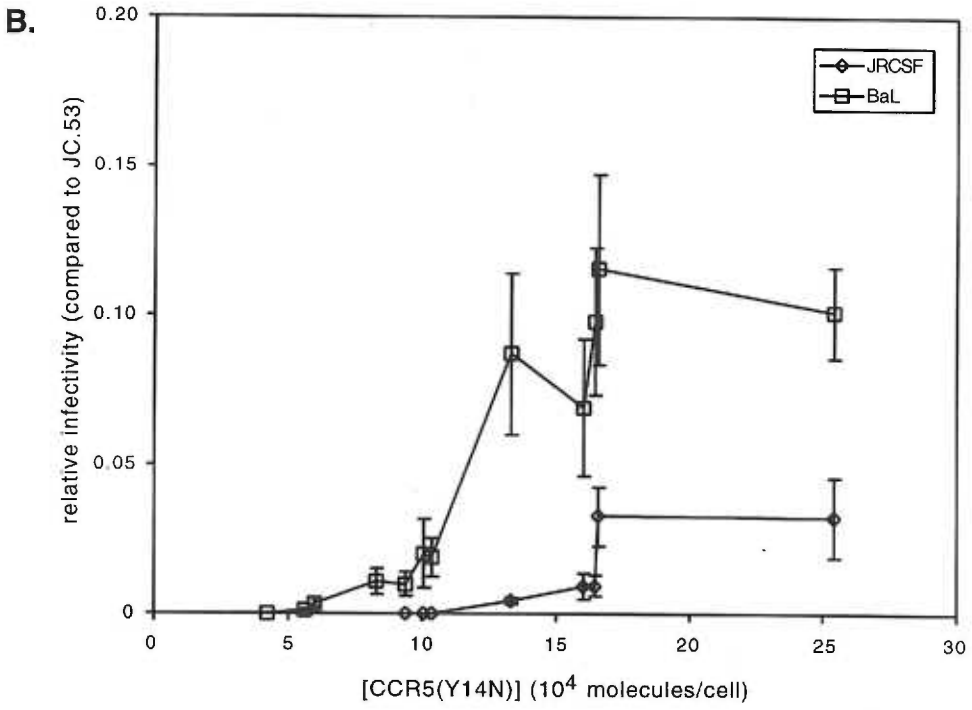
B.
0.20
0.15
0.10
0.05
0
relative infectivity (compared to JC.53)
JRCSF
BaL
0
5
10
15
20
25
30
[CCR5(Y14N)] (10^4 molecules/cell)

Figure 4-5. Syncytium formation in infected cultures is affected by Y14N and G163R substitutions.

The number of foci containing syncytia were counted in 4 assays from from the data plotted in Fig 4-4 for each virus (JRCSF and BaL) on two cell lines from each CCR5 panel. The wild-type cell lines were JC.10 and JC.53, the Y14N cell lines were YD2 and YB8, and the G163R cell lines were JGR.H4 and JGR.H11. For expression levels of wild-type or mutant CCR5 in each cell line see Table 4-1. The percent of foci containing syncytia from each assay were averaged and are shown ± SEM. ND=not done (no value is reported for the infections of YD2 cells by the JCRSF isolate because insufficient foci were available to accurately determine the percent syncytia). Qualitatively similar results were obtained for the number of nuclei per syncytium (results not shown).

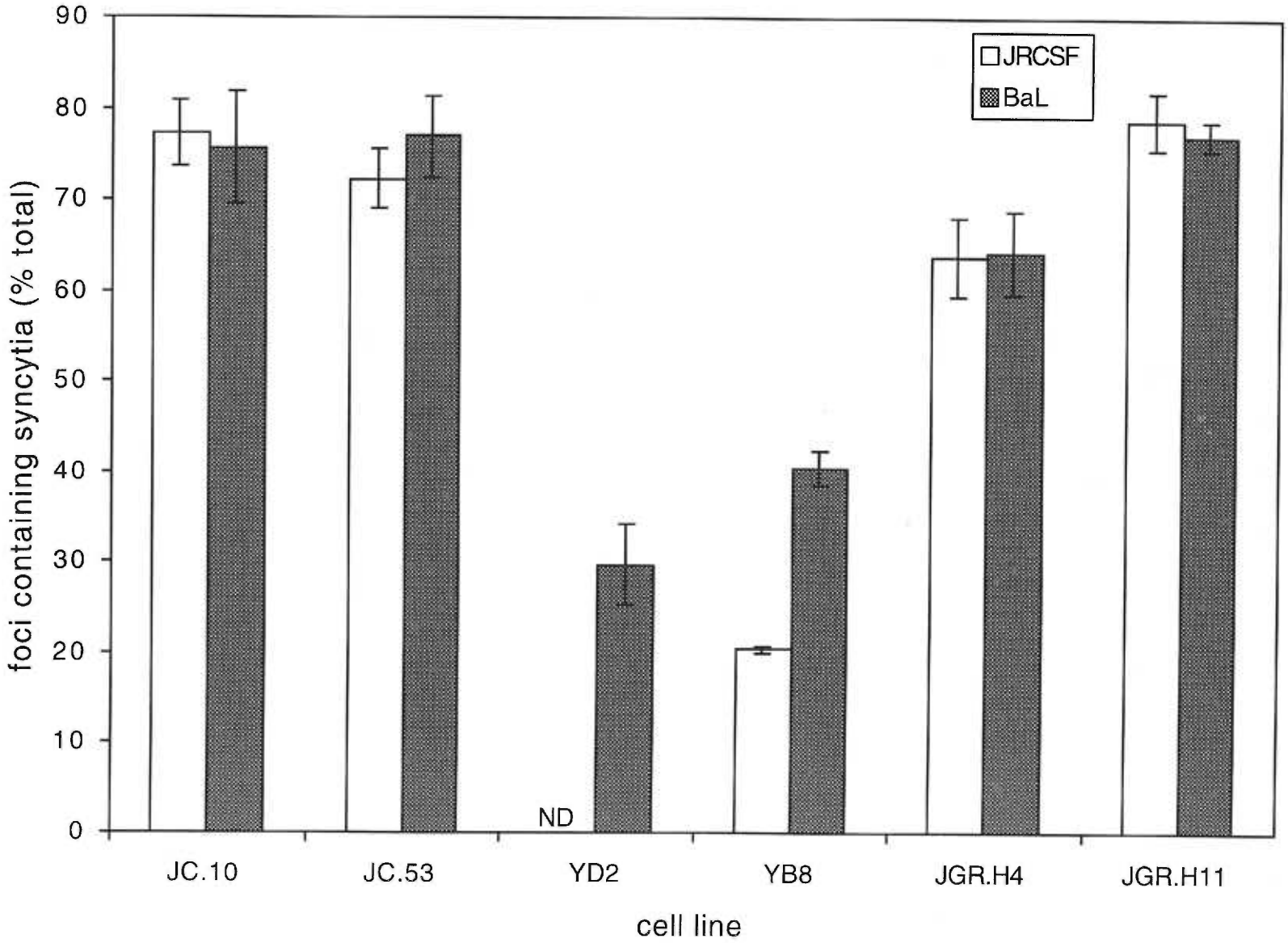
90
80
70
60
50
40
30
20
10
0
foci containing syncytia (% total)
JRCSF
BaL
ND
JC.10
JC.53
YD2
YB8
JGR.H4
JGR.H11
cell line

Figure 4-6. Mathematical analysis of infections mediated by CCR5(G163R) and CCR5(Y14N).

The data in Fig 4-4 were analyzed according to the mathematical model (equation 9) derived in Materials and Methods. The relative infectivity at the highest concentration of mutant CCR5 that was assayed was used as the value of E_{rel}, and all other i_{rel} values which were defined were plotted as $\log[i_{rel}(E_{rel}-i_{rel})]$ versus log[CCR5]. Only data points where [CCR5] is at subsaturating concentrations can be plotted in this analysis, because where $E_{rel}=i_{rel}$ equation 9 is undefined. In addition, not all of the cell lines shown in Table 4-1 were assayed with the CCR5(Y14N) adapted variants of JRCSF described below. Therefore, the number of data points in Fig 4-6 is not the same for each virus isolate, but represents all of the informative data available. The values derived from the CCR5(G163R) panel are shown with filled symbols: BaL (circles) and JRCSF (squares). From the CCR5(Y14N) panel (open symbols), the isolates used were BaL (circles), three independent isolates of JRCSF which have increased efficiencies of fusion (E_{rel}) on the CCR5(Y14N) panel (YB8 and JYN.4 adapted, squares and triangles) (142). The JRCSF/JYN.4 adapted isolate also exhibits an increased affinity for CCR5(Y14N) (142), as demonstrated by the upward shift of the curve.

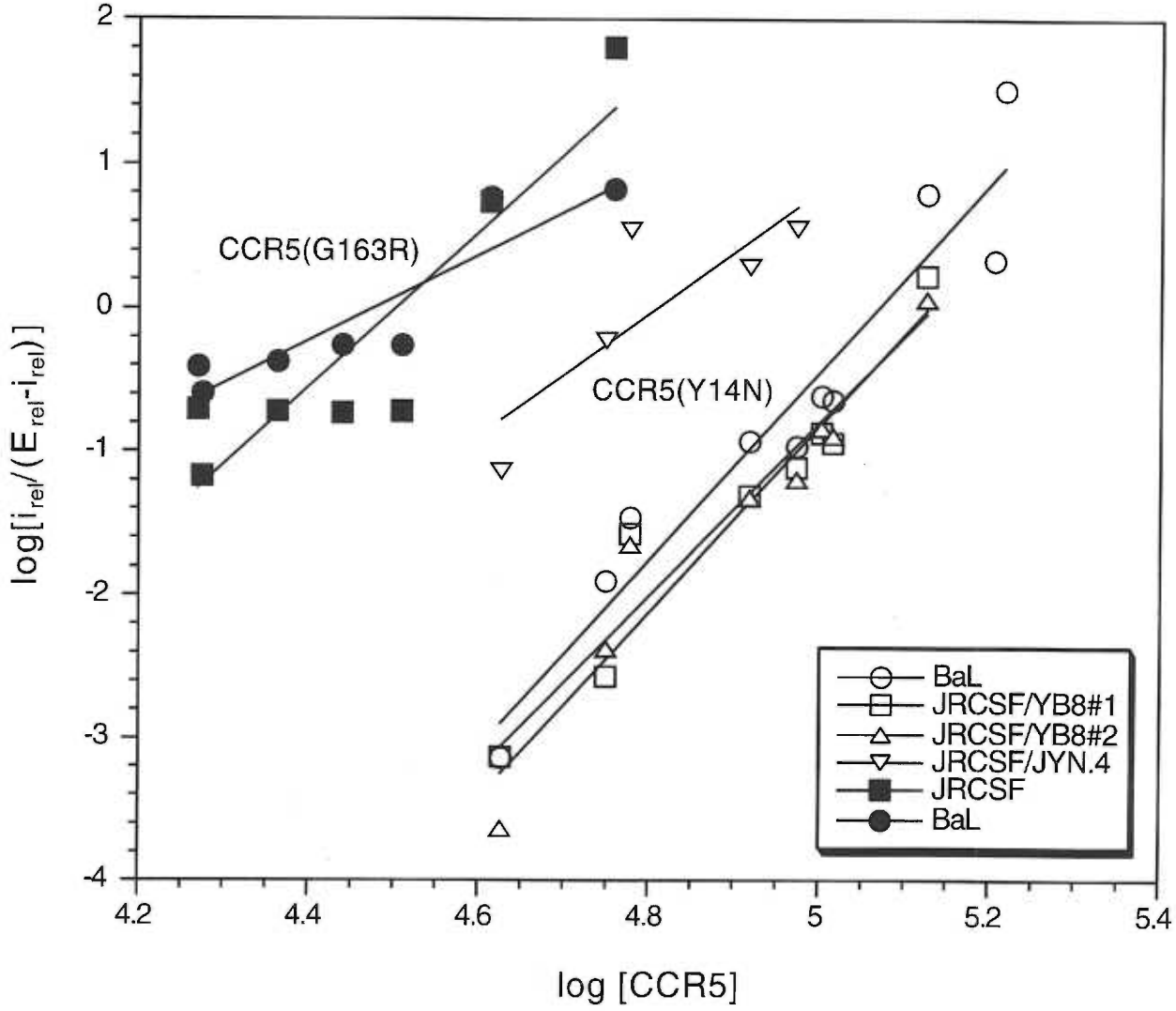
2
1
0
-1
-2
-3
-4
4.2
4.4
4.6
4.8
5
5.2
5.4
log [CCR5]
log[i_rel/(E_rel-i_rel)]
CCR5(G163R)
CCR5(Y14N)
BaL
JRCSF/YB8#1
JRCSF/YB8#2
JRCSF/JYN.4
JRCSF
BaL

Chapter 5. Discussion

Determinants of CCR5 coreceptor activity

The work described in detail in the preceding chapters has been part of an ongoing effort to elucidate the active site and mechanism of action of HIV-1 coreceptors. Here, I will discuss the efforts to map the determinants of CCR5 coreceptor activity for R5 isolates of HIV-1. As mentioned in the Introduction, CCR5 is thought to be the most important coreceptor for HIV-1 transmission and for early stages of infection *in vivo*. For these reasons we and others have chosen to study the interactions of CCR5 with R5 HIV-1 isolates. We believe these results will provide a model for the interaction of coreceptors with HIV-1 and other primate lentiviruses.

Experimental approaches. Several experimental approaches have been employed to map the structures involved in coreceptor activity. In addition, several systems for assessing coreceptor activity are routinely used. Initial experiments employed the use of chimeric coreceptors, splicing human CCR5 with non-functional, but related coreceptors, such as mouse CCR5 or human CCR2. Site-directed mutagenesis has been utilized for fine mapping of amino acids which appear to play a role in coreceptor function. Finally, mapping of epitopes recognized by some mouse mAbs directed against CCR5 which can inhibit coreceptor activity has also proven useful.

The methodology employed can have a significant impact on the results of an experiment designed to assess coreceptor function. A common system is the cell-cell fusion, or syncytia formation, assay. Cells expressing the *env* gene of a molecular clone of R5 HIV-1 (effector cells) are fused with cells expressing CD4 and a coreceptor construct (target cells). A reporter gene in the target cell is activated after fusion with the effector cell. The most common system uses recombinant vaccinia viruses to express high levels of T7 RNA polymerase and Env proteins in the effector cells. The target cells are transiently transfected with coreceptors and CD4 and a luciferase gene driven by the T7 promoter (53, 65, 155, 184). When fusion between the effector and target cells

occurs, the reporter gene is induced and cell extracts are assayed for its activity. These systems allow for sensitive detection of cell-cell fusion, but the reporter assays have not been shown to respond linearly to the number of fusion events. Thus, it is difficult to compare the relative activities of different coreceptors using reporter assays. In addition, the process of cell-cell membrane fusion may differ from virus-cell membrane fusion because the spontaneous inactivation of virions makes them more sensitive to coreceptor alterations which weaken the interaction of gp120 with the coreceptor (see below and Chapter 4).

Another common system utilizes virions which are produced by an HIV-1 provirus in which the *env* gene has been substituted with a reporter gene. When this provirus is cotransfected into producer cells with an Env expression plasmid, virions are produced which can undergo a single infection cycle and produce the reporter gene product in the infected cells (55, 71, 81, 184, 194). This assay system also relies on detection of an enzymatic activity in cell lysates which is not necessarily proportional to the number of infections. In addition, pseudotyped virions are produced at low efficiencies from transiently transfected cells. An alternative virus based approach is the use of a focal infectivity assay. In this system, high titer replication competent virions are used to infect cells expressing CD4 and a coreceptor. The infection status of cells is then assayed within two to three days, before large amounts of virus can be produced from the infected cells. This is typically done by staining cells for expression of viral proteins, either by immunocytochemistry (37), or by immunofluorescent flow cytometry (6). These techniques are proportional to the input virus (37, 90) and sensitive to viral inactivation (see Chapter 4).

Transient expression of coreceptors in the target cells can lead to a broad distribution of surface expression levels. In cell lines transformed by the SV40 large T antigen such as human embryonic kidney 293T cells (293T cells) or COS-7 cells, coreceptors are expressed to very high levels because coreceptors are typically expressed

from a plasmid with an SV40 origin of replication. If a coreceptor binds to gp120 with low affinity, but efficiently activates fusion of the viral and cellular membranes, overexpression of the mutant coreceptor is expected to overcome the effects of reduced affinity. Therefore, overexpression of coreceptors in the target cells may mask effects of low affinity coreceptors in most coreceptor assays. The expression level of CD4 can also affect the outcome of coreceptor assays. Platt *et al* have shown that coreceptor activities show an interdependence on CD4 and CCR5 expression levels (144). The cell surface level of CD4 is thought to alter the number of CCR5 binding sites because CD4 binding is required for the formation of the CCR5 binding site (100, 101, 151, 177, 193). Most of the initial studies in this field have utilized cell-cell fusion assays and transient overexpression of mutant or chimeric coreceptors. Therefore, the results may be biased toward the identification of sites which affect the efficiency of coreceptor mediated membrane fusion, as opposed to those which affect only binding of HIV-1 to the coreceptor. We used an immunocytochemical focal infectivity assay on transiently transfected HeLa cells stably expressing human CD4 (90) for most of the coreceptor function studies described in the preceding chapters. While this assay suffers some of the same drawbacks, additional studies described in Chapter 4 have employed the use of HeLa-CD4 cell clones stably expressing discrete amounts of the CCR5 coreceptor. Careful assessment of the coreceptor expression levels in these clones has allowed us to determine the effects of CCR5 concentrations on coreceptor activity.

For most R5 isolates of HIV-1, both human CCR2 and the mouse homologue of CCR5 (mCCR5) show no detectable HIV-1 coreceptor activity (154). Therefore chimeras between these nonfunctional, but related, chemokine receptors and human CCR5 (hCCR5) have been employed to map the domains which are required for coreceptor function. However, domains of the nonfunctional receptors may have structural features which have a positive or a negative effect on coreceptor function (21, 98). Therefore, the reference protein sequences present in chimeras are not always

neutral in their effects on activity. These effects can profoundly distort results of chimera studies.

The amino-terminal region. CCR5 is a 7TM receptor, and therefore has four extracellular and four intracellular domains. Attention has been focused on the extracellular regions because the interaction of CCR5 with gp120 takes place at the extracellular face of the plasma membrane. The assignment of the topology of CCR5 and the locations of its transmembrane domains has been made based on homology to other 7TM receptors whose topologies are known. The extracellular regions are the amino-terminal region (NT) and the three extracellular loops (ECLs). The NTs of CCR5 and of other chemokine receptors are characterized by a number of acidic residues and tyrosines preceding the single cysteine. The NT of CCR5 is approximately 30 amino acids in length, with the cysteine residue 20 amino acids from the amino-terminus.

Numerous studies have shown the NT of CCR5 to be important for R5 HIV-1 coreceptor activity (6, 21, 52, 55, 60-62, 71, 98, 148, 155, 184). Chimeras in which the NT of hCCR5 replaces the NT of mCCR5 or CCR2 have been reported to be active coreceptors in cell-cell fusion assays using effector cells expressing several prototypical R5 HIV-1 *env* genes (21, 52, 155, 184). Atchison *et al* found that the NT of hCCR5 in an mCCR5 background was a partially active coreceptor for one R5 HIV-1 isolate in a focal infectivity assay, and the NT of hCCR5 in the CCR2 background resulted in complete activity (6). However, the reverse chimeras, which have the mCCR5 or CCR2 NT domains in an otherwise hCCR5 background, also mediate cell-cell fusion (21, 52, 139, 155), and infection (6). Some discrepancies in these data are apparent. For example, Picard *et al* found that the NT of hCCR5 was insufficient to confer cell-cell fusion activity on mCCR5 using effector cells expressing the *env* gene from the ADA isolate (139), contradicting the results of Bieniasz *et al* using nearly the same system (21). These results might be explained by the choice of the mCCR5 allele (see below), or receptor expression levels, because Bieniasz *et al* used COS-7 and 293T cells as the

target cells (21, 139). Additionally, Farzan *et al* found that a chimera containing the NT domain of CCR2 is unable to mediate the entry of R5 HIV-1 isolates (60), in contrast to the work of Atchison *et al* who expressed this chimera in COS-7 cells (6). Overall, these results suggest that the NT domain of hCCR5 has a positive effect on HIV-1 fusion in the mCCR5 or CCR2 context, but that the remainder of the molecule also has a positive effect in the context of the NT from an inactive coreceptor.

Our results with chimeras of hCCR5 and mouse CCR5 also suggest that the NT domain is important for coreceptor function (see Chapter 2). For instance, an inactive chimera with the mouse NT and ECL1 regions is made partially active as a coreceptor for multiple isolates of R5 HIV-1 by the addition of the human NT region. In addition to mouse/human chimeras, we also studied the coreceptor activities of CCR5 alleles from AGMs. We found that AGMs are highly polymorphic at the CCR5 locus, with a common allele that differs from the wild-type AGM CCR5 by an amino acid substitution in the NT domain of tyrosine 14 for asparagine (see Chapter 2 and Appendix A). We showed that this substitution (Y14N) nearly eliminates coreceptor activity for R5 HIV-1 isolates in the context of AGM CCR5 and hCCR5. We have also shown that this substitution inhibits infections by SIV_{mac} (from the SIV_{smm} group, see Chapter 2) and SIV_{agm} (see Appendix A), suggesting that this site is critical for infections by diverse primate lentiviruses. Further analysis of the amino acid requirements at position 14 suggest that phenylalanine, and to a greater extent glutamate, can partially substitute for the wild-type tyrosine in hCCR5 (see Chapter 4). Farzan *et al* have reported that tyrosine 14 is one of four tyrosines in the NT domain of CCR5 which is sulfated, and that sulfation of tyrosines in the NT is required for HIV-1 infection (62). Thus, we speculate that the partial activity of glutamate and phenylalanine result from the preference of HIV-1 for both the aromatic and anionic character of the wild-type tyrosine sulfate moiety at this position. Asparagine is the least active substitution for all of the R5 HIV-1 isolates examined, and we have shown that a portion of the CCR5(Y14N) molecules are modified

by N-linked glycosylation of asparagine 14 (see Chapter 4). As discussed in Chapter 4, we believe that the glycosylated portion of CCR5(Y14N) is incapable of binding MIP1β or interacting with HIV-1. The unglycosylated portion of CCR5(Y14N) binds MIP1β with high affinity (Chapter 4) and transduces a signal in response to ligands (data not shown). This substitution not only reduces the coreceptor activity of CCR5, but N-linked glycosylation might also reduce the effective cell surface concentration of CCR5, which is correlated with a delay in disease progression in humans (see Introduction). We hypothesize that the AGM(Y14N) allele may have arisen in the AGM population because this substitution slows or alters the pathogenicity of SIV_{agm} *in vivo*, a speculation which will require additional experimental investigation (see Appendix A). We conclude that tyrosine 14 of CCR5 is a critical amino acid which contributes to R5 HIV-1 coreceptor activity.

Additional work has supported the conclusion that critical amino acids exist within the NT region of CCR5 for R5 HIV-1 coreceptor activity, despite the observation that the NT of mCCR5 or CCR2 may have full or partial function in the context of the remainder of CCR5 (55, 61, 148, 153). Ross *et al* showed that the mutations S7V, N13D, and Y15G partially inhibit cell-cell fusion, but they saw less of an effect with an E18A substitution (153). A series of mutagenesis experiments were performed in which many charged or polar residues predicted to lie on the extracellular surface of CCR5 were changed to alanine (55, 71, 148). These studies demonstrated that, aside from the four cysteines, the only single amino acid substitutions which impaired infection with a pseudotyped virus were in the NT region (55, 71, 148). Specifically, they found that D2A, Y10A, D11A, Y14A, Y15A, S17A, and E18A substitutions in wild-type CCR5 inhibit CCR5 mediated entry of the JRFL R5 isolate of HIV-1, whereas the K22A or Q22A substitutions have no effect (55, 148). Farzan *et al* also performed alanine scanning mutagenesis of many of the charged or polar amino acids in the extracellular domains of CCR5. They found that Y10A, D11A, Y14A, Y15A, E18A, Q21A, and

K22A substitutions in hCCR5 all significantly reduce entry of the YU2 R5 HIV-1 isolate (61). The lack of agreement from these studies about the roles of residues 2, 18, 21, and 22 can probably be attributed to differences in the isolates tested, the expression levels of CCR5 and CD4 in the target cells, and the assay method employed. However there is considerable agreement that anionic and tyrosine residues between amino acids 10 and 18 of CCR5 are critical to coreceptor function in these assay systems.

It has recently been reported that the tyrosine residues in the NT of CCR5 (Y3, Y10, Y14, and Y15) can be modified by sulfation (62). This modification occurs in the trans-Golgi and is usually found on tyrosines that are near acidic residues. Treatment with chlorate inhibits sulfation and also inhibits binding of MIP1β and gp120 from the an R5 isolate of HIV-1 (62). The results discussed above clearly indicate that at least three of the four sulfated tyrosines are critical determinants of R5 HIV-1 coreceptor activity, and many of the critical acidic amino acids may play a role in recognition by tyrosylprotein sulfotransferase (62). Any of the four tyrosines in the NT of CCR5 can be sulfated when the others are mutated to aspartate, suggesting that all four are probably sulfated (62). Other chemokine receptors including all those known to have HIV-1 coreceptor activity have similar tyrosine and acidic amino acid motifs in the NT domain and may also be sulfated (62). Our data show that CCR5(Y14N) is efficiently sulfated, including the form that is modified by N-linked glycosylation, suggesting that mutation of this residue to asparagine or addition of an N-linked oligosaccharide does not dramatically disturb the sulfation of the neighboring tyrosines (Chapter 4). We think that sulfation of tyrosine 14 is likely to be important for R5 HIV-1 infection because the anionic residue glutamate can substitute in part for the tyrosine. However, we cannot completely rule out the possibility that mutation of tyrosine 14 alters the sulfation of a neighboring tyrosine and has indirect effects on HIV-1 infection.

These studies show that the NT of CCR5 is a major determinant of coreceptor activity. Specifically acidic and tyrosine sulfate moieties between amino acids 10 and 18

have been shown to play a major role in coreceptor function in both cell-cell fusion and infectivity assays. It is probable that the NT domain forms part of the HIV-1 binding site, although it could also be important for maintaining the conformation of the another site required for binding of gp120 to CCR5.

Extracellular loop 2. The ECL2 domain (c.a., 30 amino acids) of CCR5 has also been implicated in coreceptor activity. Analysis of the coreceptor activities of chimeras indicates that the extracellular loops of hCCR5 confer coreceptor activity in the presence of the NT domains of CCR2 or mCCR5 (6, 21, 52, 139, 155). Some studies have shown that human ECL2 confers coreceptor activity in the context of an otherwise inactive chimera (6, 155) or in the context of mCCR5 (6) in cell-cell fusion (155) and infection (6) assays. Alkhatib *et al* have shown that ECL2 of hCCR5 confers partial activity in the CCR2 background, whereas the reverse chimera with ECL2 of CCR2 in the hCCR5 background was completely inactive (2). The discrepancies among these studies are likely to result from the choice of assay system or the expression levels of coreceptor and CD4. An ECL2 specific mouse anti-human CCR5 mAb inhibits both infection of R5 HIV-1 isolates and binding of R5 gp120 to CCR5 (194). We confirmed the ability of this monoclonal to inhibit R5 HIV-1 infections and mapped its binding site to an epitope that includes lysine 171 in ECL2 (see Chapter 3). The epitope recognized by 2D7 has further been shown to include glutamate 172 and to depend on the native conformation of CCR5 (103, 121, 135).

We found that introduction of only the NIH/Swiss mouse ECL2 sequence into hCCR5 prohibited infections by multiple R5 isolates of HIV-1 (see Chapter 2). Any chimera which included the NIH/Swiss mouse ECL2 sequence was completely inactive in our coreceptor assay. In contrast, the same chimera made with the ECL2 from C57BL6 mouse CCR5 was partially active as an HIV-1 coreceptor. NIH/Swiss mouse CCR5 differs from C57BL6 mouse CCR5 in ECL2 by a single amino acid substitution of proline 183 to leucine. These results indicate that substitution of a single amino acid in

ECL2 inhibits infections by an already attenuated coreceptor which has six other amino acid changes in ECL2 when compared to hCCR5. However, we have not seen any effect of introducing a P183L into hCCR5 in the absence of any other changes (data not shown). Ross *et al* have found that an S180P mutation alone, or Y184H and S185T substitutions together reduce the coreceptor activity of hCCR5 (153). These substitutions were all present in the attenuated chimera that we assayed which contains the C57BL6 mouse ECL2 in hCCR5. These results suggest that critical amino acids in ECL2 may exist, but that the effects of substitutions in this region on CCR5 coreceptor activity are more obvious when the substitutions are introduced into human CCR5 in combination. Residues in ECL2 may make critical contacts with gp120, or the structure of the loop might affect another region of CCR5 which is important for gp120 binding.

AGM CCR5 differs from that of rhesus macaques by three amino acid substitutions and human CCR5 by nine amino acid substitutions (Chapter 3). Arginine at amino acid 163 is unique to AGM CCR5 among these three primates and is the only unique AGM substitution predicted to be exposed on the extracellular surface of CCR5. AGM CCR5 is relatively inactive as a coreceptor for HIV-1 compared to hCCR5 (Chapters 2 and 3) and rhesus CCR5 (36). Based on these observations, we tested the ability of a G163R mutation in hCCR5 to modulate infections by R5 HIV-1 isolates. This substitution inhibited infections by all tested R5 isolates of HIV-1 (Chapter 3). Additionally, an R163G mutation in AGM CCR5 confers substantial coreceptor activity. Similar effects were seen when gp120 binding was assayed. These results suggest that the region near glycine 163 represents a critical site for coreceptor activity near the ECL2 domain of CCR5. Therefore, we assayed the coreceptor activity of additional CCR5 mutations at glycine 163 (Chapter 4). Interestingly, most of the tested amino acid substitutions retained substantial coreceptor activity. G163K was almost fully active, suggesting that the presence of a basic amino acid at position 163 is not sufficient to inhibit coreceptor function. Likewise, the nearly full activity of a G163P substitution

suggests that flexibility of the main-chain at amino acid 163 is not required for coreceptor activity. The two least active substitutions were G163R and G163W, even though both were well expressed. These results suggest that the presence of a bulky side chain at position 163 of CCR5 may occlude a site critical for the interaction of gp120 with CCR5. It is possible that gp120 may directly contact glycine 163, or that the conformations of other extracellular regions are altered by substitutions at this position. We consider the second possibility unlikely because CCR5(G163R) is a high-affinity receptor for MIP1α and MIP1β, and transduces a signal in response to ligand binding (Chapter 3).

Other extracellular regions of CCR5. Less evidence has been presented for a critical role of ECL1 and ECL3 of CCR5 in forming the coreceptor active site. Several studies have shown that mutation of any of the four extracellular cysteines of CCR5, including those in ECL1 and ECL3, reduces its coreceptor activity, presumably because of the loss of a disulfide bond important for maintaining the tertiary structure of the extracellular domains (23, 71, 148). ECL3 does not differ between mouse and human CCR5s, and many chimera studies have been uninformative about the role of this loop in coreceptor function, including our own. CCR2 chimeras have shown that placing ECL3 of CCR2 in the context of CCR5 reduces HIV-1 coreceptor activity in an infection assay (2). However, another study using a cell-cell fusion assay found that ECL3 of CCR2 reduced coreceptor activity only in the context of parental chimeras containing one other extracellular domain of CCR2 (155). Because the parental chimeras were active in their assay, these results also suggest that ECL3 plays a role in CCR5 coreceptor activity. However, those CCR5s which have alanine mutations of charged or polar residues in hCCR5 ECL3 and are well expressed retain coreceptor activity (61, 71).

Two groups found that introduction of ECL1 of mCCR5 or CCR2 into an otherwise active parental chimera reduces coreceptor activity for some isolates (6, 21). We found that introduction of mouse ECL1 into hCCR5 reduces coreceptor activity (Chapter 2). We also found that the substitution of both the NT and ECL1 domains of

mCCR5 into hCCR5 completely eliminates coreceptor activity, whereas the substitution of either region alone reduces activity, but does not eliminate it. We also found that a single amino acid change in ECL1 further reduces the HIV-1 coreceptor activity of the attenuated AGM CCR5 coreceptor. This substitution, arginine for glutamine at residue 93, does not inhibit infection in our assay when introduced into hCCR5 (data not shown). Alanine scanning mutagenesis studies have also failed to find individual substitutions within ECL1 which reduce the coreceptor function of CCR5 (61, 71). These results demonstrate that multiple substitutions in ECL1 or ECL3, or substitutions in these regions in the context of an attenuated coreceptor, can reduce the efficiency of CCR5 mediated infection or membrane fusion. Critical amino acid substitutions which exert these effects in isolation have not been found. Thus, ECL1 and ECL3 may contribute directly to an interaction with HIV-1, but it is more likely that substitutions in these domains exert their effects by altering the structure of other critical domains. Further investigation will be required to fully clarify the roles of ECL1 and ECL3 in mediating CCR5 coreceptor activity.

CCR5 determinants for gp120 binding and membrane fusion

The previous section describes the primary structural features which are required for CCR5 coreceptor function. Many of the studies described above used cell-cell fusion assays. These studies demonstrate a direct role for CCR5 in mediating membrane fusion because viral proteins other than Env are not expressed in the effector cells, and additional steps of the viral life cycle are not required to generate the observed signal in these assays. However, these studies do not necessarily require a direct interaction of CCR5 with the viral Env proteins. Other studies have demonstrated the direct interaction of CCR5 with purified monomeric gp120 (177, 193). These studies showed that incubating cells expressing CCR5 with R5 gp120 inhibits the binding of a radiolabeled chemokine ligand (either MIP1α or MIP1β) in a CD4 dependent manner (177, 193). Another study has shown that gp120 from an X4 HIV-1 strain can be coimmunoprecipitated in a complex with CXCR4 and CD4 (101). These results support the hypothesis that virions that have been primed by the interaction with CD4 bind directly to coreceptor molecules, and that this interaction induces the conformational changes in the Env trimer that results in membrane fusion.

In some cases, decreased coreceptor activity of CCR5 has been associated with a decreased ability to bind gp120s derived from R5 isolates of HIV-1. Farzan *et al* showed that the Y15A and E18A substitutions in the NT also completely inhibit binding of radiolabeled gp120 to CCR5 in the presence of sCD4 (61). The same group also showed that inhibition of tyrosine sulfation by chlorate inhibits binding of gp120 to CCR5 (62). An assay in which R5 gp120 is used to compete with mAb 2D7 (a mouse anti-human CCR5 ECL2 antibody) binding to CCR5 has identified Y15A, D2A, D11A, and E18A substitutions in CCR5 which disrupt gp120 binding (55, 148). To a lesser extent, Y14A and S17A substitutions in CCR5 also disrupt gp120 binding (55, 148). We have found that the Y14N substitution completely inhibits R5 gp120 binding to CCR5 as determined by competition of radiolabeled chemokine binding by gp120 in the presence of

membrane-associated CD4 (see Chapter 4). The G163R substitution was shown to inhibit gp120 binding in this assay and in direct binding assays using radiolabeled gp120 and sCD4 (Chapters 3 and 4). The mouse anti-human CCR5 monoclonal antibodies 2D7 and 3A9 which bind to ECL2 and NT domains, respectively, efficiently inhibit binding of radiolabeled gp120 to CCR5 in the presence of sCD4 (194).

Some interesting discrepancies have been noted between the gp120 binding capability of mutant or chimeric CCR5s and their coreceptor activity. For instance, Baik and coworkers noted that high affinity binding of gp120 to chimeric receptor is not required for coreceptor activity in their transient transfection assay (9). We also found that the gp120 binding activities of human and AGM CCR5s mutated at amino acid 163 do not completely correlate with their coreceptor activity in transiently transfected cells using our standard infection assay (Chapter 3). For example, AGM CCR5 retains approximately 20% of the coreceptor activity of hCCR5, yet exibits very little gp120 binding capacity in any of the assays performed in Chapter 3. We hypothesize that such discrepancies may be due to mutations in AGM CCR5 which reduce the affinity of CCR5 for gp120, but do not inhibit the ability of a virion·CCR5 complex to trigger membrane fusion once it is formed. Overexpression of the mutant CCR5s in the coreceptor assay gives measurable coreceptor activity because the low affinity binding can be overcome by mass-action driving the formation of the virion·CCR5 complex. Indeed, G163R is a candidate for such a mutation because the CCR5(G163R) mutant CCR5 retains significant coreceptor activity. Alternatively, mutations in CCR5 may both reduce the affinity of CCR5 for gp120 and the activity of the gp120·CCR5 complex.

We designed an experimental approach to distinguish between these possible effects of the Y14N and G163R mutations on coreceptor function (see Chapter 4). We engineered HeLa/CD4 cell lines to stably express various amounts of CCR5(Y14N) or CCR5(G163R) in the presence of a constant amount of CD4 (HI-J cells, c.a., 1.5×10^5 CD4/cell). A retroviral vector which expresses the appropriate CCR5 coding sequence

was used for this purpose. Cell clones were established by limiting dilution cloning, and the surface expression was quantitated by immunological methods utilizing saturating amounts of mAb 2D7. Each cell clone was then assayed for coreceptor activity. Platt *et al* have shown that HI-J cells are efficiently infected when they express very low levels of wild-type CCR5 (c.a., 10^3 CCR5/cell), but remain uninfected in the absence of CCR5 (144). Cells expressing approximately 10 times less CD4 require more CCR5 for cells to be maximally infected (c.a., 10^4 CCR5/cell) (144). These results show that infections are inefficient at low concentrations of both CCR5 and CD4 . This implies that inactivation or dissociation of bound virions must occur, because the virus adsorption is not dependent on CCR5, and cells with increased levels of CCR5 are efficiently infected (see Chapter 4 for further details). If inactivation did not occur, two cell lines with the same level of CD4 would be efficiently infected regardless of the levels of CCR5, because the formation of the necessary virion·CCR5 complex would eventually occur. Indeed, the assumption of virion inactivation or dissociation is implicit in all infection assays in which differing infectivities are seen. In such an assay it appears that viruses are in a "race" between fusion and inactivation or dissociation. We propose that fusion requires the formation of an appropriate virion·$CD4_n$·$CCR5_m$ complex (see below). Thus, in the studies of Platt *et al* utilizing HI-J cells expressing wild-type CCR5, the binding of CCR5 to virions is saturated at very low CCR5 levels because of the high-affinity of wild-type CCR5 for the virion·$CD4_n$ complex formed by cell-associated virions. In cells expressing low levels of CD4, fewer virion·$CD4_n$ complexes are available for binding to CCR5 and higher levels of CCR5 are required to form the same number of virion·$CD4_n$·$CCR5_m$ complexes.

Based on this reasoning, we predicted that if a mutant CCR5 protein has a low affinity for the virion·$CD4_n$ complex, a higher concentration of mutant CCR5 will be required to saturate the available complexes compared to wild-type CCR5. Indeed, at least 150 and 30 fold higher CCR5(Y14N) and CCR5(G163R) cell surface

concentrations, respectively, are required relative to wild-type CCR5 for maximum infectivity of two different R5 HIV-1 isolates (Chapter 4). As mentioned above and in Chapter 4, only the approximately 40% of the cell surface CCR5(Y14N) molecules that escape N-linked glycosylation are thought to be capable of interacting with HIV-1 virions. This interpretation suggests that the 150 fold difference in the apparent affinity for virion associated gp120 compared to wild-type CCR5 may only be a 60 fold difference when corrected for glycosylation. Regardless, it is clear that the CCR5(Y14N) coreceptor interacts very inefficiently with virion associated gp120, in agreement with our results using monomeric gp120 (see above and Chapter 4). Cells expressing high levels of CCR5(G163R) are infected as efficiently as cells expressing wild-type CCR5. In contrast, the infections mediated by the CCR5(Y14N) cell clones plateau at levels much lower than those for cells expressing wild-type CCR5. This effect is predicted to occur if the complex of virion·$CD4_n$·$CCR5(Y14N)_m$ is less active at promoting fusion than is the complex containing wild-type CCR5. Thus, the Y14N substitution appears to alter both the formation of the competent complex and its ability to trigger membrane fusion. This effect appears to be at the level of fusion because it is also seen when infected cells are assayed for their ability to fuse with other cells (Chapter 4).

We conclude that formation of a complex between the virion, CD4, and CCR5 are required to promote membrane fusion. The G163R and Y14N substitutions inhibit the formation of this complex by reducing the affinity of the mutant CCR5 for the virion·$CD4_n$ complex. In addition, the Y14N substitution also reduces the activity of this complex once it is formed. The simplest explanation for this observation is that the association of CCR5 with the virion is reversible, and that the Y14N mutation reduces the rate constant of the irreversible reaction which takes place after assembly of the complex (see Chapter 4). Another explanation is that some proportion of the cell surface CCR5(Y14N) molecules are capable of binding to gp120, but not capable of triggering fusion. This seems unlikely given that different plateaus are reached for different virus

strains, and the inefficient fusion mediated by this coreceptor can be overcome by compensating mutations in gp120 (142).

Cooperation of multiple CCR5s in HIV-1 infection

In Chapter 4 we present plots of infectivity *versus* cell surface CCR5 concentration for panels of cell lines expressing CCR5(Y14N) and CCR5(G163R). An interesting feature of these plots is the apparent sigmoid shape. We believe that this sigmoid shape must reflect a requirement for multiple coreceptors to mediate HIV-1 infections. The requirement is most likely to occur at the step of membrane fusion, because these mutations also affect syncytia formation in a concentration dependent manner. In addition, an X4 virus is unaffected by varying the amounts of wild-type CCR5 (144), or CCR5(G163R) and CCR5(Y14N) (data not shown) in these cells. We propose a model in Chapter 4 which allows us to estimate the number of CCR5 receptors that must be in a complex with cell-associated virions to promote infection. This is a simplified model which reflects those aspects of the infection process which we believe most sensitively affect the outcome of our infection assay. In this model, adsorbed virions are only able to infect cells when they are associated with n CD4 molecules and m CCR5 molecules. The results of Platt and coworkers have shown that CD4 and CCR5 expression levels affect the number of infections observed in this assay (144). Therefore, free CD4 and CCR5 are thought to be in equilibrium with virion associated CD4 and CCR5. At low levels of CD4 and CCR5, fewer virions on average are associated with n CD4 and m CCR5, and the rate of infections is limited. This can be overcome by adding more CD4 or CCR5 and shifting the equilibrium in favor of forming the infection competent complex. This explains the interdependence of CD4 and CCR5 levels for infection. The number of CCR5 that can associate with the competent complex is limited by the number of CD4s associated with the virion. Thus when modeling the dependence of infections on CCR5 concentration we can start with the concentration of virion·$CD4_n$ complexes capable of forming the competent complex. Addition of CCR5 to this complex will eventually result in a complex of virion·$CD4_n$·$CCR5_m$. Ideally, this step should be modeled as a number of sequential additions of CCR5 to the virion·$CD4_n$

complex. However, we have modeled this as the addition of *m* CCR5s to the virion·$CD4_n$ complex in order to obtain an estimate of *m*. It should be noted that this is not the only limitation in our model and there are a number of reasons to believe our calculated values of *m* to be approximations. These limitations are detailed in the Discussion section of Chapter 4. For our purposes we believe this model to be adequate to obtain a first approximation of the number *m* of CCR5s required for infection by R5 HIV-1 virions.

This model can be written as:

$$v{\cdot}CD4_n + mCCR5 \rightleftarrows v{\cdot}CD4_n{\cdot}CCR5_m \longrightarrow \text{infection}$$

Where v represents an adsorbed virion. This model requires that inactivation and infection be competing processes. In a culture containing many adsorbed virions the number of infections is dependent on the rate of infection, which is in turn dependent on the concentration of the competent complex. When CD4 is limiting, the concentration of $v{\cdot}CD4_n$ is below saturation, and the concentration of the complex is less than if CD4 were saturating. When CCR5 is limiting the concentration of the complex is likewise reduced. Thus, this model predicts the results of the previous experiments with wild-type CCR5 (144). By integrating the number of infections expected from this model over the course of our assay, we can mathematically describe the infectivity as a function of the concentration of CCR5 molecules on the cell surface. The derivation of the equation describing this function can be found in Chapter 4. The results obtained with wild-type CCR5 could not be fit to this equation, because of the difficulty in obtaining cell clones and accurately determining the cell surface CCR5 concentration at the very low CCR5 surface densities that would be required to perform this analysis with wild-type CCR5. However, since both CCR5(G163R) and CCR5(Y14N) have a decreased affinity for cell-associated virions the infectivity versus CCR5 concentration curves contain sufficient data to model mathematically. The results are also summarized in Chapter 4. We found that for both virus isolates assayed on the CCR5(G163R) cell panel, and for three of the four virus isolates assayed on the CCR5(Y14N) panel, the linear correlation coefficient of

the fit to our equation was greater than 0.9, indicating a good agreement with the model. Furthermore, these fits predicted similar values of *m*, which are in the range of 4 to 6. Thus, we conclude that the number of CCR5s required for infection is probably in the range of 4 to 6. While this is an approximation, it is interesting to note that similar numbers of influenza A hemagglutinin trimers are required to form a fusion pore (14, 25, 46). We hypothesize that the requirement for multiple CCR5s to cooperate in HIV-1 infection is a result of the need to form a fusion pore from multiple Env trimers. This hypothesis will require further experimentation to test. In addition, better models and experimental systems will be needed to more accurately determine the number of CCR5s required for HIV-1 infection.

Appendix A. Polymorphism in the CCR5 gene of African green monkeys and effects on SIV_{agm} infection.

In addition to the primary receptor, CD4, members of the family of seven transmembrane domain chemokine receptors have been recently identified as coreceptors necessary for infection by diverse isolates of HIV-1, HIV-2, and SIV (3, 18, 36, 38, 50, 53, 54, 56, 65, 116). CCR5, a receptor for the CC-chemokines MIP1α, MIP1β, and RANTES, has been identified as the major coreceptor for macrophage-tropic (M-tropic) isolates of HIV-1 (38, 50, 53, 54) and SIV isolates from rhesus macaques, African green monkeys (AGMs), sooty mangabeys, and chimpanzees (36, 51, 56, 80, 93, 116). Additionally, two orphan receptors related to CC- and CXC-chemokine receptors, Bonzo (STRL33) and BOB (GPR15), have been identified as coreceptors for HIV-1 and SIVs from rhesus macaques and AGMs (51, 59, 80, 93).

We previously reported, based on sequencing of genomic DNA, that the CCR5 locus of AGMs is highly polymorphic and that amino acid changes at Tyr14 and Gln93 to Asn and Arg, respectively, dramatically reduced the ability of wild-type AGM CCR5 to function as a coreceptor for M-tropic HIV-1 (98). We hypothesized that amino acid changes in AGM CCR5 may have arisen as a result of selective pressure from primate lentiviruses which have infected AGMs throughout the course of AGM speciation (4, 20, 88, 89, 99, 128). We have extended these observations by sequencing genomic DNA from 23 AGMs and three AGM cell lines, and by analyzing the coreceptor usage of SIV isolates derived from AGMs.

Genomic DNA from 23 AGMs (kindly provided by Drs. Jonathan Allan and Francois Barré-Sinoussi) and three AGM cell lines (CV-1, ATCC CCL-70; BS-C-1, ATCC CCL-26; and Vero, ATCC CCL-81) were prepared by standard methods (7). Two approximately 600 bp PCR products were generated by amplifying the genomic DNA with a proofreading thermostable DNA polymerase (*Pfu*, Stratagene, used according to manufacturer's recommendations) with the primers CCR5F (5'

cggcggggatccGGGTGGAACAAGATGGATTATC 3') and AGMR (5' ACTGTATGGAAAATGAGAGCTGC 3') or with the primers AGMF2 (5' CTCCCAAGAATCATCTTTACCAG 3') and CCR5R (5' gccgccctcgagCCACTTGAGTCCGTGTCACAAG 3'), where the lowercase sequences denote 5' extensions which are not derived from CCR5 sequences. The purified PCR products were then sequenced by automated sequencing in both directions using the same primers, allowing for analysis of the entire coding region of CCR5. In addition, this allowed for the sequence to be determined from both strands for all except the 5' and 3' ends of approximately 20 bp. Fig. 1 shows a comparison of polymorphisms observed in the 26 genomic DNA sequences analyzed, mapped onto the amino acid sequence of wild-type AGM CCR5. The sequences of the two alleles from CV-1 cells had previously been determined (98) and the Y14N polymorphism found in AGM clone 1 was easily detected by this method.

The polymorphism at nucleotide 40 (numbered from the first base of the coding sequence) of T for an A (T40A) was the most common substitution seen in this analysis (Fig. 1). Of the 52 alleles sequenced (26 genomic samples), 19 are predicted to have this base change which results in the Y14N amino acid change. This polymorphism was found exclusively in DNA samples from the tantalus subspecies of AGMs, with the exception of the CV-1 cell line which has this coding change linked to an L352F coding change. This makes Y14N the most common allele in this subspecies. Out of 12 tantalus samples, 4 were heterozygous at amino acid 14, 7 were homozygous for the Asn codon, and 1 was homozygous for the Tyr codon. The only other coding nucleotide substitutions found in the tantalus subspecies were A439G and A278G, both of which were heterozygous with the wild-type base. These two nucleotide substitutions result in V147M and Q93R amino acid substitutions, respectively. The V147M change was found in a tantalus monkey which was heterozygous for Y14N, and because the full length coding sequences have not yet been cloned, the linkage of these substitutions was not

determined. The Q93R coding change was found in the only tantalus monkey which was homozygous for Tyr at amino acid 14, and since no other coding changes were found in this DNA sample, it represents a unique allele. This allele was also found in the absence of any other coding changes in a sabaeus monkey which was heterozygous for this coding change. Therefore, this allele also represents a common polymorphism, although the frequency of the allele and any possible subspecies specificity will require a larger sample size to determine. Another coding nucleotide change was found in codon 93, resulting in a Gln to Lys substitution. This was found in a cell line of grivet subspecies origin, and in a DNA sample from a vervet animal. Both animal's CCR5 sequences were heterozygous for this substitution, and the vervet Q93K coding change was determined to be linked to an S38T coding change found in the same animal. This animal also harbored a D13N coding change which was found to be on the other allele. The D13N coding change was found only once in this analysis. However, another group has reported finding this coding change in an AGM DNA sample, suggesting it may also be a common allele (57). A non-coding nucleotide change was found at nucleotide 84 which occurred in 9 AGM CCR5 alleles. Linkage of this non-coding polymorphism was not determined, but it must be associated with at least two different amino acid sequences, suggesting its origin predates some coding polymorphisms. Additional coding and non-coding changes which occurred only once in our samples are shown in Fig. 1. In summary, these results show that AGM CCR5 alleles with alterations of the coding sequence are common. Truncations, deletions, or frameshifts were not observed. The most common coding changes observed in AGM CCR5 occurred at two sites in the CCR5 protein product. These sites are D13-Y14 in the amino-terminal domain, and Q93 in the first extracellular loop.

From this analysis, we calculate an amino acid substitution rate of 1.6×10^{-3} from the presence of 29 coding changes in 26 genomic DNA samples (52 alleles of 352 amino acid each). This estimate is roughly in accordance with the rate of 2.1×10^{-3} recently

reported for 39 human CCR5 sequences from 27 individuals by Zhang et al (201). In contrast to AGM CCR5, the coding changes seen in human CCR5 appear to be distributed throughout the CCR5 coding sequence, whereas many coding changes in AGM CCR5 are clustered at two sites, D13-Y14 and Q93. 24 of 29 coding changes in the AGM CCR5s sequenced in this analysis occurring at one of these three amino acids. These regions of CCR5 are known to be important for coreceptor function for primate lentiviruses. It has recently been reported by Martin et al that the gp120 protein from SIV_{mac239} binds to rhesus CCR5 in a manner that is independent of CD4, but requires CD4 to bind to human CCR5. The change of amino acid 13 from Asp to Asn was responsible for the difference observed (117). Other studies have implicated residues 13 and 15 (153) and 13 and 14 (98) as important sites for coreceptor function. We also showed that the Q93R substitution reduces infectivity by HIV-1 in the context of the wild-type AGM protein (98). It is possible that some of the polymorphism seen in AGM CCR5 is a result of selective pressure from endogenous SIVs, since even partial resistance to SIVs could lead to an evolutionary advantage. It would then be expected that these coding changes would alter the ability of AGM CCR5 to function as a coreceptor for some SIV_{agm} isolates.

In order to evaluate the functional consequences of these polymorphisms in SIV_{agm} infections, the coreceptor activities of AGM CCR5s containing some of the coding changes were evaluated for four strains of SIV_{agm}. The CCR5 constructs for wild-type AGM, AGM(Y14N,L352F), AGM(Q93R), and NIH/Swiss mouse were previously described (98). Molt-4 clone 8 cells infected with SIV_{agm} strains 12, Cpa266, and Cpa27 (45, 92) were obtained from the AIDS Research and Reference Reagent Program, Division of AIDS, NIAID, NIH: contributed by Dr. Ronald Desrosiers. Supernatants were harvested over the period of two weeks in culture and filtered through a 0.45 μm pore size filter, and used at dilutions of 1:2 to 1:10. The grivet SIV_{agm} strain gri-1 (67), was obtained as virus containing tissue culture supernatants (AIDS Research and

Reference Reagent Program, Division of AIDS, NIAID, NIH: contributed by Dr. Jonathan Allan), which were incubated with Molt 4 clone 8 cells (AIDS Research and Reference Reagent Program, Division of AIDS, NIAID, NIH: contributed by Dr. Ronald Desrosiers), and supernatants were harvested as above. Infectivity was determined by a focal infectivity assay as previously described (37, 96). Briefly, viral supernatants were incubated with HeLa/CD4 cells (clone HI-J) (90). Cells were stained 72 hours later by incubating with pooled heat inactivated serum from four SIV_{agm} infected AGMs at 1:1000 (kindly provided by Dr. Ronald Desrosiers), with 1:500 HRP conjugated rabbit anti-monkey IgG antibody (Sigma), and with the HRP chromogenic substrate 3-amino-9-ethylcarbazole (Sigma). When incubated with HI-J cells, the virus strains 12, Cpa266, Cpa27, and gri-1 exhibited low levels of infection which increase upon transient expression of human CCR5 by calcium phosphate transfection of a pcDNA3-CCR5 expression plasmid (data not shown). The average percentage of foci in mock versus human CCR5 transfected cells was between 3% and 18%, and this background appears to be due to the presence of Bonzo on the surface of HeLa cells (data not shown). Staining was specific to SIV_{agm} infections as no staining was seen when virus was omitted and was CD4 dependent (data not shown).

The ability of these viruses to use the wild-type AGM, AGM(Y14N, L352F), AGM(Q93R), and mouse CCR5s as coreceptors was determined by subtracting the background numbers of foci on mock (pcDNA3 alone) transfected HeLa/CD4 cells, from those transfected with various pcDNA3 CCR5 expression plasmids. The titers are shown as percentages of those seen with human CCR5 (Fig. 2). All four isolates had a similar pattern of coreceptor usage. These SIV_{agm} isolates utilized wild-type AGM as efficiently as human CCR5 for entry into HI-J cells. The average titer was 95% that of human CCR5 and taken together, the values were not significantly different from human CCR5 in a paired comparison t-test (P=0.3; N=12). In contrast to HIV-1, which does not use AGM(Y14N, L352F) CCR5 in this assay and exhibits only ~3% of human CCR5 titers

with AGM(Q93R) CCR5 (98), all four isolates were able to use AGM(Y14N,L352F) and AGM(Q93R) CCR5 to a significant level above background ($P \leq 0.005$; N=12 versus mock transfected for the four isolates together), but less efficiently than human or wild-type AGM CCR5s ($P \leq 0.001$; N=12 versus human CCR5). The average activity of AGM(Y14N, L352F) was 12% of human CCR5, and that of AGM(Q93R) was 46% of human CCR5. In our previous report, SIV_{mac251} was shown to utilize the AGM(Q93R) protein as efficiently as human CCR5, and titers with AGM(Y14N, L352F) were approximately 20% of those observed with human CCR5 (98). None of the isolates was able to use mouse CCR5 for infection (P=0.1; N=12). These results suggest that the SIV_{agm} viruses may be adapted to efficiently utilize the wild-type AGM CCR5 as a coreceptor, in contrast to HIV-1, which utilizes this coreceptor only approximately 20% as efficiently as human CCR5 in this assay (98, 166). Interestingly, we previously found that SIV_{mac251} can also use AGM CCR5 as efficiently as human CCR5 (98). The results suggest that mutations in CCR5 found in AGMs can reduce the efficiency of coreceptor usage. Specifically, the Y14N and Q93R mutations which occur in the extracellular amino-terminal and extracellular loop 1 regions significantly reduced SIV_{agm} titers. Because the coreceptors are overexpressed in this assay, usage of these coreceptors may be even further reduced in the physiological context. We believe that this pattern of coreceptor usage represents an ongoing process of host-virus coevolution, as AGMs are thought to have been infected with SIVs since the differentiation of AGM subspecies (4, 20, 88, 89, 99, 128).

Presently, these results are incomplete. The functional consequences of the D13N, Q93K, and other mutations were not evaluated. Only four isolates of SIV_{agm} were evaluated in this study, and further studies with additional SIV_{agm} viruses from other subspecies will be of value in evaluating the importance of CCR5 polymorphism in SIV_{agm}/AGM coevolution. In particular, isolates derived from tantalus monkeys should

be evaluated, given the prevalence of the Y14N polymorphism in this subspecies and the importance of this residue in SIV_{agm} and HIV-1 infections (98).

Figures

Figure A-1. Summary of nucleotide substitutions in the coding region of 26 AGM genomic DNA samples.

Genomic DNA samples were sequenced as described in the text. The origin of the 26 AGM sample were: 3 cell lines, 3 vervets, 8 sabaeus, 12 tantalus. The electropherograms from the automated sequencing were scanned manually to determine the nucleotide sequences. Heterozygous bases were readily apparent by this method. The nucleotide sequence changes compared to the AGM consensus sequence are mapped onto the amino acid coding sequence. If a codon contained a non-synonymous (coding) change it is highlighted in black. If a codon contained a synonymous nucleotide change it is highlighted in gray. Next to each amino acid whose codon contained polymorphic bases are listed the base change relative to the consensus sequence (i.e., T40A). For non-synonymous mutations, the amino acid change that results is listed in parentheses. Below this is listed the number of alleles from each source of genomic DNA in which this change is found.

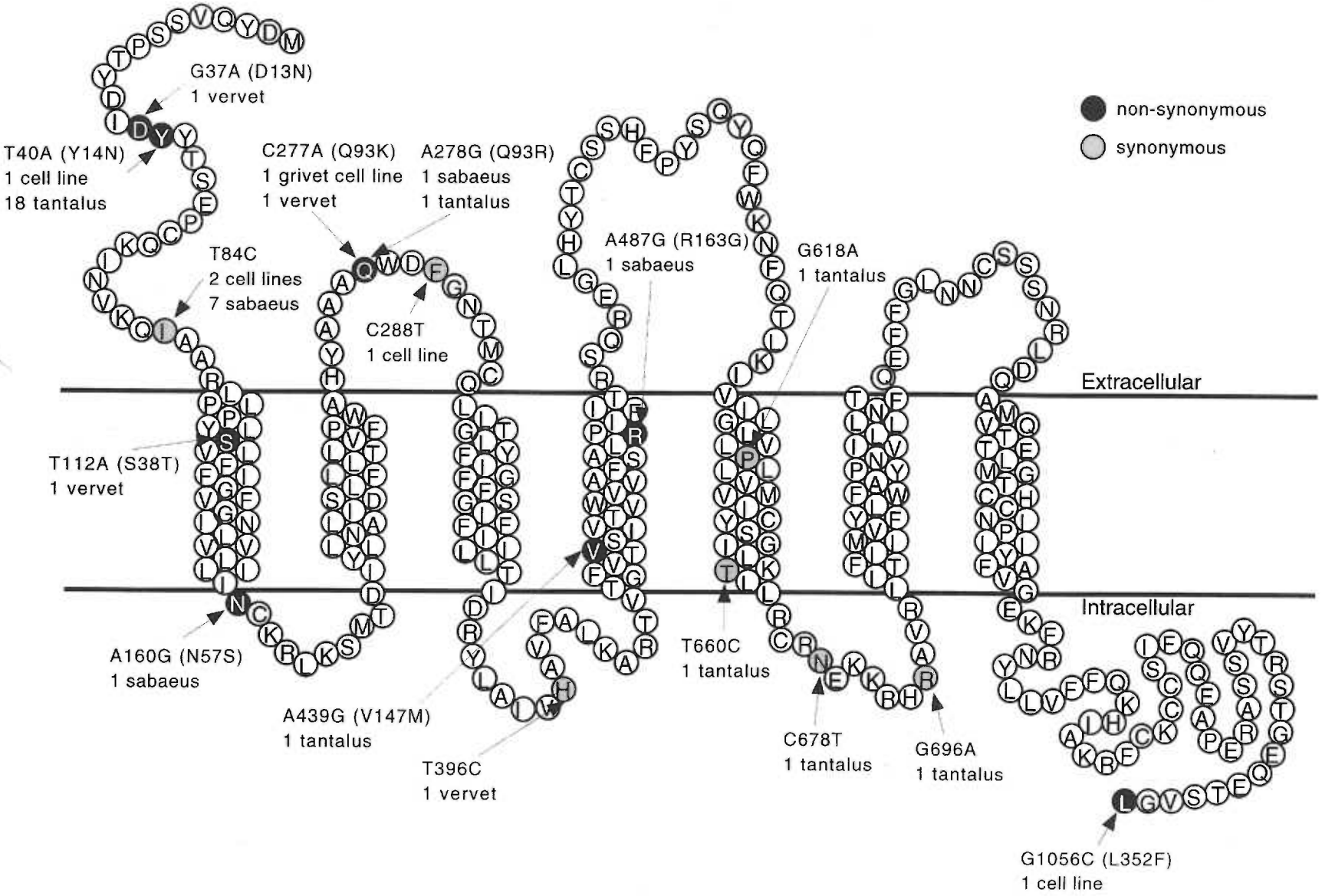
non-synonymous
synonymous
Extracellular
Intracellular
G37A (D13N)
1 vervet
T40A (Y14N)
1 cell line
18 tantalus
C277A (Q93K)
1 grivet cell line
1 vervet
A278G (Q93R)
1 sabaeus
1 tantalus
T84C
2 cell lines
7 sabaeus
C288T
1 cell line
A487G (R163G)
1 sabaeus
G618A
1 tantalus
T112A (S38T)
1 vervet
A160G (N57S)
1 sabaeus
A439G (V147M)
1 tantalus
T396C
1 vervet
T660C
1 tantalus
C678T
1 tantalus
G696A
1 tantalus
G1056C (L352F)
1 cell line

Figure A-2. SIV_{agm} infections of HeLa/CD4 cells expressing AGM, AGM(Y14N, L352F), AGM(Q93R), and mouse CCR5s.

Cells were transfected by the calcium phosphate method with 20 μg pcDNA3 expression plasmid for the CCR5 shown, stained as described in the text, and counted. Bars represent the percent of the human CCR5 titer from the same experiment, after subtracting the titers on mock transfected cells. Error bars represent SEM for three experiments.

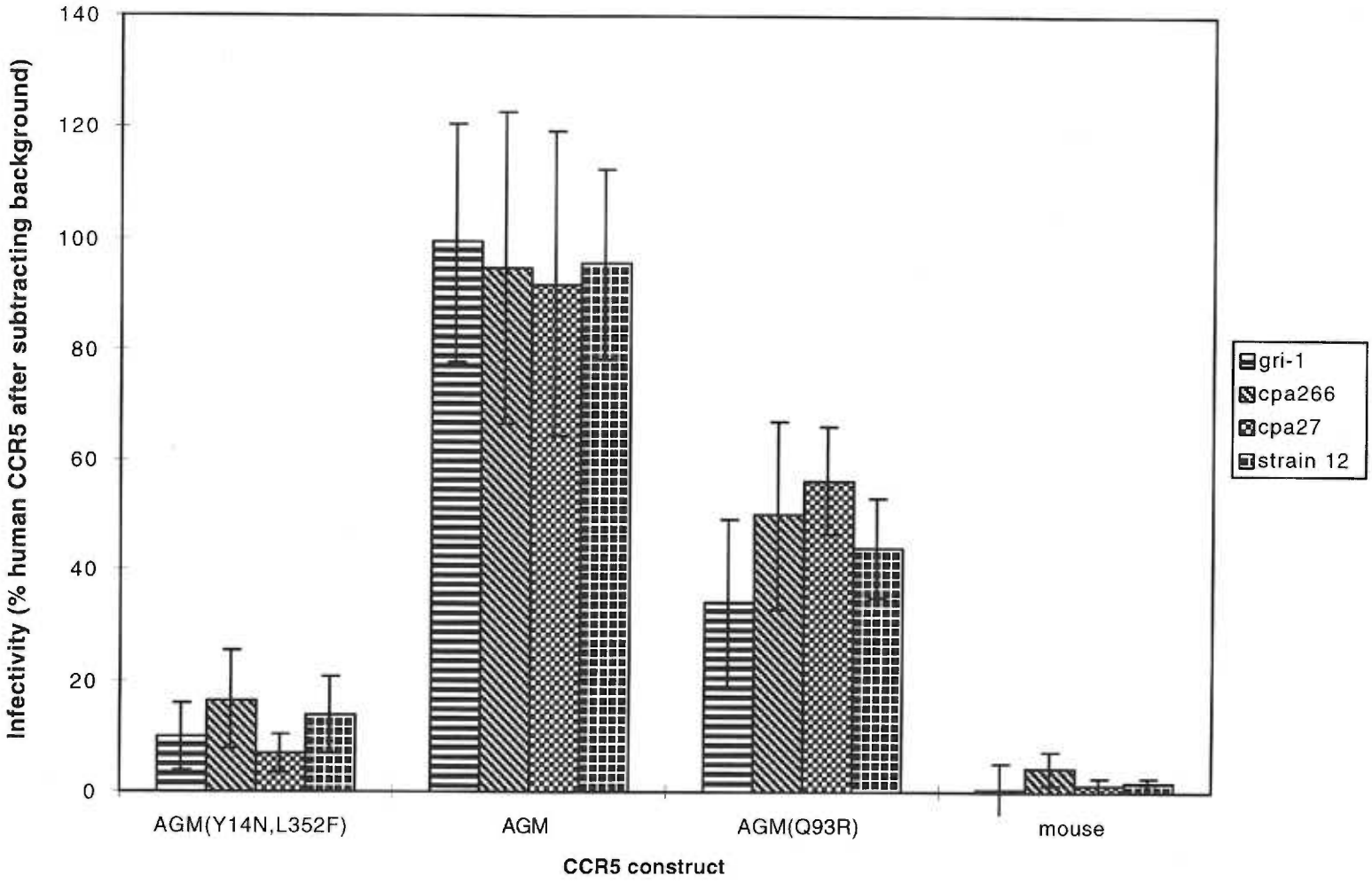
Infectivity (% human CCR5 after subtracting background)
140
120
100
80
60
40
20
0
AGM(Y14N,L352F)
AGM
AGM(Q93R)
mouse
CCR5 construct
gri-1
cpa266
cpa27
strain 12

References

1. Alizon, M., P. Sonigo, F. Barre-Sinoussi, J. C. Chermann, P. Tiollais, L. Montagnier, and S. Wain-Hobson. 1984. Molecular cloning of lymphadenopathy-associated virus. Nature. 312:757-60.
2. Alkhatib, G., S. S. Ahuja, D. Light, S. Mummidi, E. A. Berger, and S. K. Ahuja. 1997. CC chemokine receptor 5-mediated signaling and HIV-1 Co-receptor activity share common structural determinants. Critical residues in the third extracellular loop support HIV-1 fusion. J Biol Chem. 272:19771-6.
3. Alkhatib, G., C. Combadiere, C. C. Broder, Y. Feng, P. E. Kennedy, P. M. Murphy, and E. A. Berger. 1996. CC CKR5: a RANTES, MIP-1α, MIP-1β receptor as a fusion cofactor for macrophage-tropic HIV-1. Science. 272:1955-8.
4. Allan, J. S., M. Short, M. E. Taylor, S. Su, V. M. Hirsch, P. R. Johnson, G. M. Shaw, and B. H. Hahn. 1991. Species-specific diversity among simian immunodeficiency viruses from African green monkeys. J Virol. 65:2816-28.
5. Ansari-Lari, M. A., X.-M. Liu, M. L. Metzker, A. R. Rut, and R. A. Gibbs. 1997. The extent of genetic variation in the CCR5 gene. Nat Genet. 16:221-222.
6. Atchison, R. E., J. Gosling, F. S. Monteclaro, C. Franci, L. Digilio, I. F. Charo, and M. A. Goldsmith. 1996. Multiple extracellular elements of CCR5 and HIV-1 entry: dissociation from response to chemokines. Science. 274:1924-6.
7. Ausubel, F. M., R. Brent, R. E. Kingston, D. D. Moore, J. G. Seidman, J. A. Smith, and K. Struhl (ed.). 1994. Current Protocols in Molecular Biology. John Wiley & Sons, Inc., New York, NY.
8. Baba, M., O. Nishimura, N. Kanzaki, M. Okamoto, H. Sawada, Y. Iizawa, M. Shiraishi, Y. Aramaki, K. Okonogi, Y. Ogawa, K. Meguro, and M. Fujino. 1999. A small-molecule, nonpeptide CCR5 antagonist with highly potent and selective anti-HIV-1 activity. Proc Natl Acad Sci U S A. 96:5698-703.

9. Baik, S. S., R. W. Doms, and B. J. Doranz. 1999. HIV and SIV gp120 binding does not predict coreceptor function. Virology. 259:267-73.

10. Balter, M. 1999. AIDS now world's fourth biggest killer. Science. 284:1101.

11. Balter, M. 1998. On World AIDS Day, a shadow looms over southern Africa. Science. 282:1790-1.

12. Benjamini, E., G. Sunshine, and S. Leskowitz. 1996. Immunology: a short course, third ed. Wiley-Liss, Inc., New York, NY.

13. Benkirane, M., D. Y. Jin, R. F. Chun, R. A. Koup, and K. T. Jeang. 1997. Mechanism of transdominant inhibition of CCR5-mediated HIV-1 infection by ccr5Δ32. J Biol Chem. 272:30603-6.

14. Bentz, J. 1999. Minimal aggregate size and minimal fusion unit for the first fusion pore of influenza hemagglutinin mediated membrane fusion. Biophys J. In press.

15. Berg, H. C., and E. M. Purcell. 1977. Physics of chemoreception. Biophys J. 20:193-219.

16. Berger, E. A., R. W. Doms, E. M. Fenyo, B. T. Korber, D. R. Littman, J. P. Moore, Q. J. Sattentau, H. Schuitemaker, J. Sodroski, and R. A. Weiss. 1998. A new classification for HIV-1. Nature. 391:240.

17. Berger, E. A., P. M. Murphy, and J. M. Farber. 1999. Chemokine receptors as HIV-1 coreceptors: roles in viral entry, tropism, and disease. Annu Rev Immunol. 17:657-700.

18. Berson, J. F., D. Long, B. J. Doranz, J. Rucker, F. R. Jirik, and R. W. Doms. 1996. A seven-transmembrane domain receptor involved in fusion and entry of T-cell-tropic human immunodeficiency virus type 1 strains. J Virol. 70:6288-95.

19. Bestwick, R. K., S. L. Kozak, and D. Kabat. 1988. Overcoming interference to retroviral superinfection results in amplified expression and transmission of cloned genes. Proc Natl Acad Sci U S A. 85:5404-8.

20. Bibollet-Ruche, F., C. Brengues, A. Galat-Luong, G. Galat, X. Pourrut, N. Vidal, F. Veas, J. P. Durand, and G. Cuny. 1997. Genetic diversity of simian immunodeficiency viruses from West African green monkeys: evidence of multiple genotypes within populations from the same geographical locale. J Virol. 71:307-13.

21. Bieniasz, P. D., R. A. Fridell, I. Aramori, S. S. Ferguson, M. G. Caron, and B. R. Cullen. 1997. HIV-1-induced cell fusion is mediated by multiple regions within both the viral envelope and the CCR-5 co-receptor. Embo J. 16:2599-609.

22. Binley, J. M., R. Wyatt, E. Desjardins, P. D. Kwong, W. Hendrickson, J. P. Moore, and J. Sodroski. 1998. Analysis of the interaction of antibodies with a conserved enzymatically deglycosylated core of the HIV type 1 envelope glycoprotein 120. AIDS Res Hum Retroviruses. 14:191-8.

23. Blanpain, C., B. Lee, J. Vakili, B. J. Doranz, C. Govaerts, I. Migeotte, M. Sharron, V. Dupriez, G. Vassart, R. W. Doms, and M. Parmentier. 1999. Extracellular cysteines of CCR5 are required for chemokine binding, but dispensable for HIV-1 coreceptor activity. J Biol Chem. 274:18902-8.

24. Bleul, C. C., M. Farzan, H. Choe, C. Parolin, I. Clark-Lewis, J. Sodroski, and T. A. Springer. 1996. The lymphocyte chemoattractant SDF-1 is a ligand for LESTR/fusin and blocks HIV-1 entry. Nature. 382:829-33.

25. Blumenthal, R., D. P. Sarkar, S. Durell, D. E. Howard, and S. J. Morris. 1996. Dilation of the influenza hemagglutinin fusion pore revealed by the kinetics of individual cell-cell fusion events. J Cell Biol. 135:63-71.

26. Boring, L., J. Gosling, F. S. Monteclaro, A. J. Lusis, C. L. Tsou, and I. F. Charo. 1996. Molecular cloning and functional expression of murine JE (monocyte chemoattractant protein 1) and murine macrophage inflammatory protein 1α receptors: evidence for two closely linked C-C chemokine receptors on chromosome 9. J Biol Chem. 271:7551-8.

27. Brady, R. L., E. J. Dodson, G. G. Dodson, G. Lange, S. J. Davis, A. F. Williams, and A. N. Barclay. 1993. Crystal structure of domains 3 and 4 of rat CD4: relation to the NH2- terminal domains. Science. 260:979-83.

28. Brown, D. A., and E. London. 1998. Functions of lipid rafts in biological membranes. Annu Rev Cell Dev Biol. 14:111-36.

29. Brown, P. O. 1997. Integration, p. 161-203. *In* J. M. Coffin and S. H. Hughes and H. E. Varmus (ed.), Retroviruses. Cold Spring Harbor Laboratory Press, Plainview, NY.

30. Caffrey, M., M. Cai, J. Kaufman, S. J. Stahl, P. T. Wingfield, D. G. Covell, A. M. Gronenborn, and G. M. Clore. 1998. Three-dimensional solution structure of the 44 kDa ectodomain of SIV gp41. Embo J. 17:4572-84.

31. Ceresa, B. P., and L. E. Limbird. 1994. Mutation of an aspartate residue highly conserved among G-protein-coupled receptors results in nonreciprocal disruption of α2-adrenergic receptor-G-protein interactions. A negative charge at amino acid residue 79 forecasts α2A-adrenergic receptor sensitivity to allosteric modulation by monovalent cations and fully effective receptor/G-protein coupling. J Biol Chem. 269:29557-64.

32. Chackerian, B., N. L. Haigwood, and J. Overbaugh. 1995. Characterization of a CD4-expressing macaque cell line that can detect virus after a single replication cycle and can be infected by diverse simian immunodeficiency virus isolates. Virology. 213:386-94.

33. Chan, D. C., D. Fass, J. M. Berger, and P. S. Kim. 1997. Core structure of gp41 from the HIV envelope glycoprotein. Cell. 89:263-73.

34. Chan, D. C., and P. S. Kim. 1998. HIV entry and its inhibition. Cell. 93:681-4.

35. Chen, C. A., R. E. Kingston, H. Okayama, and R. F. Selden. 1994. Transfection of DNA into eukaryotic cells, p. 9.1.1-9.2.6. *In* F. M. Ausubel and R. Brent and R. E. Kingston and D. D. Moore and J. G. Seidman and J. A. Smith and K. Struhl

(ed.), Current Protocols in Molecular Biology, vol. 1. John Wiley & Sons, Inc., New York, NY.

36. Chen, Z., P. Zhou, D. D. Ho, N. R. Landau, and P. A. Marx. 1997. Genetically divergent strains of simian immunodeficiency virus use CCR5 as a coreceptor for entry. J Virol. 71:2705-14.

37. Chesebro, B., and K. Wehrly. 1988. Development of a sensitive quantitative focal assay for human immunodeficiency virus infectivity. J Virol. 62:3779-88.

38. Choe, H., M. Farzan, Y. Sun, N. Sullivan, B. Rollins, P. D. Ponath, L. Wu, C. R. Mackay, G. LaRosa, W. Newman, N. Gerard, C. Gerard, and J. Sodroski. 1996. The β-chemokine receptors CCR3 and CCR5 facilitate infection by primary HIV-1 isolates. Cell. 85:1135-48.

39. Cocchi, F., A. L. DeVico, A. Garzino-Demo, S. K. Arya, R. C. Gallo, and P. Lusso. 1995. Identification of RANTES, MIP-1α, and MIP-1β as the major HIV-suppressive factors produced by CD8+ T cells. Science. 270:1811-5.

40. Cocchi, F., A. L. DeVico, A. Garzino-Demo, A. Cara, R. C. Gallo, and P. Lusso. 1996. The V3 domain of the HIV-1 gp120 envelope glycoprotein is critical for chemokine-mediated blockade of infection. Nat Med. 2:1244-7.

41. Coffin, J. M. 1991. Retroviridae and their replication., p. 645-708. *In* B. M. Fields and D. M. Knipe (ed.), Fundamental Virology, second ed. Raven Press, Ltd., New York.

42. Connor, R. I., K. E. Sheridan, D. Ceradini, S. Choe, and N. R. Landau. 1997. Change in coreceptor use coreceptor use correlates with disease progression in HIV-1 infected individuals. J Exp Med. 185:621-8.

43. Cooper, N., P. L. Earl, O. Elroy-Stein, and B. Moss. 1994. Expression of proteins in mammalian cells using vaccinia, p. 16.15.1-16.19.9. *In* F. M. Ausubel and R. Brent and R. E. Kingston and D. D. Moore and J. G. Seidman and J. A. Smith and

K. Struhl (ed.), Current Protocols in Molecular Biology, vol. 2. John Wiley & Sons, Inc., New York, NY.

44. Dalgleish, A. G., P. C. Beverley, P. R. Clapham, D. H. Crawford, M. F. Greaves, and R. A. Weiss. 1984. The CD4 (T4) antigen is an essential component of the receptor for the AIDS retrovirus. Nature. 312:763-7.

45. Daniel, M. D., Y. Li, Y. M. Naidu, P. J. Durda, D. K. Schmidt, C. D. Troup, D. P. Silva, J. J. MacKey, H. W. d. Kestler, P. K. Sehgal, and et al. 1988. Simian immunodeficiency virus from African green monkeys. J Virol. 62:4123-8.

46. Danieli, T., S. L. Pelletier, Y. I. Henis, and J. M. White. 1996. Membrane fusion mediated by the influenza virus hemagglutinin requires the concerted action of at least three hemagglutinin trimers. J Cell Biol. 133:559-69.

47. Davis, C. B., I. Dikic, D. Unutmaz, C. M. Hill, J. Arthos, M. A. Siani, D. A. Thompson, J. Schlessinger, and D. R. Littman. 1997. Signal transduction due to HIV-1 envelope interactions with chemokine receptors CXCR4 or CCR5. J Exp Med. 186:1793-8.

48. Dean, M., M. Carrington, C. Winkler, G. A. Huttley, M. W. Smith, R. Allikmets, J. J. Goedert, S. P. Buchbinder, E. Vittinghoff, E. Gomperts, S. Donfield, D. Vlahov, R. Kaslow, A. Saah, C. Rinaldo, R. Detels, and S. J. O'Brien. 1996. Genetic restriction of HIV-1 infection and progression to AIDS by a deletion allele of the CKR5 structural gene. Hemophilia Growth and Development Study, Multicenter AIDS Cohort Study, Multicenter Hemophilia Cohort Study, San Francisco City Cohort, ALIVE Study. Science. 273:1856-62.

49. Dejucq, N., G. Simmons, and P. R. Clapham. 1999. Expanded tropism of primary human immunodeficiency virus type 1 R5 strains to CD4(+) T-cell lines determined by the capacity to exploit low concentrations of CCR5. J Virol. 73:7842-7.

50. Deng, H., R. Liu, W. Ellmeier, S. Choe, D. Unutmaz, M. Burkhart, P. Di Marzio, S. Marmon, R. E. Sutton, C. M. Hill, C. B. Davis, S. C. Peiper, T. J. Schall, D. R. Littman, and N. R. Landau. 1996. Identification of a major co-receptor for primary isolates of HIV-1. Nature. 381:661-6.

51. Deng, H. K., D. Unutmaz, V. N. KewalRamani, and D. R. Littman. 1997. Expression cloning of new receptors used by simian and human immunodeficiency viruses. Nature. 388:296-300.

52. Doranz, B. J., Z. H. Lu, J. Rucker, T. Y. Zhang, M. Sharron, Y. H. Cen, Z. X. Wang, H. H. Guo, J. G. Du, M. A. Accavitti, R. W. Doms, and S. C. Peiper. 1997. Two distinct CCR5 domains can mediate coreceptor usage by human immunodeficiency virus type 1. J Virol. 71:6305-14.

53. Doranz, B. J., J. Rucker, Y. Yi, R. J. Smyth, M. Samson, S. C. Peiper, M. Parmentier, R. G. Collman, and R. W. Doms. 1996. A dual-tropic primary HIV-1 isolate that uses fusin and the β-chemokine receptors CKR-5, CKR-3, and CKR-2b as fusion cofactors. Cell. 85:1149-58.

54. Dragic, T., V. Litwin, G. P. Allaway, S. R. Martin, Y. Huang, K. A. Nagashima, C. Cayanan, P. J. Maddon, R. A. Koup, J. P. Moore, and W. A. Paxton. 1996. HIV-1 entry into CD4+ cells is mediated by the chemokine receptor CC-CKR-5. Nature. 381:667-73.

55. Dragic, T., A. Trkola, S. W. Lin, K. A. Nagashima, F. Kajumo, L. Zhao, W. C. Olson, L. Wu, C. R. Mackay, G. P. Allaway, T. P. Sakmar, J. P. Moore, and P. J. Maddon. 1998. Amino-terminal substitutions in the CCR5 coreceptor impair gp120 binding and human immunodeficiency virus type 1 entry. J Virol. 72:279-85.

56. Edinger, A. L., A. Amedee, K. Miller, B. J. Doranz, M. Endres, M. Sharron, M. Samson, Z. H. Lu, J. E. Clements, M. Murphey-Corb, S. C. Peiper, M. Parmentier, C. C. Broder, and R. W. Doms. 1997. Differential utilization of CCR5

by macrophage and T cell tropic simian immunodeficiency virus strains. Proc Natl Acad Sci U S A. 94:4005-10.

57. Edinger, A. L., C. Blanpain, K. J. Kunstman, S. M. Wolinsky, M. Parmentier, and R. W. Doms. 1999. Functional Dissection of CCR5 Coreceptor Function through the Use of CD4-Independent Simian Immunodeficiency Virus Strains. J Virol. 73:4062-4073.

58. Emini, E. A., and H. Y. Fan. 1997. Immunological and pharmacological approaches to the control of retroviral infections, p. 637-706. *In* J. M. Coffin and S. H. Hughes and H. E. Varmus (ed.), Retroviruses. Cold Spring Harbor Laboratory Press, Plainview, NY.

59. Farzan, M., H. Choe, K. Martin, L. Marcon, W. Hofmann, G. Karlsson, Y. Sun, P. Barrett, N. Marchand, N. Sullivan, N. Gerard, C. Gerard, and J. Sodroski. 1997. Two orphan seven-transmembrane segment receptors which are expressed in CD4-positive cells support simian immunodeficiency virus infection. J Exp Med. 186:405-11.

60. Farzan, M., H. Choe, K. A. Martin, Y. Sun, M. Sidelko, C. R. Mackay, N. P. Gerard, J. Sodroski, and C. Gerard. 1997. HIV-1 entry and macrophage inflammatory protein-1β-mediated signaling are independent functions of the chemokine receptor CCR5. J Biol Chem. 272:6854-7.

61. Farzan, M., H. Choe, L. Vaca, K. Martin, Y. Sun, E. Desjardins, N. Ruffing, L. Wu, R. Wyatt, N. Gerard, C. Gerard, and J. Sodroski. 1998. A tyrosine-rich region in the N terminus of CCR5 is important for human immunodeficiency virus type 1 entry and mediates an association between gp120 and CCR5. J Virol. 72:1160-4.

62. Farzan, M., T. Mirzabekov, P. Kolchinsky, R. Wyatt, M. Cayabyab, N. P. Gerard, C. Gerard, J. Sodroski, and H. Choe. 1999. Tyrosine sulfation of the amino terminus of CCR5 facilitates HIV-1 entry. Cell. 96:667-76.

63. Fass, D., S. C. Harrison, and P. S. Kim. 1996. Retrovirus envelope domain at 1.7 angstrom resolution. Nat Struct Biol. 3:465-9.

64. Fauci, A. S., and R. C. Desrosiers. 1997. Pathogenesis of HIV and SIV, p. 587-635. *In* J. M. Coffin and S. H. Hughes and H. E. Varmus (ed.), Retroviruses. Cold Spring Harbor Laboratory Press, Plainview, NY.

65. Feng, Y., C. C. Broder, P. E. Kennedy, and E. A. Berger. 1996. HIV-1 entry cofactor: functional cDNA cloning of a seven-transmembrane, G protein-coupled receptor. Science. 272:872-7.

66. Finzi, D., J. Blankson, J. D. Siliciano, J. B. Margolick, K. Chadwick, T. Pierson, K. Smith, J. Lisziewicz, F. Lori, C. Flexner, T. C. Quinn, R. E. Chaisson, E. Rosenberg, B. Walker, S. Gange, J. Gallant, and R. F. Siliciano. 1999. Latent infection of CD4+ T cells provides a mechanism for lifelong persistence of HIV-1, even in patients on effective combination therapy. Nat Med. 5:512-7.

67. Fomsgaard, A., V. M. Hirsch, J. S. Allan, and P. R. Johnson. 1991. A highly divergent proviral DNA clone of SIV from a distinct species of African green monkey. Virology. 182:397-402.

68. Fraser, C. M., F. Z. Chung, C. D. Wang, and J. C. Venter. 1988. Site-directed mutagenesis of human β-adrenergic receptors: substitution of aspartic acid-130 by asparagine produces a receptor with high-affinity agonist binding that is uncoupled from adenylate cyclase. Proc Natl Acad Sci U S A. 85:5478-82.

69. Frey, S., M. Marsh, S. Gunther, A. Pelchen-Matthews, P. Stephens, S. Ortlepp, and T. Stegmann. 1995. Temperature dependence of cell-cell fusion induced by the envelope glycoprotein of human immunodeficiency virus type 1. J Virol. 69:1462-72.

70. Gao, F., E. Bailes, D. L. Robertson, Y. Chen, C. M. Rodenburg, S. F. Michael, L. B. Cummins, L. O. Arthur, M. Peeters, G. M. Shaw, P. M. Sharp, and B. H. Hahn.

1999. Origin of HIV-1 in the chimpanzee Pan troglodytes troglodytes. Nature. 397:436-41.

71. Genoud, S., F. Kajumo, Y. Guo, D. Thompson, and T. Dragic. 1999. CCR5-Mediated human immunodeficiency virus entry depends on an amino-terminal gp120-binding site and on the conformational integrity of all four extracellular domains. J Virol. 73:1645-8.

72. Goldstein, B. 1989. Diffusion limited effects of receptor clustering. Comments Theoretical Biology. 1:109-127.

73. Gosling, J., F. S. Monteclaro, R. E. Atchison, H. Arai, C. L. Tsou, M. A. Goldsmith, and I. F. Charo. 1997. Molecular uncoupling of C-C chemokine receptor 5-induced chemotaxis and signal transduction from HIV-1 coreceptor activity. Proc Natl Acad Sci U S A. 94:5061-6.

74. Grivel, J. C., and L. B. Margolis. 1999. CCR5- and CXCR4-tropic HIV-1 are equally cytopathic for their T-cell targets in human lymphoid tissue. Nat Med. 5:344-6.

75. Hahn, B. H., G. M. Shaw, S. K. Arya, M. Popovic, R. C. Gallo, and F. Wong-Staal. 1984. Molecular cloning and characterization of the HTLV-III virus associated with AIDS. Nature. 312:166-9.

76. Hanna, Z., D. G. Kay, N. Rebai, A. Guimond, S. Jothy, and P. Jolicoeur. 1998. Nef harbors a major determinant of pathogenicity for an AIDS-like disease induced by HIV-1 in transgenic mice. Cell. 95:163-75.

77. Harlow, E., and D. Lane. 1988. Antibodies: A Laboratory Manual. Cold Spring Harbor Laboratory, Cold Spring Harbor, NY.

78. Harouse, J. M., A. Gettie, R. C. Tan, J. Blanchard, and C. Cheng-Mayer. 1999. Distinct pathogenic sequela in rhesus macaques infected with CCR5 or CXCR4 utilizing SHIVs. Science. 284:816-9.

79. Helseth, E., U. Olshevsky, C. Furman, and J. Sodroski. 1991. Human immunodeficiency virus type 1 gp120 envelope glycoprotein regions important for association with the gp41 transmembrane glycoprotein. J Virol. 65:2119-23.

80. Hill, C. M., H. Deng, D. Unutmaz, V. N. Kewalramani, L. Bastiani, M. K. Gorny, S. Zolla-Pazner, and D. R. Littman. 1997. Envelope glycoproteins from human immunodeficiency virus types 1 and 2 and simian immunodeficiency virus can use human CCR5 as a coreceptor for viral entry and make direct CD4-dependent interactions with this chemokine receptor. J Virol. 71:6296-304.

81. Hill, C. M., D. Kwon, M. Jones, C. B. Davis, S. Marmon, B. L. Daugherty, J. A. DeMartino, M. S. Springer, D. Unutmaz, and D. R. Littman. 1998. The Amino Terminus of Human CCR5 Is Required for Its Function as a Receptor for Diverse Human and Simian Immunodeficiency Virus Envelope Glycoproteins. Virology. 248:357-71.

82. Hoffman, T. L., C. C. LaBranche, W. Zhang, G. Canziani, J. Robinson, I. Chaiken, J. A. Hoxie, and R. W. Doms. 1999. Stable exposure of the coreceptor-binding site in a CD4-independent HIV- 1 envelope protein. Proc Natl Acad Sci U S A. 96:6359-64.

83. Huang, Y., W. A. Paxton, S. M. Wolinsky, A. U. Neumann, L. Zhang, T. He, S. Kang, D. Ceradini, Z. Jin, K. Yazdanbakhsh, K. Kunstman, D. Erickson, E. Dragon, N. R. Landau, J. Phair, D. D. Ho, and R. A. Koup. 1996. The role of a mutant CCR5 allele in HIV-1 transmission and disease progression. Nat Med. 2:1240-3.

84. Hung, C. S., N. Vander Heyden, and L. Ratner. 1999. Analysis of the critical domain in the V3 loop of human immunodeficiency virus type 1 gp120 involved in CCR5 utilization. J Virol. 73:8216-26.

85. Hunter, E. 1997. Viral entry and receptors, p. 71-119. *In* J. M. Coffin and S. H. Hughes and H. E. Varmus (ed.), Retroviruses. Cold Spring Harbor Laboratory Press, Plainview, NY.

86. Ivey-Hoyle, M., J. S. Culp, M. A. Chaikin, B. D. Hellmig, T. J. Matthews, R. W. Sweet, and M. Rosenberg. 1991. Envelope glycoproteins from biologically diverse isolates of immunodeficiency viruses have widely different affinities for CD4. Proc Natl Acad Sci U S A. 88:512-6.

87. Jiang, S. 1997. HIV-1--co-receptors binding. Nat Med. 3:367-8.

88. Jin, M. J., H. Hui, D. L. Robertson, M. C. Müller, F. Barré-Sinoussi, V. M. Hirsch, J. S. Allan, G. M. Shaw, P. M. Sharp, and B. H. Hahn. 1994. Mosaic genome structure of simian immunodeficiency virus from west African green monkeys. Embo J. 13:2935-47.

89. Johnson, P. R., A. Fomsgaard, J. Allan, M. Gravell, W. T. London, R. A. Olmsted, and V. M. Hirsch. 1990. Simian immunodeficiency viruses from African green monkeys display unusual genetic diversity. J Virol. 64:1086-92.

90. Kabat, D., S. L. Kozak, K. Wehrly, and B. Chesebro. 1994. Differences in CD4 dependence for infectivity of laboratory-adapted and primary patient isolates of human immunodeficiency virus type 1. J Virol. 68:2570-7.

91. Kato, K., H. Sato, and Y. Takebe. 1999. Role of naturally occurring basic amino acid substitutions in the human immunodeficiency virus type 1 subtype E envelope V3 loop on viral coreceptor usage and cell tropism. J Virol. 73:5520-6.

92. Kikukawa, R., Y. Koyanagi, S. Harada, N. Kobayashi, M. Hatanaka, and N. Yamamoto. 1986. Differential susceptibility to the acquired immunodeficiency syndrome retrovirus in cloned cells of human leukemic T-cell line Molt-4. J Virol. 57:1159-62.

93. Kirchhoff, F., S. Pohlmann, M. Hamacher, R. E. Means, T. Kraus, K. Uberla, and P. Di Marzio. 1997. Simian immunodeficiency virus variants with differential T-

cell and macrophage tropism use CCR5 and an unidentified cofactor expressed in CEMx174 cells for efficient entry. J Virol. 71:6509-16.

94. Klatzmann, D., E. Champagne, S. Chamaret, J. Gruest, D. Guetard, T. Hercend, J. C. Gluckman, and L. Montagnier. 1984. T-lymphocyte T4 molecule behaves as the receptor for human retrovirus LAV. Nature. 312:767-8.

95. Kozak, S. L., S. E. Kuhmann, E. J. Platt, and D. Kabat. 1999. Roles of CD4 and coreceptors in binding, endocytosis, and proteolysis of gp120 envelope glycoproteins derived from human immunodeficiency virus type 1. J Biol Chem. 274:23499-507.

96. Kozak, S. L., E. J. Platt, N. Madani, F. E. Ferro, Jr., K. Peden, and D. Kabat. 1997. CD4, CXCR-4, and CCR-5 dependencies for infections by primary patient and laboratory-adapted isolates of human immunodeficiency virus type 1. J Virol. 71:873-82.

97. Kuhmann, S. E., and D. Kabat. 1999. unpublished data.

98. Kuhmann, S. E., E. J. Platt, S. L. Kozak, and D. Kabat. 1997. Polymorphisms in the CCR5 genes of African green monkeys and mice implicate specific amino acids in infections by simian and human immunodeficiency viruses. J Virol. 71:8642-56.

99. Kurth, R., and S. Norley. 1994. Simian immunodeficiency viruses of African green monkeys. Curr Top Microbiol Immunol. 188:21-33.

100. Kwong, P. D., R. Wyatt, J. Robinson, R. W. Sweet, J. Sodroski, and W. A. Hendrickson. 1998. Structure of an HIV gp120 envelope glycoprotein in complex with the CD4 receptor and a neutralizing human antibody. Nature. 393:648-59.

101. Lapham, C. K., J. Ouyang, B. Chandrasekhar, N. Y. Nguyen, D. S. Dimitrov, and H. Golding. 1996. Evidence for cell-surface association between fusin and the CD4-gp120 complex in human cell lines. Science. 274:602-5.

102. Layne, S. P., M. J. Merges, M. Dembo, J. L. Spouge, and P. L. Nara. 1990. HIV requires multiple gp120 molecules for CD4-mediated infection. Nature. 346:277-9.

103. Lee, B., M. Sharron, C. Blanpain, B. J. Doranz, J. Vakili, P. Setoh, E. Berg, G. Liu, H. R. Guy, S. R. Durell, M. Parmentier, C. N. Chang, K. Price, M. Tsang, and R. W. Doms. 1999. Epitope mapping of CCR5 reveals multiple conformational states and distinct but overlapping structures involved in chemokine and coreceptor function. J Biol Chem. 274:9617-26.

104. Lee, B., M. Sharron, L. J. Montaner, D. Weissman, and R. W. Doms. 1999. Quantification of CD4, CCR5, and CXCR4 levels on lymphocyte subsets, dendritic cells, and differentially conditioned monocyte-derived macrophages. Proc Natl Acad Sci U S A. 96:5215-20.

105. Leonard, C. K., M. W. Spellman, L. Riddle, R. J. Harris, J. N. Thomas, and T. J. Gregory. 1990. Assignment of intrachain disulfide bonds and characterization of potential glycosylation sites of the type 1 recombinant human immunodeficiency virus envelope glycoprotein (gp120) expressed in Chinese hamster ovary cells. J Biol Chem. 265:10373-82.

106. Li, Y., H. Hui, C. J. Burgess, R. W. Price, P. M. Sharp, B. H. Hahn, and G. M. Shaw. 1992. Complete nucleotide sequence, genome organization, and biological properties of human immunodeficiency virus type 1 in vivo: evidence for limited defectiveness and complementation. J Virol. 66:6587-600.

107. Littman, D. R. 1998. Chemokine receptors: keys to AIDS pathogenesis? Cell. 93:677-80.

108. Liu, R., W. A. Paxton, S. Choe, D. Ceradini, S. R. Martin, R. Horuk, M. E. MacDonald, H. Stuhlmann, R. A. Koup, and N. R. Landau. 1996. Homozygous defect in HIV-1 coreceptor accounts for resistance of some multiply-exposed individuals to HIV-1 infection. Cell. 86:367-77.

109. Locati, M., and P. M. Murphy. 1999. Chemokines and chemokine receptors: biology and clinical relevance in inflammation and AIDS. Annu Rev Med. 50:425-40.

110. Luciw, P. A., S. J. Potter, K. Steimer, D. Dina, and J. A. Levy. 1984. Molecular cloning of AIDS-associated retrovirus. Nature. 312:760-3.

111. Madani, N., and D. Kabat. 1998. An endogenous inhibitor of human immunodeficiency virus in human lymphocytes is overcome by the viral Vif protein. J Virol. 72:10251-5.

112. Madani, N., S. L. Kozak, M. P. Kavanaugh, and D. Kabat. 1998. gp120 envelope glycoproteins of human immunodeficiency viruses competitively antagonize signaling by coreceptors CXCR4 and CCR5. Proc Natl Acad Sci U S A. 95:8005-10.

113. Maddon, P. J., A. G. Dalgleish, J. S. McDougal, P. R. Clapham, R. A. Weiss, and R. Axel. 1986. The T4 gene encodes the AIDS virus receptor and is expressed in the immune system and the brain. Cell. 47:333-48.

114. Malashkevich, V. N., D. C. Chan, C. T. Chutkowski, and P. S. Kim. 1998. Crystal structure of the simian immunodeficiency virus (SIV) gp41 core: conserved helical interactions underlie the broad inhibitory activity of gp41 peptides. Proc Natl Acad Sci U S A. 95:9134-9.

115. Malashkevich, V. N., B. J. Schneider, M. L. McNally, M. A. Milhollen, J. X. Pang, and P. S. Kim. 1999. Core structure of the envelope glycoprotein GP2 from Ebola virus at 1.9- A resolution. Proc Natl Acad Sci U S A. 96:2662-7.

116. Marcon, L., H. Choe, K. A. Martin, M. Farzan, P. D. Ponath, L. Wu, W. Newman, N. Gerard, C. Gerard, and J. Sodroski. 1997. Utilization of C-C chemokine receptor 5 by the envelope glycoproteins of a pathogenic simian immunodeficiency virus, SIVmac239. J Virol. 71:2522-7.

117. Martin, K. A., R. Wyatt, M. Farzan, H. Choe, L. Marcon, E. Desjardins, J. Robinson, J. Sodroski, C. Gerard, and N. P. Gerard. 1997. CD4-Independent binding of SIV gp120 to rhesus CCR5. Science. 278:1470-3.

118. McDougal, J. S., M. S. Kennedy, J. M. Sligh, S. P. Cort, A. Mawle, and J. K. Nicholson. 1986. Binding of HTLV-III/LAV to T4+ T cells by a complex of the 110K viral protein and the T4 molecule. Science. 231:382-5.

119. McDougal, J. S., A. Mawle, S. P. Cort, J. K. Nicholson, G. D. Cross, J. A. Scheppler-Campbell, D. Hicks, and J. Sligh. 1985. Cellular tropism of the human retrovirus HTLV-III/LAV. I. Role of T cell activation and expression of the T4 antigen. J Immunol. 135:3151-62.

120. Meyer, A., A. J. Coyle, A. E. Proudfoot, T. N. Wells, and C. A. Power. 1996. Cloning and characterization of a novel murine macrophage inflammatory protein-1α receptor. J Biol Chem. 271:14445-51.

121. Mirzabekov, T., N. Bannert, M. Farzan, W. Hofmann, P. Kolchinsky, L. Wu, R. Wyatt, and J. Sodroski. 1999. Enhanced expression, native purification, and characterization of CCR5, a principal HIV-1 coreceptor. J Biol Chem. 274:28745-50.

122. Monck, J. R., and J. M. Fernandez. 1996. The fusion pore and mechanisms of biological membrane fusion. Curr Opin Cell Biol. 8:524-33.

123. Mondor, I., M. Moulard, S. Ugolini, P. J. Klasse, J. Hoxie, A. Amara, T. Delaunay, R. Wyatt, J. Sodroski, and Q. J. Sattentau. 1998. Interactions among HIV gp120, CD4, and CXCR4: dependence on CD4 expression level, gp120 viral origin, conservation of the gp120 COOH- and NH2-termini and V1/V2 and V3 loops, and sensitivity to neutralizing antibodies. Virology. 248:394-405.

124. Mondor, I., S. Ugolini, and Q. J. Sattentau. 1998. Human immunodeficiency virus type 1 attachment to HeLa CD4 cells is CD4 independent and gp120 dependent and requires cell surface heparans. J Virol. 72:3623-34.

125. Monteclaro, F. S., and I. F. Charo. 1996. The amino-terminal extracellular domain of the MCP-1 receptor, but not the RANTES/MIP-1α receptor, confers chemokine selectivity. Evidence for a two-step mechanism for MCP-1 receptor activation. J Biol Chem. 271:19084-92.

126. Moore, J. P., and J. Binley. 1998. HIV. Envelope's letters boxed into shape. Nature. 393:630-1.

127. Moore, J. P., L. C. Burkly, R. I. Connor, Y. Cao, R. Tizard, D. D. Ho, and R. A. Fisher. 1993. Adaptation of two primary human immunodeficiency virus type 1 isolates to growth in transformed T cell lines correlates with alterations in the responses of their envelope glycoproteins to soluble CD4. AIDS Res Hum Retroviruses. 9:529-39.

128. Müller, M. C., N. K. Saksena, E. Nerrienet, C. Chappey, V. M. Hervé, J.-P. Durand, P. Legal-Campodonico, M. C. Lang, J. P. Digoutte, A. J. Georges, M.-C. Georges-Courbot, P. Sonigo, and F. Barré-Sinoussi. 1993. Simian immunodeficiency viruses from central and western Africa: evidence for a new species-specific lentivirus in tantalus monkeys. J Virol. 67:1227-35.

129. Murphy, P. M. 1994. The molecular biology of leukocyte chemoattractant receptors. Annu Rev Immunol. 12:593-633.

130. Naif, H. M., S. Li, M. Alali, A. Sloane, L. Wu, M. Kelly, G. Lynch, A. Lloyd, and A. L. Cunningham. 1998. CCR5 expression correlates with susceptibility of maturing monocytes to human immunodeficiency virus type 1 infection. J Virol. 72:830-6.

131. Nir, S., M. P. de Lima, C. Larsen, J. Wilschut, D. Hoekstra, and N. Düzgünes. 1993. Kinetics and extent of virus-cell aggregation and fusion, p. 437-452. *In* J. Bentz (ed.), Viral fusion mechanisms. CRC Press, Inc., Boca Raton, FL.

132. Norley, S. G. 1996. SIVagm infection of its natural African green monkey host. Immunol Lett. 51:53-8.

133. Oberlin, E., A. Amara, F. Bachelerie, C. Bessia, J. L. Virelizier, F. Arenzana-Seisdedos, O. Schwartz, J. M. Heard, I. Clark-Lewis, D. F. Legler, M. Loetscher, M. Baggiolini, and B. Moser. 1996. The CXC chemokine SDF-1 is the ligand for LESTR/fusin and prevents infection by T-cell-line-adapted HIV-1. Nature. 382:833-5.

134. Olbrich, H., A. E. Proudfoot, and M. Oppermann. 1999. Chemokine-induced phosphorylation of CC chemokine receptor 5 (CCR5). J Leukoc Biol. 65:281-5.

135. Olson, W. C., G. E. Rabut, K. A. Nagashima, D. N. Tran, D. J. Anselma, S. P. Monard, J. P. Segal, D. A. D. Thompson, F. Kajumo, Y. Guo, J. P. Moore, P. J. Maddon, and T. Dragic. 1999. Differential Inhibition of Human Immunodeficiency Virus Type 1 Fusion, gp120 Binding, and CC-Chemokine Activity by Monoclonal Antibodies to CCR5. J Virol. 73:4145-4155.

136. Pelchen-Matthews, A., N. Signoret, P. J. Klasse, A. Fraile-Ramos, and M. Marsh. 1999. Chemokine receptor trafficking and viral replication. Immunol Rev. 168:33-49.

137. Penn, M. L., J. C. Grivel, B. Schramm, M. A. Goldsmith, and L. Margolis. 1999. CXCR4 utilization is sufficient to trigger CD4+ T cell depletion in HIV- 1-infected human lymphoid tissue. Proc Natl Acad Sci U S A. 96:663-8.

138. Pesenti, E., C. Pastore, F. Lillo, A. G. Siccardi, D. Vercelli, and L. Lopalco. 1999. Role of CD4 and CCR5 levels in the susceptibility of primary macrophages to infection by CCR5-dependent HIV type 1 isolates. AIDS Res Hum Retroviruses. 15:983-7.

139. Picard, L., G. Simmons, C. A. Power, A. Meyer, R. A. Weiss, and P. R. Clapham. 1997. Multiple extracellular domains of CCR5 contribute to human immunodeficiency virus type 1 entry and fusion. J Virol. 71:5003-5011.

140. Piguet, V., O. Schwartz, S. Le Gall, and D. Trono. 1999. The downregulation of CD4 and MHC-I by primate lentiviruses: a paradigm for the modulation of cell surface receptors. Immunol Rev. 168:51-63.

141. Platt, E. J., S. L. Kozak, and D. Kabat. 2000. Critical role of enhanced CD4 affinity in laboratory-adaptation of human immunodeficiency virus type-1. AIDS Res Hum Retroviruses. In press.

142. Platt, E. J., S. E. Kuhmann, and D. Kabat. 1999. unpublished data.

143. Platt, E. J., N. Madani, S. L. Kozak, and D. Kabat. 1997. Infectious properties of human immunodeficiency virus type 1 mutants with distinct affinities for the CD4 receptor. J Virol. 71:883-90.

144. Platt, E. J., K. Wehrly, S. E. Kuhmann, B. Chesebro, and D. Kabat. 1998. Effects of CCR5 and CD4 cell surface concentrations on infections by macrophagetropic isolates of human immunodeficiency virus type 1. J Virol. 72:2855-64.

145. Premack, B. A., and T. J. Schall. 1996. Chemokine receptors: gateways to inflammation and infection. Nat Med. 2:1174-8.

146. Pretet, J. L., A. C. Zerbib, M. Girard, J. G. Guillet, and C. Butor. 1997. Chimpanzee CXCR4 and CCR5 act as coreceptors for HIV type 1. AIDS Res Hum Retroviruses. 13:1583-7.

147. Rabson, A. B., and B. J. Graves. 1997. Synthesis and processing of viral RNA, p. 587-635. *In* J. M. Coffin and S. H. Hughes and H. E. Varmus (ed.), Retroviruses. Cold Spring Harbor Laboratory Press, Plainview, NY.

148. Rabut, G. E., J. A. Konner, F. Kajumo, J. P. Moore, and T. Dragic. 1998. Alanine substitutions of polar and nonpolar residues in the amino-terminal domain of CCR5 differently impair entry of macrophage-and dualtropic isolates of human immunodeficiency virus type 1. J Virol. 72:3464-8.

149. Rana, S., G. Besson, D. G. Cook, J. Rucker, R. J. Smyth, Y. Yi, J. D. Turner, H. H. Guo, J. G. Du, S. C. Peiper, E. Lavi, M. Samson, F. Libert, C. Liesnard, G.

Vassart, R. W. Doms, M. Parmentier, and R. G. Collman. 1997. Role of CCR5 in infection of primary macrophages and lymphocytes by macrophage-tropic strains of human immunodeficiency virus: resistance to patient-derived and prototype isolates resulting from the Δ*ccr5* mutation. J Virol. 71:3219-27.

150. Raport, C. J., J. Gosling, V. L. Schweickart, P. W. Gray, and I. F. Charo. 1996. Molecular cloning and functional characterization of a novel human CC chemokine receptor (CCR5) for RANTES, MIP-1β, and MIP-1α. J Biol Chem. 271:17161-6.

151. Rizzuto, C. D., R. Wyatt, N. Hernandez-Ramos, Y. Sun, P. D. Kwong, W. A. Hendrickson, and J. Sodroski. 1998. A conserved HIV gp120 glycoprotein structure involved in chemokine receptor binding. Science. 280:1949-53.

152. Rollins, T. E., S. Siciliano, and M. S. Springer. 1988. Solubilization of the functional C5a receptor from human polymorphonuclear leukocytes. J Biol Chem. 263:520-6.

153. Ross, T. M., P. D. Bieniasz, and B. R. Cullen. 1998. Multiple residues contribute to the inability of murine CCR-5 to function as a coreceptor for macrophage-tropic human immunodeficiency virus type 1 isolates. J Virol. 72:1918-24.

154. Ross, T. M., P. D. Bieniasz, and B. R. Cullen. 1999. Role of chemokine receptors in HIV-1 infection and pathogenesis. Adv Virus Res. 52:233-67.

155. Rucker, J., M. Samson, B. J. Doranz, F. Libert, J. F. Berson, Y. Yi, R. J. Smyth, R. G. Collman, C. C. Broder, G. Vassart, R. W. Doms, and M. Parmentier. 1996. Regions in β-chemokine receptors CCR5 and CCR2b that determine HIV-1 cofactor specificity. Cell. 87:437-46.

156. Ryu, S. E., A. Truneh, R. W. Sweet, and W. A. Hendrickson. 1994. Structures of an HIV and MHC binding fragment from human CD4 as refined in two crystal lattices. Structure. 2:59-74.

157. Samson, M., O. Labbe, C. Mollereau, G. Vassart, and M. Parmentier. 1996. Molecular cloning and functional expression of a new human CC-chemokine receptor gene. Biochemistry. 35:3362-7.

158. Samson, M., F. Libert, B. J. Doranz, J. Rucker, C. Liesnard, C. M. Farber, S. Saragosti, C. Lapoumeroulie, J. Cognaux, C. Forceille, G. Muyldermans, C. Verhofstede, G. Burtonboy, M. Georges, T. Imai, S. Rana, Y. Yi, R. J. Smyth, R. G. Collman, R. W. Doms, G. Vassart, and M. Parmentier. 1996. Resistance to HIV-1 infection in caucasian individuals bearing mutant alleles of the CCR-5 chemokine receptor gene. Nature. 382:722-5.

159. Sattentau, Q. J., J. P. Moore, F. Vignaux, F. Traincard, and P. Poignard. 1993. Conformational changes induced in the envelope glycoproteins of the human and simian immunodeficiency viruses by soluble receptor binding. J Virol. 67:7383-93.

160. Scarlatti, G., E. Tresoldi, Björndal, R. Fredriksson, C. Colognesi, H. K. Deng, M. S. Malnati, A. Plebani, A. G. Siccardi, D. R. Littman, E. M. Fenyö, and P. Lusso. 1997. In vivo evolution of HIV-1 co-receptor usage and sensitivity to chemokine-mediated suppression. Nat Med. 3:1259-65.

161. Schmidt, N. J., E. H. Lennette, C. W. Shon, and J. Dennis. 1964. The sensitivity of grivet monkey kidney cell line BS-C-1 for propagation and isolation of certain human viruses. Am J Public Health. 54:1522-1530.

162. Schmidtmayerova, H., M. Alfano, G. Nuovo, and M. Bukrinsky. 1998. Human immunodeficiency virus type 1 T-lymphotropic strains enter macrophages via a CD4- and CXCR4-mediated pathway: replication is restricted at a postentry level. J Virol. 72:4633-42.

163. Schuitemaker, H., M. Koot, N. A. Kootstra, M. W. Dercksen, R. E. de Goede, R. P. van Steenwijk, J. M. Lange, J. K. Schattenkerk, F. Miedema, and M. Tersmette. 1992. Biological phenotype of human immunodeficiency virus type 1

clones at different stages of infection: progression of disease is associated with a shift from monocytotropic to T-cell-tropic virus population. J Virol. 66:1354-60.

164. Schwartz, M. 1976. The adsorption of coliphage lambda to its host: effect of variations in the surface density of receptor and in phage-receptor affinity. J Mol Biol. 103:521-36.

165. Siciliano, S. J., B. L. Daugherty, J. A. DeMartino, and M. S. Springer. 1999. manuscript in preparation.

166. Siciliano, S. J., S. E. Kuhmann, Y. Weng, N. Madani, M. S. Springer, J. E. Lineberger, R. Danzeisen, M. D. Miller, M. P. Kavanaugh, J. A. DeMartino, and D. Kabat. 1999. A Critical Site in the Core of the CCR5 Chemokine Receptor Required for Binding and Infectivity of Human Immunodeficiency Virus Type 1. J Biol Chem. 274:1905-1913.

167. Siciliano, S. J., T. E. Rollins, J. DeMartino, Z. Konteatis, L. Malkowitz, G. Van Riper, S. Bondy, H. Rosen, and M. S. Springer. 1994. Two-site binding of C5a by its receptor: an alternative binding paradigm for G protein-coupled receptors. Proc Natl Acad Sci U S A. 91:1214-8.

168. Siess, D. C., S. L. Kozak, and D. Kabat. 1996. Exceptional fusogenicity of Chinese hamster ovary cells with murine retroviruses suggests roles for cellular factor(s) and receptor clusters in the membrane fusion process. J Virol. 70:3432-9.

169. Simon, F., P. Mauclère, P. Roques, I. Loussert-Ajaka, M. C. Müller-Trutwin, S. Saragosti, M. C. Georges-Courbot, F. Barré-Sinoussi, and F. Brun-Vézinet. 1998. Identification of a new human immunodeficiency virus type 1 distinct from group M and group O. Nat Med. 4:1032-7.

170. Simon, J. H., N. C. Gaddis, R. A. Fouchier, and M. H. Malim. 1998. Evidence for a newly discovered cellular anti-HIV-1 phenotype. Nat Med. 4:1397-400.

171. Skehel, J. J., and D. C. Wiley. 1998. Coiled coils in both intracellular vesicle and viral membrane fusion. Cell. 95:871-4.

172. Speck, R. F., K. Wehrly, E. J. Platt, R. E. Atchison, I. F. Charo, D. Kabat, B. Chesebro, and M. A. Goldsmith. 1997. Selective employment of chemokine receptors as human immunodeficiency virus type 1 coreceptors determined by individual amino acids within the envelope V3 loop. J Virol. 71:7136-9.

173. Stewart, G. 1998. Chemokine genes--beating the odds. Nat Med. 4:275-7.

174. Swanstrom, R., and J. W. Wills. 1997. Synthesis, assembly, and processing of viral proteins, p. 587-635. *In* J. M. Coffin and S. H. Hughes and H. E. Varmus (ed.), Retroviruses. Cold Spring Harbor Laboratory Press, Plainview, NY.

175. Telesnitsky, A., and S. P. Goff. 1997. Reverse transcriptase and the generation of retroviral DNA, p. 121-160. *In* J. M. Coffin and S. H. Hughes and H. E. Varmus (ed.), Retroviruses. Cold Spring Harbor Laboratory Press, Plainview, NY.

176. Thali, M., J. P. Moore, C. Furman, M. Charles, D. D. Ho, J. Robinson, and J. Sodroski. 1993. Characterization of conserved human immunodeficiency virus type 1 gp120 neutralization epitopes exposed upon gp120-CD4 binding. J Virol. 67:3978-88.

177. Trkola, A., T. Dragic, J. Arthos, J. M. Binley, W. C. Olson, G. P. Allaway, C. Cheng-Mayer, J. Robinson, P. J. Maddon, and J. P. Moore. 1996. CD4-dependent, antibody-sensitive interactions between HIV-1 and its co-receptor CCR-5. Nature. 384:184-7.

178. Tuttle, D. L., J. K. Harrison, C. Anders, J. W. Sleasman, and M. M. Goodenow. 1998. Expression of CCR5 increases during monocyte differentiation and directly mediates macrophage susceptibility to infection by human immunodeficiency virus type 1. J Virol. 72:4962-9.

179. Van Riper, G., S. Siciliano, P. A. Fischer, R. Meurer, M. S. Springer, and H. Rosen. 1993. Characterization and species distribution of high affinity GTP-coupled receptors for human rantes and monocyte chemoattractant protein 1. J Exp Med. 177:851-6.

180. Vogt, V. M. 1997. Retroviral virions and genomes, p. 587-635. *In* J. M. Coffin and S. H. Hughes and H. E. Varmus (ed.), Retroviruses. Cold Spring Harbor Laboratory Press, Plainview, NY.

181. Wang, C. D., M. A. Buck, and C. M. Fraser. 1991. Site-directed mutagenesis of α 2A-adrenergic receptors: identification of amino acids involved in ligand binding and receptor activation by agonists. Mol Pharmacol. 40:168-79.

182. Wang, J. H., Y. W. Yan, T. P. Garrett, J. H. Liu, D. W. Rodgers, R. L. Garlick, G. E. Tarr, Y. Husain, E. L. Reinherz, and S. C. Harrison. 1990. Atomic structure of a fragment of human CD4 containing two immunoglobulin-like domains. Nature. 348:411-8.

183. Wang, W. K., T. Dudek, Y. J. Zhao, H. G. Brumblay, M. Essex, and T. H. Lee. 1998. CCR5 coreceptor utilization involves a highly conserved arginine residue of HIV type 1 gp120. Proc Natl Acad Sci U S A. 95:5740-5.

184. Wang, Z., B. Lee, J. L. Murray, F. Bonneau, Y. Sun, V. Schweickart, T. Zhang, and S. C. Peiper. 1999. CCR5 HIV-1 coreceptor activity. Role of cooperativity between residues in N-terminal extracellular and intracellular domains. J Biol Chem. 274:28413-9.

185. Wei, P., M. E. Garber, S. M. Fang, W. H. Fischer, and K. A. Jones. 1998. A novel CDK9-associated C-type cyclin interacts directly with HIV-1 Tat and mediates its high-affinity, loop-specific binding to TAR RNA. Cell. 92:451-62.

186. Weiss, R. A. 1983. How does HIV cause AIDS? Science. 260:1273-1279.

187. Weiss, R. A., and R. W. Wrangham. 1999. From Pan to pandemic. Nature. 397:385-6.

188. Weissenhorn, W., L. J. Calder, S. A. Wharton, J. J. Skehel, and D. C. Wiley. 1998. The central structural feature of the membrane fusion protein subunit from the Ebola virus glycoprotein is a long triple-stranded coiled coil. Proc Natl Acad Sci U S A. 95:6032-6.

189. Weissenhorn, W., A. Carfi, K. H. Lee, J. J. Skehel, and D. C. Wiley. 1998. Crystal structure of the Ebola virus membrane fusion subunit, GP2, from the envelope glycoprotein ectodomain. Mol Cell. 2:605-16.

190. Weissenhorn, W., A. Dessen, S. C. Harrison, J. J. Skehel, and D. C. Wiley. 1997. Atomic structure of the ectodomain from HIV-1 gp41. Nature. 387:426-30.

191. Weissman, D., R. L. Rabin, J. Arthos, A. Rubbert, M. Dybul, R. Swofford, S. Venkatesan, J. M. Farber, and A. S. Fauci. 1997. Macrophage-tropic HIV and SIV envelope proteins induce a signal through the CCR5 chemokine receptor. Nature. 389:981-5.

192. Wu, H., P. D. Kwong, and W. A. Hendrickson. 1997. Dimeric association and segmental variability in the structure of human CD4. Nature. 387:527-30.

193. Wu, L., N. P. Gerard, R. Wyatt, H. Choe, C. Parolin, N. Ruffing, A. Borsetti, A. A. Cardoso, E. Desjardin, W. Newman, C. Gerard, and J. Sodroski. 1996. CD4-induced interaction of primary HIV-1 gp120 glycoproteins with the chemokine receptor CCR-5. Nature. 384:179-83.

194. Wu, L., G. LaRosa, N. Kassam, C. J. Gordon, H. Heath, N. Ruffing, H. Chen, J. Humblias, M. Samson, M. Parmentier, J. P. Moore, and C. R. Mackay. 1997. Interaction of chemokine receptor CCR5 with its ligands: multiple domains for HIV-1 gp120 binding and a single domain for chemokine binding. J Exp Med. 186:1373-81.

195. Wu, L., W. A. Paxton, N. Kassam, N. Ruffing, J. B. Rottman, N. Sullivan, H. Choe, J. Sodroski, W. Newman, R. A. Koup, and C. R. Mackay. 1997. CCR5 levels and expression pattern correlate with infectability by macrophage-tropic HIV-1, in vitro. J Exp Med. 185:1681-91.

196. Wyatt, R., E. Desjardin, U. Olshevsky, C. Nixon, J. Binley, V. Olshevsky, and J. Sodroski. 1997. Analysis of the interaction of the human immunodeficiency virus

type 1 gp120 envelope glycoprotein with the gp41 transmembrane glycoprotein. J Virol. 71:9722-31.

197. Wyatt, R., P. D. Kwong, E. Desjardins, R. W. Sweet, J. Robinson, W. A. Hendrickson, and J. G. Sodroski. 1998. The antigenic structure of the HIV gp120 envelope glycoprotein. Nature. 393:705-11.

198. Wyatt, R., J. Moore, M. Accola, E. Desjardin, J. Robinson, and J. Sodroski. 1995. Involvement of the V1/V2 variable loop structure in the exposure of human immunodeficiency virus type 1 gp120 epitopes induced by receptor binding. J Virol. 69:5723-33.

199. Xiao, L., S. M. Owen, I. Goldman, A. A. Lal, J. J. deJong, J. Goudsmit, and R. B. Lal. 1998. CCR5 coreceptor usage of non-syncytium-inducing primary HIV-1 is independent of phylogenetically distinct global HIV-1 isolates: delineation of consensus motif in the V3 domain that predicts CCR-5 usage. Virology. 240:83-92.

200. Yang, Z. N., T. C. Mueser, J. Kaufman, S. J. Stahl, P. T. Wingfield, and C. C. Hyde. 1999. The crystal structure of the SIV gp41 ectodomain at 1.47 A resolution. J Struct Biol. 126:131-44.

201. Zhang, L., C. D. Carruthers, T. He, Y. Huang, Y. Cao, G. Wang, B. Hahn, and D. D. Ho. 1997. HIV type 1 subtypes, coreceptor usage, and CCR5 polymorphism. AIDS Res Hum Retroviruses. 13:1357-66.

202. Zhang, Y. J., and J. P. Moore. 1999. Will multiple coreceptors need to be targeted by inhibitors of human immunodeficiency virus type 1 entry? J Virol. 73:3443-8.

203. Zhu, T., H. Mo, N. Wang, D. S. Nam, Y. Cao, R. A. Koup, and D. D. Ho. 1993. Genotypic and phenotypic characterization of HIV-1 from patients with primary infection. Science. 261:1179-81.